Doctoral theses at NTNU, 2024:37

Janelle Shari Weir

Motifs of Order

Emergent Self-Organization and Complex Dynamics in Biological Neural Networks

Doctoral thesis

NTNU
Norwegian University of Science and Technology
Thesis for the Degree of
Philosophiae Doctor
Faculty of Medicine and Health Sciences
Department of Neuromedicine and Movement Science

NTNU
Norwegian University of
Science and Technology

Janelle Shari Weir

Motifs of Order

Emergent Self-Organization and Complex Dynamics in Biological Neural Networks

Thesis for the Degree of Philosophiae Doctor

Trondheim, February 2024

Norwegian University of Science and Technology
Faculty of Medicine and Health Sciences
Department of Neuromedicine and Movement Science

NTNU
Norwegian University of
Science and Technology

NTNU
Norwegian University of Science and Technology

Thesis for the Degree of Philosophiae Doctor

Faculty of Medicine and Health Sciences
Department of Neuromedicine and Movement Science

ISBN 978-82-326-7676-7 (printed ver.)
ISBN 978-82-326-7675-0 (electronic ver.)
ISSN 1503-8181 (printed ver.)
ISSN 2703-8084 (online ver.)

Doctoral theses at NTNU, 2024:37

Printed by NTNU Grafisk senter

Nerve cells in a dog's olfactory bulb (detail), from Camillo Golgi's *Sulla fina anatomia degli organi centrali del Sistema nervosa* (1885) ---- Source: The Public Domain Review

"We cannot reject, a priori, the possibility that the inextricable forest of the brain, the last branches and leaves of which we imagine ourselves to have discerned, does not still possess some enigmatic system of filaments binding the neuronal whole, as creepers attach the trees of tropical forests. This is an idea which, appearing to us with the prestige of unity and of simplicity, has exerted and still exerts, a powerful attraction for even the most serene of spirits. True, it would be very convenient and very economical ... if all the nerve centers were made up of a continuous intermediary network [...]. Unfortunately, nature seems unaware of our intellectual need for convenience and unity, and very often takes delight in complication and diversity".

Santiago Ramón y Cajal, Nobel Lecture – December 12, 1906.

Norsk Sammendrag: Motiv av Orden

Den normale funksjonen av nevrale nettverk avhenger av den koordinerte interaksjonen mellom ulike elementer innenfor informasjonsbehandlingshierarkiet. Disse elementene spenner fra enkeltceller på mikronivå, til nevrale ansamlinger på mesonivå og til hele nettverk på makronivå. Selv om mye fortsatt er usikkert om hvordan grupper av celler i hjernen organiserer seg i funksjonelle hierarkier og hvordan interaksjoner mellom ulike kretsnivåer støtter hjernefunksjon, gir siste fremskritt innen metodikk og modelleringsteknikker lovende muligheter for å utforske disse prosessene i mer detalj. I dette doktorgrads prosjektet brukte jeg en tverrfaglig tilnærming for å få en mer omfattende forståelse av disse prosessene; avanserte modellering av biologiske nevrale nettverk *in vitro*, analyse av nettverkets selvorganisering og utvikling av funksjon gjennom teorien om komplekse systemer, samt definering og analyse av strukturelle og funksjonelle forhold mellom ulike nettverks elementer ved bruk av nettverksteori.

Gjennom hele denne avhandlingen legger jeg vekt på den uadskillelige sammenhengen mellom struktur, funksjon og selvorganisering i nevrale nettverk, samtidig som jeg fremhever relevansen av en reduksjonistisk tilnærming for å forbedre vår forståelse av disse komplekse mikro-mesonivåfenomenene. Ved å strippe hjernen ned til sine bestanddeler, nevroner og nevrale forsamlinger, kan vi få en dypere forståelse av hvordan den fungerer som en helhet. Dette reduksjonistiske perspektivet blir også komplementert av en mer helhetlig tilnærming som tar hensyn til de fremskapte egenskapene til komplekse systemer, det vil si at funksjonalitet oppstår fra interaksjoner og kollektive atferder fra de ulike elementene. Dette betyr at for å virkelig forstå komplekse systemer, må vi undersøke interaksjonene mellom elementer på ulike nivåer av nettverksorganiseringen slik at vi kan få innsikt i hvordan endringer i deres interaksjoner kan påvirke den overordnede nettverksfunksjonen. For å gjøre dette ble eksperimentene i dette prosjektet utviklet for å påvirke den komplekse nettverksdynamikken på ulike nivåer (hemming av synaptisk overføring på mikronivå ved bruk av DREADDs, og forstyrrelse av axon forbindelser mellom nevrale nettverk på mesonivå ved bruk av mutert tau) for å undersøke det overordnede nettverksvaret og om responsen kan fremme fremme eller hindre funksjonelle adaptive prosesser.

Navn kandidat: Janelle Shari Weir
Institutt: Nevromedisin og Bevegelsesvitenskap
Veiledere: Professor Ioanna Sandvig PhD, Professor Axel Sandvig MD, PhD
Finansieringskilder: Forskningsradet; NFR IKT Pluss; Self-Organizing Computational Substrates (SOCRATES) Grant nummer: 270961

Ovennevnte avhandling er funnet verdig til å forsvares offentlig
for graden PhD i medisin, Doctor Philosophiae.

To my incredible mother,

Your words of wisdom have inspired me to strive for excellence in all aspects of my life and provided the foundation upon which I build my academic pursuits.

Motifs of Order: Emergent Self-organization and Complex Dynamics in Biological Neural Networks

The normal function of neural networks hinges on the coordinated interaction among various elements within the information processing hierarchy. These elements range from single cells at the microscale, neural assemblies at the mesoscale, to entire networks at the macroscale. Though much remains uncertain about how cell assemblies in the brain self-organize into functional hierarchies and how interactions between different circuit levels elicit behavior, advances in methodologies and modelling techniques offer promising avenues for exploring these processes in greater depth. In this PhD research project, I applied a multidisciplinary approach to obtain a more comprehensive understanding of these processes; modelling biological neural networks *in vitro*, analyzing the networks´ self-organization and the emergence of function through complex systems theory, and defining and analyzing the structural and functional relationships between elements using network theory.

Throughout this thesis, I emphasize the inextricable relationship between structure, function, and self-organization in neural networks, while highlighting the relevance of a reductionist approach to enhance our understanding of these complex micro-mesoscale phenomena. By scaling down the brain to its constituent parts, neurons, and neural assemblies, we can gain a deeper understanding of how it functions. This reductionist perspective is also complemented by a more holistic one that considers the emergent properties of complex systems, i.e., functionality arises from the interactions and collective behaviors of the different elements. This means that to truly understand complex systems, we need to investigate the interactions between elements at different levels of network organization so we can gain insight into how changes in these interactions may affect overall network behavior. To do so, the experiments in this project were developed to perturb complex network dynamics at different scales (inhibition of synaptic transmission at the microscale using DREADDs, and disruption of axonal connections at the mesoscale using mutated tau) to investigate the overall network response and whether the response may be adaptive or maladaptive. I firmly believe that these studies can provide us with a deeper understanding of the underlying mechanisms of network response in varying conditions and help us determine whether we can leverage them to facilitate functional recovery in damaged networks or treat neuropathological conditions. I hope that this is effectively conveyed in this thesis.

Name of candidate: Janelle Shari Weir
Institute: Neuromedicine and Movement Science
Supervisors: Prof. Ioanna Sandvig PhD, Prof., Axel Sandvig MD, PhD
Funding source: Research Council of Norway (RCN) IKT Plus; Self-Organizing Computational Substrates (SOCRATES) Grant number: 270961

Acknowledgments

This research project was conducted at the Department of Neuromedicine and Movement Science at the Norwegian University of Science and Technology (NTNU), under the guidance of Professors Ioanna Sandvig and Axel Sandvig.

I would like to express my deepest gratitude to my main supervisor, Ioanna, and co-supervisor, Axel, for taking me on as a master student and providing me with the opportunity to undertake my PhD research project in their group. Your unwavering support, invaluable expertise, and constant encouragement throughout my academic journey have been instrumental in shaping this thesis. Moreover, your exceptional mentorship and kindness have been pivotal in my growth as a researcher and made my experience both in the group and in Norway truly remarkable.

I would also like to extend my heartfelt appreciation to my colleagues, past and present, for their camaraderie, collaboration, and willingness to share their knowledge. I am grateful for the vibrant intellectual environment you have created, which has challenged me to learn more and enjoy research. To Ola, Vibeke, Vegard, and the rest of the group, I have learned so much from you, and I am grateful for the laughs and fun social events that made the grueling lab hours and extensive failures more bearable. I would also like to thank Rajeev for his collaboration, knowledge, and expertise, which have been instrumental to my work.

I am also immensely grateful to my loving partner, Thomas, for their never-ending support and patience during this challenging and rewarding undertaking. You are a constant source of inspiration. To my colleagues and dear friends Katrine, and Christiana, thank you for being an incredible support system and for always being there to lend an ear and offer words of encouragement. Your bona fide friendship has helped me maintain balance and perspective. To Madison and Fairooz, thank you for the wonderful girl dates that brought so much laughter, comfort, and the much-needed break from the rigors of academia. Your friendship will forever be a cherished part of my journey. And to my bffls Kimberley (Canada) and Janvee (USA), you've gifted me the most extraordinary friendship that allows us to grow separately but never apart. Thank you both for being a major part of my journey, loving and supporting me across every ocean.

Finally, to my mom and sisters, thank you for believing in me from the very beginning. Your constant encouragement, love, and understanding have been the driving force behind my pursuit of knowledge and personal growth. And to everyone else who have played a part, big or small, in my academic and personal growth, I extend my gratitude to you. Your contributions and influence have shaped my journey in profound ways.

Preface

The theory of the independent neuron – which Spanish neuroanatomist Santiago Ramón y Cajal deduced as the building block of the nervous system – challenged the concept of the brain as a continuous nerve network in the 1890s. In the decades that followed, an explosion of research confirmed an intricate neuroanatomy, structure, and function derived from the dynamic interactions of diverse neuron types in a bottom-up sequence. This evidence has firmly established the brain's network as an extraordinarily complex self-organizing system.

Brain network complexity arises from several factors including:

1. ***Structural complexity*** – Billions of neurons and trillions of synapses coordinate to form highly interconnected networks.

2. ***Functional complexity*** – Different regions of the brain carry out different functions that are interconnected and functionally specialized.

3. ***Temporal complexity*** – Neural activity is highly dynamic and changes over time. The activity that arises is also highly unique to the structural and functional layout of the network, with various rhythmic patterns associated with specific cognitive processing.

4. ***Neuroplasticity*** – Neural networks can adapt and change in response to experience. This allows for reorganization of neural connections to modify function in response to environmental stimuli.

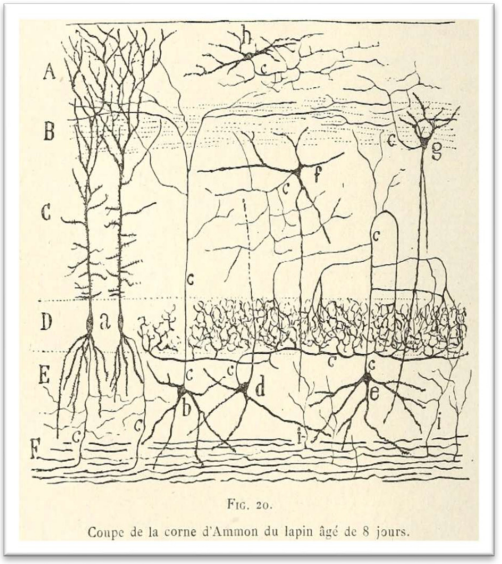

Figure 1. Illustration from Santiago Ramon y Cajal's *Les nouvelles idées sur la structure du système nerveux: chez l'homme et chez les vertébrés* (1894) Source : The Public Domain Review.

5. ***Heterogeneity*** – Neurons and synapses in the brain are highly diverse in terms of their properties and function. Each neuron type has several hundred connections, creating local circuits that connect to larger circuits.

My motivation for undertaking this neuroscientific enquiry was to investigate self-organizing neural network behavior at the mesoscale neuronal assembly level and understand the interrelationship among these complex processes in healthy and perturbed conditions. There is still a great deal of uncertainty surrounding many of these mechanisms, so the best thing we can do is approach them with an open mind, knowing that the answers may still be light years away.

Janelle Shari Weir – July 2023 – Trondheim

Table of Contents

List of Papers

Paper I

***Weir, Janelle S.**, *Christiansen, Nicholas., Sandvig, Axel., Sandvig Ioanna.

(Shared first authorship)*

Selective inhibition of excitatory synaptic transmission alters the emergent bursting dynamics of *in vitro* neural network.

(Published in *Frontiers in Neural Circuits,* February 2023, doi: 10.3389/fncir.2023.1020487)

Paper II

Weir, Janelle S., Huse Ramstad, Ola., Sandvig, Axel., Sandvig, Ioanna.

Selective inhibition of excitatory synaptic transmission alters functional organization and efficiency in cortical neural networks.

(Preprint, *BioRxiv,* July 2023, doi: https://doi.org/10.1101/2023.07.05.547785)

Paper III

***Weir, Janelle S.,** *Hanssen, Katrine S., Winter-Hjelm, Nicolai., Sandvig, Axel., Sandvig, Ioanna.

*(*Shared first authorship)*

Altered structural organization and functional connectivity in feedforward neural networks after induced perturbation.

(Preprint, *BioRxiv,* September 2023, doi: https://doi.org/10.1101/2023.09.12.557339)

List of Figures

Abbreviations (in order of appearance)

TCA	Thalamocortical axon
LGN	Lateral geniculate nucleus
LTP	Long-term potentiation
LTD	Long-term depression
DTI	Diffusion tensor imaging
DSI	Diffusion spectrum imaging
MRI	Magnetic resonance imaging
fMRI	Functional magnetic resonance imaging
EEG	Electroencephalography
MEG	Magnetoencephalography
E – I	Excitatory – Inhibitory
GABA	y-Aminobutyric acid
NMDA	N-methyl-d-aspartate
GDP	Giant depolarizing potentials
IBI	Interburst interval
ISI	Interspike interval
PSP	Postsynaptic potential
AD	Alzheimer's disease
TBI	Traumatic brain injury
SD	Spreading depolarization
ESCs	Embryonic stem cells
iPSCs	Induced pluripotent stem cells
PDLO	Poly-dl-ornithine
PLO	Poly-l-ornithine
PEI	Poly-ethylenimine
ECM	Extracellular matrix
MEA	Micro-electrode arrays
mMEA	Multiwell micro electrode arrays
HD CMOS	High density complementary metal-oxide semi-conductor
AAV	Adeno-associated virus
DREADD	Designer Receptors Exclusively Activated by Designer Drugs

GPCR	G-protein coupled receptors
GIRK	G-protein inward rectifying potassium channels
CaMKIIa	Calcium calmodulin dependent protein kinase II Alpha
CNO	Clozapine-N-oxide
DCZ	Deschloroclozapine
GFP	Green fluorescent protein
DIV	Days in vitro
PBS	Phosphate-buffered saline
STDP	Spike-timing dependent plasticity
BG	Basal Ganglia
CB	Cerebellum

1 Introduction

Can we ever fully unravel the complexities of the human brain? This is one of the prevailing questions in modern neuroscience, and a recursive problem since the researcher is the brain, studying itself. While advances in research methodology have allowed us to explore the brain in more depth than ever before, there is still a lot we may unfortunately, never fully understand. Its sheer scale, uniqueness and constantly evolving nature make it challenging to establish general principles that fully capture the diverse range of functionalities that gives rise to intricate human experiences.

To combat the challenge of scale, we can approach the brain from a viewpoint which scales it down to its basic components i.e., neurons, and elucidate their interactions that create the more complex architectures of the brain. Appropriately, the key principles of emergence i.e., that at any level or across levels, the behavior and function of a system are greater than the sum of its parts (Gazzaniga 2010), can provide an appropriate theory to describe how the brain and other complex systems operate. The brain evolved from a natural process of self-assembly, where the behavior of lower-level neural processes influence the behavior of higher-level units through hierarchical connections between them (Newsome 2009). Thus, to begin to understand complex behavior of the whole, we must consider its multiscale organization, and how multiscale interactions contribute to functional output. In the following sections, I will give an overview of complexity in brain networks from a rudimentary level of cellular organization, to how this organization ultimately drives complex function and behavior.

1.1 Overview of early brain organization and network formation

In the human brain, dynamic changes take place beginning during the embryonic stage of development, lasting well into adulthood, and arguably continuing throughout life. By embryonic day 42, neurogenesis commences, and neuroblasts begin their migration from proliferative regions near the cerebral ventricle along radial pathways towards the pia (Sidman and Rakic 1973) **(Figure 2)**. As cerebral expansion continues with cellular proliferation in the ventricular and subventricular zones, newly born neuroblasts migrate towards the cortical plate and pia along radial processes and the surfaces of earlier arrived neurons to take their position in the cerebral cortex in an 'inside-out' sequence (Angevine and Sidman 1961, Angevine 1965, Berry and Rogers 1965). In this 'inside-out' organization, the deeper layer of the cortex is composed of older neurons, while younger neurons settle sequentially to make up laminae VI, V, IV, III and II. The outermost layer, the marginal zone, goes on to become layer I (Bystron, Blakemore et al. 2008).

With the exception of the striatum granulosum, where development seems to take place in an 'outside-in' sequence (Angevine 1965), the rest of the cortex has an 'inside-out' formation which suggests that the later neurons must migrate through differentiated neurons that are already elaborating their dendrites and axons. This reverse order of cell migration is crucial for the attainment of intracortical synaptic

connections; the axons of migrating immature neurons are directed inwards towards the deep layers making up the white matter, and make contact with the somata or developing dendritic trees of the cells that arrived previously forming axo-dendritic connections (Angevine and Sidman 1961, Molliver, Kostovic´ et al. 1973).

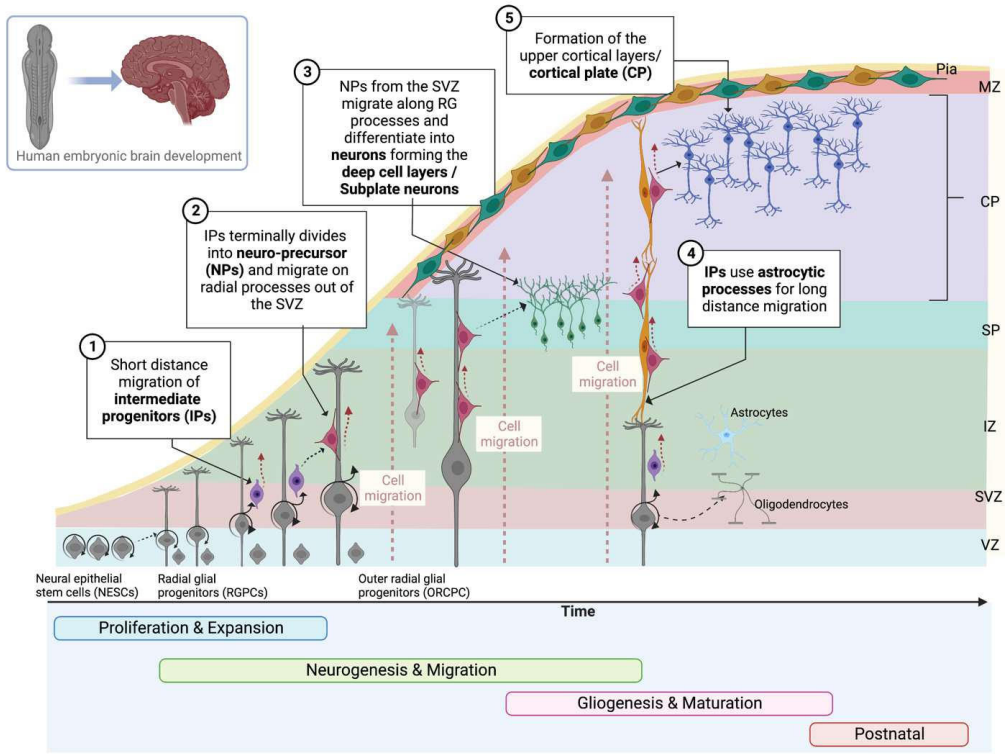

Figure 2. Development of the human cortex and early neural network formation. The processes involved in the formation of the brain are diverse, operate on precise spatial scales and may overlap considerably in their timing. The genetic coding that initiates a developmental process only needs to provide enough information to move the process along to a point where new cues can specify further steps. Thus, there is a clear hierarchical interaction where each level is constrained by the specifications dictated by the level below it (Ackerman 1992). These processes are ongoing, with each developmental stage characterized by a meticulous process of cellular organization and refinement. This implies that the brain is also both structurally and functionally dissimilar at different timepoints throughout life. Nonetheless, a dynamically complex and ordered system emerges from the independent actions of transcription factors, growth factors, guidance molecules, cellular interactions and perhaps others that are not yet identified. Any small disruption, deficiency, or perturbation to any of these underlying processes can have adverse consequences for the entire system. Abbreviations: MZ, Marginal Zone; CP, Cortical Plate; SP, Subplate; IZ, Intermediate Zone; SVZ, Sub-ventricular Zone; VZ, Ventricular Zone. *© Janelle S. Weir. Created in Biorender.com*

The earlier arrived neurons go on to establish simple connections with each other to create a coarse scaffolding of a neural network. They also aid in thalamocortical axon (TCA) pathfinding connectivity and play an essential role in the formation of the first neural circuits from the thalamus towards the cortical layer IV (Ohtaka-Maruyama 2020). While most of these early processes including cell division, migration, differentiation and early network formation are often described as 'activity-independent' due to the absence of neurotransmission, recent research suggests that subplate neurons may be neuronally active in early development and send signals to migrating new-born neurons via synapse-like interactions (Ohtaka-Maruyama, Okamoto et al. 2018). These interactions cause an increase in intracellular calcium concentration in new-born neurons as they pass through the subplate layer, and triggers a switch in the mode of migration from radial neuronal migration into locomotion (Ohtaka-Maruyama 2020). However, though subplate neurons may exhibit some spontaneous activity in early development to aid in cerebral organization, the mechanisms of cell migration, neuronal and regional differentiation, axon guidance and connectivity are chiefly directed by patterns of genetically specified molecular cues, growth and transcription factors (Goodman and Shatz 1993, Bystron, Blakemore et al. 2008). The discussion of these factors, pathways and guidance cues is beyond the scope of this research however relevant studies and reviews exist (Goodman and Shatz 1993, Tessier-Lavigne and Goodman 1996, Hirabayashi, Itoh et al. 2004, Plachez and Richards 2005, Wolman, Sittaramane et al. 2008, Munji, Choe et al. 2011, Namba, Kibe et al. 2014, McCormick and Gupton 2020).

Ultimately, the very early formation of neural networks requires that developing neurons (and axonal projections) navigate a dynamic microenvironment to make the correct connections at their target regions while avoiding navigational errors. Prenatal growth enhancing factors promote an overproduction of neurons and synapses with low precision connections; many of which will be eliminated over time and thus provide an opportunity to correct any wiring errors (Ackerman 1992). These early connections are extremely malleable, and are amended by experience-expectant synaptogenesis (Munji, Choe et al. 2011) and by ongoing spontaneous neuronal activity (Shatz 1990). This makes the early brain network a basic, rudimentary connected structure with crude cortical maps of the core compartments of the cerebral and cerebellar cortex on which subsequent experience-driven refinements can be made (Goodman and Shatz 1993).

1.1.1 Neuroplasticity and self-organization in neural networks

After the activity-independent phase of early brain development, the next major stage is a dynamic process of interaction among maturing neurons – the building blocks of the whole system – to form complex self-guided scaffolds of neural networks. This dynamic process describes the inherent capacity of the system to self-organize in a bottom-up manner (Karsenti 2008), in which structure and function evolve concomitantly with an increase in complexity and efficiency **(Figure 3)**. Neuroplasticity mechanisms are

heavily involved in self-organization, and there is a very active and ongoing interaction among elements across multiple organizational scales in the brain, which coordinate to form ordered neural structures.

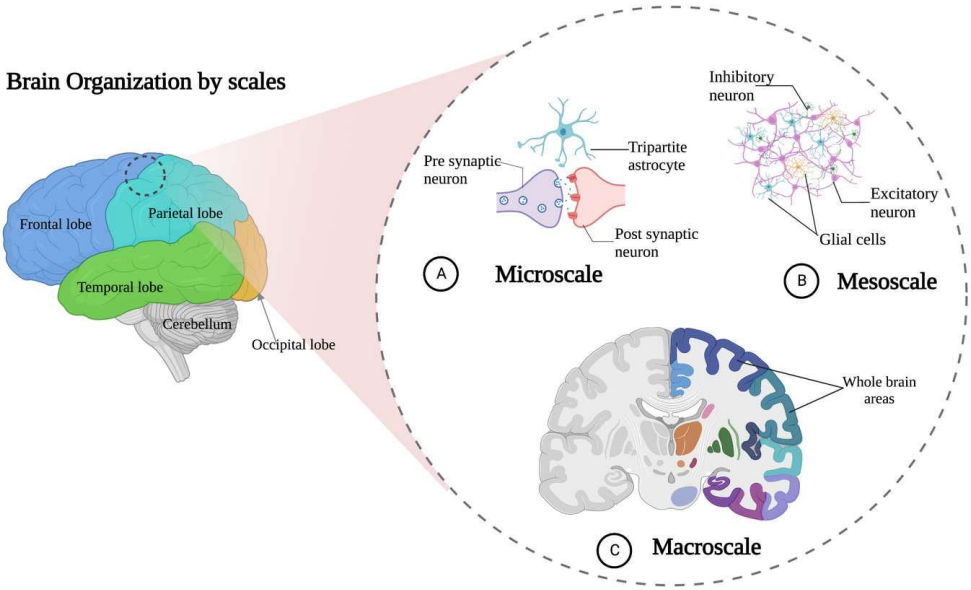

Figure 3. Schematic representation of the bottom-up process of self-organization in the brain. (A) Microscale organization where the synapse serves as a specialized junction for expediting fast point-to-point communication between presynaptic and postsynaptic neurons in intercellular interactions (Südhof 2018). Astrocytes are also active partners in the synaptic process and play a crucial role in brain function. **(B)** Mesoscale organization involves the interaction between diverse neuronal assemblies, or cell-type specific architectures with both local and long-range connections. These mesoscale structures also involve recurring motifs of interconnected neurons with distinct types of connections between them e.g., feedforward or feedback motifs. **(C)** Macroscale organization involve whole cortical areas and associated connections. *© Janelle S. Weir. Created in Biorender.com.*

Previous paragraphs have elucidated that prenatal neurogenesis and the formation of a functional brain foundation are regulated by patterns of genetic expression that dictate everything from mitotic activity to the differentiation of neurons. Postnatal development, however, is largely dependent on exogeneous sensory experience to refine neural structures and create those specific patterns of connectivity that characterize different neural networks in the mature brain. During early developmental progress, there is a comparatively short period termed the "critical development period" where sensory circuits are incredibly sensitive to both positive and negative stimuli (Knudsen 2004). During this period, adequate stimuli are needed for growing and differentiating various systems, and inadequate stimuli may permanently alter these structures (Trojan and Pokorny 1999). Interestingly, internally generated spontaneous activity has been shown to drive activity dependent synaptic modelling in some of these systems well before the onset of sensory responsiveness (Katz and Shatz 1996). For example, evidence showed that spontaneous electrical activity is needed for the refinement of ganglion cell axon connections within the lateral geniculate nucleus (LGN) before the onset of visual perception (Shatz and Stryker 1988, Wong, Meister et al. 1993). Conversely, blocking this activity hinders the process of segregating

retinogeniculate afferents into eye-specific layers (Shatz and Stryker 1988) and may block visual responsivity. Internally generated spontaneous activity may be critical for some processes, however, sensory development at critical periods is mostly dictated by sensory input. This has been widely studied and confirmed in systems for ocular representation in mammals (Hubel, Wiesel et al. 1977, Antonini and Stryker 1993), filial imprinting in precocial birds (Ramsay and Hess 1954, Bolhuis and Honey 1998) and song learning in the forebrain of songbirds (Doupe and Solis 1997) among others. Similarly, sensory deprivation during the development of the circuits responsible for these functions can result in the withdrawal of synaptic branches and rapid axonal rearrangements (Antonini and Stryker 1993) leading to potentially adverse behavioral outcomes.

Although stimuli during early development have a uniquely potent role in shaping the patterns of connectivity in neural networks, subsequent experience and learning throughout lifetime cause further structural and functional changes – within the enduring constraints established by critical period modifications (Knudsen 2004) – which can reinforce or nullify initial connectivity patterns. This involves a broad spectrum of changes governed by activity-dependent mechanisms **(Figure 4)** consistent with the Hebbian-based model of learning and plasticity (Hebb 1949, Bliss and Lomo 1973, Turrigiano, Abbott et al. 1994, Holtmaat and Svoboda 2009, Collingridge, Peineau et al. 2010, Fauth and Tetzlaff 2016, Jackman and Regehr 2017).

The Hebbian theory posits that repeated and enduring post-synaptic activation by the pre-synaptic neuron induces Long Term Potentiation (LTP), thereby strengthening those connections (Hebb 1949, Bliss and Lomo 1973, Komatsu and Iwakiri 1992). Synaptic connections that are not reinforced will experience Long Term Depression (LTD) and a reduction in their synaptic efficacy (Artola and Singer 1993, Bear and Malenka 1994, Artola, Hensch et al. 1996, Collingridge, Peineau et al. 2010). These mechanisms must also be gated to prevent irrelevant activity from inducing inappropriate modifications. Thus, homeostatic plasticity exists as a counterbalance to provide a negative feedback response to sustained alterations in network activity, and stabilize changes to preserve synaptic strengths and the overall dynamic range of activity (Turrigiano 1999, Turrigiano 2017, Ma, Turrigiano et al. 2019, Harrell, Pimentel et al. 2021, Kavalali and Monteggia 2023).

In addition, changes in synaptic activity and network function are also driven by activity dependent morphological modifications of dendritic spines. Strong lines of evidence indicate that learning and novel sensory experiences induce the rapid formation of new dendritic spines, while also resulting in the pruning of some existing spines that were formed during early development (Yang, Pan et al. 2009). Despite ongoing plasticity, new spines formed by novel experiences and those formed during early development which survived experience-dependent elimination are preserved, and provide an integral and stable structural basis for lifelong learning and memory retention (Yang, Pan et al. 2009).

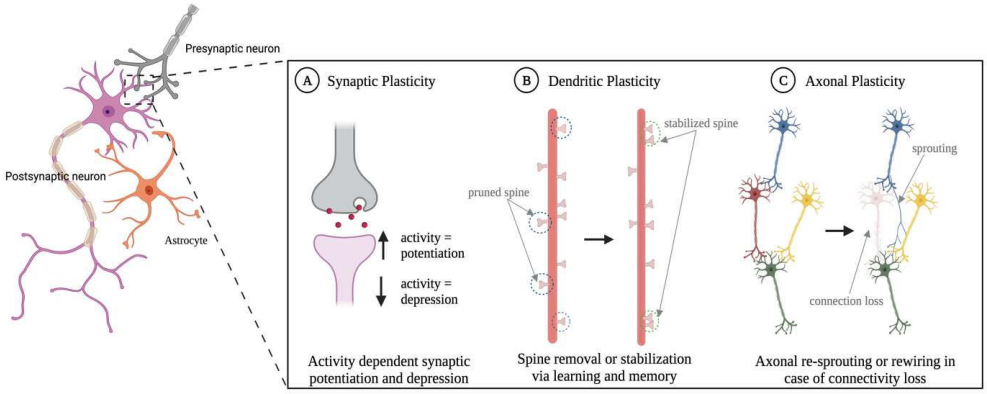

Figure 4. Mechanisms of neuroplasticity in neural networks. (A) Schematic representation of synaptic plasticity occurring between the transmitting (pre-synaptic) and receiving (post-synaptic) neuron to induce either the strengthening (potentiation) or weakening (depression) of synaptic efficacy (indicated by arrows) (Hebb 1949, Bliss and Lomo 1973, Jackman and Regehr 2017). The efficiency of information propagation between connections is also self-reinforcing such that more stimulation correlates to more effective information flow, resulting in **LTP**. Inadequate stimulation and no self-reinforcement reduce information propagation efficiency and result in **LTD** (Gilson, Burkitt et al. 2009, Henderson and Gong 2018). Concurrently, as recurrent activity-dependent positive feedback works to strengthen or weaken connections in the developing network, network activity is stabilized in a homeostatic manner to maintain activity within an optimal dynamic range (Bliss and Lomo 1973, Turrigiano and Nelson 2000). **(B)** Schematic illustration showing some dendritic changes due to neuroplasticity. Dendritic spines change dynamically throughout life and are either pruned, stabilized or new spines added (dotted circles) in response to levels of synaptic activation. While dendritic structures remain stable, the lifetime of spines can vary greatly and there is a prominent relationship between spine turnover and sensory-dependent synaptic formation and elimination (Trachtenberg, Chen et al. 2002). The dynamic changes in dendritic spine density, appearance and disappearance play a significant role in learning and memory formation in neural networks (Holtmaat and Svoboda 2009, Baltaci, Mogulkoc et al. 2019). **(C)** Schematic representation showing one axonal mechanism of neuroplasticity and repair. Collateral sprouting from healthy axons is an important rerouting mechanism to re-establish synaptic communication with other healthy regions of the network after neuron loss, injury, or lesion (Dancause, Barbay et al. 2005, Gatto 2020). Neuroplastic axonal reorganization after network damage contribute significantly to the restitution of network function. Abbreviations: LTP, Long-Term potentiation, LTD, Long-Term depression. Figure adapted from (Gatto 2020). *© Janelle S. Weir. Created in Biorender.com.*

While the previous paragraphs expounded on neuroplasticity at the microscale between synapses, the same processes are also continually active at the meso-and macroscale levels as well. The brain is dominated by hierarchical multi-layered sub- and supra-networks distributed within macroscopic regions, and both Hebbian and homeostatic plasticity are needed to establish and maintain synaptic connections within and between these layered networks. For many parts of the brain, the emergence of local network structure depends on correlation-sensitive plasticity mechanisms to stabilize recurrent and reciprocal connections (Gilson, Burkitt et al. 2009, Singer 2021). For instance, neighboring cells that are tuned to respond to similar stimuli and are represented by adjacent neurons are interconnected to form topographic orientation maps in the visual cortex (Hubel and Wiesel 1962, von der Malsburg 1973), and tonotopic maps in the auditory cortex (Jahan, Pan et al. 2015, Jahan, Elliott et al. 2018). These maps or functional modules are interconnected with each other such that cellular activity promotes robust activity-

dependent synaptic modifications within and between them. Disrupting synaptic activity during their wiring can alter their formation (Shatz and Stryker 1988, Ruthazer and Stryker 1996), indicating that activity-dependent mechanisms are vital for self-organization at the different scales (Érdi and Barna 1984, Kaiser and Hilgetag 2010). It is also suggested that the modular connectivity and self-organization capacity of neural networks are independent of each other but are mutually reinforcing in a way that ensures that both structural and functional capacity are developed simultaneously (Okujeni and Egert 2019, Dresp-Langley 2020). Thus, the more that the network learns, the more active connections will be established, effectively increasing its learning capabilities as well (Dresp-Langley 2020). These organizational and connectivity rules are evolutionarily conserved mechanisms that enhance efficiency and effective information processing in neural networks.

1.2 Small worlds and rich clubs

An emerging field of human brain mapping and network neuroscience makes use of complex network theory to analyze large-scale neurophysiological data to create structural and functional network graphs. Structural network graphs represent physical anatomical structures and connections and are constructed from diffusion tensor imaging (DTI) (van den Heuvel and Sporns 2013, Misic and Sporns 2016), diffusion spectrum imaging (DSI) (Lohse, Bassett et al. 2014), or conventional magnetic resonance imaging (MRI) data (Scholtens, Schmidt et al. 2014). Functional network graphs are derived from statistical descriptions of time series data obtained from functional MRI (fMRI) (Kaiser and Hilgetag 2010, Meunier, Lambiotte et al. 2010), electroencephalography (EEG) (Li, Li et al. 2023) and magnetoencephalography (MEG) data (Bullmore and Sporns 2009, Sato, Safar et al. 2023). The results of these high-resolution anatomical maps show that different brain regions are grouped into semiautonomous modules that are highly correlated with a core cortical processing **(Figure *5*)**.

These modules interact through dense intra-modular neurite connections and sparse long-distance inter-modular axonal connections (van den Heuvel and Sporns 2013, Misic and Sporns 2016). Similarly, network graphs constructed from electrophysiological recordings from neurons *in vitro* also reveal a similar topology with distinct modules, dense intra-modular connections, and sparse inter-modular connections (Bettencourt, Stephens et al. 2007, Downes, Hammond et al. 2012, Poli, Pastore et al. 2015, Poli, Pastore et al. 2016, Antonello, Varley et al. 2022). The modular organization in networks facilitates a balance between network structural segregation of specialized processing and functional integration of rapid and efficient global information transmission (Singer 1986, Watts and Strogatz 1998, Singer 2009, van den Heuvel and Sporns 2013), which are core features of complex systems with a small-world topology (Scholtens, Schmidt et al. 2014).

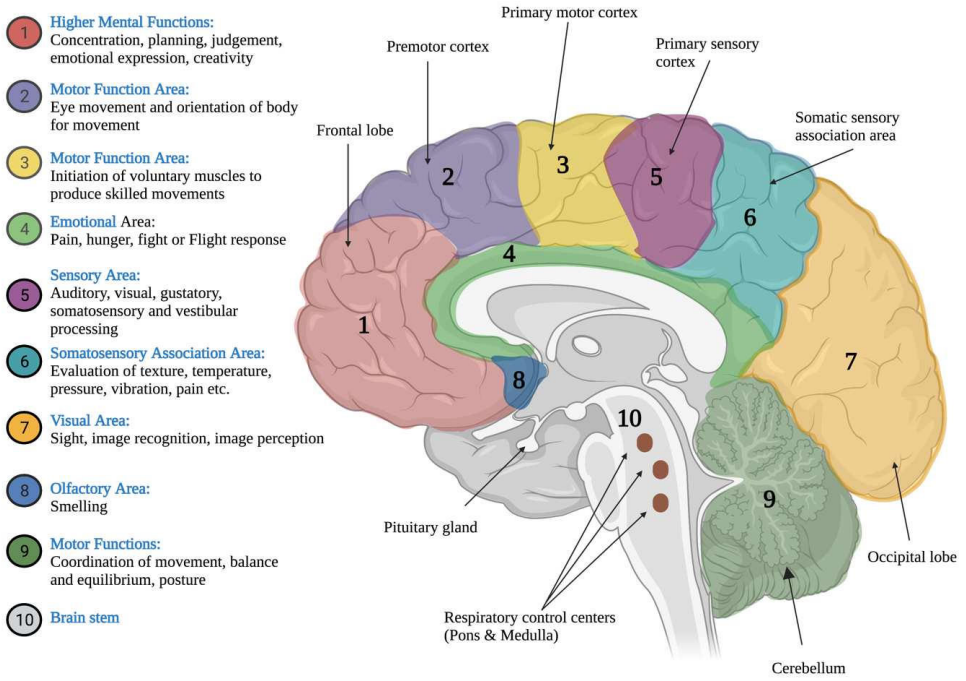

Figure 5. Structural segregation and functional organization in the brain. The earliest evidence indicating a non-random structural – functional organization in the brain comes from pioneering work by German anatomist Korbinian Brodmann, who in 1909 presented maps of cortical areas, showing distinguishable brain subdivisions based on cytoarchitectonic patterns derived from the original primitive six-layered cytoarchitecture (Garey 1999). Brodmann's parcellation of the brain into 52 distinguishable areas based on regional variations and consistent homologous distribution of cells and complex internal structures (Strotzer 2009), are still widely regarded more than 100 years later. Each of these areas is shown to correlate highly with a core cortical processing e.g. Brodmann's Areas 3, 1 and 2 (Intermediate, Caudal and Rostral Postcentral Areas) represent the primary somatosensory projection cortex and are responsible for somatosensory perception (Strotzer 2009) (represented in the figure as number 6). Since then, modern technology has enabled further parcellation of major brain areas to include more locally distributed clusters of functionally related cortical regions. Network-based analyses of MRI brain imaging data reveal dense meshwork of interconnected neurons that share common inputs and targets (Bassett and Sporns 2017, Faber, Antoneli et al. 2019) and provide information about the structural organization in local networks. Furthermore, fMRI is used to estimate functional connectivity between regions by assessing whether the perceived relationship between areas is statistically related or not, or if there are statistical dependence between them. Such analyses have concluded a strong correspondence for example, between cognitive function and structural discreet and functionally related brain modules (Bertolero, Yeo et al. 2015). Abbreviations: MRI, magnetic resonance imaging, fMRI, functional magnetic resonance imaging. *© Janelle S. Weir. Created in Biorender.com.*

These network graphs represent simple models of the real underlying connectome where the neural networks are delineated into a series of measurable nodes (neurons or regions) and connecting edges (white matter tracts or axons) (Sporns and Honey 2006, Downes, Hammond et al. 2012) **(Figure 6)**. Though structural connections are highly predictive of functional connections (Bullmore and Sporns 2009), edges in functional networks do not necessarily represent anatomical connectivity, and thus, there are functional connections between structurally unconnected node pairs (van den Heuvel and Sporns 2013). Of course, there are other important caveats to consider about these graphs. For example, the use of a single edge to describe an entire axonal pathway may overlook how information is distributed via the

convergence/divergence of presynaptic axons, as identified, for example, in the vertebrate retina (Gamlin, Zhang et al. 2020). Notwithstanding, defining nodes and edges in structural and functional networks enables us to determine dynamics of communication and information transfer, information processing, and the reciprocity of structure-function relations in neural networks.

1.2.1 Small-world communication and information processing

In previous paragraphs, I stated that neural network topology assumes a hierarchical organization over multiple spatial scales (Bullmore and Sporns 2009, Poli, Pastore et al. 2016); a hierarchy I have also illustrated in **Figure 6** to convey the interconnected nature between levels.

In small world complex networks, the hierarchical manner in which information flows and is processed is closely linked to inherent principles that govern the organization of connections. The majority of connections in the network are short-range edges, which represent the dense connectivity between neighboring nodes within a module. Nodes that are not otherwise edge-linked to each other are connected via hubs at higher levels in the hierarchy. For example, provincial hubs have greater intra-module connections and play a pivotal role in the function realized by its module, while connector hubs will play a central role in transferring information from its module to the rest of the network via long-range edges (Bettencourt, Stephens et al. 2007) **(Figure 6)**. Long-range edges preferentially link to hub regions and greatly reduce pathlengths for faster, more direct global information transfers between modules, though they are expensive in terms of energy and volume (Bullmore and Sporns 2012). This hierarchical organization dictates that information propagates in a bottom-up manner through the different processing stages i.e., nodes → hubs → rich-clubs → rest of network, with each level of the hierarchy providing responses of increasing complexity.

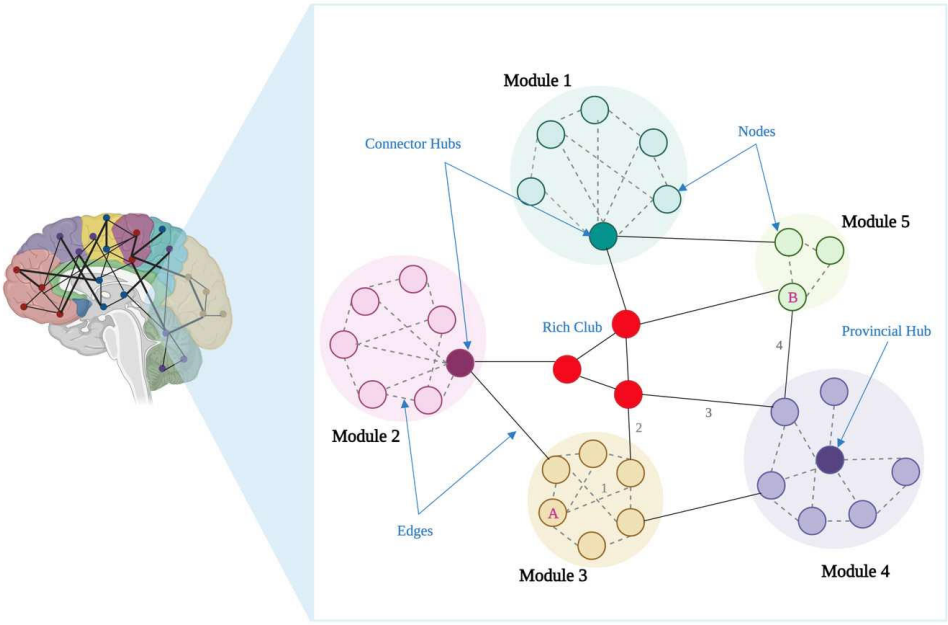

Figure 6. Graph theoretical schematic of complex neural network structural and functional organization. The convergence of neuroscience with the theoretical perspectives of mathematics and computational tools of network science, has made it possible to generate structural connective maps of brain networks across multiple spatial scales and in parallel, shed new light on neural network dynamics (Sporns, Tononi et al. 2005, Boccaletti, Latora et al. 2006). High clustering of nodes in modules signify high intra-modular connectivity with relatively sparse connections with the nodes of other modules. Long range connections are constrained by Euclidean distance and the number of connections linking two nodes is limited by the physical space available to accommodate axons and neurites (Sporns 2013, Bertolero, Yeo et al. 2015, Cohen and D'Esposito 2016). Thus, rapid information transmission between modules is achieved by few long distant connections, or via hubs (as illustrated by the numbered edges (n = 4) connecting nodes A and B in Modules 3 and 5 respectively). As hubs typically have very high degree i.e., having larger than average number of edges than other nodes, they receive information from various parts of the network. Structural segregation is mediated by modules and provincial hubs; which are high degree nodes primarily connected to other nodes in the same module (Hagmann, Cammoun et al. 2008, van den Heuvel and Sporns 2011, van den Heuvel, Kahn et al. 2012, Alstott, Panzarasa et al. 2014, de Lange, Ardesch et al. 2019). Functional integration is typically mediated by connector hubs and rich clubs (van den Heuvel and Sporns 2011, van den Heuvel, Kahn et al. 2012, Alstott, Panzarasa et al. 2014, de Lange, Ardesch et al. 2019). *© Janelle S. Weir. Created in Biorender.com.*

The idealized construction I described is biologically adapted for the conservation of energy and the maximization of efficiency. Anatomically localized and functionally specialized modules conserve space and biological material by reducing the average length of axonal projections, while functionally integrative hubs conserve conduction time by reducing the average axonal delay (Rubinov, Ypma et al. 2015). By minimizing the average length of projections and inter-neuronal communication delay, networks are adapted for faster and more efficient transmission of information throughout the brain. These conserved principles across information-processing complex systems unequivocally satisfy optimization criteria necessary for maximizing communication efficiency and minimizing wiring cost in the brain (Bullmore and Bassett 2011).

In general, the metabolic cost for establishing and maintaining axons, plus neural communication via synaptic transmission increases with wiring volume (Raichle and Mintun 2006, Bullmore and Sporns 2012, Tomasi, Wang et al. 2013), so there are functional advantages for minimizing the connection distances of intra- and inter-modular edges (Raichle and Mintun 2006, Tomasi, Wang et al. 2013). Furthermore, since living organisms are designed according to the guiding principles of economy and efficiency – possessing remarkable abilities to conserve energy thus enabling us to function at optimal levels without expending unnecessary effort – communication dynamics within neural networks are also shaped by a trade-off between energy conservation in terms of metabolic cost and wiring optimization, and the ability to maximize communication efficiency through a specific topology (Chen, Hall et al. 2006, Achard and Bullmore 2007, Bullmore and Sporns 2012, Avena-Koenigsberger, Yan et al. 2019). Hubs and rich clubs perform the bulk of computation in the network and are crucial for global communication (Hilgetag, Burns et al. 2000, Hilgetag and Goulas 2020) because of their strategic position in the hierarchy above nodes. This also implies that communication efficiency in neural networks is inversely proportional to the distance between processing nodes (Chen, Hall et al. 2006, Bullmore and Sporns 2012) since traversing hubs greatly reduces path lengths. Results from large-scale statistical analyses of connectivity datasets support that communication efficiency between different areas of different modalities and information integration is largely mediated by few, highly connected hubs (Zamora-López, Zhou et al. 2009, Liang, Hsu et al. 2018, Faber, Timme et al. 2019). Also, recordings from neural assemblies found that rich clubs tend to transfer much more information than other nodes in the network (Nigam, Shimono et al. 2016) and are often traversed by a majority of short paths between areas of the network (Schroeter, Charlesworth et al. 2015).

These findings also have significant relevance for information processing; as studies suggest an association between higher intelligence and higher brain network efficiency (Li, Liu et al. 2009, van den Heuvel, Stam et al. 2009, Langer, Pedroni et al. 2012, Hilger, Ekman et al. 2017, Koenis, Brouwer et al. 2018). If high global efficiency is beneficial for information processing and increases cognitive abilities, then it seems logical that low global efficiency would also be correlated with low processing and cognition. This theory is supported by evidence that showed that low cognitive performance is correlated with decreased global integration and efficiency in individuals with alcohol use disorder (Wang, Zhao et al. 2018), small vessel disease (Schroeter, Charlesworth et al. 2015), multiple sclerosis (Shu, Liu et al. 2011) and mild cognitive impairment (Berlot, Metzler-Baddeley et al. 2016). Thus, the high correlation between cognitive performance and anatomical network organization (McColgan, Seunarine et al. 2015) signifies an important relationship between neural network structure and function.

1.3 Does neural network structure dictate function?

A key question of intense neuroscience research intrigue remains: To what extent does network structure influence its distributed functional properties? While empirical studies using large data sets of whole brain recordings provide fascinating insights into this structure – function relationship, a refined answer remains elusive. In the next sections and throughout the rest of this thesis, I will regard function as the electrophysiological dynamics exhibited by the active network, rather than the set of behaviors subserved by a particular brain region (Honey, Thivierge et al. 2010). One of the key insights from the study of complex systems is that neural network function emerges from specific arrangements of heterogeneous neuron populations making up multi-level micro-and mesoscale hierarchical local circuits embedded within the macroscale system. Each local circuit exhibits precise and patterned spontaneous and task-evoked physiological activity that changes over time and with temporal resolution. By investigating the underlying structural interactions that produce the repertoire of activity displayed by networks, we may come closer to answering our question at the top of this paragraph.

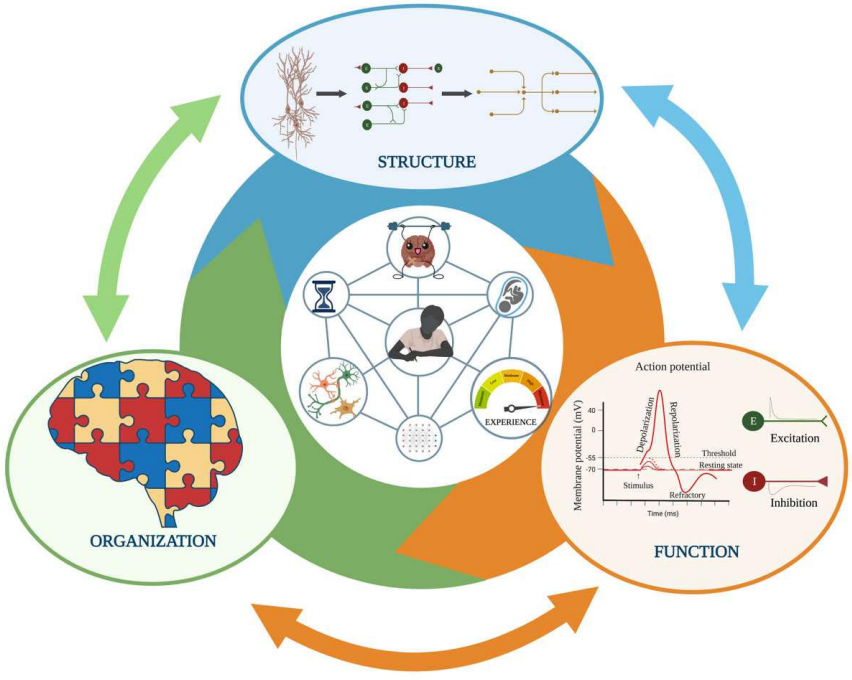

Figure 7. The reciprocity of structure, function, and organization in the brain. Network structure is composed of diverse cell types interacting to create micro-network motifs. These motifs interconnect to form large scale topographic maps (Luo 2021), and enable specialized functions through convergent and divergent signal processing. Neurons hyperpolarize or depolarize in response to neurotransmitters binding to postsynaptic receptors, causing repeated patterns of E-I innervations throughout the network. These different patterns of activation and suppression in motifs drive the initiation and execution of function. Motifs of different function self-organize to create large hierarchical networks that make up the brain. Structure, function, and organization are thus self-reinforced through neuroplasticity and learning beginning from prenatal development and continuing throughout adulthood. *© Janelle S. Weir. Created in Biorender.com.*

1.3.1 Excitatory – inhibitory neurons: backbone of neural network function

During network development, diverse ensembles of neural cells — including principal cells and an array of interneurons (McColgan, Seunarine et al. 2015) — are established in functionally relevant neural circuits that form the foundation of network structure. The coordinated activity between these two cell types is vital in shaping neural activity and drives network function **(Figure 7)**. The concept that network function is driven by glutamatergic excitation (E) and GABAergic inhibition (I) is not new. One early paper pointed out that the fundamental tenet of neural networks is that "*all nervous processes of any complexity are dependent upon the interactions of excitatory and inhibitory cells*" (Wilson and Cowan 1972). This is evidenced by the highly non-random organization of E-I neuron types that can be found all over the brain including in the cerebellum (Ohtaka-Maruyama, Okamoto et al. 2018), the striatum (Markram, Toledo-Rodriguez et al. 2004, Booker and Vida 2018), the hippocampus (McKenzie 2018), and the neocortex (DeFelipe, Alonso-Nanclares et al. 2002).

In the context of emergence and network organization, spontaneous interactions between E-I neuron types create heterogenous topologies of recurring subnetworks or motifs throughout the neural network (Milo, Shen-Orr et al. 2002) that have incredible influence on function. These motifs are characterized by specific patterns of connectivity (Milo, Shen-Orr et al. 2002) **(Figure 7)** and result in different information processing streams that can create feedforward, feedback, diverging, converging or recurrent activity (Jiang, Wang et al. 2013) that produce different functional outcomes for the network. A number of studies, particularly in the neocortex, have investigated the organization of diverse classes of E-I neurons and found that there is significant functional and organizational diversity in their connectivity (Rieubland, Roth et al. 2014, Straub, Saulnier et al. 2016). The functional outcomes achieved by such diverse patterns of neuron connections are a testament to the complexity and sophistication of the brain. For instance, interneurons in the neocortex L2/3 selectively make synapses at various parts of L5 pyramidal neurons and drive inactivation in one area of the circuit whilst the connections in other areas facilitate signal amplification, depending on which stream of connectivity is activated (Jiang, Wang et al. 2013). Similarly, *in vivo* initiation or suppression of dendritic complex spiking in L5 pyramidal neurons has been found to be mediated by upstream feedback inhibitory to inhibitory innervation between L1 interneurons connecting to L2/3 interneurons (Jiang, Wang et al. 2013).

Analyzing E-I interactions through the application of complex network theory implies that distinct functional subclasses of nodes located at various points along the information processing stream in motifs play a crucial role in maintaining balanced E-I neural activity. Research has demonstrated that there exists spontaneous segregation of excitation and inhibition in networks within cortical columns, with the average activity of nodes being strongly correlated with their degree (Markram, Toledo-Rodriguez et al. 2004, Jiang, Wang et al. 2013, Neske, Patrick et al. 2015). For hubs, their influence on the overall network is determined by the ratio of inhibitory or excitatory inputs they receive. If input is predominantly excitatory,

the resulting activity will be strongly excitatory and if input is predominantly inhibitory, there will be a strong inhibitory influence on the network (Rieubland, Roth et al. 2014). Taking all of these into account, we can agree that the structural organization of E-I neurons creates the dynamics necessary for complex processing, defines signal propagation rules at the circuit level, and determines network performance. These constraints also shape the repertoire of collective activities, from single spikes to bursts and synchrony, that give rise to network functions. I will elaborate on these complex activities in the following section.

1.3.2 Collective dynamics of E-I interactions shape spontaneous neural activity

Diverse patterns of E-I connections and balance between E-I synaptic transmission play a crucial role in the stability of neural networks. Also, network topology and network activity are mutually dependent in a reciprocal relationship with activity-dependent neuroplasticity (Rubinov, Sporns et al. 2009). Neurons communicate with each other via spikes, which are action potentials generated through depolarizing action of ion channels and the release of neurotransmitters. In the immature brain, γ-aminobutyric acid (GABA), the main inhibitory neurotransmitter in the mature brain, along with $GABA_A$ receptors ($GABA_AR$) are depolarizing (Malagarriga, Villa et al. 2015). GABA operates in synergy with functional *N*-methyl d-aspartate receptors (NMDARs) that are present even before synapses are established (Tremblay, Lee et al. 2016, Booker and Vida 2018). The depolarizing effects of GABA, $GABA_AR$s and NMDARs produce primitive network-driven patterns of electrical activity – the giant depolarizing potentials (GDP) (Ben-Ari 2001) - which underly activity-dependent development and wiring of the immature neural network (Ben-Ari 2002). GABA exerts its conventional inhibitory action after sufficient excitatory and inhibitory synapses are formed, thus replacing the primitive patterns of network activity with more diverse and elaborate ones.

The maturity of inhibitory control coincides with the emergence of spontaneous network bursts both *in vivo* (Khazipov, Sirota et al. 2004, Khazipov and Luhmann 2006, Minlebaev, Ben-Ari et al. 2007, Egorov and Draguhn 2013, Luhmann and Khazipov 2018, Graf, Rahmati et al. 2022) and *in vitro* (Mooney, Penn et al. 1996, Ben-Ari 2001, Wagenaar, Nadasdy et al. 2006, Wagenaar, Pine et al. 2006). These early bursts – events of ~0.5s long period of extensive spiking across the network interspersed by ~7s long quiescent interburst intervals (IBIs) (Teppola, Acimovic et al. 2019) – are fundamental for Hebbian refinement of the neural network during development. Since the activiy is self-reinforcing, information propagation efficiency increases through LTP while non-self-reinforced, inefficient pathways are restructured through LTD (Dresp-Langley 2020), as been shown with memory reinforcement (Fauth and van Rossum 2019).

With maturity, complexity in both structural and functional dynamics also increases in neural networks in ways that facilitate learning, memory encoding and cognition. In other words, the adult network will exhibit more complexity in spikes and burst patterns compared with the immature network (Sadeh, Silver et al. 2017, Sadeh and Clopath 2020). As such, bursts occur across various brain regions in complex processing

(Llinás and Steriade 2006, Leleo and Segev 2021, Kim, Kim et al. 2023) and their features are often characteristic electrophysiological indicators of maturity in neural networks. Bursts create larger and stronger electrical signals that can be more reliable than single spikes in transferring information (Lisman 1997). It has been proposed that sending short bursts instead of single spikes circumvents the probability of synaptic transmission failure and ensures that at least one spike reaches its target (Lisman 1997). Furthermore, shorter interspike intervals (ISIs) increase the chance of multiple spikes occurring within a burst, thereby triggering synaptic transmission that can create larger postsynaptic potentials (PSPs) than single spikes (Izhikevich, Desai et al. 2003). Bursts can also facilitate selective communication without involving long term synaptic modifications. Complementing Lisman's theory (Lisman 1997), Izhikevich et.al proposed that because different postsynaptic neurons possess distinct resonance frequencies, utilizing bursts with varying interspike frequencies allows the presynaptic neuron to selectively influence some postsynaptic targets and not others (Izhikevich, Desai et al. 2003). Therefore, although bursts are characterized by stereotypical trains of action potentials, they can also exhibit different interspike frequencies based on the properties of the neurons and the overall network activity. This makes them a more efficient means of communicating information in mature neural networks.

In addition to bursts, neural networks also exhibit highly complex temporal dynamics, which include but are not limited to the correlated firing between two or more neurons that creates synchronized activity (Singer 1999, Salinas and Sejnowski 2001). Several studies support the hypothesis that synchrony plays an essential role in the emergence of function within complex systems (Jackson, Gee et al. 2003, Uhlhaas, Pipa et al. 2009, Nowak, Vallacher et al. 2017). Much like bursts, previous studies noted that synchronous inputs can be more effective than single inputs at conveying information (Softky and Koch 1993, Usrey, Reppas et al. 1998). In addition, one group of neurons can affect another group in a range of different ways; either by modifying the firing rate or through correlations between local neurons in a postsynaptic group, depending on the input received from a presynaptic group (Salinas and Sejnowski 2001). The impact of input correlations on postsynaptic neurons is often dependent on E-I signals arriving in balanced or unbalanced neurons (Salinas and Sejnowski 2000). In all cases, correlation of activity can increase the variability of network output and contributes to the complex functional properties of neural networks. On the one hand, synchrony is suggested to be associated with cognitive functions that require large-scale integration of distributed neural activity (Schnitzler and Gross 2005). For example, they play a salient role in short-term memory (Lisman and Idiart 1995, Siegel, Warden et al. 2009), attention (Fries, Reynolds et al. 2001) and the encoding of sensory inputs (Gray, König et al. 1989). On the other hand, abnormal synchrony is implicated in some cognitive disorders including schizophrenia, autism and Alzheimer's disease (AD) (Uhlhaas and Singer 2006). Therefore, networks develop specific patterns of synchronous and asynchronous activity that can be correlated with both distinct cognitive processing or network pathology (Sadeh and Clopath 2020, Sanzeni, Akitake et al. 2020). Also, the ability of neurons to synchronize and propagate information is inextricably linked to the topological organization of their long - and short – range structural connections (Buzsáki, Geisler et al. 2004). As a result, small-world

architectures can increase synaptic transmission efficiency for both functional and dysfunctional network behaviours.

1.3.3 Neural network robustness and resilience to damage or perturbation

In healthy conditions, neural network structural organization is beneficial for fast integrative processing and high communication efficiency. However, this organization also acts as a convenient highway for spreading perturbations by providing direct pathways and integration among brain regions. For example, in focal epilepsy, seizures may start and remain localized, or spread to other nodes in the network via connections (Moosavi, Jirsa et al. 2022). In conditions such as severe traumatic brain injury (TBI) or ischemic stroke, a class of pathological waves called "spreading depolarizations" (SD) propagate slowly through cerebral gray matter (1 to 9 mm/min)(Hinzman, Wilson et al. 2016) and result in subsequent suppression of synaptic activity (Somjen 2001, Johann, Ashlyn et al. 2019). The propagation of these aberrant activations cause widespread metabolic crises in the network with increased intracellular calcium, and can cause lasting loss of neuron function (Somjen 2001).

Small-world organization also renders neural networks vulnerable in the event of structural damage or targeted attacks (Kaiser and Hilgetag 2004). For example, damage to network hub regions can cause large disturbances in the overall network function (van den Heuvel and Sporns 2011, Crossley, Mechelli et al. 2014, de Reus and van den Heuvel 2014, Li, Liao et al. 2016, Tu, Ma et al. 2021). In addition, lesions to functional hubs rather than an anatomical area can produce severe behavioral deficits (Warren, Power et al. 2014, Osada, Adachi et al. 2015, Gordon, Lynch et al. 2018) and disrupt inter-regional information integration (Honey and Sporns 2008). Because these central nodes are so crucial for the performance of all cognitive tasks and functions, neuropathological conditions with distributed, aberrant effects including schizophrenia (van den Heuvel, Sporns et al. 2013), major depressive disorder (Zhao, Swati et al. 2019) and autism spectrum disorder (Benkarim, Paquola et al. 2021) are all typically accompanied by disruptions in functional connectivity among core brain nuclei (or hubs). In many other neural disorders, dysfunction is highly correlated with severe anatomical impairments in specific brain modules as in Parkinson's disease with degeneration of dopaminergic neurons in the substantia nigra (Giguère, Burke Nanni et al. 2018, Aman 2022), AD with progressive degeneration in the entorhinal cortex (de Haan, Mott et al. 2012), expressive aphasia with Broca's area damage (Sreedharan, Chandran et al. 2020) and cognitive impairment or personality changes resulting from frontal lobe damage (Janowsky, Shimamura et al. 1989, Van Horn, Irimia et al. 2012).

Despite the adverse effects of perturbations, neural networks can exhibit remarkable resilient in the face of changing conditions. Although the process of network resilience during a metabolic crisis remains unclear, as it often results in secondary brain injury due to neuron death, neural networks still possess the ability to reorganize functions to compensate for structural damage. One reason for this is that although modular organization enables specialized processing in separate brain areas, function is widely distributed

across network levels and not centralized to a specific subnetwork or module. According to John's theory of multipotentiality, any brain region can contribute to the mediation of a diversity of function, such that if the structural integrity of an area is compromised, the function can also reorganize within intact areas (John 1980). Furthermore, functional plasticity allows subnetworks with an initial function to spontaneously adapt to perform a different function to compensate for network damage (Dresp-Langley 2020). Such reorganization strategies are largely mediated by plasticity of synaptic efficacies, and ensure that the network can often withstand attacks or failures without losing its overall performance and can quickly recover, adapt or return to its initial functional state after perturbation (Dresp-Langley 2020).

Importantly, neural systems also are characterized by redundancy so that different patterns of interactions between network components can produce similar circuit performance (Prinz, Bucher et al. 2004, Marder 2011). In neural network studies, the shortest path represents one possible communication route between processing nodes in the functional subnetwork. However, there are alternative anatomical and functional pathways (De Vico Fallani, Rodrigues et al. 2011, Di Lanzo, Marzetti et al. 2012) that allow neural networks to reconfigure to compensate for the critical consequences of perturbations. This is evidenced by electrical stimulation studies that revealed that neural networks can evolve towards a new dynamic state by modifying their underlying functional connectivity both *in vitro* (Poli, Pastore et al. 2015) and *in vivo* (Teskey, Monfils et al. 2002, Huang, Hajnal et al. 2019, Bloch, Greaves-Tunnell et al. 2022). Similarly, large-scale brain reorganization, for example of the somatosensory cortex, has been reported to result from deafferentation following spinal cord injury (Tandon, Kambi et al. 2009, Kambi, Halder et al. 2014) and amputation (Simoes, Bramati et al. 2012). Considering all this, it will remain crucial for researchers to investigate the adaptive capacity of neural networks to better understand how we can harness these mechanisms to improve functional outcomes and facilitate recovery after neural network damage.

2. Aims and Objectives

Neural networks respond differently under changing conditions, thus, understanding the underlying mechanisms of network function can be crucial for making informed predictions about future behavior. The goal of this PhD project was to characterize emergent properties of neural networks and elucidate complex network dynamics at the micro-mesoscale level of network organization in healthy and perturbed conditions.

Key research questions:

I. How do neural networks exhibit emergent properties at the micro-mesoscale level of network organization?

II. What are the key characteristics of complex network dynamics observed in healthy neural networks?

III. How do perturbations affect emergent properties and network dynamics?

IV. What are the specific changes in network structural and functional organization that occur under perturbed conditions?

V. How do perturbations affect the stability and resilience of neural networks?

VI. What insights can be gained from studying the complex dynamics of healthy and perturbed neural networks and how can their emergent properties help us predict future behavior?

The key objectives included:

I. Establish and optimize a robust *in vitro* model that recapitulates the micro-mesoscale development and organization of neural networks.

II. Characterize the emergent properties and network dynamics of healthy neural networks.

III. Develop optimized protocols to selectively perturb neural networks using controlled experimental conditions to simulate pathophysiological scenarios.

IV. Quantify and analyze the changes in emergent dynamics of perturbed neural networks compared to healthy baseline to understand the effects of perturbation on network structural and functional processes.

3. Overview of main methods

3.1 In vitro neural networks as a reductionist model for studying complex and dynamic brain processes.

Considering the complexity of the brain and the difficulty of accessing it, studying neural networks is a major challenge for researchers, who are still attempting to understand neurological behavior and how the brain develops strategies to either repair damaged neural circuits or arrest neurodegeneration. A well-tested approach to overcome accessibility is to use *in vitro* cell cultures of animal-derived primary neurons, embryonic stem cells (ESCs) or healthy human and patient-derived induced pluripotent stem cells (iPSCs)(Takahashi, Tanabe et al. 2007, Vazin and Freed 2010, Amin, Maccione et al. 2016, Wang, Kong et al. 2018, Valderhaug, Heiney et al. 2021, van Niekerk, Kawaguchi et al. 2022) to examine mechanisms involved in neural network connectivity, communication, function, and dysfunction.

Protocols for preparing, culturing, and maintaining *in vitro* neural networks vary depending on the cell types involved. Hence, to determine highly reproducible procedures to routinely culture different cell types, numerous assays are often required. In the studies presented in this thesis, primary neurons were obtained from commercially available sources along with their recommended protocols (ThermoFisher Scientific, AS), which greatly reduced optimization time. Based on previous *in vitro* experiments (Fiskum, Sandvig et al. 2021, Hanssen, Witter et al. 2023, Weir, Christiansen et al. 2023), a combination of biochemical substrates such as poly-dl-ornithine (PDLO), poly-l-ornithine (PLO), or poly-ethylenimine (PEI), together with extra-cellular matrix (ECM) glycoproteins such as Matrigel, Geltrex and Laminin, were determined as the best cell adhesion promoters on both micro-electrode arrays (MEAs) and multi-nodal MEAs (mMEAs). In addition, primary neurons survive best when established as co-cultures with primary astrocytes, as astrocytes are consistently found to increase neuron attachment, viability, and maturity (Wang and Cynader 1999, Aebersold, Thompson-Steckel et al. 2018). Good handling routines are also essential to increasing survivability and maturity. Therefore, primary cell cultures require nutrient rich media, routine media changes in a sterile environment to prevent contamination, and maintenance in a stable external environment achieved by keeping them at 37°C in a CO_2 incubator **(Figure 8)**.

Despite the limited functional complexity and dissociation from sensory inputs, networks of cultured neurons can provide robust recapitulation of *in vivo* processes. A core feature is that the *in vitro* architecture of densely innervated neurons allows for self-generated and self-sustained network activation (Braitenburg and Shuz 1998). Moreover, cultured primary neurons maintain their intrinsic morphological and electrophysiological properties: they form neurites and synapses, self-organize into complex interconnected topologies, and exhibit emergent network-driven activity which serves to establish long term synaptic and structural connections necessary for function, and survival (Katz and Shatz 1996, Ben-Ari 2001).

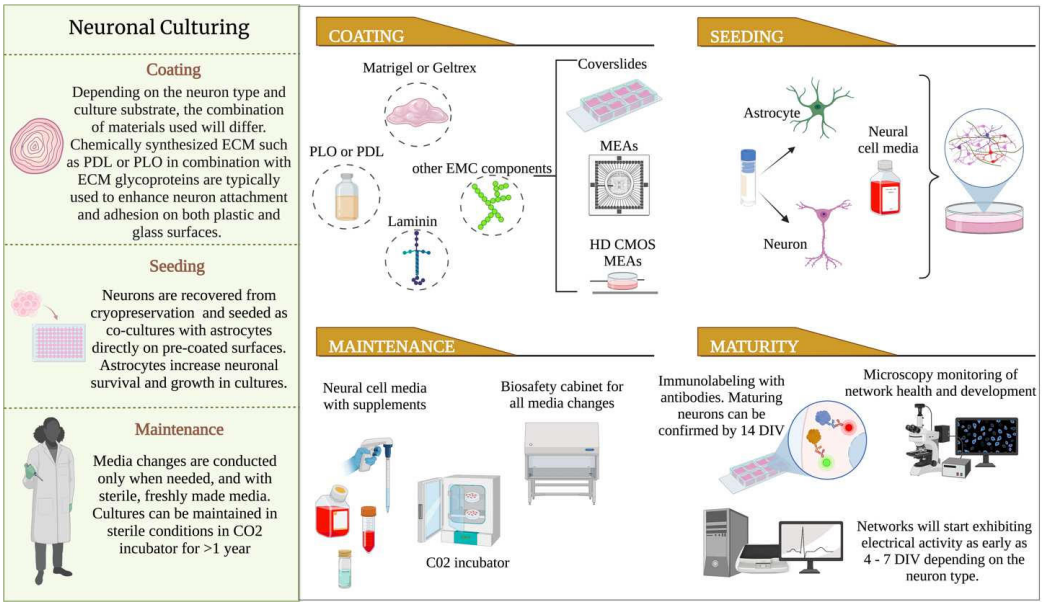

Figure 8. Typical experimental procedures involved in neuronal culturing. Depending on the cell type protocol, coating procedures for the culture vessel may take anywhere from 2 hours to 3 days to complete. Next, cells derived from commercial sources are thawed and seeded along with astrocytes on the pre-coated surfaces. Cultures are maintained in sterile conditions, with regular media changes to enhance survival and maturity. *© Janelle S. Weir. Created in Biorender.com.*

Within hours of seeding dissociated primary neurons, cells begin to form a rudimentary scaffold of the neural network (Goodman and Shatz 1993), which is subsequently refined to strengthen some connections and pathways, while pruning others (Piochon, Kano et al. 2016, Millan, Torres et al. 2018). Within a few days, neurons start to exhibit a range of age-dependent electrophysiological activity – including primitive spikes, bursts and network wide synchronous activation – that dynamically changes as the network develops (Ben-Ari 2001, Opitz, De Lima et al. 2002, Chiappalone, Bove et al. 2006, Wagenaar, Pine et al. 2006), similar to *in vivo* neural networks (Ben-Ari 2001, Simao, Silva et al. 2018). This spontaneous electrophysiological activity directs network configuration towards a small-world topology (Poli, Pastore et al. 2015), enabling the network to follow similar communication efficiency rules as *in vivo* networks.

Together, these features make *in vitro* neural networks an attractive modelling approach to capture some fundamental aspects of self-organization and dynamic structural and functional behaviors of brain networks at a reductionist level. Most importantly, these model systems give us easy access to network mechanisms and allow us to selectively manipulate neural processes to induce perturbation, study neuropathology, and enable us to make better assumptions about grand and subtle changes in complex network dynamics.

3.2 Capturing neural network spontaneous activity using multi-electrode arrays

To fully capitalize on the advantages of *in vitro* neural network modelling, planar multi-electrode arrays (MEAs) systems are used to capture extracellular electrophysiological information about biological networks at high spatial and temporal resolutions (Jones, Livi et al. 2011). Neurons are seeded and grown directly on top of pre-coated glass substrates embedded with electrically independent metal micro electrodes. The microelectrodes in these devices detect fluctuations in the extracellular ionic concentration in their measurable vicinity upon the occurrence of an action potential (Jones, Livi et al. 2011).

Conventional MEAs provided a few tens of electrode sites (Pine 1980), however, new generations of high-density complementary metal-oxide semi-conductor (HD CMOS) arrays with thousands of electrodes covering a few square millimeters **(Figure 9)** provide the capacity to simultaneously record from several thousands of neurons (Berdondini, Overstolz et al. 2001, Malerba, Amin et al. 2018, Lonardoni, Amin et al. 2019, Miccoli, Lopez et al. 2019) with excellent signal to noise characteristics. This has significantly increased the spatiotemporal recording resolution and facilitated monitoring of dynamic changes in electrophysiological behavior. We can capture the rate of action potentials (spikes), groups of closely occurring spikes (bursts) (Wagenaar, Pine et al. 2006, Weir, Christiansen et al. 2023), signal propagation and avalanches (Beggs and Plenz 2003) in real-time and over long term (Potter and DeMarse 2001).

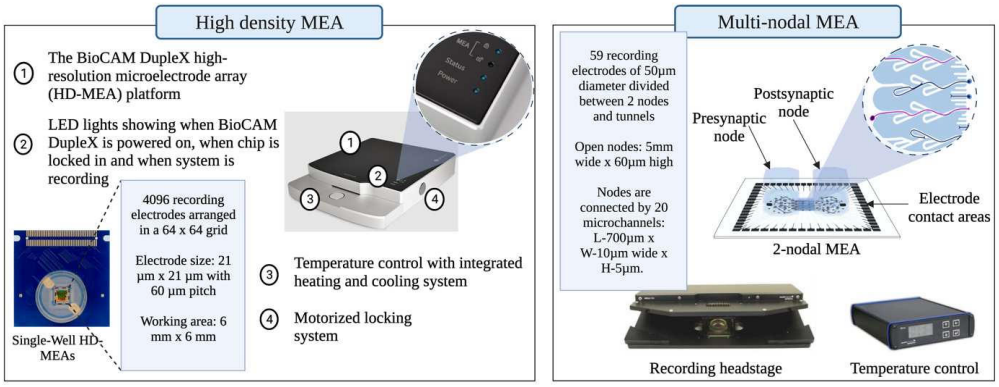

Figure 9. Schematic of MEAs and microfluidics for recording neural network activity. The HD MEAs and head-stage used in the studies were purchased from 3Brain AG, (Switzerland). The mMEAs were manufactured in house with custom developed protocols (van de Wijdeven, Ramstad et al. 2018) and designed to segregate neuron populations within different nodes. In the design used here, the presynaptic axons (red) enter the tunnels from the presynaptic node and exit in the post synaptic node. The postsynaptic axons (blue) are looped back, effectively preventing them from exiting in the presynaptic node (Winter-Hjelm, Tomren et al. 2022). *© Janelle S. Weir. Created in Biorender.com.*

While it is important to passively record the activity of neurons, certain aspects of neural network behavior such as learning and memory require external stimuli (Jones, Livi et al. 2011) in order to fully appreciate network dynamics. Thus, MEAs may have dual functionalities to both record activity and selectively deliver an electrical stimulus that can evoke response (Wagenaar, Pine et al. 2004, Wagenaar, Madhavan et al. 2005, Takayama and Kida 2016). However, despite their many advantages, limitations do also exist. For example, extracellular signal amplitudes tend to be small ~80–100 μV (Lonardoni, Amin et al. 2019), or may come from multiple cells within the recording vicinity rather than from a single neuron. This in turn may require high and low frequency filtering of the data, event detection, and spike sorting (Rey, Pedreira et al. 2015) to differentiate the activity of different neurons. Nevertheless, high density MEAs offer an unprecedented spatiotemporal resolution capable of capturing single cell or subcellular bioelectrical activity (Frey, Egert et al. 2009, Lonardoni, Amin et al. 2019), and thus provide solutions for these limitations.

A second type of device, the multi-nodal microfluidic interfaced with MEA (mMEA) **(Figure 9)**, has also emerged as useful tools for modelling hierarchical modular networks *in vitro* by segregating neural populations using microchannels only permissible by axons (Taylor, Rhee et al. 2003, Gladkov, Pigareva et al. 2017, van de Wijdeven, Ramstad et al. 2018, Winter-Hjelm, Tomren et al. 2022). These devices provide unique advantages to control afferent and efferent connections within neural networks, thereby recapitulating aspects of the modular topological organization found in the brain. mMEA platforms are necessary and powerful *in vitro* tools for acquiring a comprehensive view of healthy network development, as well as pathology and disease progression between different parts of the network. Application is widespread from being used for localized drug delivery (Bruno, Colistra et al. 2020), investigating the effects of pharmacologically active substances (Takayama, Ostuni et al. 2001, Peterman, Noolandi et al. 2004), to modelling neuropathy and neurodegeneration (Kunze, Meissner et al. 2011, Hallinan, Vargas-Caballero et al. 2019). Neural networks modelled on both MEAs and mMEAs, are also widely used to study small-world structural and functional connectivity, and communication efficiency in different contexts (Pastore, Massobrio et al. 2018, van de Wijdeven, Ramstad et al. 2018, Shen, Wu et al. 2019, van de Wijdeven, Ramstad et al. 2019).

3.3 Selective in vitro manipulation using adeno-associated viruses

As mentioned in previous paragraphs, to adequately study specific aspects of network behavior *in vitro*, some degree of external input or perturbation is required in addition to recording spontaneous activity. To target the specific mechanisms at the cellular and sub-cellular levels that drive neural activity and network behavior, the application of advanced and revolutionary methods is needed. While there are many viral and non-viral tools available for these purposes, in staying within the scope of this thesis, I will only discuss adeno-associated viruses (AAV).

AAV is a group of small, simple, helper dependent, non-pathogenic and single stranded DNA viruses (Wang and Gao 2014) used as a standard tool for the delivery of genes in classes of cells in neural systems (Betley and Sternson 2011). The distinct gene expression patterns of neuron types can be exploited to deliver genetically encoded molecular tools via their specific promoter regions, that can drive transgene expression in the corresponding genes (Betley and Sternson 2011, Wiebe, Huang et al. 2023). For neural network manipulation, transgenes that permit visualization and perturbation of neurons are ubiquitously used. The promoter and transgene of interest are packaged within the capsid of a serotype (Au, Isalan et al. 2022). Different AAV serotypes interact with cellular proteins in different ways, and thus the final transduction efficiency can vary significantly among them (Wu, Asokan et al. 2006). Therefore, rigorous testing of viral vectors is necessary to identify the most suitable variant. As AAV transduction in primary neurons *in vitro* has not been widely applied, labor intensive pilot tests and protocol optimization were conducted to establish the appropriate viral concentration for high transduction efficiency (Malik, Maronski et al. 2012) and minimal cytotoxic effects in our research.

3.3.1 AAV2/1 – hM4Di – mCherry – CaMKIIa – DREADDs

Designer Receptors Exclusively Activated by Designer Drugs (DREADDs) are engineered G-protein coupled receptors (GPCRs) based on human muscarinic (hM) acetylcholine receptors. In neurons, G-proteins couple to various downstream effectors to modulate second messengers and regulate neuronal excitability (Roth 2019). The perturbation objective in Papers I and II was to selectively inhibit excitatory signal transmission within networks, therefore, I used the human M4 receptor – which activates Gi-family protein inwardly rectifying potassium channels (GIRKs), thereby attenuating neuronal signal transmission (Urban and Roth 2015) **(Figure 10)**. AAV vectors were constructed with the excitatory cell type specific promoter calcium calmodulin dependent protein kinase II alpha (CaMKIIa). As CaMKIIa is selectively expressed at excitatory synapses on excitatory neurons (Liu and Murray 2012), this promoter ensured selective viral infectivity in excitatory neurons only. Human muscarinic DREADDs are also engineered to be physiologically inert to their endogenous ligand acetylcholine, have minimal basal activity and are only activated by a designer exogeneous ligand such as clozapine-N-oxide (CNO) (Stachniak, Ghosh et al. 2014), and more recently deschloroclozapine (DCZ) – which has a higher affinity to DREADDs and lower off target effects compared to CNO (Nagai, Miyakawa et al. 2020).

Several tests were conducted to deduce the optimal concentration of DCZ for *in vitro* use, onset of network response, length of exposure before cytotoxicity, and effects of repeated exposure. I found that 10uM was sufficient to induce silencing within 1 hour, however, higher concentrations resulted in cytotoxic cell death after 48 hours. I also noted that chronic DCZ exposure for > 4 hours resulted in faster network deterioration over time due to increased cell death. Thus, 10uM for 2 hours was the most effective exposure time to capture network changes while still preserving the integrity of the network for long-term monitoring (Paper II).

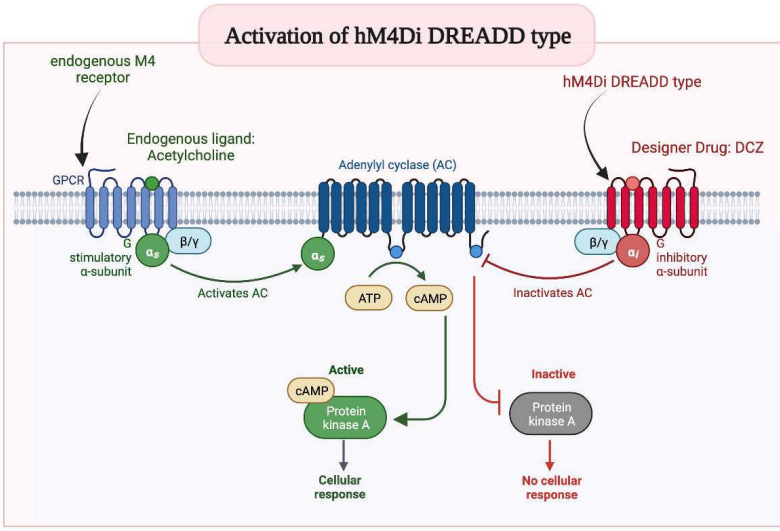

Figure 10. DREADDs in neural networks. The receptor is a genetically modified version of the muscarinic acetylcholine receptor. The receptor is inert to acetylcholine, and only becomes activated by a designer drug such as DCZ. This unique feature of DREADDs make it an invaluable tool for researchers to manipulate the activity of specific neurons. *© Janelle S. Weir. Created in Biorender.com.*

In Paper II, I wanted to cause more enduring structural and functional changes to the network, so 10uM for 2 hours repeated over 3 consecutive days was done instead of increasing the DCZ concentration or exposure time per application. This ensured that I could induce changes while preserving the health of the network for long term monitoring. One obvious limitation here is that this combination of DREADDs and DCZ, to our knowledge, has not been used in *in vitro* neural networks, and thus, saturation due to prolonged ligand binding has not been clearly evaluated.

3.3.2 AAV8 – GFP – 2a – P301LTau

For Paper III, a mutated form of human tau was used to induce perturbation in healthy 2-nodal *in vitro* neural networks with unidirectional, feedforward afferent – efferent connections (presynaptic and postsynaptic nodes respectively) **(Figure 9)**. The viral vector production and purification was performed in house at the Viral Vector Core Facility at the Kavli Institute for Systems Neuroscience (NTNU), and kindly gifted to us by Dr. Christiana Bjørkli. The human mutated tau was introduced to the healthy network in the presynaptic node **(Figure 9)** after the network had reached structural and electrophysiological maturity at 28 DIV. Rigorous tests were conducted to optimize the transduction efficiency and viral sequestering in the presynaptic node. This was achieved by maintaining a higher volume of media in the postsynaptic node, such that the valvular design of the mMEA axonal tunnels restricted backwards media flow and effectively created an impenetrable barrier (Forster, Bardell et al. 1995, Winter-Hjelm, Tomren et al. 2022).

4. Synopses of Papers: Methods

This section describes the key methodology involved in each of the papers that comprise this thesis. Detailed experimental method is described in each of the papers.

Paper I | Selective inhibition of excitatory synaptic transmission alters the emergent bursting dynamics of in vitro neural networks.

In Paper I, rat cortical neurons were seeded as co-cultures with 15% rat cortical astrocytes (both obtained from ThermoFisher) on AXION multiwell MEAs and maintained in a 5% CO_2 incubator at 37°C with regular media changes done every 2 – 3 days. At 7 DIV, networks were transduced using AAV2/1 vector encoding inhibitory hM4Di-CaMKIIa-DREADDs. Following transduction, hM4Di DREADDs expression was confirmed within 4 days by the mCherry fluorescent tag encoded in the vector that allowed for visualization early after transduction. Electrophysiological recordings of spontaneous network activity commenced on 9 DIV. At 14 DIV, transduced networks were treated with the designer synthetic ligand DCZ. The experimental protocol is illustrated in **Figure 11**. Briefly, 20 minutes baseline recordings were conducted for all networks, then then either PBS (vehicle) or DCZ (drug) diluted in cell media was added directly to the networks for a final concentration of 10 µM (at 14 DIV, 21 DIV and 28 DIV). The networks were incubated for 1, then, network activity was recorded for 1-hour with PBS or DCZ to capture network response to the perturbation. After this recording, 3 x 50% media changes were carried out to remove the PBS or DCZ from the networks before returning them to the incubator. Recordings were done at 12 hours and 24 hours after the wash out to assess network recovery. Control networks did not receive any treatment, so 1 x 100% media change was done to maintain similar conditions in media concentration. The bursting profile and network synchrony were analyzed offline using custom protocols.

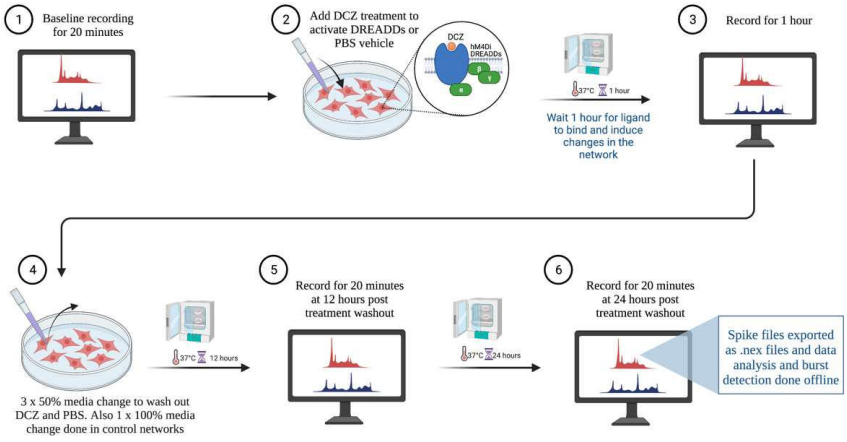

Figure 11. Schematic of the workflow. Figure from: (Weir, Christiansen et al. 2023).

Paper II |Selective inhibition of excitatory synaptic transmission alters functional organization and efficiency in cortical in vitro neural networks.

In Paper II, rat cortical neurons were seeded as co-cultures with 15% rat cortical astrocytes (both obtained from ThermoFisher) on high density CMOS MEAs and maintained in a 5% CO_2 incubator at 37°C with regular media changes done every 2 – 3 days. The networks were transduced at 7 DIV with AAV2/1-hM4Di-CaMKIIa-DREADDs using the protocol developed from Paper I. After transduction, DREADDs expression was confirmed using parallel immunocytochemistry to assess mCherry expression in the networks at 14 DIV. Electrophysiological recordings commenced on 14 DIV. At 25 DIV, the networks showed dense neurite interconnectivity based on assessments made by microscopy evaluations. They also exhibited robust and widespread bursts that originated at distinctive areas and propagated throughout the rest of the network. This behavior further supported that the network was highly interconnected. Baseline recordings of 15 minutes were made of all networks, then the experimental networks were treated with DCZ diluted in cell media at a final concentration of 10 µM and incubated for 2 hours. This concentration and time of exposure to DCZ was determined from previously optimized protocol for Paper I. After the incubation period, 3 x 50% media changes were done to wash out the DCZ and the networks were returned to the incubator to recover. This experimental protocol with DCZ inhibition was repeated for 3 days at 25, 26 and 27 DIV. Electrophysiological data to assess network recovery from acute perturbation was captured at 28, 32, 36, 40 and 42 DIV. Data analyses was conducted offline using custom protocols.

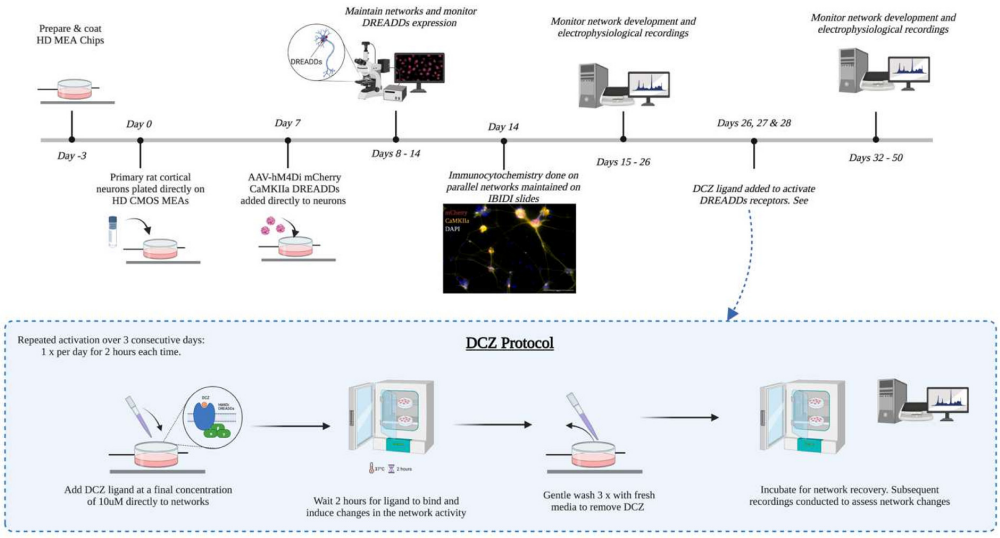

Figure 12. Schematic of experiment methods. Figure from: (Weir, Huse Ramstad et al. 2023).

Paper III | Altered structural organization and functional connectivity in feedforward neural networks after induced perturbation.

In Paper III, rat cortical neurons were seeded as co-cultures with 15% rat cortical astrocytes (both obtained from ThermoFisher) on unidirectional 2-nodal microfluidic chips interfaced with MEAs (created in-house at the Nanolab, NTNU). The networks were maintained in a 5% CO_2 incubator at 37°C with regular media changes done every other day. Electrophysiological recordings commenced on 14 DIV and 15 minutes recordings were done every other day until 28 DIV, at which point networks were determined to be both structurally and functionally mature. Structural maturity was confirmed at 21 DIV via microscopy assessment and parallel immunocytochemistry. AT 28 DIV, the networks were transduced using AAV8 vector encoding experimental GFP-2A-P301L tau protein to overexpress human mutated tau in the presynaptic network / node on the microfluidic chips. The titer for *in vitro* transduction was determined at 3 x 10^2 viral particles per neuron based on previous protocol tests. After transduction, mutated tau protein expression was confirmed within 2 days by the GFP fluorescent tag encoded in the vector that allowed for visualization early after transduction. Structural changes in the networks were monitored by microscopy visualization and imaging over the lifetime of the network. The network behavior was monitored after transduction by recording spontaneous electrophysiological activity every other day from 31 DIV until 47 DIV. Additionally, from 31 DIV, electrical stimulations of 800mV for 1 minute was applied at the most active electrode (detected during the spontaneous activity recording) and the evoked activity was captured. Network firing rate, bursting profile within each node, and signal propagation between nodes were analyzed offline in Matlab (R2021b) using adapted and custom scripts.

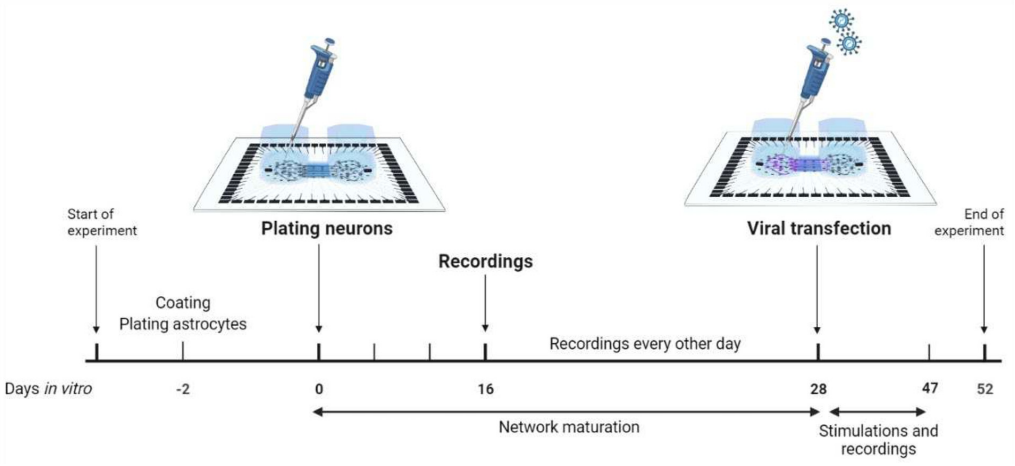

Figure 13. Timeline of experimental process. Figure from: (Weir, JS., Hanssen, K., et.al. 2023).

5. Synopses of Papers: Results

Paper I | Selective inhibition of excitatory synaptic transmission alters the emergent bursting dynamics of in vitro neural networks.

Janelle Shari Weir*, Nicholas Christiansen*, Axel Sandvig, Ioanna Sandvig
Published in Frontiers in Neural Circuits, February 2023, doi: 10.3389/fncir.2023.1020487
*Shared first authorship

The aim of this study was to investigate changes in neural network dynamics, i.e., network bursting behavior and synchrony, in response to selective inhibition of excitatory synaptic transmission using DREADDs. In this study, we conducted recordings of up to 2 hours each session over a period of 5 weeks. Our results demonstrated that all *in vitro* neural networks follow a trend of gradually increasing firing rate, burst rate and network burst rate as the network reach maturity between 28 DIV and 32 DIV, and gradual decline in synchrony between 9 DIV and 18 DIV. We also successfully transduced hM4Di-DREADDs in *in vitro* neural networks, induced transient silencing of network activity (at 14 DIV, 21 DIV and 28 DIV) using the novel ligand DCZ (for 2 hours), and recorded the network response both during and following wash out.

Our results showed that during perturbation, the inhibited networks exhibited significantly lower firing and burst activity compared to PBS treated and control unperturbed networks, which maintained robust spiking and bursting activity. We also demonstrated that inhibited networks were able to recover bursting activity within 1 hour of DCZ exposure. This activity was significantly higher than what was observed prior to inhibition. We also showed that in the PBS treated and control unperturbed networks, there was a general decline in network synchrony between 9 DIV and 28 DIV, however following DCZ treatment at 14 DIV, inhibited networks began exhibiting significant increases in overall network synchrony that lasted between 18 DIV and 32 DIV. Similarly, inhibited networks also exhibited significantly higher burstiness between 21 DIV and 28 DIV compared to PBS treated and control unperturbed networks. We also recorded network activity 12 hours and 24 hours after inhibition and found that across all 3 perturbation days, inhibited networks reduced the level of bursts and synchronization, indicating active adaptive mechanisms in the networks.

This study provides valuable insights into how the characteristics of network activity, particularly network bursts and synchrony, may change in response to selective inhibition of excitatory transmission; and how these dynamics change as the network adapt and restore normal dynamics.

Paper II | Selective inhibition of excitatory synaptic transmission alters functional organization and efficiency in cortical in vitro neural networks.

Janelle Shari Weir, Ola Huse Ramstad, Axel Sandvig, Ioanna Sandvig
Preprint, BioRxiv 2023, doi: https://doi.org/10.1101/2023.07.05.547785

As a follow up from Paper I, the aim of this study was to investigate network responses at the structural and functional organization level to transient disruption of excitatory synaptic transmission. Neural networks were transduced with hM4Di-DREADDs and we induced transient silencing of network activity using DCZ. Networks were silenced for 2 hours at 25 DIV, 26 DIV and 27 DIV, with wash out done after each treatment.

Our results showed that at 26 DIV and prior to inhibition, neural networks had self-organized into a modular topology on the CMOS MEAs, with each recording electrode signifying a single node belonging to a specific module. Following inhibition at 26 DIV, neural networks experienced transient disruption in segregated processing, which manifested as modular de-clustering, and decreases in clustering coefficient and participation coefficient. In addition, network integration capabilities appeared to decrease, indicated by a decline in the average number of connections that each node had with other nodes in the network. Furthermore, we found that perturbation also resulted in an increase in path lengths suggesting an overall less efficient network as signal transmission would traverse more edges.

Following perturbation and between 32 DIV and 40 DIV, we found that neural networks recovered the modular structure with nodes having higher spatial distance compared to being positioned closer together at 21 and 26 DIV. In addition, both mean degree and path lengths were restored by 40 DIV i.e., >300 connections on average, and <0.2 intermodular path length. This indicates that the networks reconfigured towards high integration of signals, with reduced path lengths to achieve higher efficiency.

The current findings of this paper compliment the findings of Paper I and suggest that the changes observed in structural and functional organization may be directly linked to changes in network bursting activity and network synchrony. De-clustering of modules allows for more flexible and efficient network communication in various contexts, including perturbation. This suggests that global activation increases as inhibited networks lose their structural boundaries, possibly to restore synaptic drive with and across the perturbed areas of the network. Induced inhibition may trigger compensatory increases in global synaptic transmission that would contribute to increased synchronization in the network. These findings contribute to our understanding of structural adaptability and the dynamic nature of neural network reorganization capacity following perturbation.

Paper III | Altered structural organization and functional connectivity in feedforward neural networks after induced perturbation.

Janelle Shari Weir*, Katrine Sjaastad Hanssen*, Axel Sandvig, Ioanna Sandvig
Preprint, BioRxiv, September 2023, doi: https://doi.org/10.1101/2023.09.12.557339
*Shared first authorship

The key aims of this study was to monitor and record dynamic changes in structural organization of neural connections, and electrophysiological activity in neural networks with evolving perturbation. We engineered neural networks as two-nodal unidirectional feedforward assemblies and selectively induced expression of human mutated tau in the presynaptic nodes at 28 DIV. Our results showed that prior to induced expression of human mutated tau, neural networks exhibited a diverse range of electrophysiological behavior including gradually increasing intranodal spikes, bursts, and network bursts between 16 DIV and 28 DIV. They had also achieved dense intranodal neurite connectivity, as well as both structural and functional internodal connectivity between the pre- and postsynaptic nodes. We found that electrical stimulation of one electrode in the presynaptic node elicited a spike response with a delay in the postsynaptic node, and that the networks exhibited spontaneous burst propagation between the nodes. These findings validated that our networks had achieved a feedforward functional connectivity mode with the presynaptic node providing input to the postsynaptic node.

Perturbation by induced human mutated tau protein to the presynaptic node resulted in extensive neurite retraction from the entry zone close to the microtunnels within 4 days, followed by subsequent neurite retraction from the exit zone close to the microtunnels in the postsynaptic node within a week. This indicates that the loss of synaptic input from the presynaptic node triggered intranodal reorganization within the postsynaptic node. No neurite retraction was observed in healthy control networks during the same observation period. Furthermore, induced perturbation also resulted in changes in intranodal electrophysiological activity, which manifested as an overall decrease in both firing rate and burst rate in the perturbed networks from 31 DIV onwards, contrary to increases observed in the control unperturbed networks during the same period. Also, during the same period there was an increase in both network burst size and synchrony in the perturbed networks, but not in the healthy control networks.

We also demonstrated that electrical stimulation within the presynaptic node of perturbed networks failed to elicit a spike response in the postsynaptic node between 31 and 47 DIV. There was no spike response to stimulation by 40 DIV in the perturbed presynaptic node. By contrast, in the healthy control networks, there were spike responses in the presynaptic node for all days of stimulation, with gradually lower responses over time in the postsynaptic nodes. Together, the findings of this study are highly significant as they highlight the concomitant occurrence of structural reorganization and functional activity changes in neural networks with ongoing perturbations. Most importantly, we've modelled and captured mechanisms that are challenging to detect using *in vivo* methods.

6 Discussion

"If future science reserves big surprises and wonderful conquests for us, it must be supposed that she will complete and develop our knowledge indefinitely, while still starting from the present facts".

Santiago Ramón y Cajal, Nobel Lecture – December 12, 1906

6.1 Emergence of electrophysiological activities in neural networks

Emergent self-organization is a fascinating phenomenon observed in biological systems, including neural networks *in vitro*. As stated in the introductory section, this is the ability of the system to spontaneously acquire high order organization through the interactions among lower-level components without any external input or control. In the brain, early network organization and neural network formation emerges through a well-orchestrated spatio-temporal manner that relies heavily on activity-independent processes in the absence of neurotransmission (Ohtaka-Maruyama 2020). Later, the network is shaped through sensory-evoked activity-dependent mechanisms. The transcription factors and growth molecules that guide and support the initial network formation are largely absent *in vitro*, and thus must be substituted via exogeneous sources (Hanssen, Witter et al. 2023) in order to recapitulate network developmental processes. Still, one could argue that the initial stages of *in vitro* network development is somewhat analogous to that of *in vivo* networks as both are characterized by immature neurite connections and very little spontaneous neural activity (Tierney and Nelson 2009, Luhmann and Khazipov 2018).

Only through the interconnectedness of neurons do we see the emergence of network level phenomena. This phenomenon is similar to how individual cells in the human body work together to perform complex tasks. Just as a single cell cannot carry out all the functions necessary for the body to operate, a single neuron cannot generate the complexity observed at the network level. Moreover, for neurons to avoid pruning and remain part of the functional network, it is crucial that they generate some bioelectrical activity and establish connections early. We already know that early spontaneous activity is a crucial part of the overall network development, but it also significantly reduces the probability of single neuron cell death, while also facilitating coordinated integration of immature neurons into the emerging network (Warm, Bassetti et al. 2022). The catalytic impact of early bioelectrical activity leads to the establishment of more evolved connection patterns via the formation of mesoscale motifs composed of neuron aggregates with improved synaptic strengths. These motifs also spontaneously generate activity among them, thus creating more complex topologies. High levels and complex patterns of innervation is associated with the interconnectivity of different motifs (Luo 2021), leading to the diverse spatial and temporal patterns of activation that includes bursts, network bursts and network synchronization (Wagenaar, Pine et al. 2006, Li, Zhou et al. 2007, Huang, Chang et al. 2017), that we observe in our *in vitro* neural network.

Our findings from Paper I and Paper III align with these previous studies by showing that neural networks begin to generate spontaneous activity shortly after seeding neurons, starting with low levels of activity during early development and gradually progressing to more robust patterns over the course of maturity. Interestingly, our results in Paper I prior to any perturbation also revealed a gradual decrease in synchrony between 9 DIV and 21 DIV, which persisted until approximately 21 DIV, with a slight increase at 32 DIV (Weir, Christiansen et al. 2023). Similarly, in Paper III prior to perturbation, we observed a decrease in synchrony between 16 DIV and 28 DIV, followed by a slight increase at 33 DIV, which then remained relatively stable until 47 DIV. These findings highlight a consistent decline in network synchrony during early development and before any perturbation, followed by a slight increase and stabilization after 32 DIV. This pattern stands in contrast to perturbed conditions, where significantly higher synchrony was evident within 36 to 48 hours of perturbation and persisted throughout the course of the study. This distinction is significant because it sheds light on the various conditions under which neural networks may exhibit synchronous activity.

One implication of these observations is that during early development, lower synchrony might be required for the selective strengthening of synapses for promoting diversity in postsynaptic resonance frequencies and enabling more complex processing later (Izhikevich, Desai et al. 2003). This notion aligns with studies in sensory systems, where information processing and performance (Beaman, Eagleman et al. 2017, Waschke, Tune et al. 2019) and the fidelity of novel information encoding (Hirata and Castro-Alamancos 2011, Pachitariu, Lyamzin et al. 2015) were improved in lower synchronous network states. Furthermore, synchrony appears to increase in more mature networks, potentially playing an integrative role in the processing of more complex information. Processes such as spike-timing dependent plasticity (STDP) for example, which are associated with more mature and intricate regulation of NMDAR and ion channels (Dan and Poo 2004), benefit from some level of synchrony (Anisimova, van Bommel et al. 2023). Thus, synchrony likely serves multiple specific functions in neural networks, which may be influenced by the developmental stage of the network and its specific goals. Intuitively, one might think that high synchrony in the early development would play a more salient role for the integration of immature neurons into the network, given its involvement in widespread correlated activation of multiple neurons. However, the observed decrease in synchrony alongside the dramatic increase in bursts in both Paper I and Paper III indicates that these dynamics serve distinct roles at different developmental stages, rather than merely representing different types of neuron or network activations.

Another noteworthy observation in these findings pertains to the relationship between electrophysiological activity and the structural – functional organization of the networks. This aspect is particularly interesting in the context of our results from Paper III, where we observed the progressive development of a feedforward network in the two-nodal unidirectional mMEAs. This was evident through the significant propagation of bursts from the presynaptic node, which provided input to the postsynaptic node. The evidence of burst propagation also indicated a corresponding increase in structural / synaptic maturity

since signal transmission relies on robust synaptic connections between different components of the neural network, with the activity itself reinforcing the strength of these connections. These findings provide compelling evidence for the dynamic and intricate connection between the structural properties of neural networks and their functional properties, underscoring the significant correlation between self-organization and emergence. However, it is important to reiterate that self-organization emphasizes the network's structure arising from the interactions among its components, whereas the concept of emergence emphasizes that higher-level properties or behaviors cannot be solely deduced or predicted from the properties of individual components or their interactions (Mainzer 2008). This crucial distinction is essential for understanding the behavior of biological neural networks, as it highlights the non-linearity of complex systems.

6.2 Embracing unpredictability: Unraveling non-linear dynamics of neural interactions

While there are certain aspects of neural network behavior that can be predicted – such as the age-dependent developmental trajectory of network activity described in previous paragraphs – the formation of motifs within each network can create unexpected patterns of activity at higher levels of organization. Though individual neurons may either depolarize or hyperpolarize in response to neurotransmission, their collective behavior is highly non-linear, which makes complex phenomena intrinsically unpredictable in character (Roberts and Robinson 2012, Yang, Solis-Escalante et al. 2016). The overall behavior of each network is then greatly influenced by factors such as the distinctive patterns of connectivity between excitatory and inhibitory neurons (Jang, Chung et al. 2020), the firing rates and timing of firing of individual neurons and the strength of connections between neurons. These factors combine to create complex spatiotemporal patterns of neural activity that underlie network function. Furthermore, nonlinearity is a prominent feature during learning, especially in the refinement of functional connectivity in motor skill learning. Researchers have established specific loop circuits between the frontoparietal cortices and the associative region of the Basal Ganglia (BG) and Cerebellum (CB), and the motor cortices with the motor region of the BG and CB that function in parallel (Hikosaka, Nakamura et al. 2002, Chen, Wang et al. 2022). Interestingly, Chen et. al. also found that activation patterns in these circuits may change depending on the stage of motor learning associated with skilled performance i.e., expert vs amateur vs novice (Chen, Wang et al. 2022). These dynamic interactions and diverse processing in motifs contribute to the emergence of higher-order cognitive functions and the brain's remarkable computational capabilities.

In a linear system, the output or behavior is typically directly proportional to the input. However, in the context of *in vitro* neural networks, the intricacy of the relationship between inputs and outputs stems from random, self-driven interactions within the network, leading to unpredictable behavior that go beyond the intrinsic characteristics of its constituents. The overall development and bottom-up process remains the same for all networks, but the underlying neural network structure does not adhere strictly to linear relationships. Unique local connectivity patterns exert significant influence on the inputs received by

different regions of the network. This observation provides valuable insights into the wide-ranging activity profiles exhibited by *in vitro* neural networks, even when they are maintained under comparable recording and microenvironmental contexts. It is essential to recognize that although *in vitro* neural networks serve as a reductionist model of brain networks, they still consist of tens of thousands of neurons that, to a large extent, retain much of the intrinsic programming rules governing network development *in vivo*. These rules encompass various aspects such as diversity in synapse development and modulation, and the formation of motifs and their interconnectedness. Consequently, these networks exhibit high level of complexity, similar to the brain where we can establish general principles of development and processing, while still allowing for individual variability. Therefore, it is not surprising that *in vitro* neural networks also exhibit inherent variability. This observation is commonly reported across studies when *in vitro* neural networks are recorded for extended timeframes and study periods (van Pelt, Wolters et al. 2004, Gal, Eytan et al. 2010). Variability is often apparent through differences in firing rates, burst frequency and size, and burst duration (van Pelt, Wolters et al. 2004) due to the non-linear interactions that regulate neuron sensitivity to different levels of input (Channell, Fuwape et al. 2009, Mensi, Hagens et al. 2016), or activity history based on the activity of neighboring neurons (Schiff, So et al. 1996).

Therefore, the onus is on researchers to devise suitable approaches for capturing network dynamics effectively, if any meaningful inferences are to be drawn regarding network function. As shown in Papers I and III, individual networks exhibit differing activity ranges, with varying firing rates and bursts rates at different days of recordings. Notably, by conducting recordings spanning up to 30 minutes each and monitoring networks over several weeks, we were able to identify significant trends in average activity notwithstanding variability. Moreover, the convergence of our findings with those of others who have also conducted longitudinal recordings (Habibey, Striebel et al. 2022) further strengthens the validity and reliability of our results. Consequently, we can confidently use these *in vitro* models to draw comparisons and establish general assumptions about neural network behavior.

6.3 All Hands-on Deck! Adaptability and resilience in the face of perturbation

Understanding that complex and dynamic behaviors arise from self-driven interactions between micro and mesoscale components within the network enables us to intervene in the system and study its responses. We also know that in nonlinear systems, small changes in initial conditions – such as variations in excitation or inhibition – can have significant impacts on neural network behavior (Roberts and Robinson 2012). Furthermore, the ability of neural networks to respond to perturbations is contingent on nonlinearity, which creates possibilities for adaptability and computational flexibility (He and Yang 2021). For instance, non-linear E-I interactions contribute to information processing by either amplifying or suppressing signals based on their relative strengths (Murphy-Baum and Taylor 2018, Kastner, Ozuysal et al. 2019). When this balance is disrupted, i.e., by transient inhibition of excitatory synaptic transmission as in Paper I, the dynamic adjustment of neural responses allows for optimal processing by appropriately

regulating the subsequent activity. This manifested in our networks as an increase in burstiness and synchrony, possibly related to decreased inhibitory drive due to modified pre and postsynaptic inhibitory responses (Maffei 2011, Rozov, Valiullina et al. 2017, Chiu, Barberis et al. 2019). Studies of sensory neurons in the retina yielded dramatic parallels where strong presynaptic inhibition decreased synaptic depression whilst concurrently increasing excitatory activity with low ISI (Sagdullaev, Eggers et al. 2011), so as to suggest the possibility of burst-like activity as was observed in our study.

These compensatory responses to perturbation signify active homeostatic plasticity processes playing a critical role in maintaining the stability and functionality of the networks. One key aspect is the scaling of synaptic physiology, which helps to regulate the strength of synaptic connections by ensuring that the overall activity levels remain within an optimal range, and prevents firing rates from becoming overly saturated or suppressed during environmental changes (Turrigiano, Leslie et al. 1998, Pozo and Goda 2010). The ability to regulate synaptic function also ensures that during periods of reduced neural activity the network will not reach extremes of hypo- excitability. In addition to adjusting synaptic function, there may also be an active process controlling the temporal patterning of neural activity, causing an increase in synchronization in response to perturbation. Our results from Papers I and III revealed an intriguing contrast in terms of synchronization trends. Perturbed networks displayed an increased synchrony following perturbation, while control networks exhibited decreased synchronization overtime. This observation was particularly interesting in Paper III, where the overall firing and burst rates of the perturbed network decreased over time, but not those of healthy controls. This suggested a direct correlation between the increase in synchrony and functional impairment within the networks. Specifically, because the heightened synchrony coincided with progressive neurite retractions and disconnected internodal connectivity. As mentioned in previous paragraphs, the presence of synchrony in the network and its impact on overall network function appear to be influenced by factors beyond the functional level alone, but also take into account the structural aspects of the network.

The relationship between network synchrony and structure is two-fold; first, synchronized activity co-evolve with network topology creating a feedback loop between structure and dynamics (Assenza, Gutiérrez et al. 2011). Second, the network's structural features can modulate synchronization levels as elements adjust input processing based on aggregate information available to them (Sorrentino and Ott 2008). Interconnected neurons receive inputs from many neighbors about the state of the network, and this collective information can guide decision-making and influence synchronization levels. For example, in Paper III, prolonged exposure to induced human mutated tau resulted in extensive axonal retraction from microtunnels and subsequent reorganization within nodes concomitantly with increased synchronization. This in conjunction with the overall low firing rates suggested a compensatory tactic by the perturbed networks to sustain inter-neuronal interactions and possibly functional integration. This theory is logical since hyperphosphorylated tau has the potential to interfere with the structural integrity of the affected network, subsequently leading to heightened neuron stress and inflammation, which in turn

can trigger apoptotic or neurotic call death (Dong, Yu et al. 2022, Thal and Tomé 2022). Therefore, if extensive neuron death contributed to the decrease in overall firing and bursts, then the network would need to increase synchrony in response low network levels to counteract potential hypoactivity (Chowdhury and Hell 2018). Also, in addition to improving information processing (Bernardo, Clara et al. 2011) and enhancing the signal-to-noise ratio of neural signals (Jang, Chung et al. 2020), increasing synchrony can enable networks to integrate information more easily (Buehlmann and Deco 2010, Li, Mi et al. 2018) by promoting mutual influence throughout the network. This means that by synchronizing activity, neurons in the perturbed networks can collectively process information in a more coherent and collaborative manner.

6.4 Never function without structure

It remains imperative to understand the interaction between structure, function, and the unpredictable dynamics created by nonlinearity in order to unravel the intrinsic adaptability of neural networks to respond to changes in their conditions. Combined, the findings from Papers I and II demonstrated that when neural networks are subjected to perturbation such as the interference with synaptic processes, the underlying structural features can change and influence the ability of the network to maintain its functional integrity. Robust structural network properties such as modular organization and distributed paths, can exhibit resilience by redistributing the information flow and adapting their functioning. This aligns with perturbation studies using external stimulation to show that neural networks can evolve towards new dynamic states by modifying their underlying connectivity (Poli, Pastore et al. 2015, Bloch, Greaves-Tunnell et al. 2022). In Paper II, networks responded to perturbation by transiently de-clustering modules and increasing the path lengths between them, which occurred within the same time frame as increased network bursting and synchronization (as presented in Paper I). These network changes are not random. Previous studies have demonstrated that de-clustering of specialized modules enables more efficient information transmission and increases network integration (Park and Friston 2013, Joanna Su Xian, Kwun Kei et al. 2019). Furthermore, this increase in efficiency and integration is also associated with increased synchrony (Buehlmann and Deco 2010, Palmigiano, Geisel et al. 2017, Li, Mi et al. 2018), further highlighting how structure and function are mutually reinforcing even in perturbation.

The interrelationship between structure and function is not solely limited to the network's ability to withstand perturbations. Adaptive processes such as plasticity mechanisms within the network, can be guided by the underlying structural properties to determine the network's capacity to recover and re-establish its functionality. For example, when the function of nodes or connections are disrupted, the structural features of the network can guide the rewiring of connections or the activation of latent pathways to restore functional connectivity. This may account for the connectivity changes observed, for example, after a stroke (Blaschke, Hensel et al. 2021) where functional recovery processes are often accompanied by an increase in path lengths (Park, Chang et al. 2011, Zhang, Zhang et al. 2017) and/or a decrease in

clustering (Wang, Yu et al. 2010); both phenomena have also been reported in Paper II. Based on topological considerations, this also implies a shift from small-worldness to random network organization in the brain (Wang, Yu et al. 2010) suggesting a less optimized reorganization involved in regaining function. It is important to note that in our *in vitro* neural networks, this less optimized topology was transient since the network was able to reconfigure by resuming modular organization and short paths. This could reflect the differences between the *in vitro* and the *in vivo* conditions where the latter are significantly larger systems, have more pathways, and are associated with more complex processing and behaviors. Other factors such as widespread inflammatory responses (Golia, Poggini et al. 2019, Lecca, Jung et al. 2022) can also make it harder for these neural plasticity mechanisms to mitigate functional impairment *in vivo*. Notwithstanding, the key takeaway is that adaptive response is intricately intertwined with the network's structural characteristics and flexibility which allows it to contingently reorganize to compensate for disturbances.

Finally, the topology of small-world complex networks with high clustering and hierarchical organization can have a profound impact on the spread of perturbations and their influence on overall network function. For one, network hubs which serve as the focal points for information exchange, enhance the potential for synchronization to emerge within the network (Senden, Deco et al. 2014, Schmidt, LaFleur et al. 2015, Kim, Harris et al. 2022). Their dense interconnectivity facilitates mutuality – where the flow of information among areas with direct connections influence each other – and can shape synchrony in the network (Wang and Chen 2002, Senden, Deco et al. 2014, Vlasov and Bifone 2017). This can have adverse ramifications for brain function, for example, driving certain neuropathology characterized by high synchrony such as epilepsy (Xin, Anastasia et al. 2021) and schizophrenia (de la Iglesia-Vaya, Escartí et al. 2014). Therefore, we must consider whether an increase in synchronization arises from adaptive mechanisms in the perturbed networks (as suggested by Papers I and II) or whether the network structure merely promoted the propagation of perturbation effects (implied by Paper III with concomitant synchrony increase and functional impairment).

To determine which explanation is more likely, further investigation and analyses are required. This may involve examining additional data, conducting more experiments with higher samples sizes, or employing computational models to simulate the network dynamics and observe how perturbations affect synchronization patterns. Understanding the origin of increased synchronization may be crucial, as it can inform interventions and therapeutic strategies towards restoring network function. If synchronization is found to be adaptive, it might be leveraged to promote recovery or enhance network resilience. On the other hand, if it is maladaptive, efforts can be directed towards mitigating or disrupting the synchronization to restore normal network functioning. The ultimate goal would be to gain a deeper understanding of the underlying mechanisms at play and distinguish between adaptive and maladaptive responses in perturbed networks.

Considerations and future directions

A multidisciplinary approach to studying complex network dynamics is challenging but holds great promise for advancing our understanding of the brain and its functions. Modelling neural networks *in vitro* offers a way to study and understand the inner working of neural networks without causing harm or violating ethical boundaries regarding the extent to which we can probe the network or alter structural and functional processes. This allows researchers with study certain isolated aspects of cellular and circuit behavior, without the constraints and potential risks associated with studying them directly *in vivo*. These advantages create a wide array of research questions that we can explored to fully comprehend various aspects of brain complexity.

Despite these incredible advantages, it is important to reiterate that *in vitro* neural networks only represent a small circuit of biological components, thereby being a reductionist approach to studying the brain. Widely used *in vitro* models lack insights into multicellular interactions, as other cell types such as oligodendrocytes, vascular cells, and immune cells with vital roles in brain function tend to be absent in such models. Nevertheless, neurons form intricate networks based on the intrinsic rules governing self-organization, synaptic plasticity and synaptic transmission thus making *in vitro* neural networks highly complex systems. Therefore, such models serve as valuable and robust complementary or alternative approaches to *in vivo* models. They provide a means to delve into the fundamental micro- and mesoscale interactions that underly complex phenomena at the macroscale level. Understanding these interactions is of paramount importance for gaining insights into the grander picture of neural functioning.

A promising outlook lies in the diligent focus on network data analysis. By developing robust tools and more standardized methods, researchers can attain a more comprehensive understanding of complex biological data (Milano, Agapito et al. 2022). This may necessitate the use of innovative algorithms and a sophisticated understanding of how complex systems operate. The key is to ensure that these methods build upon each other, so that we can capture nuances in neural activity, investigate more deeply, and extract more information about neural behavior in healthy and perturbed conditions (Guo, Sosa et al. 2022). Future research can also greatly benefit from a continued multidisciplinary approach that integrates theoretical modelling, empirical studies of biological networks, and computational simulations. This holistic approach enables the discovery of hidden patterns, relationships, and subtle correlations within neural data that may otherwise remain undetectable. This combined approach can accelerate progress in the development of predictive models capable of discerning dynamics associated with specific stimuli or behaviors and empower us to make accurate predictions about how neural networks might respond under varying conditions. The latter is important for our ability to understand and selectively engage neuroplasticity to promote functional recovery after perturbation and is of paramount importance for clinical translation of preclinical findings.

Conclusion

The field of network neuroscience offers complex and exciting opportunities to deepen our comprehension of the brain and its functionalities. By employing a meticulous and systematic approach to modelling biological neural networks, we can obtain invaluable insights into network emergent self-organization and devise novel strategies to enhance network functionality during and after perturbations. The enigmatic nature of self-organization, non-linear excitatory-inhibitory interactions, and their contributions to emergence in the brain pose significant obstacles to neuroscientists. Nevertheless, unravelling the intricacies of these complex dynamics stands as a pivotal task that can benefit greatly from the use of *in vitro* modelling and the exploration of complex micro-mesoscale interactions. Therefore, the goal of this PhD project was to characterize self-organizing and emergent properties of biological neural networks and elucidate complex micro-mesoscale network dynamics in healthy and perturbed conditions.

The key findings of my PhD project can be summarised as follows:

1. *In vitro* neural networks of dissociated cortical neurons exhibit highly intricate behaviors that adhere to the inherent programs of age-dependent network development and self-organization found in the brain.
2. Our protocols for monitoring and recording long timeframes of network electrophysiological activity over several weeks enabled us to capture subtle and ongoing changes in perturbed networks that would otherwise be difficult to observe *in vivo*.
3. Both increased synchronization (functional response) and de-clustering of modules (structural response) emerged as compensatory mechanisms to restore function in neural networks after selectively silencing excitatory synaptic transmission (Papers I and II). Both responses seemed to be self-reinforcing.
4. When mesoscale structural components (mutated tau affecting axons) were perturbed for a prolonged period, synchronization increased concomitantly with impaired function (bursts and propagation between nodes) and structure (axonal retraction) (Paper III).

Overall, these findings demonstrate that disrupting functional network dynamics affects structural dynamics and vice versa at different scales of network organization. It is therefore imperative to conduct further investigation into the underlying mechanisms of network response in these changing conditions to determine whether we can leverage them to aid functional recovery in damaged networks or treat neuropathological phenomena. These findings also provide meaningful insights into my research questions and meet the objectives outlined for this research project.

References:

Achard, S. and E. Bullmore (2007). "Efficiency and Cost of Economical Brain Functional Networks." PLOS Computational Biology **3**(2): e17.

Ackerman, S. (1992). Discovering the Brain. Washington (DC), National Academies Press (US)

Copyright © 1992 by the National Academy of Sciences.

Aebersold, M. J., G. Thompson-Steckel, A. Joutang, M. Schneider, C. Burchert, C. Forró, S. Weydert, H. Han and J. Vörös (2018). "Simple and Inexpensive Paper-Based Astrocyte Co-culture to Improve Survival of Low-Density Neuronal Networks." Front Neurosci **12**.

Alstott, J., P. Panzarasa, M. Rubinov, E. T. Bullmore and P. E. Vertes (2014). "A unifying framework for measuring weighted rich clubs." Sci Rep **4**: 7258.

Aman, Y. (2022). "Selective loss among dopaminergic neurons in Parkinson's disease." Nature Aging **2**(6): 462-462.

Amin, H., A. Maccione, F. Marinaro, S. Zordan, T. Nieus and L. Berdondini (2016). "Electrical Responses and Spontaneous Activity of Human iPS-Derived Neuronal Networks Characterized for 3-month Culture with 4096-Electrode Arrays." Front Neurosci **10**.

Angevine, J. B., Jr. (1965). "Time of neuron origin in the hippocampal region. An autoradiographic study in the mouse." Exp Neurol Suppl: Suppl 2:1-70.

Angevine, J. B. and R. L. Sidman (1961). "Autoradiographic Study of Cell Migration during Histogenesis of Cerebral Cortex in the Mouse." Nature **192**(4804): 766-768.

Anisimova, M., B. van Bommel, R. Wang, M. Mikhaylova, J. S. Wiegert, T. G. Oertner and C. E. Gee (2023). "Spike-timing-dependent plasticity rewards synchrony rather than causality." Cerebral Cortex **33**(1): 23-34.

Antonello, P. C., T. F. Varley, J. Beggs, M. Porcionatto, O. Sporns and J. Faber (2022). "Self-organization of in vitro neuronal assemblies drives to complex network topology." Elife **11**.

Antonini, A. and M. P. Stryker (1993). "Rapid remodeling of axonal arbors in the visual cortex." Science **260**(5115): 1819-1821.

Artola, A., T. Hensch and W. Singer (1996). "Calcium-induced long-term depression in the visual cortex of the rat in vitro." J Neurophysiol **76**(2): 984-994.

Artola, A. and W. Singer (1993). "Long-term depression of excitatory synaptic transmission and its relationship to long-term potentiation." Trends Neurosci **16**(11): 480-487.

Assenza, S., R. Gutiérrez, J. Gómez-Gardeñes, V. Latora and S. Boccaletti (2011). "Emergence of structural patterns out of synchronization in networks with competitive interactions." Sci Rep **1**: 99.

Au, H. K. E., M. Isalan and M. Mielcarek (2022). "Gene Therapy Advances: A Meta-Analysis of AAV Usage in Clinical Settings." Frontiers in Medicine **8**.

Avena-Koenigsberger, A., X. Yan, A. Kolchinsky, M. P. van den Heuvel, P. Hagmann and O. Sporns (2019). "A spectrum of routing strategies for brain networks." PLoS Comput Biol **15**(3): e1006833.

Baltaci, S. B., R. Mogulkoc and A. K. Baltaci (2019). "Molecular Mechanisms of Early and Late LTP." Neurochem Res **44**(2): 281-296.

Bassett, D. S. and O. Sporns (2017). "Network neuroscience." Nat Neurosci **20**(3): 353-364.

Beaman, C. B., S. L. Eagleman and V. Dragoi (2017). "Sensory coding accuracy and perceptual performance are improved during the desynchronized cortical state." Nat Commun **8**(1): 1308.

Bear, M. F. and R. C. Malenka (1994). "Synaptic plasticity: LTP and LTD." Curr Opin Neurobiol **4**(3): 389-399.

Beggs, J. M. and D. Plenz (2003). "Neuronal avalanches in neocortical circuits." J Neurosci **23**(35): 11167-11177.

Ben-Ari, Y. (2001). "Developing networks play a similar melody." Trends Neurosci **24**(6): 353-360.

Ben-Ari, Y. (2002). "Excitatory actions of gaba during development: the nature of the nurture." Nat Rev Neurosci **3**(9): 728-739.

Benkarim, O., C. Paquola, B.-y. Park, S.-J. Hong, J. Royer, R. Vos de Wael, S. Lariviere, S. Valk, D. Bzdok, L. Mottron and B. C. Bernhardt (2021). "Connectivity alterations in autism reflect functional idiosyncrasy." Communications Biology **4**(1): 1078.

Berdondini, L., T. Overstolz, N. F. d. Rooij, M. Koudelka-Hep, M. Wany and P. Seitz (2001). High-density microelectrode arrays for electrophysiological activity imaging of neuronal networks. ICECS 2001. 8th IEEE International Conference on Electronics, Circuits and Systems (Cat. No.01EX483).

Berlot, R., C. Metzler-Baddeley, M. A. Ikram, D. K. Jones and M. J. O'Sullivan (2016). "Global Efficiency of Structural Networks Mediates Cognitive Control in Mild Cognitive Impairment." Frontiers in Aging Neuroscience **8**.

Bernardo, P., M. Clara, L. Eric Carl, K. Svetlana, L. Simona, O. Marco, R. Alessandro Di, T. Giulio and M. F. Ghilardi (2011). "Modulation of Gamma and Theta Spectral Amplitude and Phase Synchronization Is Associated with the Development of Visuo-Motor Learning." The Journal of Neuroscience **31**(41): 14810.

Berry, M. and A. W. Rogers (1965). "The migration of neuroblasts in the developing cerebral cortex." J Anat **99**(Pt 4): 691-709.

Bertolero, M. A., B. T. Yeo and M. D'Esposito (2015). "The modular and integrative functional architecture of the human brain." Proc Natl Acad Sci U S A **112**(49): E6798-6807.

Betley, J. N. and S. M. Sternson (2011). "Adeno-Associated Viral Vectors for Mapping, Monitoring, and Manipulating Neural Circuits." Human Gene Therapy **22**(6): 669-677.

Bettencourt, L. M., G. J. Stephens, M. I. Ham and G. W. Gross (2007). "Functional structure of cortical neuronal networks grown in vitro." Phys Rev E Stat Nonlin Soft Matter Phys **75**(2 Pt 1): 021915.

Blaschke, S. J., L. Hensel, A. Minassian, S. Vlachakis, C. Tscherpel, S. U. Vay, M. Rabenstein, M. Schroeter, G. R. Fink, M. Hoehn, C. Grefkes and M. A. Rueger (2021). "Translating Functional Connectivity After Stroke: Functional Magnetic Resonance Imaging Detects Comparable Network Changes in Mice and Humans." Stroke **52**(9): 2948-2960.

Bliss, T. V. and T. Lomo (1973). "Long-lasting potentiation of synaptic transmission in the dentate area of the anaesthetized rabbit following stimulation of the perforant path." J Physiol **232**(2): 331-356.

Bloch, J., A. Greaves-Tunnell, E. Shea-Brown, Z. Harchaoui, A. Shojaie and A. Yazdan-Shahmorad (2022). "Network structure mediates functional reorganization induced by optogenetic stimulation of non-human primate sensorimotor cortex." iScience **25**(5): 104285.

Boccaletti, S., V. Latora, Y. Moreno, M. Chavez and D. U. Hwang (2006). "Complex networks: Structure and dynamics." Physics Reports **424**(4): 175-308.

Bolhuis, J. J. and R. C. Honey (1998). "Imprinting, learning and development: from behaviour to brain and back." Trends in Neurosciences **21**(7): 306-311.

Booker, S. A. and I. Vida (2018). "Morphological diversity and connectivity of hippocampal interneurons." Cell Tissue Res **373**(3): 619-641.

Braitenburg, V. and A. Shuz (1998). Cortex: statistics and geometry of neuronal connectivity. New York, Springer.

Bruno, G., N. Colistra, G. Melle, A. Cerea, A. Hubarevich, L. Deleye, F. De Angelis and M. Dipalo (2020). "Microfluidic Multielectrode Arrays for Spatially Localized Drug Delivery and Electrical Recordings of Primary Neuronal Cultures." Front Bioeng Biotechnol **8**: 626.

Buehlmann, A. and G. Deco (2010). "Optimal Information Transfer in the Cortex through Synchronization." PLOS Computational Biology **6**(9): e1000934.

Bullmore, E. and O. Sporns (2009). "Complex brain networks: graph theoretical analysis of structural and functional systems." Nat Rev Neurosci **10**(3): 186-198.

Bullmore, E. and O. Sporns (2012). "The economy of brain network organization." Nat Rev Neurosci **13**(5): 336-349.

Bullmore, E. T. and D. S. Bassett (2011). "Brain graphs: graphical models of the human brain connectome." Annu Rev Clin Psychol **7**: 113-140.

Buzsáki, G., C. Geisler, D. A. Henze and X.-J. Wang (2004). "Interneuron Diversity series: Circuit complexity and axon wiring economy of cortical interneurons." Trends in Neurosciences **27**(4): 186-193.

Bystron, I., C. Blakemore and P. Rakic (2008). "Development of the human cerebral cortex: Boulder Committee revisited." Nature Reviews Neuroscience **9**(2): 110-122.

Channell, P., I. Fuwape, A. B. Neiman and A. L. Shilnikov (2009). "Variability of bursting patterns in a neuron model in the presence of noise." J Comput Neurosci **27**(3): 527-542.

Chen, B. L., D. H. Hall and D. B. Chklovskii (2006). "Wiring optimization can relate neuronal structure and function." Proceedings of the National Academy of Sciences of the United States of America **103**(12): 4723-4728.

Chen, T. T., K. P. Wang, C. J. Huang and T. M. Hung (2022). "Nonlinear refinement of functional brain connectivity in golf players of different skill levels." Sci Rep **12**(1): 2365.

Chiappalone, M., M. Bove, A. Vato, M. Tedesco and S. Martinoia (2006). "Dissociated cortical networks show spontaneously correlated activity patterns during in vitro development." Brain Res **1093**(1): 41-53.

Chiu, C. Q., A. Barberis and M. J. Higley (2019). "Preserving the balance: diverse forms of long-term GABAergic synaptic plasticity." Nat Rev Neurosci **20**(5): 272-281.

Chowdhury, D. and J. W. Hell (2018). "Homeostatic synaptic scaling: molecular regulators of synaptic AMPA-type glutamate receptors." F1000Res **7**: 234.

Cohen, J. R. and M. D'Esposito (2016). "The Segregation and Integration of Distinct Brain Networks and Their Relationship to Cognition." J Neurosci **36**(48): 12083-12094.

Collingridge, G. L., S. Peineau, J. G. Howland and Y. T. Wang (2010). "Long-term depression in the CNS." Nat Rev Neurosci **11**(7): 459-473.

Crossley, N. A., A. Mechelli, J. Scott, F. Carletti, P. T. Fox, P. McGuire and E. T. Bullmore (2014). "The hubs of the human connectome are generally implicated in the anatomy of brain disorders." Brain **137**(Pt 8): 2382-2395.

Dan, Y. and M.-m. Poo (2004). "Spike Timing-Dependent Plasticity of Neural Circuits." Neuron **44**(1): 23-30.

Dancause, N., S. Barbay, S. B. Frost, E. J. Plautz, D. Chen, E. V. Zoubina, A. M. Stowe and R. J. Nudo (2005). "Extensive cortical rewiring after brain injury." J Neurosci **25**(44): 10167-10179.

de Haan, W., K. Mott, E. C. van Straaten, P. Scheltens and C. J. Stam (2012). "Activity dependent degeneration explains hub vulnerability in Alzheimer's disease." PLoS Comput Biol **8**(8): e1002582.

de la Iglesia-Vaya, M., M. J. Escartí, J. Molina-Mateo, L. Martí-Bonmatí, M. Gadea, F. X. Castellanos, E. J. Aguilar García-Iturrospe, M. Robles, B. B. Biswal and J. Sanjuan (2014). "Abnormal synchrony and effective connectivity in patients with schizophrenia and auditory hallucinations." NeuroImage: Clinical **6**: 171-179.

de Lange, S. C., D. J. Ardesch and M. P. van den Heuvel (2019). "Connection strength of the macaque connectome augments topological and functional network attributes." Netw Neurosci **3**(4): 1051-1069.

de Reus, M. A. and M. P. van den Heuvel (2014). "Simulated rich club lesioning in brain networks: a scaffold for communication and integration?" Front Hum Neurosci **8**: 647.

De Vico Fallani, F., F. A. Rodrigues, L. da Fontoura Costa, L. Astolfi, F. Cincotti, D. Mattia, S. Salinari and F. Babiloni (2011). "Multiple pathways analysis of brain functional networks from EEG signals: an application to real data." Brain Topogr **23**(4): 344-354.

DeFelipe, J., L. Alonso-Nanclares and J. I. Arellano (2002). "Microstructure of the neocortex: comparative aspects." J Neurocytol **31**(3-5): 299-316.

Di Lanzo, C., L. Marzetti, F. Zappasodi, F. De Vico Fallani and V. Pizzella (2012). "Redundancy as a graph-based index of frequency specific MEG functional connectivity." Comput Math Methods Med **2012**: 207305.

Dong, Y., H. Yu, X. Li, K. Bian, Y. Zheng, M. Dai, X. Feng, Y. Sun, Y. He, B. Yu, H. Zhang, J. Wu, X. Yu, H. Wu and W. Kong (2022). "Hyperphosphorylated tau mediates neuronal death by inducing necroptosis and inflammation in Alzheimer's disease." Journal of Neuroinflammation **19**(1): 205.

Doupe, A. J. and M. M. Solis (1997). "Song- and order-selective neurons develop in the songbird anterior forebrain during vocal learning." J Neurobiol **33**(5): 694-709.

Downes, J. H., M. W. Hammond, D. Xydas, M. C. Spencer, V. M. Becerra, K. Warwick, B. J. Whalley and S. J. Nasuto (2012). "Emergence of a Small-World Functional Network in Cultured Neurons." Plos Computational Biology **8**(5).

Dresp-Langley, B. (2020). "Seven properties of self-organization in the human brain." Big Data and Cognitive Computing **4**(2): 10.

Egorov, A. V. and A. Draguhn (2013). "Development of coherent neuronal activity patterns in mammalian cortical networks: Common principles and local hetereogeneity." Mechanisms of Development **130**(6): 412-423.

Érdi, P. and G. Barna (1984). "Self-organizing mechanism for the formation of ordered neural mappings." Biological Cybernetics **51**(2): 93-101.

Faber, J., P. C. Antoneli, G. Via, N. S. Araújo, D. J. L. L. Pinheiro and E. Cavalheiro (2019). Critical elements for connectivity analysis of brain networks.

Faber, S. P., N. M. Timme, J. M. Beggs and E. L. Newman (2019). "Computation is concentrated in rich clubs of local cortical networks." Netw Neurosci **3**(2): 384-404.

Fauth, M. and C. Tetzlaff (2016). "Opposing Effects of Neuronal Activity on Structural Plasticity." Front Neuroanat **10**: 75.

Fauth, M. J. and M. C. van Rossum (2019). "Self-organized reactivation maintains and reinforces memories despite synaptic turnover." Elife **8**.

Fiskum, V., A. Sandvig and I. Sandvig (2021). "Silencing of Activity During Hypoxia Improves Functional Outcomes in Motor Neuron Networks in vitro." Frontiers in Integrative Neuroscience **15**.

Forster, F. K., R. L. Bardell, M. A. Afromowitz, N. R. Sharma and A. P. Blanchard (1995). DESIGN, FABRICATION AND TESTING OF FIXED-VALVE MICRO-PUMPS.

Frey, U., U. Egert, F. Heer, S. Hafizovic and A. Hierlemann (2009). "Microelectronic system for high-resolution mapping of extracellular electric fields applied to brain slices." Biosensors and Bioelectronics **24**(7): 2191-2198.

Fries, P., J. H. Reynolds, A. E. Rorie and R. Desimone (2001). "Modulation of oscillatory neuronal synchronization by selective visual attention." Science **291**(5508): 1560-1563.

Gal, A., D. Eytan, A. Wallach, M. Sandler, J. Schiller and S. Marom (2010). "Dynamics of excitability over extended timescales in cultured cortical neurons." J Neurosci **30**(48): 16332-16342.

Gamlin, C. R., C. Zhang, M. A. Dyer and R. O. L. Wong (2020). "Distinct Developmental Mechanisms Act Independently to Shape Biased Synaptic Divergence from an Inhibitory Neuron." Curr Biol **30**(7): 1258-1268.e1252.

Garey, L. J. (1999). The basic laminar pattern of the cerebral cortex. Brodmann's 'Localisation in the Cerebral Cortex'. L. J. Garey. Imperial College**:** 13-36.

Gatto, R. (2020). "Molecular and microstructural biomarkers of neuroplasticity in neurodegenerative disorders through preclinical and diffusion magnetic resonance imaging studies." Journal of Integrative Neuroscience **19**: 571-592.

Gazzaniga, M. S. (2010). "Neuroscience and the correct level of explanation for understanding mind. An extraterrestrial roams through some neuroscience laboratories and concludes earthlings are not grasping how best to understand the mind-brain interface." Trends Cogn Sci **14**(7): 291-292.

Giguère, N., S. Burke Nanni and L.-E. Trudeau (2018). "On Cell Loss and Selective Vulnerability of Neuronal Populations in Parkinson's Disease." Frontiers in Neurology **9**.

Gilson, M., A. N. Burkitt, D. B. Grayden, D. A. Thomas and J. L. van Hemmen (2009). "Emergence of network structure due to spike-timing-dependent plasticity in recurrent neuronal networks. I. Input selectivity–strengthening correlated input pathways." Biological Cybernetics **101**(2): 81-102.

Gladkov, A., Y. Pigareva, D. Kutyina, V. Kolpakov, A. Bukatin, I. Mukhina, V. Kazantsev and A. Pimashkin (2017). "Design of Cultured Neuron Networks in vitro with Predefined Connectivity Using Asymmetric Microfluidic Channels." Sci Rep **7**(1): 15625.

Golia, M. T., S. Poggini, S. Alboni, S. Garofalo, N. Ciano Albanese, A. Viglione, M. A. Ajmone-Cat, A. St-Pierre, N. Brunello, C. Limatola, I. Branchi and L. Maggi (2019). "Interplay between inflammation and neural plasticity: Both immune activation and suppression impair LTP and BDNF expression." Brain Behav Immun **81**: 484-494.

Goodman, C. S. and C. J. Shatz (1993). "Developmental Mechanisms That Generate Precise Patterns of Neuronal Connectivity." Cell **72**: 77-98.

Gordon, E. M., C. J. Lynch, C. Gratton, T. O. Laumann, A. W. Gilmore, D. J. Greene, M. Ortega, A. L. Nguyen, B. L. Schlaggar, S. E. Petersen, N. U. F. Dosenbach and S. M. Nelson (2018). "Three Distinct Sets of Connector Hubs Integrate Human Brain Function." Cell Reports **24**(7): 1687-1695.e1684.

Graf, J., V. Rahmati, M. Majoros, O. W. Witte, C. Geis, S. J. Kiebel, K. Holthoff and K. Kirmse (2022). "Network instability dynamics drive a transient bursting period in the developing hippocampus in vivo." Elife **11**.

Gray, C. M., P. König, A. K. Engel and W. Singer (1989). "Oscillatory responses in cat visual cortex exhibit inter-columnar synchronization which reflects global stimulus properties." Nature **338**(6213): 334-337.

Guo, M. G., D. N. Sosa and R. B. Altman (2022). "Challenges and opportunities in network-based solutions for biological questions." Briefings in Bioinformatics **23**(1): bbab437.

Habibey, R., J. Striebel, F. Schmieder, J. Czarske and V. Busskamp (2022). "Long-term morphological and functional dynamics of human stem cell-derived neuronal networks on high-density micro-electrode arrays." Frontiers in Neuroscience **16**.

Hagmann, P., L. Cammoun, X. Gigandet, R. Meuli, C. J. Honey, V. J. Wedeen and O. Sporns (2008). "Mapping the structural core of human cerebral cortex." PLoS Biol **6**(7): e159.

Hallinan, G. I., M. Vargas-Caballero, J. West and K. Deinhardt (2019). "Tau Misfolding Efficiently Propagates between Individual Intact Hippocampal Neurons." The Journal of Neuroscience **39**(48): 9623.

Hanssen, K. S., M. P. Witter, A. Sandvig, I. Sandvig and A. Kobro-Flatmoen (2023). "Dissection and culturing of adult lateral entorhinal cortex layer II neurons from APP/PS1 Alzheimer model mice." Journal of Neuroscience Methods **390**: 109840.

Harrell, E. R., D. Pimentel and G. Miesenböck (2021). "Changes in Presynaptic Gene Expression during Homeostatic Compensation at a Central Synapse." J Neurosci **41**(14): 3054-3067.

He, F. and Y. Yang (2021). "Nonlinear System Identification of Neural Systems from Neurophysiological Signals." Neuroscience **458**: 213-228.

Hebb, D. (1949). The Organization of Behavior, McGill University, John Wiley & Sons, New York, USA.

Hebb, D. O. (1949). The Organization of behaviour: A Neurosychologycal Approach. , John Wiley & Sons.

Henderson, J. A. and P. Gong (2018). Functional mechanisms underlie the emergence of a diverse range of plasticity phenomena. PLoS Comput Biol. **14**.

Hikosaka, O., K. Nakamura, K. Sakai and H. Nakahara (2002). "Central mechanisms of motor skill learning." Curr Opin Neurobiol **12**(2): 217-222.

Hilger, K., M. Ekman, C. J. Fiebach and U. Basten (2017). "Efficient hubs in the intelligent brain: Nodal efficiency of hub regions in the salience network is associated with general intelligence." Intelligence **60**: 10-25.

Hilgetag, C. C., G. A. Burns, M. A. O'Neill, J. W. Scannell and M. P. Young (2000). "Anatomical connectivity defines the organization of clusters of cortical areas in the macaque monkey and the cat." Philos Trans R Soc Lond B Biol Sci **355**(1393): 91-110.

Hilgetag, C. C. and A. Goulas (2020). "'Hierarchy' in the organization of brain networks." Philos Trans R Soc Lond B Biol Sci **375**(1796): 20190319.

Hinzman, J. M., J. A. Wilson, A. T. Mazzeo, M. R. Bullock and J. A. Hartings (2016). "Excitotoxicity and Metabolic Crisis Are Associated with Spreading Depolarizations in Severe Traumatic Brain Injury Patients." J Neurotrauma **33**(19): 1775-1783.

Hirabayashi, Y., Y. Itoh, H. Tabata, K. Nakajima, T. Akiyama, N. Masuyama and Y. Gotoh (2004). "The Wnt/beta-catenin pathway directs neuronal differentiation of cortical neural precursor cells." Development **131**(12): 2791-2801.

Hirata, A. and M. A. Castro-Alamancos (2011). "Effects of cortical activation on sensory responses in barrel cortex." J Neurophysiol **105**(4): 1495-1505.

Holtmaat, A. and K. Svoboda (2009). "Experience-dependent structural synaptic plasticity in the mammalian brain." Nature Reviews Neuroscience **10**(9): 647-658.

Honey, C. J. and O. Sporns (2008). "Dynamical consequences of lesions in cortical networks." Human Brain Mapping **29**(7): 802-809.

Honey, C. J., J. P. Thivierge and O. Sporns (2010). "Can structure predict function in the human brain?" Neuroimage **52**(3): 766-776.

Huang, Y., B. Hajnal, L. Entz, D. Fabó, J. L. Herrero, A. D. Mehta and C. J. Keller (2019). "Intracortical Dynamics Underlying Repetitive Stimulation Predicts Changes in Network Connectivity." J Neurosci **39**(31): 6122-6135.

Huang, Y. T., Y. L. Chang, C. C. Chen, P. Y. Lai and C. K. Chan (2017). "Positive feedback and synchronized bursts in neuronal cultures." PLoS One **12**(11): e0187276.

Hubel, D. H. and T. N. Wiesel (1962). "Receptive fields, binocular interaction and functional architecture in the cat's visual cortex." J Physiol **160**(1): 106-154.

Hubel, D. H., T. N. Wiesel and S. LeVay (1977). "Plasticity of ocular dominance columns in monkey striate cortex." Philos Trans R Soc Lond B Biol Sci **278**(961): 377-409.

Izhikevich, E. M., N. S. Desai, E. C. Walcott and F. C. Hoppensteadt (2003). "Bursts as a unit of neural information: selective communication via resonance." Trends Neurosci **26**(3): 161-167.

Jackman, S. L. and W. G. Regehr (2017). "The Mechanisms and Functions of Synaptic Facilitation." Neuron **94**(3): 447-464.

Jackson, A., V. J. Gee, S. N. Baker and R. N. Lemon (2003). "Synchrony between neurons with similar muscle fields in monkey motor cortex." Neuron **38**(1): 115-125.

Jahan, I., K. L. Elliott and B. Fritzsch (2018). "Understanding Molecular Evolution and Development of the Organ of Corti Can Provide Clues for Hearing Restoration." Integrative and Comparative Biology **58**(2): 351-365.

Jahan, I., N. Pan, K. L. Elliott and B. Fritzsch (2015). "The quest for restoring hearing: Understanding ear development more completely." Bioessays **37**(9): 1016-1027.

Jang, H. J., H. Chung, J. M. Rowland, B. A. Richards, M. M. Kohl and J. Kwag (2020). "Distinct roles of parvalbumin and somatostatin interneurons in gating the synchronization of spike times in the neocortex." Science Advances **6**(17): eaay5333.

Janowsky, J. S., A. P. Shimamura, M. Kritchevsky and L. R. Squire (1989). "Cognitive impairment following frontal lobe damage and its relevance to human amnesia." Behav Neurosci **103**(3): 548-560.

Jiang, X., G. Wang, A. J. Lee, R. L. Stornetta and J. J. Zhu (2013). "The organization of two new cortical interneuronal circuits." Nat Neurosci **16**(2): 210-218.

Joanna Su Xian, C., N. Kwun Kei, T. Jesisca, W. Chenhao, P. Jia-Hou, C. L. June, W. L. C. Michael and Z. Juan Helen (2019). "Longitudinal Changes in the Cerebral Cortex Functional Organization of Healthy Elderly." The Journal of Neuroscience **39**(28): 5534.

Johann, M. P., H.-L. Ashlyn, S. Claire, J. M. Carissa, E. M. Kathryn, J. P. Natalie, Z. Haikun, C. W. Shuttleworth and A. M. Russell (2019). "Spreading Depolarizations Occur in Mild Traumatic Brain Injuries and Are Associated with Postinjury Behavior." eneuro **6**(6): ENEURO.0070-0019.2019.

John, E. R. (1980). Multipotentiality: A Statistical Theory of Brain Function—Evidence and Implications. The Psychobiology of Consciousness. J. M. Davidson and R. J. Davidson. Boston, MA, Springer US**:** 129-146.

Jones, I. L., P. Livi, M. K. Lewandowska, M. Fiscella, B. Roscic and A. Hierlemann (2011). "The potential of microelectrode arrays and microelectronics for biomedical research and diagnostics." Analytical and Bioanalytical Chemistry **399**(7): 2313-2329.

Kaiser, M. and C. Hilgetag (2010). "Optimal hierarchical modular topologies for producing limited sustained activation of neural networks." Frontiers in Neuroinformatics **4**.

Kaiser, M. and C. C. Hilgetag (2004). "Edge vulnerability in neural and metabolic networks." Biological Cybernetics **90**(5): 311-317.

Kambi, N., P. Halder, R. Rajan, V. Arora, P. Chand, M. Arora and N. Jain (2014). "Large-scale reorganization of the somatosensory cortex following spinal cord injuries is due to brainstem plasticity." Nature Communications **5**(1): 3602.

Karsenti, E. (2008). "Self-organization in cell biology: a brief history." Nat Rev Mol Cell Biol **9**(3): 255-262.

Kastner, D. B., Y. Ozuysal, G. Panagiotakos and S. A. Baccus (2019). "Adaptation of Inhibition Mediates Retinal Sensitization." Curr Biol **29**(16): 2640-2651.e2644.

Katz, L. C. and C. J. Shatz (1996). "Synaptic activity and the construction of cortical circuits." Science **274**(5290): 1133-1138.

Kavalali, E. T. and L. M. Monteggia (2023). "Rapid homeostatic plasticity and neuropsychiatric therapeutics." Neuropsychopharmacology **48**(1): 54-60.

Khazipov, R. and H. J. Luhmann (2006). "Early patterns of electrical activity in the developing cerebral cortex of humans and rodents." Trends Neurosci **29**(7): 414-418.

Khazipov, R., A. Sirota, X. Leinekugel, G. L. Holmes, Y. Ben-Ari and G. Buzsaki (2004). "Early motor activity drives spindle bursts in the developing somatosensory cortex." Nature **432**(7018): 758-761.

Kim, M., R. E. Harris, A. F. DaSilva and U. Lee (2022). "Explosive Synchronization-Based Brain Modulation Reduces Hypersensitivity in the Brain Network: A Computational Model Study." Frontiers in Computational Neuroscience **16**.

Kim, Y., S. Kim, W. K. Ho and S. H. Lee (2023). "Burst firing is required for induction of Hebbian LTP at lateral perforant path to hippocampal granule cell synapses." Mol Brain **16**(1): 45.

Knudsen, E. I. (2004). "Sensitive periods in the development of the brain and behavior." J Cogn Neurosci **16**(8): 1412-1425.

Koenis, M. M. G., R. M. Brouwer, S. C. Swagerman, I. L. C. van Soelen, D. I. Boomsma and H. E. Hulshoff Pol (2018). "Association between structural brain network efficiency and intelligence increases during adolescence." Hum Brain Mapp **39**(2): 822-836.

Komatsu, Y. and M. Iwakiri (1992). "Low-threshold Ca2+ channels mediate induction of long-term potentiation in kitten visual cortex." J Neurophysiol **67**(2): 401-410.

Kunze, A., R. Meissner, S. Brando and P. Renaud (2011). "Co-pathological connected primary neurons in a microfluidic device for Alzheimer studies." Biotechnol Bioeng **108**(9): 2241-2245.

Langer, N., A. Pedroni, L. R. Gianotti, J. Hänggi, D. Knoch and L. Jäncke (2012). "Functional brain network efficiency predicts intelligence." Hum Brain Mapp **33**(6): 1393-1406.

Lecca, D., Y. J. Jung, M. T. Scerba, I. Hwang, Y. K. Kim, S. Kim, S. Modrow, D. Tweedie, S.-C. Hsueh, D. Liu, W. Luo, E. Glotfelty, Y. Li, J.-Y. Wang, Y. Luo, B. J. Hoffer, D. S. Kim, R. A. McDevitt and N. H. Greig (2022). "Role of chronic neuroinflammation in neuroplasticity and cognitive function: A hypothesis." Alzheimer's & Dementia **18**(11): 2327-2340.

Leleo, E. G. and I. Segev (2021). "Burst control: Synaptic conditions for burst generation in cortical layer 5 pyramidal neurons." PLoS Comput Biol **17**(11): e1009558.

Li, C., P. Li, Y. Zhang, N. Li, Y. Si, F. Li, Z. Cao, H. Chen, B. Chen, D. Yao and P. Xu (2023). "Effective Emotion Recognition by Learning Discriminative Graph Topologies in EEG Brain Networks." IEEE Transactions on Neural Networks and Learning Systems: 1-15.

Li, L., Y. Mi, W. Zhang, D.-H. Wang and S. Wu (2018). "Dynamic Information Encoding With Dynamic Synapses in Neural Adaptation." Frontiers in Computational Neuroscience **12**.

Li, R., W. Liao, Y. Li, Y. Yu, Z. Zhang, G. Lu and H. Chen (2016). "Disrupted structural and functional rich club organization of the brain connectome in patients with generalized tonic-clonic seizure." Hum Brain Mapp **37**(12): 4487-4499.

Li, Y., Y. Liu, J. Li, W. Qin, K. Li, C. Yu and T. Jiang (2009). "Brain anatomical network and intelligence." PLoS Comput Biol **5**(5): e1000395.

Li, Y., W. Zhou, X. Li, S. Zeng, M. Liu and Q. Luo (2007). "Characterization of synchronized bursts in cultured hippocampal neuronal networks with learning training on microelectrode arrays." Biosens Bioelectron **22**(12): 2976-2982.

Liang, X., L. M. Hsu, H. Lu, A. Sumiyoshi, Y. He and Y. Yang (2018). "The Rich-Club Organization in Rat Functional Brain Network to Balance Between Communication Cost and Efficiency." Cereb Cortex **28**(3): 924-935.

Lisman, J. E. (1997). "Bursts as a unit of neural information: making unreliable synapses reliable." Trends Neurosci **20**(1): 38-43.

Lisman, J. E. and M. A. P. Idiart (1995). "Storage of 7 ± 2 Short-Term Memories in Oscillatory Subcycles." Science **267**(5203): 1512-1515.

Liu, X.-B. and K. D. Murray (2012). "Neuronal excitability and calcium/calmodulin-dependent protein kinase type II: Location, location, location." Epilepsia **53**(s1): 45-52.

Llinás, R. R. and M. Steriade (2006). "Bursting of thalamic neurons and states of vigilance." J Neurophysiol **95**(6): 3297-3308.

Lohse, C., D. S. Bassett, K. O. Lim and J. M. Carlson (2014). "Resolving Anatomical and Functional Structure in Human Brain Organization: Identifying Mesoscale Organization in Weighted Network Representations." PLOS Computational Biology **10**(10): e1003712.

Lonardoni, D., H. Amin, S. Zordan, F. Boi, A. Lecomte, G. N. Angotzi and L. Berdondini (2019). "Active High-Density Electrode Arrays: Technology and Applications in Neuronal Cell Cultures." Adv Neurobiol **22**: 253-273.

Luhmann, H. J. and R. Khazipov (2018). "Neuronal activity patterns in the developing barrel cortex." Neuroscience **368**: 256-267.

Luo, L. (2021). "Architectures of neuronal circuits." Science **373**(6559): eabg7285.

Ma, Z., G. G. Turrigiano, R. Wessel and K. B. Hengen (2019). "Cortical Circuit Dynamics Are Homeostatically Tuned to Criticality In Vivo." Neuron **104**(4): 655-664.e654.

Maffei, A. (2011). "The many forms and functions of long term plasticity at GABAergic synapses." Neural Plast **2011**: 254724.

Mainzer, K. (2008). "The emergence of mind and brain: an evolutionary, computational, and philosophical approach." Prog Brain Res **168**: 115-132.

Malagarriga, D., A. E. P. Villa, J. Garcia-Ojalvo and A. J. Pons (2015). "Mesoscopic Segregation of Excitation and Inhibition in a Brain Network Model." PLoS Computational Biology **11**(2).

Malerba, M., H. Amin, G. N. Angotzi, A. Maccione and L. Berdondini (2018). "Fabrication of Multielectrode Arrays for Neurobiology Applications." Methods Mol Biol **1771**: 147-157.

Malik, S. Z., M. A. Maronski, M. A. Dichter and D. J. Watson (2012). "The use of specific AAV serotypes to stably transduce primary CNS neuron cultures." Methods Mol Biol **846**: 305-319.

Marder, E. (2011). "Variability, compensation, and modulation in neurons and circuits." Proceedings of the National Academy of Sciences **108**(supplement_3): 15542-15548.

Markram, H., M. Toledo-Rodriguez, Y. Wang, A. Gupta, G. Silberberg and C. Wu (2004). "Interneurons of the neocortical inhibitory system." Nat Rev Neurosci **5**(10): 793-807.

McColgan, P., K. K. Seunarine, A. Razi, J. H. Cole, S. Gregory, A. Durr, R. A. Roos, J. C. Stout, B. Landwehrmeyer, R. I. Scahill, C. A. Clark, G. Rees and S. J. Tabrizi (2015). "Selective vulnerability of Rich Club brain regions is an organizational principle of structural connectivity loss in Huntington's disease." Brain **138**(Pt 11): 3327-3344.

McCormick, L. E. and S. L. Gupton (2020). "Mechanistic advances in axon pathfinding." Current Opinion in Cell Biology **63**: 11-19.

McKenzie, S. (2018). "Inhibition shapes the organization of hippocampal representations." Hippocampus **28**(9): 659-671.

Mensi, S., O. Hagens, W. Gerstner and C. Pozzorini (2016). "Enhanced Sensitivity to Rapid Input Fluctuations by Nonlinear Threshold Dynamics in Neocortical Pyramidal Neurons." PLoS Computational Biology **12**.

Meunier, D., R. Lambiotte and E. T. Bullmore (2010). "Modular and hierarchically modular organization of brain networks." Front Neurosci **4**: 200.

Miccoli, B., C. M. Lopez, E. Goikoetxea, J. Putzeys, M. Sekeri, O. Krylychkina, S.-W. Chang, A. Firrincieli, A. Andrei, V. Reumers and D. Braeken (2019). "High-Density Electrical Recording and Impedance Imaging With a Multi-Modal CMOS Multi-Electrode Array Chip." Frontiers in Neuroscience **13**.

Milano, M., G. Agapito and M. Cannataro (2022). "Challenges and Limitations of Biological Network Analysis." BioTech (Basel) **11**(3).

Millan, A. P., J. J. Torres, S. Johnson and J. Marro (2018). "Concurrence of form and function in developing networks and its role in synaptic pruning." Nat Commun **9**(1): 2236.

Milo, R., S. Shen-Orr, S. Itzkovitz, N. Kashtan, D. Chklovskii and U. Alon (2002). "Network motifs: simple building blocks of complex networks." Science **298**(5594): 824-827.

Minlebaev, M., Y. Ben-Ari and R. Khazipov (2007). "Network Mechanisms of Spindle-Burst Oscillations in the Neonatal Rat Barrel Cortex In Vivo." Journal of Neurophysiology **97**(1): 692-700.

Misic, B. and O. Sporns (2016). "From regions to connections and networks: new bridges between brain and behavior." Curr Opin Neurobiol **40**: 1-7.

Molliver, M. E., I. Kostovic´ and H. Van Der Loos (1973). "The development of synapses in cerebral cortex of the human fetus." Brain Research **50**(2): 403-407.

Mooney, R., A. A. Penn, R. Gallego and C. J. Shatz (1996). "Thalamic Relay of Spontaneous Retinal Activity Prior to Vision." Neuron **17**(5): 863-874.

Moosavi, S. A., V. K. Jirsa and W. Truccolo (2022). "Critical dynamics in the spread of focal epileptic seizures: Network connectivity, neural excitability and phase transitions." PLoS One **17**(8): e0272902.

Munji, R. N., Y. Choe, G. Li, J. A. Siegenthaler and S. J. Pleasure (2011). "Wnt signaling regulates neuronal differentiation of cortical intermediate progenitors." J Neurosci **31**(5): 1676-1687.

Murphy-Baum, B. L. and W. R. Taylor (2018). "Diverse inhibitory and excitatory mechanisms shape temporal tuning in transient OFF α ganglion cells in the rabbit retina." J Physiol **596**(3): 477-495.

Nagai, Y., N. Miyakawa, H. Takuwa, Y. Hori, K. Oyama, B. Ji, M. Takahashi, X. P. Huang, S. T. Slocum, J. F. DiBerto, Y. Xiong, T. Urushihata, T. Hirabayashi, A. Fujimoto, K. Mimura, J. G. English, J. Liu, K. I. Inoue, K. Kumata, C. Seki, M. Ono, M. Shimojo, M. R. Zhang, Y. Tomita, J. Nakahara, T. Suhara, M. Takada, M. Higuchi, J. Jin, B. L. Roth and T. Minamimoto (2020). "Deschloroclozapine, a potent and selective chemogenetic actuator enables rapid neuronal and behavioral modulations in mice and monkeys." Nat Neurosci **23**(9): 1157-1167.

Namba, T., Y. Kibe, Y. Funahashi, S. Nakamuta, T. Takano, T. Ueno, A. Shimada, S. Kozawa, M. Okamoto, Y. Shimoda, K. Oda, Y. Wada, T. Masuda, A. Sakakibara, M. Igarashi, T. Miyata, C. Faivre-Sarrailh, K. Takeuchi and K. Kaibuchi (2014). "Pioneering axons regulate neuronal polarization in the developing cerebral cortex." Neuron **81**(4): 814-829.

Neske, G. T., S. L. Patrick and B. W. Connors (2015). "Contributions of diverse excitatory and inhibitory neurons to recurrent network activity in cerebral cortex." J Neurosci **35**(3): 1089-1105.

Newsome, W. T. (2009). "Human freedom "emergence"." Downward causation and the neurobiology of free will: 53-62.

Nigam, S., M. Shimono, S. Ito, F. C. Yeh, N. Timme, M. Myroshnychenko, C. C. Lapish, Z. Tosi, P. Hottowy, W. C. Smith, S. C. Masmanidis, A. M. Litke, O. Sporns and J. M. Beggs (2016). "Rich-Club Organization in Effective Connectivity among Cortical Neurons." J Neurosci **36**(3): 670-684.

Nowak, A., R. R. Vallacher, M. Zochowski and A. Rychwalska (2017). "Functional Synchronization: The Emergence of Coordinated Activity in Human Systems." Frontiers in Psychology **8**.

Ohtaka-Maruyama, C. (2020). "Subplate Neurons as an Organizer of Mammalian Neocortical Development." Frontiers in Neuroanatomy **14**.

Ohtaka-Maruyama, C., M. Okamoto, K. Endo, M. Oshima, N. Kaneko, K. Yura, H. Okado, T. Miyata and N. Maeda (2018). "Synaptic transmission from subplate neurons controls radial migration of neocortical neurons." Science **360**(6386): 313-317.

Okujeni, S. and U. Egert (2019). "Self-organization of modular network architecture by activity-dependent neuronal migration and outgrowth." Elife **8**.

Opitz, T., A. D. De Lima and T. Voigt (2002). "Spontaneous development of synchronous oscillatory activity during maturation of cortical networks in vitro." Journal of neurophysiology **88**(5): 2196-2206.

Osada, T., Y. Adachi, K. Miyamoto, K. Jimura, R. Setsuie and Y. Miyashita (2015). "Dynamically Allocated Hub in Task-Evoked Network Predicts the Vulnerable Prefrontal Locus for Contextual Memory Retrieval in Macaques." PLOS Biology **13**(6): e1002177.

Pachitariu, M., D. R. Lyamzin, M. Sahani and N. A. Lesica (2015). "State-dependent population coding in primary auditory cortex." J Neurosci **35**(5): 2058-2073.

Palmigiano, A., T. Geisel, F. Wolf and D. Battaglia (2017). "Flexible information routing by transient synchrony." Nat Neurosci **20**(7): 1014-1022.

Park, C. H., W. H. Chang, S. H. Ohn, S. T. Kim, O. Y. Bang, A. Pascual-Leone and Y. H. Kim (2011). "Longitudinal changes of resting-state functional connectivity during motor recovery after stroke." Stroke **42**(5): 1357-1362.

Park, H.-J. and K. Friston (2013). "Structural and Functional Brain Networks: From Connections to Cognition." Science **342**(6158): 1238411.

Pastore, V. P., P. Massobrio, A. Godjoski and S. Martinoia (2018). "Identification of excitatory-inhibitory links and network topology in large-scale neuronal assemblies from multi-electrode recordings." PLoS Comput Biol **14**(8): e1006381.

Peterman, M. C., J. Noolandi, M. S. Blumenkranz and H. A. Fishman (2004). "Localized chemical release from an artificial synapse chip." Proc Natl Acad Sci U S A **101**(27): 9951-9954.

Pine, J. (1980). "Recording action potentials from cultured neurons with extracellular microcircuit electrodes." Journal of Neuroscience Methods **2**(1): 19-31.

Piochon, C., M. Kano and C. Hansel (2016). "LTD-like molecular pathways in developmental synaptic pruning." Nat Neurosci **19**(10): 1299-1310.

Plachez, C. and L. J. Richards (2005). Mechanisms of Axon Guidance in the Developing Nervous System. Current Topics in Developmental Biology, Academic Press. **69:** 267-346.

Poli, D., V. P. Pastore, S. Martinoia and P. Massobrio (2016). "From functional to structural connectivity using partial correlation in neuronal assemblies." Journal of Neural Engineering **13**(2).

Poli, D., V. P. Pastore and P. Massobrio (2015). "Functional connectivity in in vitro neuronal assemblies." Front Neural Circuits **9**: 57.

Potter, S. M. and T. B. DeMarse (2001). "A new approach to neural cell culture for long-term studies." J Neurosci Methods **110**(1-2): 17-24.

Pozo, K. and Y. Goda (2010). "Unraveling mechanisms of homeostatic synaptic plasticity." Neuron **66**(3): 337-351.

Prinz, A. A., D. Bucher and E. Marder (2004). "Similar network activity from disparate circuit parameters." Nature Neuroscience **7**(12): 1345-1352.

Raichle, M. E. and M. A. Mintun (2006). "Brain work and brain imaging." Annu Rev Neurosci **29**: 449-476.

Ramsay, A. O. and E. H. Hess (1954). "A Laboratory Approach to the Study of Imprinting." The Wilson Journal of Ornithology **66**: 196-206.

Rey, H. G., C. Pedreira and R. Quian Quiroga (2015). "Past, present and future of spike sorting techniques." Brain Res Bull **119**(Pt B): 106-117.

Rieubland, S., A. Roth and M. Häusser (2014). "Structured connectivity in cerebellar inhibitory networks." Neuron **81**(4): 913-929.

Roberts, J. A. and P. A. Robinson (2012). "Quantitative theory of driven nonlinear brain dynamics." NeuroImage **62**(3): 1947-1955.

Roth, B. L. (2019). "How structure informs and transforms chemogenetics." Current Opinion in Structural Biology **57**: 9-16.

Rozov, A. V., F. F. Valiullina and A. P. Bolshakov (2017). "Mechanisms of Long-Term Plasticity of Hippocampal GABAergic Synapses." Biochemistry (Mosc) **82**(3): 257-263.

Rubinov, M., O. Sporns, C. van Leeuwen and M. Breakspear (2009). "Symbiotic relationship between brain structure and dynamics." BMC Neurosci **10**: 55.

Rubinov, M., R. J. F. Ypma, C. Watson and E. T. Bullmore (2015). "Wiring cost and topological participation of the mouse brain connectome." Proceedings of the National Academy of Sciences **112**(32): 10032-10037.

Ruthazer, E. S. and M. P. Stryker (1996). "The Role of Activity in the Development of Long-Range Horizontal Connections in Area 17 of the Ferret." The Journal of Neuroscience **16**(22): 7253.

Sadeh, S. and C. Clopath (2020). "Inhibitory stabilization and cortical computation." Nat Rev Neurosci.

Sadeh, S., R. A. Silver, T. D. Mrsic-Flogel and D. R. Muir (2017). "Assessing the role of inhibition in stabilizing neocortical networks requires large-scale perturbation of the inhibitory population." Journal of Neuroscience **37**(49): 12050-12067.

Sagdullaev, B. T., E. D. Eggers, R. Purgert and P. D. Lukasiewicz (2011). "Nonlinear interactions between excitatory and inhibitory retinal synapses control visual output." J Neurosci **31**(42): 15102-15112.

Salinas, E. and T. J. Sejnowski (2000). "Impact of correlated synaptic input on output firing rate and variability in simple neuronal models." J Neurosci **20**(16): 6193-6209.

Salinas, E. and T. J. Sejnowski (2001). "Correlated neuronal activity and the flow of neural information." Nat Rev Neurosci **2**(8): 539-550.

Sanzeni, A., B. Akitake, H. C. Goldbach, C. E. Leedy, N. Brunel and M. H. Histed (2020). "Inhibition stabilization is a widespread property of cortical networks." Elife **9**.

Sato, J., K. Safar, V. M. Vogan and M. J. Taylor (2023). "Functional connectivity changes during working memory in autism spectrum disorder: A two-year longitudinal MEG study." NeuroImage: Clinical **37**: 103364.

Schiff, S. J., P. So, T. Chang, R. E. Burke and T. Sauer (1996). "Detecting dynamical interdependence and generalized synchrony through mutual prediction in a neural ensemble." Physical Review E **54**(6): 6708-6724.

Schmidt, R., K. J. R. LaFleur, M. A. de Reus, L. H. van den Berg and M. P. van den Heuvel (2015). "Kuramoto model simulation of neural hubs and dynamic synchrony in the human cerebral connectome." BMC Neuroscience **16**(1): 54.

Schnitzler, A. and J. Gross (2005). "Normal and pathological oscillatory communication in the brain." Nature Reviews Neuroscience **6**(4): 285-296.

Scholtens, L. H., R. Schmidt, M. A. de Reus and M. P. van den Heuvel (2014). "Linking macroscale graph analytical organization to microscale neuroarchitectonics in the macaque connectome." J Neurosci **34**(36): 12192-12205.

Schroeter, M. S., P. Charlesworth, M. G. Kitzbichler, O. Paulsen and E. T. Bullmore (2015). "Emergence of rich-club topology and coordinated dynamics in development of hippocampal functional networks in vitro." J Neurosci **35**(14): 5459-5470.

Senden, M., G. Deco, M. A. de Reus, R. Goebel and M. P. van den Heuvel (2014). "Rich club organization supports a diverse set of functional network configurations." Neuroimage **96**: 174-182.

Shatz, C. J. (1990). "Impulse activity and the patterning of connections during CNS development." Neuron **5**(6): 745-756.

Shatz, C. J. and M. P. Stryker (1988). "Prenatal tetrodotoxin infusion blocks segregation of retinogeniculate afferents." Science **242**(4875): 87-89.

Shen, X. F., J. X. Wu, Z. F. Wang and T. Chen (2019). "Characterization of in vitro neural functional connectivity on a neurofluidic device." Electrophoresis **40**(22): 2996-3004.

Shu, N., Y. Liu, K. Li, Y. Duan, J. Wang, C. Yu, H. Dong, J. Ye and Y. He (2011). "Diffusion tensor tractography reveals disrupted topological efficiency in white matter structural networks in multiple sclerosis." Cereb Cortex **21**(11): 2565-2577.

Sidman, R. L. and P. Rakic (1973). "Neuronal migration, with special reference to developing human brain: a review." Brain Research **62**(1): 1-35.

Siegel, M., M. R. Warden and E. K. Miller (2009). "Phase-dependent neuronal coding of objects in short-term memory." Proceedings of the National Academy of Sciences **106**(50): 21341-21346.

Simao, D., M. M. Silva, A. P. Terrasso, F. Arez, M. F. Q. Sousa, N. Z. Mehrjardi, T. Saric, P. Gomes-Alves, N. Raimundo, P. M. Alves and C. Brito (2018). "Recapitulation of Human Neural Microenvironment Signatures in iPSC-Derived NPC 3D Differentiation." Stem Cell Reports **11**(2): 552-564.

Simoes, E. L., I. Bramati, E. Rodrigues, A. Franzoi, J. Moll, R. Lent and F. Tovar-Moll (2012). "Functional expansion of sensorimotor representation and structural reorganization of callosal connections in lower limb amputees." Journal of Neuroscience **32**(9): 3211-3220.

Singer, W. (1986). "The brain as a self-organizing system." Eur Arch Psychiatry Neurol Sci **236**(1): 4-9.

Singer, W. (1999). "Neuronal synchrony: a versatile code for the definition of relations?" Neuron **24**(1): 49-65, 111-125.

Singer, W. (2009). "The Brain, a Complex Self-organizing System." European Review **17**(2): 321-329.

Singer, W. (2021). "Recurrent dynamics in the cerebral cortex: Integration of sensory evidence with stored knowledge." Proceedings of the National Academy of Sciences **118**(33): e2101043118.

Softky, W. R. and C. Koch (1993). "The highly irregular firing of cortical cells is inconsistent with temporal integration of random EPSPs." J Neurosci **13**(1): 334-350.

Somjen, G. G. (2001). "Mechanisms of spreading depression and hypoxic spreading depression-like depolarization." Physiol Rev **81**(3): 1065-1096.

Sorrentino, F. and E. Ott (2008). "Adaptive synchronization of dynamics on evolving complex networks." Phys Rev Lett **100**(11): 114101.

Sporns, O. (2013). "Network attributes for segregation and integration in the human brain." Curr Opin Neurobiol **23**(2): 162-171.

Sporns, O. and C. J. Honey (2006). "Small worlds inside big brains." Proc Natl Acad Sci U S A **103**(51): 19219-19220.

Sporns, O., G. Tononi and R. Kotter (2005). "The human connectome: A structural description of the human brain." PLoS Comput Biol **1**(4): e42.

Sreedharan, S., A. Chandran, V. R. Yanamala, P. N. Sylaja, C. Kesavadas and R. Sitaram (2020). "Self-regulation of language areas using real-time functional MRI in stroke patients with expressive aphasia." Brain Imaging and Behavior **14**(5): 1714-1730.

Stachniak, T. J., A. Ghosh and S. M. Sternson (2014). "Chemogenetic synaptic silencing of neural circuits localizes a hypothalamus→midbrain pathway for feeding behavior." Neuron **82**(4): 797-808.

Straub, C., J. L. Saulnier, A. Bègue, D. D. Feng, K. W. Huang and B. L. Sabatini (2016). "Principles of Synaptic Organization of GABAergic Interneurons in the Striatum." Neuron **92**(1): 84-92.

Strotzer, M. (2009). "One Century of Brain Mapping Using Brodmann Areas*." Clinical Neuroradiology **19**(3): 179-186.

Südhof, T. C. (2018). "Towards an Understanding of Synapse Formation." Neuron **100**(2): 276-293.

Takahashi, K., K. Tanabe, M. Ohnuki, M. Narita, T. Ichisaka, K. Tomoda and S. Yamanaka (2007). "Induction of pluripotent stem cells from adult human fibroblasts by defined factors." Cell **131**(5): 861-872.

Takayama, S., E. Ostuni, P. LeDuc, K. Naruse, D. E. Ingber and G. M. Whitesides (2001). "Subcellular positioning of small molecules." Nature **411**(6841): 1016.

Takayama, Y. and Y. S. Kida (2016). "In Vitro Reconstruction of Neuronal Networks Derived from Human iPS Cells Using Microfabricated Devices." PLoS One **11**(2): e0148559.

Tandon, S., N. Kambi, L. Lazar, H. Mohammed and N. Jain (2009). "Large-scale expansion of the face representation in somatosensory areas of the lateral sulcus after spinal cord injuries in monkeys." Journal of Neuroscience **29**(38): 12009-12019.

Taylor, A. M., S. W. Rhee, C. H. Tu, D. H. Cribbs, C. W. Cotman and N. L. Jeon (2003). "Microfluidic Multicompartment Device for Neuroscience Research." Langmuir **19**(5): 1551-1556.

Teppola, H., J. Acimovic and M. L. Linne (2019). "Unique Features of Network Bursts Emerge From the Complex Interplay of Excitatory and Inhibitory Receptors in Rat Neocortical Networks." Frontiers in Cellular Neuroscience **13**.

Teskey, G. C., M. H. Monfils, P. M. VandenBerg and J. A. Kleim (2002). "Motor map expansion following repeated cortical and limbic seizures is related to synaptic potentiation." Cereb Cortex **12**(1): 98-105.

Tessier-Lavigne, M. and C. S. Goodman (1996). "The molecular biology of axon guidance." Science **274**(5290): 1123-1133.

Thal, D. R. and S. O. Tomé (2022). "The central role of tau in Alzheimer's disease: From neurofibrillary tangle maturation to the induction of cell death." Brain Research Bulletin **190**: 204-217.

Tierney, A. L. and C. A. Nelson, 3rd (2009). "Brain Development and the Role of Experience in the Early Years." Zero Three **30**(2): 9-13.

Tomasi, D., G. J. Wang and N. D. Volkow (2013). "Energetic cost of brain functional connectivity." Proc Natl Acad Sci U S A **110**(33): 13642-13647.

Trachtenberg, J. T., B. E. Chen, G. W. Knott, G. Feng, J. R. Sanes, E. Welker and K. Svoboda (2002). "Long-term in vivo imaging of experience-dependent synaptic plasticity in adult cortex." Nature **420**(6917): 788-794.

Tremblay, R., S. Lee and B. Rudy (2016). "GABAergic Interneurons in the Neocortex: From Cellular Properties to Circuits." Neuron **91**(2): 260-292.

Trojan, S. and J. Pokorny (1999). "Threoretical aspects of neuroplasticity." Physiological research **48**: 87-98.

Tu, W., Z. Ma and N. Zhang (2021). "Brain network reorganization after targeted attack at a hub region." Neuroimage **237**: 118219.

Turrigiano, G., L. F. Abbott and E. Marder (1994). "Activity-dependent changes in the intrinsic properties of cultured neurons." Science **264**(5161): 974-977.

Turrigiano, G. G. (1999). "Homeostatic plasticity in neuronal networks: the more things change, the more they stay the same." Trends Neurosci **22**(5): 221-227.

Turrigiano, G. G. (2017). "The dialectic of Hebb and homeostasis." Philos Trans R Soc Lond B Biol Sci **372**(1715).

Turrigiano, G. G., K. R. Leslie, N. S. Desai, L. C. Rutherford and S. B. Nelson (1998). "Activity-dependent scaling of quantal amplitude in neocortical neurons." Nature **391**(6670): 892-896.

Turrigiano, G. G. and S. B. Nelson (2000). "Hebb and homeostasis in neuronal plasticity." Curr Opin Neurobiol **10**(3): 358-364.

Uhlhaas, P., G. Pipa, B. Lima, L. Melloni, S. Neuenschwander, D. Nikolić and W. Singer (2009). "Neural synchrony in cortical networks: history, concept and current status." Frontiers in Integrative Neuroscience **3**.

Uhlhaas, P. J. and W. Singer (2006). "Neural synchrony in brain disorders: relevance for cognitive dysfunctions and pathophysiology." Neuron **52**(1): 155-168.

Urban, D. J. and B. L. Roth (2015). "DREADDs (designer receptors exclusively activated by designer drugs): chemogenetic tools with therapeutic utility." Annu Rev Pharmacol Toxicol **55**: 399-417.

Usrey, W. M., J. B. Reppas and R. C. Reid (1998). "Paired-spike interactions and synaptic efficacy of retinal inputs to the thalamus." Nature **395**(6700): 384-387.

Valderhaug, V. D., K. Heiney, O. H. Ramstad, G. Bråthen, W.-L. Kuan, S. Nichele, A. Sandvig and I. Sandvig (2021). "Early functional changes associated with alpha-synuclein proteinopathy in engineered human neural networks." American Journal of Physiology-Cell Physiology **320**(6): C1141-C1152.

van de Wijdeven, R., O. Ramstad, U. Bauer, Ø. Halaas, A. Sandvig and I. Sandvig (2018). "Structuring a multi-nodal neural network in vitro within a novel design microfluidic chip." Biomedical Microdevices **20**.

van de Wijdeven, R., O. Ramstad, V. Valderhaug, P. Köllensperger, A. Sandvig, I. Sandvig and Ø. Halaas (2019). "A novel lab-on-chip platform enabling axotomy and neuromodulation in a multi-nodal network." Biosensors and Bioelectronics **140**: 111329.

van de Wijdeven, R., O. H. Ramstad, U. S. Bauer, Ø. Halaas, A. Sandvig and I. Sandvig (2018). "Structuring a multi-nodal neural network in vitro within a novel design microfluidic chip." Biomedical Microdevices **20**(1): 9.

van den Heuvel, M. P., R. S. Kahn, J. Goni and O. Sporns (2012). "High-cost, high-capacity backbone for global brain communication." Proc Natl Acad Sci U S A **109**(28): 11372-11377.

van den Heuvel, M. P. and O. Sporns (2011). "Rich-club organization of the human connectome." J Neurosci **31**(44): 15775-15786.

van den Heuvel, M. P. and O. Sporns (2013). "An anatomical substrate for integration among functional networks in human cortex." J Neurosci **33**(36): 14489-14500.

van den Heuvel, M. P. and O. Sporns (2013). "Network hubs in the human brain." Trends Cogn Sci **17**(12): 683-696.

van den Heuvel, M. P., O. Sporns, G. Collin, T. Scheewe, R. C. Mandl, W. Cahn, J. Goñi, H. E. Hulshoff Pol and R. S. Kahn (2013). "Abnormal rich club organization and functional brain dynamics in schizophrenia." JAMA Psychiatry **70**(8): 783-792.

van den Heuvel, M. P., C. J. Stam, R. S. Kahn and H. E. Hulshoff Pol (2009). "Efficiency of functional brain networks and intellectual performance." J Neurosci **29**(23): 7619-7624.

Van Horn, J. D., A. Irimia, C. M. Torgerson, M. C. Chambers, R. Kikinis and A. W. Toga (2012). "Mapping connectivity damage in the case of Phineas Gage." PLoS One **7**(5): e37454.

van Niekerk, E. A., R. Kawaguchi, C. Marques de Freria, K. Groeniger, M. C. Marchetto, S. Dupraz, F. Bradke, D. H. Geschwind, F. H. Gage and M. H. Tuszynski (2022). "Methods for culturing adult CNS neurons reveal a CNS conditioning effect." Cell Rep Methods **2**(7): 100255.

van Pelt, J., P. S. Wolters, M. A. Corner, W. L. Rutten and G. J. Ramakers (2004). "Long-term characterization of firing dynamics of spontaneous bursts in cultured neural networks." IEEE Trans Biomed Eng **51**(11): 2051-2062.

Vazin, T. and W. J. Freed (2010). "Human embryonic stem cells: derivation, culture, and differentiation: a review." Restor Neurol Neurosci **28**(4): 589-603.

Vlasov, V. and A. Bifone (2017). "Hub-driven remote synchronization in brain networks." Scientific Reports **7**(1): 10403.

von der Malsburg, C. (1973). "Self-organization of orientation sensitive cells in the striate cortex." Kybernetik **14**(2): 85-100.

Wagenaar, D. A., R. Madhavan, J. Pine and S. M. Potter (2005). "Controlling bursting in cortical cultures with closed-loop multi-electrode stimulation." J Neurosci **25**(3): 680-688.

Wagenaar, D. A., Z. Nadasdy and S. M. Potter (2006). "Persistent dynamic attractors in activity patterns of cultured neuronal networks." Phys Rev E Stat Nonlin Soft Matter Phys **73**(5 Pt 1): 051907.

Wagenaar, D. A., J. Pine and S. M. Potter (2004). "Effective parameters for stimulation of dissociated cultures using multi-electrode arrays." J Neurosci Methods **138**(1-2): 27-37.

Wagenaar, D. A., J. Pine and S. M. Potter (2006). "An extremely rich repertoire of bursting patterns during the development of cortical cultures." BMC Neurosci **7**: 11.

Wang, D. and G. Gao (2014). "State-of-the-art human gene therapy: part I. Gene delivery technologies." Discov Med **18**(97): 67-77.

Wang, F., J. Kong, Y. Y. Cui, P. Liu and J. Y. Wen (2018). "Is Human-induced Pluripotent Stem Cell the Best Optimal?" Chin Med J (Engl) **131**(7): 852-856.

Wang, L., C. Yu, H. Chen, W. Qin, Y. He, F. Fan, Y. Zhang, M. Wang, K. Li, Y. Zang, T. S. Woodward and C. Zhu (2010). "Dynamic functional reorganization of the motor execution network after stroke." Brain **133**(4): 1224-1238.

Wang, X. and G. Chen (2002). "Synchronization in Small-World Dynamical Networks." I. J. Bifurcation and Chaos **12**: 187-192.

Wang, X. F. and M. S. Cynader (1999). "Effects of astrocytes on neuronal attachment and survival shown in a serum-free co-culture system." Brain Res Brain Res Protoc **4**(2): 209-216.

Wang, Y., Y. Zhao, H. Nie, C. Liu and J. Chen (2018). "Disrupted Brain Network Efficiency and Decreased Functional Connectivity in Multi-sensory Modality Regions in Male Patients With Alcohol Use Disorder." Frontiers in Human Neuroscience **12**.

Warm, D., D. Bassetti, J. Schroer, H. J. Luhmann and A. Sinning (2022). "Spontaneous Activity Predicts Survival of Developing Cortical Neurons." Frontiers in Cell and Developmental Biology **10**.

Warren, D. E., J. D. Power, J. Bruss, N. L. Denburg, E. J. Waldron, H. Sun, S. E. Petersen and D. Tranel (2014). "Network measures predict neuropsychological outcome after brain injury." Proceedings of the National Academy of Sciences **111**(39): 14247-14252.

Waschke, L., S. Tune and J. Obleser (2019). "Local cortical desynchronization and pupil-linked arousal differentially shape brain states for optimal sensory performance." Elife **8**.

Watts, D. J. and S. H. Strogatz (1998). "Collective dynamics of 'small-world' networks." Nature **393**(6684): 440-442.

Weir, J. S., N. Christiansen, A. Sandvig and I. Sandvig (2023). "Selective inhibition of excitatory synaptic transmission alters the emergent bursting dynamics of in vitro neural networks." Frontiers in Neural Circuits **17**.

Wiebe, S., Z. Huang, R. J. Ladak, A. Skalecka, R. Cagnetta, J. C. Lacaille, A. Aguilar-Valles and N. Sonenberg (2023). "Cell-type-specific translational control of spatial working memory by the cap-binding protein 4EHP." Mol Brain **16**(1): 9.

Wilson, H. R. and J. D. Cowan (1972). "Excitatory and inhibitory interactions in localized populations of model neurons." Biophys J **12**(1): 1-24.

Winter-Hjelm, N., Å. B. Tomren, P. Sikorski, A. Sandvig and I. Sandvig (2022). Structure-Function Dynamics of Engineered, Modular Neuronal Networks with Controllable Afferent-Efferent Connectivity, bioRxiv.

Wolman, M. A., V. K. Sittaramane, J. J. Essner, H. J. Yost, A. Chandrasekhar and M. C. Halloran (2008). "Transient axonal glycoprotein-1 (TAG-1) and laminin-alpha1 regulate dynamic growth cone behaviors and initial axon direction in vivo." Neural Dev **3**: 6.

Wong, R. O., M. Meister and C. J. Shatz (1993). "Transient period of correlated bursting activity during development of the mammalian retina." Neuron **11**(5): 923-938.

Wu, Z., A. Asokan and R. J. Samulski (2006). "Adeno-associated Virus Serotypes: Vector Toolkit for Human Gene Therapy." Molecular Therapy **14**(3): 316-327.

Xin, R., B. Anastasia, L. H. John and K. Jaideep (2021). "Connectivity and Neuronal Synchrony during Seizures." The Journal of Neuroscience **41**(36): 7623.

Yang, G., F. Pan and W. B. Gan (2009). "Stably maintained dendritic spines are associated with lifelong memories." Nature **462**(7275): 920-924.

Yang, Y., T. Solis-Escalante, F. C. T. van der Helm and A. C. Schouten (2016). "A Generalized Coherence Framework for Detecting and Characterizing Nonlinear Interactions in the Nervous System." IEEE Trans Biomed Eng **63**(12): 2629-2637.

Zamora-López, G., C. Zhou and J. Kurths (2009). "Graph analysis of cortical networks reveals complex anatomical communication substrate." Chaos **19**(1): 015117.

Zhang, J., Y. Zhang, L. Wang, L. Sang, J. Yang, R. Yan, P. Li, J. Wang and M. Qiu (2017). "Disrupted structural and functional connectivity networks in ischemic stroke patients." Neuroscience **364**: 212-225.

Zhao, Q., Z. N. K. Swati, H. Metmer, X. Sang and J. Lu (2019). "Investigating executive control network and default mode network dysfunction in major depressive disorder." Neuroscience Letters **701**: 154-161.

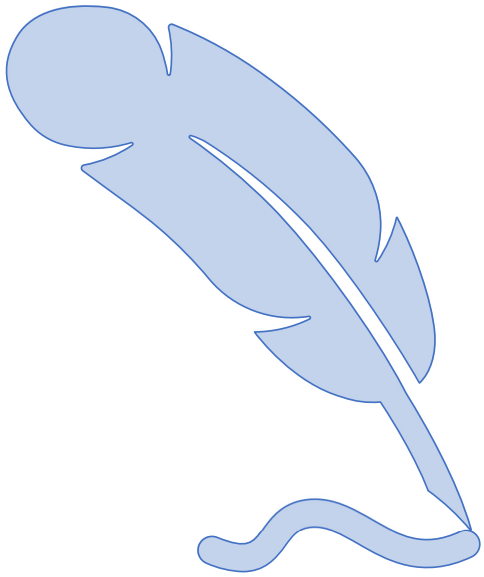

PAPER I

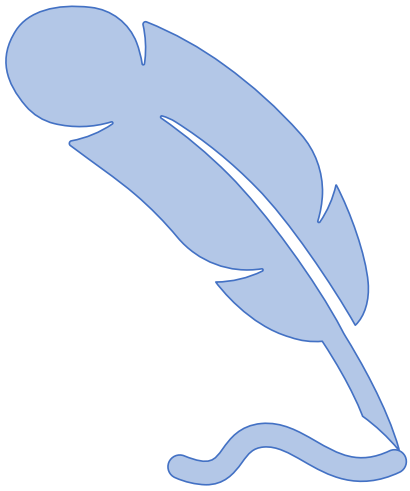

frontiers | Frontiers in Neural Circuits

TYPE Original Research
PUBLISHED 16 February 2023
DOI 10.3389/fncir.2023.1020487

OPEN ACCESS

EDITED BY
David Parker,
University of Cambridge, United Kingdom

REVIEWED BY
Wei Meng,
Jiangxi Science and Technology Normal University, China
John M. Beggs,
Indiana University Bloomington, United States

*CORRESPONDENCE
Ioanna Sandvig
✉ ioanna.sandvig@ntnu.no
Janelle Shari Weir
✉ janelle.s.weir@ntnu.no

†These authors have contributed equally to this work

RECEIVED 16 August 2022
ACCEPTED 31 January 2023
PUBLISHED 16 February 2023

CITATION
Weir JS, Christiansen N, Sandvig A and Sandvig I (2023) Selective inhibition of excitatory synaptic transmission alters the emergent bursting dynamics of *in vitro* neural networks.
Front. Neural Circuits 17:1020487.
doi: 10.3389/fncir.2023.1020487

Selective inhibition of excitatory synaptic transmission alters the emergent bursting dynamics of *in vitro* neural networks

Janelle Shari Weir[1*†], Nicholas Christiansen[1†], Axel Sandvig[1,2,3,4] and Ioanna Sandvig[1*]

[1]Department of Neuromedicine and Movement Science, Faculty of Medicine and Health Sciences, Norwegian University of Science and Technology, Trondheim, Norway, [2]Department of Neurology and Clinical Neurophysiology, St. Olav's University Hospital, Trondheim, Norway, [3]Division of Neuro, Head and Neck, Department of Pharmacology and Clinical Neurosciences, Umeå University Hospital, Umeå, Sweden, [4]Division of Neuro, Head and Neck, Department of Community Medicine and Rehabilitation, Umeå University Hospital, Umeå, Sweden

Neurons *in vitro* connect to each other and form neural networks that display emergent electrophysiological activity. This activity begins as spontaneous uncorrelated firing in the early phase of development, and as functional excitatory and inhibitory synapses mature, the activity typically emerges as spontaneous network bursts. Network bursts are events of coordinated global activation among many neurons interspersed with periods of silencing and are important for synaptic plasticity, neural information processing, and network computation. While bursting is the consequence of balanced excitatory-inhibitory (E/I) interactions, the functional mechanisms underlying their evolution from physiological to potentially pathophysiological states, such as decreasing or increasing in synchrony, are still poorly understood. Synaptic activity, especially that related to maturity of E/I synaptic transmission, is known to strongly influence these processes. In this study, we used selective chemogenetic inhibition to target and disrupt excitatory synaptic transmission in *in vitro* neural networks to study functional response and recovery of spontaneous network bursts over time. We found that over time, inhibition resulted in increases in both network burstiness and synchrony. Our results indicate that the disruption in excitatory synaptic transmission during early network development likely affected inhibitory synaptic maturity which resulted in an overall decrease in network inhibition at later stages. These findings lend support to the importance of E/I balance in maintaining physiological bursting dynamics and, conceivably, information processing capacity in neural networks.

KEYWORDS

excitatory-inhibitory balance, network bursts, electrophysiology, designer receptors exclusively activated by designer drugs (DREADDs), synchrony, chemogenetic approach, cortical network, network activity

1. Introduction

Neural network dynamics emerge over the course of development *in vitro*. Spontaneous network activity starts as immature tonic spiking and primitive patterns of synchronized activity in the early phases of development (Ben-Ari, 2001) which then progresses toward more complex behavior characterized by bursts (van Pelt et al., 2004;

Fardet et al., 2018). Typically, *in vitro* neural networks start exhibiting bursts between 6 and 14 DIV (Chiappalone et al., 2006; Wagenaar et al., 2006). Such early bursts, described as "superbursts" (Stephens et al., 2012), are posited to be driven by depolarizing gamma—aminobutyric acid type A ($GABA_A$) receptors and are hallmarks of early network development. At this stage, neuronal interactions are strengthened leading to recurrent coactivation among several neurons, which manifest as network bursts. These network bursts become more recurring as the neural network reaches maturity around 21 DIV and onward, with burst profile of higher frequency, shorter burst onset and offset, and shorter duration (Chiappalone et al., 2006; Bisio et al., 2014).

Network bursts are shown to be driven by excitatory synaptic transmission (Robinson et al., 1993; Kudela et al., 2003; Teppola et al., 2019), primarily mediated by glutamatergic ionotropic N-methyl-D-aspartate (NMDA) receptors and alpha-amino-3-hydroxy-5-methyl-4-isoxazolepropionic acid (AMPA) receptors. Fast inhibition by $GABA_A$ receptors also mediates network activity and burst emergence by maintaining a balance in excitatory-inhibitory (E/I) synaptic transmission (Teppola et al., 2019). Early *in vitro* studies reported that the relationship between network age, structure and the resulting activity is due to variations in synaptic connections and the differential developmental periods of excitatory and inhibitory synaptic transmission (Burgard and Hablitz, 1994; Kamioka et al., 1996). As the network achieves adequate interconnectivity and inhibitory synapses become more functionally mature during the later stages of development, network dynamics are reported to progress from spontaneous uncorrelated firing to more complex patterns of synchronized network bursts (Kamioka et al., 1996; Opitz et al., 2002; Wagenaar et al., 2006; Baltz et al., 2010). It has been suggested that the propagation of synchronized bursts plays an important role in shifting the network from immaturity into a stage characterized by a highly diversified range of electrical signaling (Ben-Ari, 2001), rendering the network capable of complex information processing and encoding. Several *in vivo* studies have reported similar age specific correlation of the emergence of network bursts with functional circuit development in various parts of the nervous system including the hippocampus (Blankenship and Feller, 2010; Raus Balind et al., 2019), cerebellar cortex (Dizon and Khodakhah, 2011; Hoehne et al., 2020), visual cortex (Chiu and Weliky, 2001), medulla (Pena and Ramirez, 2004; Magalhaes et al., 2021), and spinal cord (Darbon et al., 2004). These findings suggest that excitatory and inhibitory synaptic maturity are important drivers of network bursts, burst characteristics and subsequent network function. The effect of selective disruption of E/I balance on bursting dynamics in neural networks may therefore reveal substantial biological insights into network function, adaptability, and robustness.

Investigating inhibitory—excitatory synaptic contribution to network burst evolution *in vivo* is challenging. This is in part because the brain comprises numerous complex multi-layered neural networks, with heterogeneous synaptic connectivity among subsets of burst-generating neurons that contribute to the dynamics of the network (Zeldenrust et al., 2018). The interweaving of different neurons and synapses at various topological and temporal scales makes it challenging to determine the relative impact of synaptic activity on physiological and pathophysiological bursting activity. Since *in vitro* neural networks represent a reductionist model of a brain network—while still maintaining salient age dependent electrophysiological dynamics (Ben-Ari, 2001; Chiappalone et al., 2006, 2007; Sun et al., 2010; Schroeter et al., 2015)—the complexity is markedly reduced, and thus enables study and selective manipulation in a controlled manner (Marom and Shahaf, 2002). Many studies have taken advantage of such reductionist *in vitro* models to investigate network burst dynamics at the synaptic level *via* manipulation that changes the balance between excitatory and inhibitory synaptic transmission. Methods such as pharmacological blockade of NMDA and AMPA receptors (Chub and O'Donovan, 1998; Li et al., 2007; Suresh et al., 2016) and membrane current blockers (Ramakers et al., 1990, 1994; van Drongelen et al., 2006) have provided significant insights into the functional contribution of synaptic receptors and intrinsic membrane currents to the generation, maintenance, duration, and propagation of network bursts. However, these approaches indiscriminately block NMDA and AMPA receptors potentially expressed in inhibitory interneurons and some glia cells (Hestrin, 1993; Geiger et al., 1995; Verkhratsky and Kirchhoff, 2007; Perez-Rando et al., 2017). In this study, we utilized hM4Di designer receptors exclusively activated by designer drugs (DREADDs) (Armbruster et al., 2007; Alexander et al., 2009; Urban and Roth, 2015; Khambhati and Bassett, 2016; Whissell et al., 2016; Panthi and Leitch, 2019; Haaranen et al., 2020a,b; Lebonville et al., 2020; Ozawa and Arakawa, 2021) to selectively inhibit excitatory synaptic transmission—*via* G-protein coupled receptors (GPCRs) in calcium/calmodulin-dependent protein kinase alpha (CaMKlla) expressing neurons—in neural networks interfaced with microelectrode arrays (MEAs). This method allows us to target and manipulate excitatory synaptic transmission with greater selectivity while minimizing unintended off-target effects. Here, networks were chemogenetically inhibited at 14, 21, and 28 DIV and their dynamics characterized in comparison to their baseline activity and to phosphate-buffered saline (PBS) vehicle and control, unperturbed networks. The internal characteristics of network bursts both during treatment (functional response to perturbation) and post-treatment (recovery of the network) were analyzed. We found that inhibition of excitatory synaptic transmission increased bursting activity, as well as increased network synchronization within the chemogenetically inhibited networks by 28 DIV. Our results suggest that the long-term maintenance of the E/I balance depends on ongoing excitatory synaptic activity, and that disruption impairs physiological processes involved in modulating synchrony in maturing neural networks.

2. Materials and methods

2.1. Culture of cortical networks on microelectrode arrays

Primary rat (Sprague Dawley) cortex neurons were obtained from ThermoFisher Scientific, USA (Cat. No: A36511). Cells were thawed and seeded as a co-culture with 15% rat primary cortical astrocytes also from ThermoFisher Scientific (Cat. No: N7745100). The cells were plated at a density of approximately 1,000 cells/mm^2 on Nunc™ Lab -Tek™ chamber slides (Cat. No. 177380) coated with Geltrex matrix (cat. No. A1413201) at a working concentration of 0.5 ug/cm^2 for 1:100 dilution, both obtained from ThermoFisher Scientific. Pre-sterilized 6-well CytoView MEA

plates were purchased from Axion BioSystems and coated with 0.5% polyethyleneimine diluted in HEPES (both from Sigma-Aldrich, USA) and 20 μg/ml natural mouse laminin (ThermoFisher Scientific) diluted in Dulbecco's phosphate-buffered saline (DPBS) according to the Axion coating protocol (Axion BioSystems, GA, USA). Cells were plated directly over the electrodes on Axion MEA plates at a density of approximately 1,500 cells/mm^2 and incubated for 4 h before topping up wells to 1 ml with media. Cells were plated and maintained in Neurobasal™ Plus Medium supplemented with 2% B-27 Plus Supplement and 0.5% GlutaMAX™ all from ThermoFisher Scientific. The culture media was also supplemented with 0.2% (1:500 dilution from a 5 μg/ml working concentration) Plasmocin™ Prophylactic (ant. mpp; InvivoGen, USA). The day of plating from cryopreservation was allocated as day 0 and 50% media changes were carried out every 2–3 days. Cells were always kept in a 5% CO_2 incubator at 37°C except during media changes and imaging. All the wells on a single Axion MEA plate were allocated to one experimental condition. This ensured that networks that received the DREADDs virus were handled separately from the control networks, which did not receive the virus.

2.2. Adeno-associated virus 2/1 hM4Di CaMKIIa-DREADDs production and *in vitro* transduction

Vector production and purification was performed in-house at the Viral Vector Core Facility (Kavli Institute, NTNU). Tittering of the viral stock was determined as approximately 10^{11} vg/ml. High viral stocks were aliquoted into 20 ul volumes and stored at −80°C. Aliquots for use were thawed on ice and remaining virus aliquoted at store at −80°C. The maximum number of thaws for any aliquot used was 3 times. At 7 DIV, the neurons were transduced by removing 80% of the cell media from the culture and directly adding a dilution of adeno-associated virus (AAV) viral particles encoding experimental hM4Di -CaMKIIa-DREADDs to the neurons (**Figure 1A**). The titer of the viral dilution used for each well was 1×10^3 viral units per neuron based on tests at different viral concentrations (results not included). The cultures were gently agitated for 30 s to ensure proper distribution of the viral particles and then incubated for 8 h. Afterward, each well was topped up to 1 ml with fresh media without Plasmocin™ Prophylactic and incubated for an additional 40 h in 5% CO_2, 37°C incubator. After the incubation period, 50% media changes were carried out as scheduled. The vector encodes mCherry which is a bright red fluorescent protein tag that makes it possible to visualize results soon after transduction (**Figure 1B**).

2.3. Immunocytochemistry

At 14 DIV, parallel hM4Di DREADD networks were immunolabeled to investigate the specificity for vector mediated hM4Di expression in the CaMKIIa positive neurons. The cultures were fixed with 4% Paraformaldehyde (PFA) for 20 min and washed with DPBS before cultures were permeabilized with a blocking solution of 0.03% Triton X-100 and 5% goat serum in DPBS for 2 h at room temperature. Following blocking, antibodies at the indicated solutions (**Table 1**) were added in a buffer of 0.01% Triton X-100 and 1% goat serum in DPBS. Nuclei were stained with Hoechst (bisbenzimide H 33342 trihydrochloride, 14533, Sigma-Aldrich, USA, 1: 5,000 dilution). Samples were washed, mounted on glass cover slides with anti-fade fluorescence mounting medium (ab104135, Abcam) and imaged. All sample images were acquired using the EVOS M5000 imaging system (Invitrogen, ThermoFisher Scientific). Images were processed using Fiji/ImageJ and Adobe Illustrator 2020 version: 24.0.0.

2.4. Extracellular electrophysiological recordings

Neural activity was recorded on the Axion Maestro Pro MEA system (Axion BioSystems, GA, USA) with an integrated temperature-controlled CO_2 incubator (temperature 37°C and 5% CO_2). Data acquisition was done through the AxIS Navigator Software version 3.1.1. Spontaneous neuronal activity was recorded across 5 weeks between 9 and 32 DIV. Spiking data was captured using the AxIS spike detector with an adaptive threshold crossing. Spikes were defined by a threshold of seven standard deviations of the internal noise level with a post/pre-spike duration of 2.16/2.84 ms of each individual electrode, and with frequency limits of 200Hz–3kHz. Spike sorting was not attempted due to high clustering of the neurons on each electrode making it challenging to reliably discern which spikes correspond to individual neurons on the electrode. Furthermore, we were interested in the network wide activity rather than the activity of individual neurons.

2.5. Chemogenetic manipulation

To investigate the network response to chemogenetic manipulation, the novel synthetic ligand DCZ (MedChemExpress) was used to activate the DREADDs receptors (Nagai et al., 2020; Bjorkli et al., 2022) to induce synaptic silencing in excitatory neurons (see **Figure 2** for workflow). In summary, MEA plates were incubated for 15 min in the Maestro Pro chamber to allow the activity to stabilize before commencing the recording. Then, baseline activity was recorded for 20 min to capture the spontaneous activity of the networks before either PBS or DCZ was added. Afterward, either PBS (vehicle) or DCZ diluted in cell media (treatment) was added to 45% media volume in the wells at a final DCZ concentration of 10 μM. Networks were incubated for 1 h and then recorded for 1 h. This 1 h recording was divided into 3 phases of 20 min recordings denoted as 1st Treatment phase, 2nd Treatment phase and 3rd Treatment phase. The recording was continuous, and the division was done offline during the analysis. After treatment, 3 × 50% media changes were performed to wash out DCZ in the inhibited networks, and 3 × 50% media changes done in the PBS treated networks. To keep all conditions similar, a full media change was carried out on the Control (CTRL) networks. Networks were recorded after washout at 12 and 24 h (see **Table 2** for overview of networks recordings and analysis done). We looked at a total of 23 networks across repeated experiments, and 17 networks from the same experiment are presented here in the main results. Six networks were excluded from the main results due to missing data points.

10.3389/fncir.2023.1020487

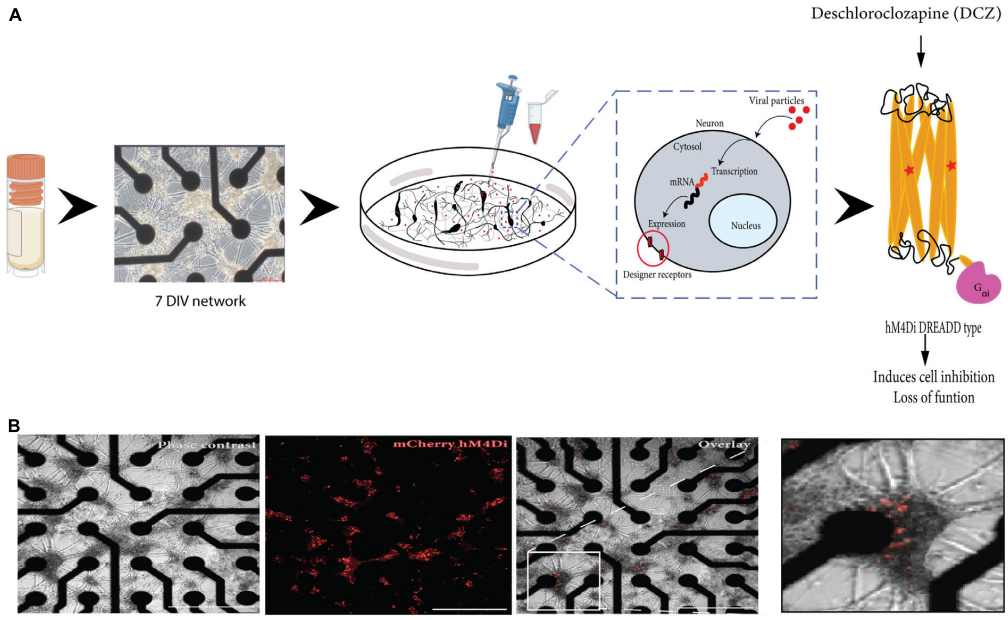

FIGURE 1
Illustration of the workflow of the study. **(A)** Cryopreserved cortical neurons were thawed and seeded on precoated microelectrode arrays (MEAs) until 7 DIV (scale bar = 200 μm). Neurons grow on top of the electrodes (black) and connect with each other across the surface. The designer receptors exclusively activated by designer drug (DREADD) protein is encoded in a replication deficient adeno-associated viral vector (AAV2/1) that is targeted for cytoplasmic gene delivery, thus circumventing genomic integration. The vector was added directly to the neurons in culture (on the MEA). The vector codes for the cell-specific promoter CaMKIIa so that mRNA transcription is targeted specifically at excitatory neurons which will be the cells that express the designer receptors. The designed DREADD hM4Di receptor has mutations at two points, which results in the receptor being insensitive to its endogenous agonist and neurotransmitter acetylcholine and instead respond only to a physiologically inert exogenous molecule (designer drug) such as deschloroclozapine (DCZ). When DCZ binds, the hM4DiR preferentially signals through the Gai/o subset of G-protein to inhibit adenylate cyclase and downstream cyclic adenosine monophosphate (cAMP) production, causing neuronal hyperpolarization and induces loss of cellular activity. **(B)** *In vitro* neural network on MEA at 12 days post adding the virus. DREADDs expression was confirmed without immunocytochemistry based on strong mCherry fluorescent expression in the network. Scale bar = 1250 μm.

TABLE 1 Overview of primary and secondary antibodies, species, and concentration.

Primaries			Secondaries		
Markers	Catalog number	Concentration	Fluorescent	Catalog number	Concentration
Ck mCherry	Ab205402 (Abcam)	1:1,000	Goat-anti-chicken AlexaFluor 568	Ab175477 (Abcam)	1:1,000
Ms calmodulin (CaMKIIa)	MA3-918 (Invitrogen)	1:250	Goat-anti-mouse AlexaFluor 568	A11019 (Invitrogen)	1:1,000
Ms NMDAR1	32-0500 (Invitrogen)	1:100	Goat-anti-mouse AlexaFluor 647	A21236 (Invitrogen)	1:1,000
Ms GABA BR1	Ab55051 (Abcam)	1:250	Goat-anti-mouse AlexaFluor 488	A11001 (Invitrogen)	1:1,000
Rb calmodulin (CaMKIIa)	Ab134041 (Abcam)	1:200	Goat-anti-rabbit AlexaFluor 568	A11011 (Invitrogen)	1:1,000
Rb glutamate decarboxylase (GAD65/67)	Ab183999 (Abcam)	1:100	Goat-anti-rabbit AlexaFluor 647	A21244 (Invitrogen)	1:1,000
Rb Map2	Ab32454 (Abcam)	1:250	Goat-anti-rabbit AlexaFluor 488	A11008 (Invitrogen)	1:1,000
Rb glial fibrillary acidic protein (GFAP)	Ab278054 (Abcam)	1:500			

2.6. Network dynamics analysis and network burst detection

The recording spike frequency was computed using the equation: $f = \frac{(spikes-1)}{\Delta t}$, where *spikes* are the total number of spikes for a recording channel and Δt is the time difference between the first and last spike included in *spikes*.

For shorter windows we define the instantaneous spike frequency of the window, f_{window}, as $f_{window} = \frac{spikes}{n\Delta t}$.

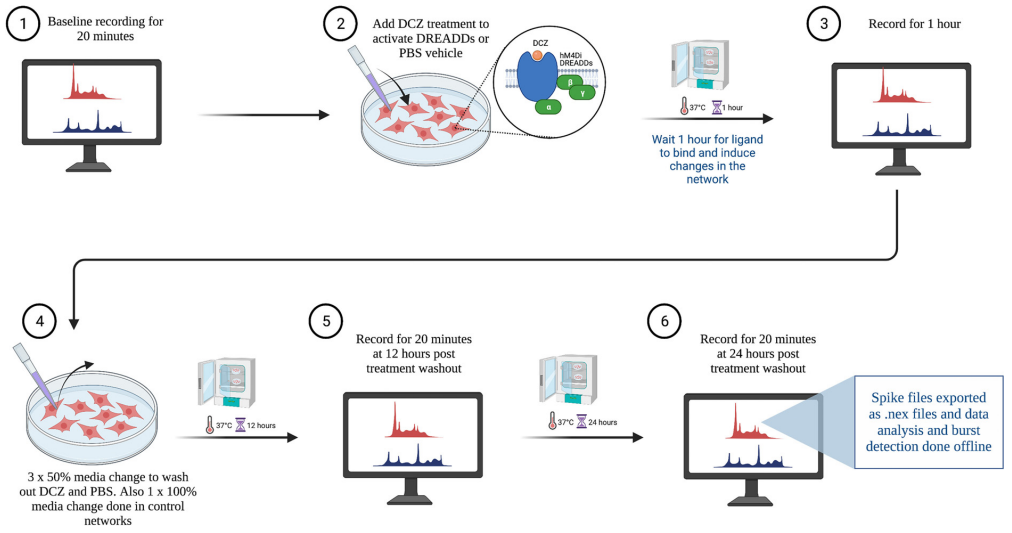

FIGURE 2
Workflow of electrophysiological recordings with treatment and wash out steps. Created with BioRender.com.

TABLE 2 Overview of networks analyzed, conditions, treatments received, and recordings done.

Neuronal networks analyzed	Conditions	Protocol	Electrophysiology recording
Control × seven networks (six included in main results)	No DREADDs, no DCZ treatment, no PBS vehicle	-	Baseline
Control × seven networks (five included in main results)	DREADDs + PBS vehicle	10% PBS in cell media	Baseline During PBS vehicle Recovery at 12 h Recovery at 24 h
Treatment × nine networks (six included in main results)	DREADDs + DCZ treatment	10 uM DCZ diluted in cell media	Baseline During DCZ treatment Recovery at 12 h Recovery at 24 h

Here, *spikes* are the spikes in the given window, n is the number of active electrodes in the recording, and Δt is the width of the window of interest. The instantaneous spike frequency was computed using a moving window of 1 s with a step size of 0.1 s, resulting in an overlap of windows for instantaneous measures.

Bursts were defined as sequences of at least four spikes with an inter spike interval (ISI) lower than a threshold of 100 ms for all electrodes (Table 3). The ISI was defined as the quiescent period between two consecutive spikes. Network bursts were defined as the collective sequences of synchronized bursts within an automatically detected ISI threshold for each well at every recording time (Bakkum et al., 2013). First, the ISI between six consecutive spikes (ISI_6) on the flattened spike train were binned on a logarithmic scale, and the peaks of the binned histograms were detected. The thresholds were centered between these two peaks on a logarithmic scale and limited to the range between at minimum 12 ms and at maximum 300 ms (Gandolfo et al., 2010; Obien et al., 2015). A network burst was detected for spikes where the interval between six consecutive spikes was below the found threshold. Please see (Chiappalone et al., 2005; Pasquale et al., 2010) for details of standard burst detection methods, also reviewed in Cotterill et al. (2016). The inter burst interval (IBI) was detected as the quiescent period between two bursts or two network bursts (NIBI). Burst analyses were also performed to identify the number of spikes in each network burst (spikes in network burst) and the count of the number of network bursts generated with the number of spikes (number of occurrence). The burstiness index of a recording was

TABLE 3 Burst and network burst detection parameters on the cumulative spike train over all electrodes.

Burst detection parameters		Network burst detection parameters	
ISI threshold	100 ms	Minimum ISI_6 threshold	12 ms
Minimum spikes in burst	4 spikes	Maximum ISI_6 threshold	300 ms
		Minimum spikes in network burst	6 spikes

defined as the amount of activity contained in the 15% most active windows of the computed instantaneous spike frequencies and provides an indication of synchronized neuronal participation in global network bursts (Wagenaar et al., 2005).

The coherence index was calculated as the standard deviation divided by the mean of the instantaneous spike frequencies. A high coherence index indicated more activity was contained in co-occurring bursts on multiple electrodes. Each parameter of all recording groups was assessed for normality using the Shapiro–Wilk test. Comparisons between groups were evaluated using the Welch's *t*-test or the Conover test in the case of normality and non-normality, respectively. Both tests were corrected with Bonferroni corrections for multiple comparisons. Statistical significance was determined if the *p*-value falls below the significance level ($p < 0.05$).

3. Results

3.1. AAV2/1 Gi-DREADD is expressed exclusively in CaMKIIa positive neurons

AAV mediated-DREADDs expression was confirmed with immunolabeling to amplify mCherry expression in target CaMKIIa positive neurons (Figure 3A). Neither inhibitory neurons (GAD65/67) (Figure 3B), nor astrocytes glial fibrillary acidic protein (GFAP) (Figure 3C) showed co-labeling with mCherry. This confirmed that there was cell specific expression of the AAV-DREADDs. Furthermore, networks at 14 DIV positively expressed GABA (Figure 4A), GABA B receptors (Figure 4B) and NMDA receptors (Figure 4C) confirming network capacity for excitatory and inhibitory signaling at this age.

In the sections that follow, we provide a detailed report of the main findings of our electrophysiological investigations and relevant analyses. Notwithstanding variability in our data, as discussed in subsequent sections, we present statistically significant results that support the hypothesis that selective inhibition alters the bursting dynamics in *in vitro* cortical networks.

3.2. Spontaneous activity and burst characteristics at baseline

Spontaneous network activity was recorded at different timepoints during the experiment for the chemogenetically inhibited networks, PBS vehicle networks and Control networks, which did not receive any treatment (hereafter referred to as DCZ networks, PBS networks and CTRL networks, respectively). The spontaneous baseline network profile before the addition of either PBS or DCZ (Step 1, in Figure 2) captured across 5 weeks is presented in Figure 5. The networks in each condition showed some variations in their activity and bursting characteristics between each recording from 9 to 32 DIV, nonetheless, the mean spontaneous network activity of all networks followed a typical trajectory of development, with increasingly more bursts as the networks reached maturity, according to previous work (Kamioka et al., 1996; Wagenaar et al., 2006). The CTRL networks exhibited more robust electrophysiological activity across several of the parameters, especially in the mean firing rate from 21 DIV onward when compared to the other networks (Figure 5A). Nonetheless, all networks had a trend of increasing mean firing rate between 9 and 28 DIV with a decrease at 32 DIV (Figure 5A), and an opposite trend in the ISI, which decreased over time until 28 DIV, then increased again by 32 DIV (Figure 5B). All networks exhibited bursting activity at 9 DIV and continued to exhibit varying degrees of bursting throughout network lifetime.

We found that the mean burstiness steadily decreased between 14 and 26 DIV for CTRL networks and between 9 and 28 DIV for PBS networks (Figure 5C). From then onward, until 32 DIV, both PBS and CTRL networks increased drastically in burstiness. Interestingly, while the DCZ networks also exhibited a decrease in burstiness between 9 and 18 DIV, these networks had a significantly higher burstiness at 21 DIV when compared to PBS ($p < 0.02$) and CTRL ($p < 0.02$) networks, and at 28 DIV compared to PBS ($p < 0.0006$) and CTRL ($p < 0.002$) networks (Figure 5C). Furthermore, the mean burst duration for all networks across the 3 conditions decreased similarly between 9 and 18 DIV, after which point the DCZ networks started to display increasingly longer bursts, which was significant at 28 DIV when compared to PBS networks ($p < 0.003$), but not CTRL networks ($p > 0.05$) (Figure 5D). The CTRL networks also displayed increasingly longer bursts during this time, while PBS networks maintained a stable burst duration between 18 and 32 DIV (Figure 5D). All networks maintained a similar trend in mean IBI and mean NIBI, with both decreased steadily between 9 and 28 DIV, with a slight increase at 32 DIV for both DCZ and CTRL networks (Figures 5E, H).

We also noticed that there was a lot of variation between day-to-day recordings in the PBS and DCZ networks for both fraction of spikes in bursts (Figure 5F) and fraction of spikes in network bursts (Figure 5G). The CTRL networks, however, maintained a very constant burst composition with > 90% spikes occurring in both isolated bursts (Figure 5F) and network bursts (Figure 5G) from 14 DIV onward. However, when we looked at network synchrony, which was measured by the coherence index, we noticed that after 18 DIV there was an overall increase in synchrony in DCZ networks at baseline, with a slight decrease between 21 and 28 DIV. Both PBS and CTRL networks exhibited decreased synchrony, with PBS networks decreasing between 9 and 28 DIV and CTRL networks between 14 and 28 DIV (Figure 5I), even though both had > 90% spikes occurring in network bursts from 18 DIV onward (Figure 5G). The increase observed in DCZ networks at 21 DIV did not differ significantly when compared to the other networks, but there were significant changes at 26 DIV compared to CTRL ($p < 0.0007$) and PBS ($p < 0.002$) networks, and at 28 DIV compared to CTRL networks ($p < 0.004$) and PBS networks ($p < 0.0004$). This increase in synchrony in DCZ networks from 18 DIV also corresponded to the observed increase in burstiness and burst durations at the same timepoint (Figures 5C, D). At 32 DIV, all networks including PBS and CTRL networks showed an increase in synchrony (Figure 5I), with only a significant difference between DCZ and CTRL networks ($p < 0.003$).

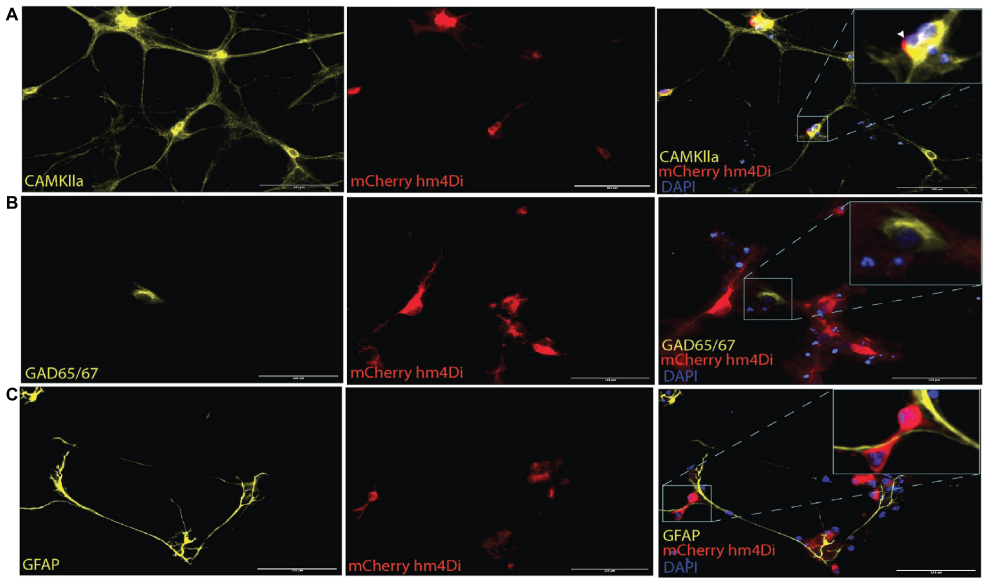

FIGURE 3
AAV2/1 hM4Di designer receptors exclusively activated by designer drugs (DREADDs) expression in neurons *in vitro*. **(A)** The mCherry antibody was used to enhance the fluorescent of the hM4Di receptors, which were positively colocalized with the somata of CaMKIIa positive neurons. **(B)** GAD65/67 expression indicated the presence of inhibitory neurons and showed no soma colocalization mCherry hM4Di expression. **(C)** Glial fibrillary acidic protein (GFAP) antibody was used to label astrocytes in the culture which also showed no soma colocalization with mCherry hM4Di expression. Scale bar = 125 μm.

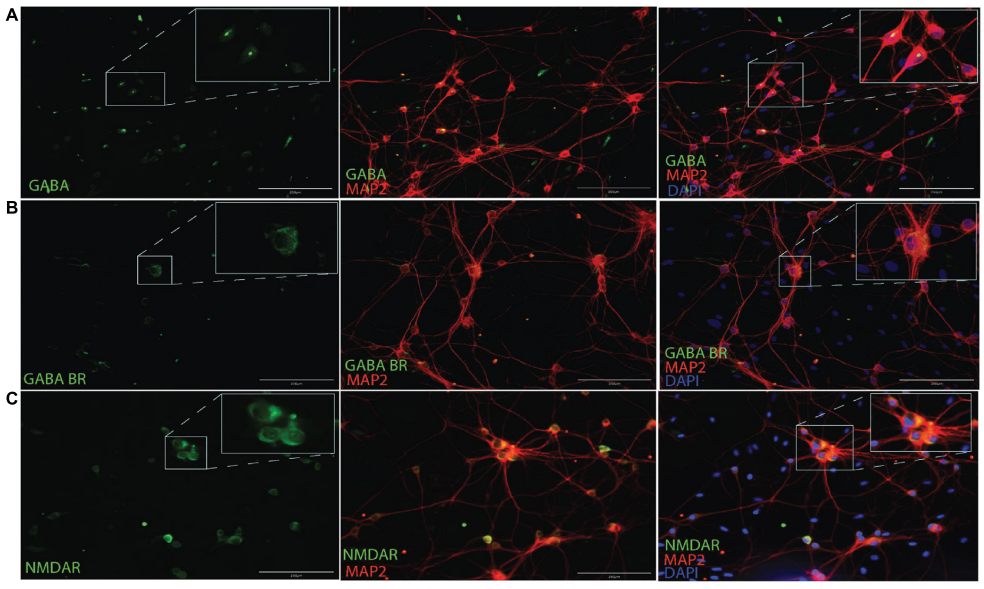

FIGURE 4
Immunocytochemistry for GABA **(A)**, GABAB receptors **(B)** and NMDA receptors **(C)** along with MAP2 neuronal cytoskeletal marker at 14 DIV. Scale bar = 200 μm.

10.3389/fncir.2023.1020487

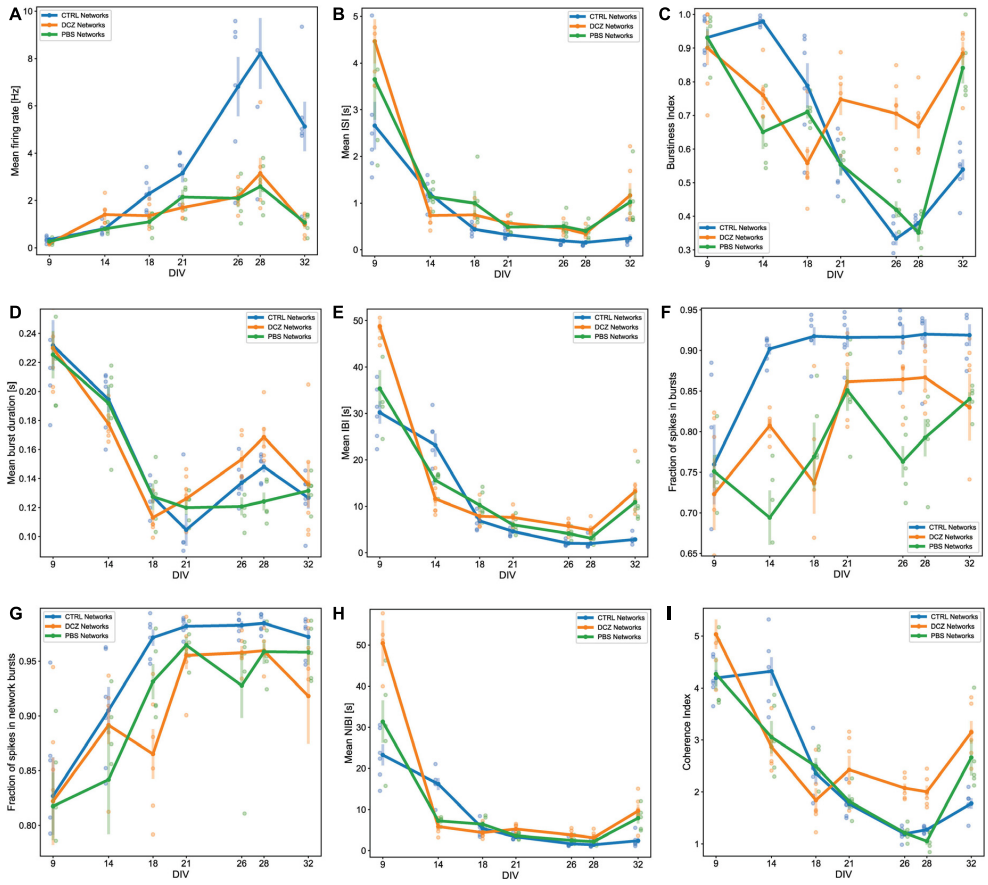

FIGURE 5
Activity and burst composition at baseline across 5 weeks of recording. Each plot presents the mean activity for all the networks in each condition [DCZ treated (n = 6), PBS vehicle (n = 5) or CTRL (n = 6)]. Network behavior for each condition is described in terms of mean firing rate **(A)**, mean inter spike intervals (ISI) **(B)**, burstiness index **(C)**, mean burst duration **(D)**, mean inter burst intervals (IBI) **(E)**, fraction of spikes in bursts **(F)**, fraction of spikes in network bursts **(G)**, mean network IBI **(H)**, and coherence index **(I)**. The solid lines with solid circles plot the mean values for all networks in one group, the shaded bars show the standard error of the mean, and the shaded circles show the individual data points (the mean activity obtained from each network in each group).

3.3. Analysis of network response and network recovery due to selective inhibition

To identify the changes in activity in the neural networks, we compared spontaneous baseline activity with activity during either DCZ treatment or PBS vehicle, as well as the network activity after DCZ removal at different time intervals. Hereafter, we refer to the recordings during DCZ treatment or PBS vehicle as "response." In these results, we have only included the analysis of the recordings done at 12 and 24 h post-washout as we were interested in the network's recovery over a longer timeframe after perturbation. These recordings will be subsequently referred to as "recovery." The response activity was analyzed in 3 phases of 20 min recordings—1st phase, 2nd phase, and 3rd phase—to better characterize dynamic network changes. The baseline activity and inhibited activity of one DCZ treated network are shown as the recording trace generated from 64 channels on the MEA (Figure 6A). Prior to DCZ application, the spontaneous firing rate at baseline was stable for the entirety of the recording, observed as regular spikes and a high occurrence of bursts containing < 10 spikes per bursts (Figure 6A, first panel labeled "Baseline"; Figures 6B, C). As expected, the application of DCZ caused a decrease in network activity and ablation of networks bursts, which was captured during the 1st phase response (Figure 6A, second panel labeled "Treatment 1st phase"). The network started exhibiting intermittent spikes and isolated bursts that gradually increased as the recording progressed (Figure 6A, third and fourth panels labeled "Treatment 2nd phase" and "Treatment 3rd phase"), indicating that network activity recovered in the presence of DCZ. We also noticed that during the 1st phase response, the DCZ

networks exhibited very low occurrences of bursts (< 2 occurrences of bursts at any timepoint during the recording period), and the occasional burst had up to 150 spikes per bursts for individual bursts (Figure 6B) and up to 800 spikes per bursts for network bursts (Figure 6C). There was also an increase in the number of burst occurrences for the 2nd and 3rd phase responses for both individual bursts and network bursts for the DCZ networks, exceeding 600 occurrences of bursts with < 10 spikes in bursts for the 3rd phase response (Figure 6B) and up to 200 occurrences of bursts with < 10 spikes in network bursts (Figure 6C). The PBS networks depicted here maintained some bursting activity during the 1st phase response, though there were lower occurrences of bursts and fewer spikes in both individual bursts and network bursts when compared to the DCZ networks (Figures 6B, C). There was, however, a gradual increase in the number of spikes in bursts at the 2nd and 3rd phase response for both individual bursts and network bursts (Figures 6B, C). The PBS networks also maintained a trend similar to DCZ networks where the most occurrences of bursts had < 10 spikes, and there were some bursts with up to 100 spikes per burst by the 3rd phase response for both individual bursts and network bursts. Unlike the inhibited networks though, which had up to 1,000 spikes per network burst by the 2nd phase response, PBS networks did not exceed 100 spikes in bursts or network bursts (Figures 6B, C).

We performed further analyses to look at both the fraction of spikes in bursts and the burstiness index for the networks at baseline, during response, and during recovery on the days that they were manipulated (14, 21, and 28 DIV). These results revealed that the CTRL networks maintained their characteristic of having > 90% of spikes located in bursts across all the recordings (baseline, response, and recovery) at 14, 21, and 28 DIV (Figures 6D–F). There were no significant changes in the fraction of spikes in bursts for CTRL networks at recovery. We noticed that there was a decrease in the fraction of spikes in bursts between baseline and 1st phase response across all the days for the PBS networks, and a slight increase during the 1 h response recording (Figures 6D–F), however, these changes were not found to be significantly different from baseline ($p > 0.05$). At 14 DIV, the PBS networks had a very quick recovery at 12 h, exhibiting > 80% of spikes in bursts which was maintained for at least 24 h. However, recovery at 12 h appeared impaired at 21 DIV, at which time point the PBS networks decreased significantly below baseline in the fraction of spikes in bursts ($p < 0.05$) (Figure 6E). Interestingly, although DCZ networks had a nonsignificant decrease in the fraction of spikes between baseline and the 1st phase response at 21 DIV, these networks stably maintained > 80% of spikes in bursts between baseline and during the 1 h response recording for all 3 days (Figures 6D–F). As expected, there was a significant decrease in the fraction of spikes in bursts after DCZ washout at 12 h compared to baseline across the 3 perturbation days. This change, however, was only significant at 21 DIV ($p < 0.005$) and 28 DIV ($p < 0.006$) (Figures 6D–F). While the CTRL networks maintained a high bursting profile at 14 DIV across all the recordings (Figure 6G), this steadily decreased until burstiness had diminished significantly by 28 DIV when compared to DCZ networks. PBS networks also had lower burstiness profiles across all the recording sessions at 28 DIV where we saw a distinct difference in burstiness at 2nd and 3rd phase responses compared to DCZ networks ($p < 0.00005$; $p < 0.00003$, respectively). The DCZ networks maintained a high burstiness especially noticeable during the 1 h response recording at 14 and 28 DIV (Figures 6G–I). However, at 21 DIV, there was a significant decrease in burstiness between baseline and the 1st phase response ($p < 0.00001$), and although there was a significant increase between 1st and 3rd phase response ($p < 0.006$), this was still significantly lower than baseline ($p < 0.05$). In addition, as can be observed in (Figures 6D–F), across all the perturbation days burstiness decreased to significant levels after washout at 12 h recovery when compared to baseline at 14 DIV ($p < 0.002$), 21 DIV ($p < 0.0000005$) and 28 DIV ($p < 0.005$). Activity in the DCZ networks did not recover to baseline levels within 24 h (Figures 6G–I).

We also found that during response at 14 DIV, the PBS and DCZ networks had overall shorter mean burst duration, and shorter mean IBI than the CTRL networks (Figures 7A, B). These differences were found to be significant when comparing DCZ with CTRL networks at 1st ($p < 0.04$), 2nd ($p < 0.04$) and 3rd ($p < 0.03$) phase responses, and PBS and CTRL networks only at 2nd ($p < 0.005$) and 3rd ($p < 0.002$) phase responses. There were no significant differences in the responses between DCZ and PBS networks. There was also a decrease in both mean burst duration and mean IBI for CTRL networks at 24 h recovery, while both DCZ and PBS networks increased in both parameters (Figures 7A, B). At 28 DIV, consistent with what was seen with the burstiness index in Figure 6I, the DCZ networks had an overall steady increase in mean burst duration during the 1 h response recording, with correspondingly longer intervals between each burst (Figures 7E, F). DCZ networks also had a decrease in both mean burst duration and mean IBI between 3rd phase response and 12 h recovery, with a slight increase in mean IBI at 24 h recovery (Figures 7E, F). Interestingly though, there was variability in the responses across the networks, especially observed at 14 and 21 DIV (Figures 7A–D). Both days showed an increase in mean burst duration at 12 h recovery for all networks, but this was sustained until 24 h only at 14 DIV (Figures 7A, C). Similarly, for both mean burst duration and mean IBI at 21 DIV, there were no significant differences in the response between any of the networks across the recordings, though there was an overall decrease in the CTRL networks compared to what was observed at 14 DIV.

3.4. Analysis of network bursts and synchrony

Since we observed that the increase in bursting activity in DCZ networks during response seemed to be a result of selective silencing, we wanted to investigate how synchronous the networks were across the different recording phases in comparison to the PBS and CTRL networks. Again, we observed that the CTRL networks exhibited between 90 and 98% of spikes consistently in network bursts across the different recording sessions and for all perturbation days (Figures 8A, C, E). However, there was notable variability in the coherence index between the networks at 14 and 21 DIV, with CTRL networks having highest values across the response phases at 14 DIV (Figure 8B). However, synchrony gradually decreased for both CTRL and PBS networks until 28 DIV, but increased for DCZ networks (Figures 8B, D, F). Though the fraction of spikes in network bursts for PBS networks decreased

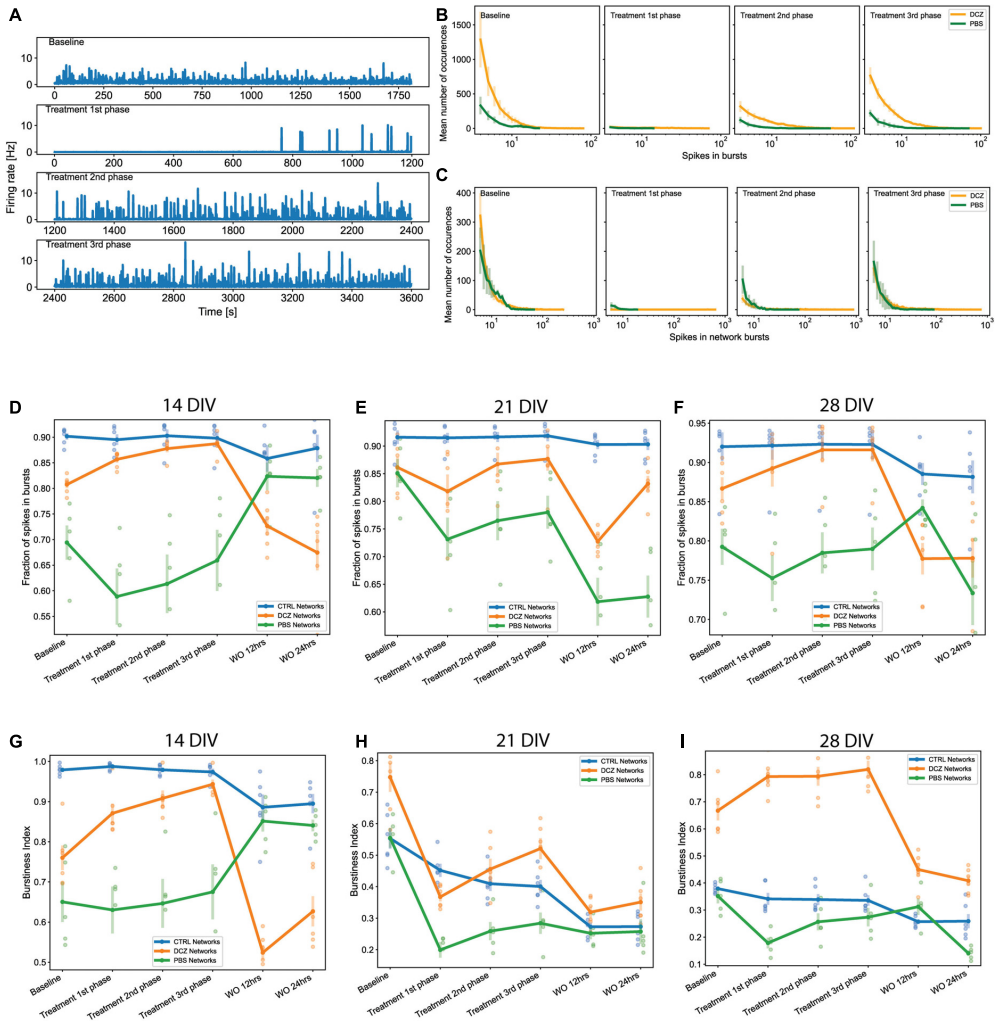

FIGURE 6
Neural network activity at baseline and in response to designer receptors exclusively activated by designer drugs (DREADDs)-mediated inhibition of excitatory synaptic transmission. Each panel in **(A)** show a trace generated from 64 recording channels of spontaneous activity of one DCZ treated network at 28 DIV. The first panel shows the 20 min recording of the spontaneous firing rate at baseline, the second, third and fourth panels show the 1st, 2nd, and 3rd phases of 20 min recordings of spontaneous activity during DCZ treatment. The *x*-axis denotes time in seconds and the *y*-axis denotes firing rate in Hz. **(B)** The spikes in bursts and **(C)** network bursts for the baseline, 1st, 2nd, and 3rd phase recordings are shown for sample DCZ treated networks ($n = 3$) and for sample PBS vehicle networks ($n = 2$). The *x*-axis denotes the number of spikes, and the *y*-axis denotes the number of burst occurrences of a given number of spikes. **(D–F)** Plots of the fraction of spikes in bursts across baseline, treatment and recovery recordings at 14, 21, and 28 DIV for all network groups ($n = 6$ for CTRL and DCZ, and $n = 5$ for PBS). The *x*-axis denotes the recording condition, and the *y*-axis denotes the percentage of spikes located in bursts. **(G–I)** Plots depicting burstiness of each network group across the baseline, treatment and recovery recordings at 14, 21, and 28 DIV. The *x*-axis denotes the recording condition, and the *y*-axis denotes the burstiness index as the fraction of activity in the 15% most active time windows. The solid lines and solid circles plot the mean values for all networks in one group, the shaded bars show the standard error of the mean, and the shaded circles show the individual data points.

between the baseline recording and the 1st phase response on all days, this was only found to be significant at 21 DIV ($p < 0.02$) (Figures 8A, C, E). The PBS networks also maintained lower synchrony than the DCZ networks during response across all days (Figures 8B, D, F). Additionally, for all the perturbation days, the DCZ networks maintained > 90% spikes in network bursts during the 1 h response recording but they did not fully recover to baseline after the media changes at 12 or 24 h (Figures 8A, C, E). Similarly, the DCZ networks also had sustained synchrony during the 1 h response recording, but reduced synchrony at 12- and 24-h recovery for all 3 perturbation days (Figures 8B, D, F). Overall, these results indicate that the inhibited networks steadily began

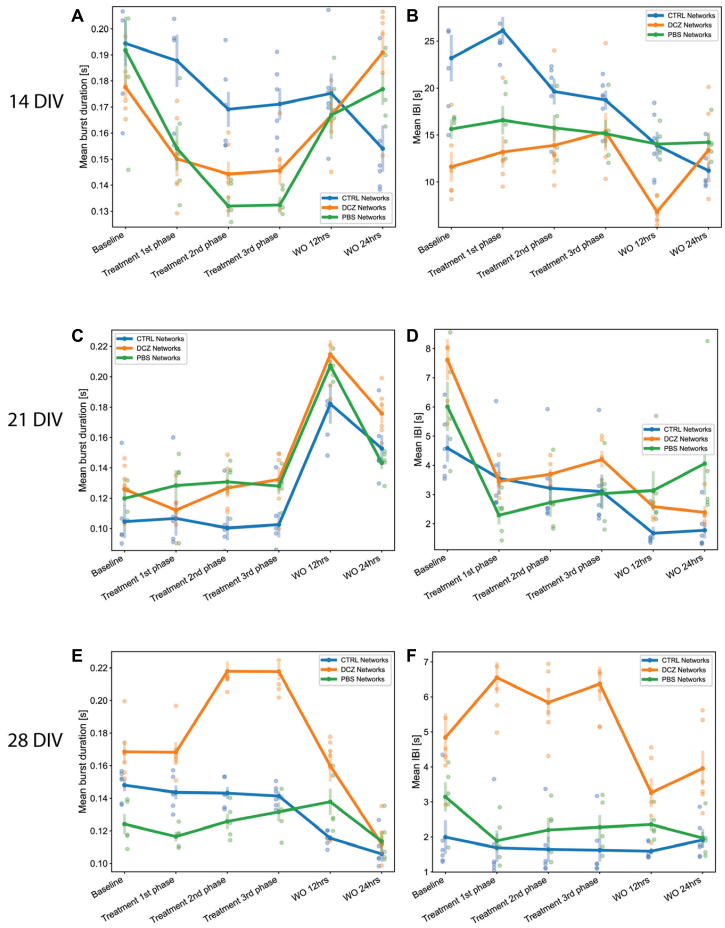

FIGURE 7
Neural network mean burst duration and mean inter burst intervals. **(A,C,E)** Plots showing the mean burst duration and **(B,D,F)** showing the mean IBIs for each network group (n = 6 for CTRL and DCZ, and n = 5 for PBS) across the baseline, treatment and recovery recordings at 14, 21, and 28 DIV. The solid lines and solid circles plot the mean values for all networks in one group, the shaded bars show the standard error of the mean, and the shaded circles show the individual data points.

developing more synchronous activity after the first perturbation session at 14 DIV but failed to recover baseline dynamics within 24 h after the perturbation.

4. Discussion

Over the last decades, an increasing amount of research is conducted to answer questions related to *in vitro* neural network development, E/I interaction, and observed spontaneous dynamic network properties in the absence of external stimuli (Latham et al., 2000). Cortical neurons *in vitro* tend to form densely connected networks by 7 DIV, as observed in this study (**Figure 1**), and by 14 DIV, the neurons had formed distinct structural organization with prominent axon fasciculation, and dendritic connections across the entire network, as well as mature excitatory and inhibitory receptors as seen in **Figure 3**. A recent study has shown that functional interactions between maturing excitatory and inhibitory synapses result in dynamic spiking activity and the emergence of network bursts (Teppola et al., 2019). Increasing either excitation or inhibition can therefore be expected to result in aberrant bursting dynamics in neural networks, thus we set out to investigate how bursting dynamics are affected and how neural networks recover when excitatory synaptic transmission is transiently inhibited. To do this, we took advantage of the unique opportunity that DREADDs provide to selectively target excitatory activity, and after transducing the networks with AAV 2/1 hM4Di CaMKlla-DREADDs, we proceeded to activate the DREADDs with DCZ at 14, 21 and 28 DIV. Our primary findings are: (1) inhibition of excitatory synaptic transmission resulted

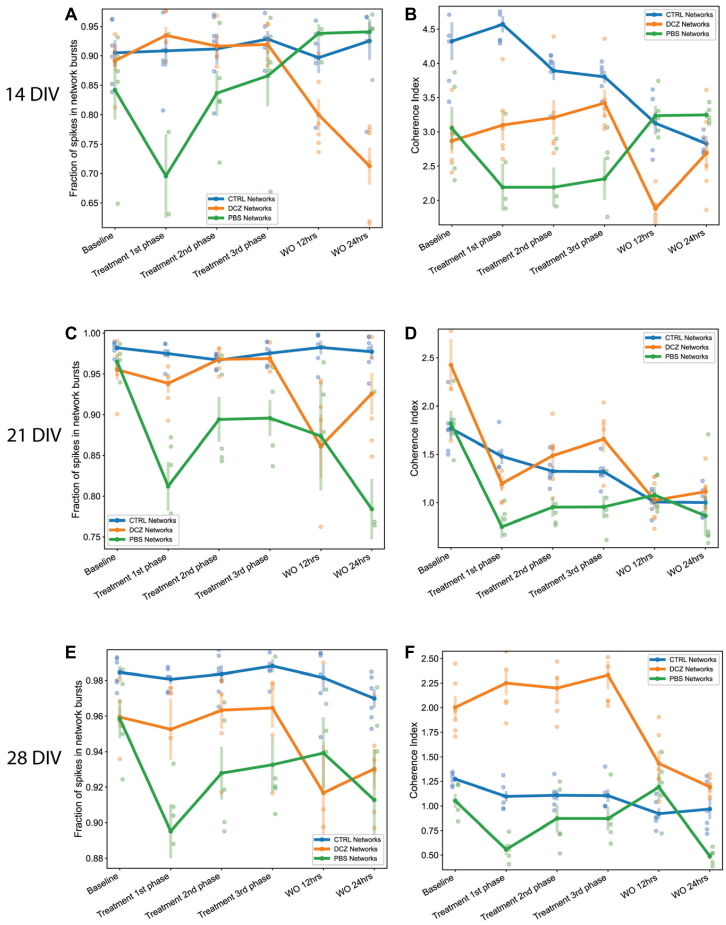

FIGURE 8
The fraction of spikes in network bursts and the measure of network synchrony across the baseline, treatment and recovery recordings at 14, 21, and 28 DIV. **(A,C,E)** Plots showing the fraction of spike in network bursts. The *x*-axis denotes the recording condition, and the *y*-axis denotes the percentage of spikes in network bursts. **(B,D,F)** Plots showing the coherence index (*y*-axis) of each network group across each recording condition (*x*-axis). The solid lines and solid circles plot the mean values for all networks in one group (n = 6 for CTRL and DCZ, and n = 5 for PBS), the shaded bars show the standard error of the mean, and the shaded circles show the individual data points.

in an increase in network burstiness by 28 DIV; (2) inhibited networks recovered activity in the presence of DCZ indicating rapid homeostatic response to network silencing; (3) by 28 DIV, inhibited networks exhibited higher synchrony and burstiness during and following selective inhibition contrary to PBS and CTRL networks that had diminished levels.

Network activity and bursting dynamics are inherently unique to each network *in vitro*, nonetheless, in our study all networks exhibited some degree of network bursting activity by 9 DIV. Early network bursts are significant for network development and maturity and are deemed to be physiologically relevant for neural information processing and synaptic plasticity (Lisman, 1997). In developing networks, bursts act as more reliable determinants of neurotransmitter release than single spikes (Lisman, 1997; Delattre et al., 2015), thus synaptic efficacy and facilitation rely on network bursts to increase the probability of postsynaptic response to presynaptic inputs. While others (Marom and Shahaf, 2002; Chiappalone et al., 2006; Wagenaar et al., 2006; Bisio et al., 2014) reported increase in network bursts toward more mature stages *in vitro* (21–28 DIV), our networks showed a propensity toward high, regular bursting activity—as can be seen in **Figures 5F, G** where over 70% of spikes occurred in bursts and network bursts—for all networks from as early as 9 DIV. Due to their early appearance, these bursts appeared to be akin to "superbursts" typically observed at earlier development, before the network establishes more mature neuronal phenotypes and before GABA receptors mature (Stephens et al., 2012) and may be driven by the early evolution of the network morphology (Kim and Lee, 2022).

Evolving network morphology plays a significant role in the electrophysiological dynamics of the networks throughout

development. Neural networks develop and mature through a bottom-up process of self-organization which can be observed everywhere in nature, from the microscopic to the macroscopic level (Turing, 1990; Kondo and Asal, 1995; Arango-Restrepo et al., 2021). The process of self-organization involves the dynamic interaction between constituent elements of a system and implies that there is a reciprocal relationship between structural organization and function (Karsenti, 2008). In physical and biological systems, self-organization is part of emergence, i.e., unpredictable interactions between known constituent elements, and drives morphogenesis (Chialvo, 2010; Dobrescu and Purcarea, 2011). Inherent to the process of self-organization of neural networks is the gradual development of complex hierarchies through local interactions (Karsenti, 2008; Sasai, 2013). Thus, each neural network can be expected to self-organize in a different way. This may explain the observed variability in the baseline activity between each experimental group, as well as between recordings from the same group as shown in **Figure 5**. It is reasonable to assume that each *in vitro* neural network will have unique mesoscale structural and functional features, such as dendritic–axonal topological arrangement, cell clustering and synaptic connections which will shape the pattern of network activity (Kaiser and Hilgetag, 2010; Klinshov et al., 2014). Neurons within clusters may receive stronger inputs, exhibit more intense activity, and contribute more to the initiation, propagation and maintenance of activity (Okujeni et al., 2017). We can still, however, confidently draw comparisons between networks given that intrinsic developmental programs, such as E/I synaptic development, govern their self-organization and emergent activity over time (Ben-Ari, 2001; Tetzlaff et al., 2010). As a result, all networks reliably exhibit consistent patterns of age dependent bursting behavior, rendering the latter a reliable measure of network development and maturity, and also network function and potential dysfunction.

It is hardly surprising that the developmental profile of total network firing and bursting activity vary from recording to recording between the networks. It should be noted that because neural activity is spontaneous and unpredictable, electrophysiological data obtained within narrow study timeframes for example < 28 DIV (Weir et al., 2015; Passaro et al., 2021), and recording time frames for example < 10 min recordings (Jimbo et al., 1999; Eytan et al., 2003; Passaro et al., 2021) may present more uniform behavior and not adequately reflect dynamic network changes. In fact, studies that monitor network activity over extended time frames have verified that neuronal dynamics can be very unstable (van Pelt et al., 2004; Gal et al., 2010). Still, variability in electrophysiological profiles may currently be underreported in the relevant literature creating a necessity for long-term investigations. In our study we monitored network activity from early development, until 32 DIV, a time frame widely accepted as a period of network maturity (Wagenaar et al., 2006). In addition, we recorded continuous spontaneous baseline activity for 20 min and, response activity for 1 h as opposed to 3–10 min recordings often reported in the literature. Our longer recordings make it easier to capture variable profiles in network activity.

Notwithstanding the variability in network activity profiles, the responses of the DCZ networks were consistent and distinct from the CTRL and PBS networks and demonstrate that selective inhibition of excitatory synaptic transmission can modulate long term network dynamics. We found that network burstiness began increasing steadily between the first and second perturbation session in DCZ networks and remained high while the PBS and CTRL networks decreased in burstiness as shown in **Figure 5C**, suggesting that selective inhibition affected the maintenance of endogenous network excitation and inhibition, and affected network bursting. Importantly, both PBS and CTRL networks showed a sustained decrease in baseline burstiness over time, as well as an overall decrease in baseline synchrony. This indicated that while bursting may be the dominant activity profile for these networks, there was still a dynamic balance being maintained between E/I, such that global inhibition may have played a role in desynchronizing the network, which may be a fundamental process in neural network development. According to studies investigating sensory coding, desynchronization in neural networks optimizes information processing and performance (Waschke et al., 2019) and may strongly improve the fidelity with which novel information is encoded (Pachitariu et al., 2015). Increased synchronization is implicated in several neurological disorders including but not limited to epilepsy and Parkinson's disease, where inhibition becomes severely impaired (Calcagnotto et al., 2005; Harrington et al., 2018). Thus, it follows that the uninhibited networks would mature and develop the appropriate excitatory and inhibitory processes necessary to maintain network activity within a healthy dynamic range and achieve desynchronization in order to optimize network information processing capabilities. The observed decrease in coherence in the DCZ networks between 9 and 18 DIV reflected what was observed in the uninhibited networks as part of the normal process of development. It is plausible that inhibition at 14 DIV may have triggered the slow synaptic plasticity process mediated by G-protein coupled signaling systems to, for example, induce long term modification of pre and postsynaptic inhibitory response (Chiu and Weliky, 2001; Rozov et al., 2017; Chiu et al., 2019). Therefore, we conclude that transient external inhibition may trigger the network to decrease endogenous inhibitory mechanisms leading to an overall increase in global activation of the neural network.

While there may be different explanations as to the cause of an increase in synchronization and a decrease in inhibition, the most plausible one may be linked to our experimental set up and methods used. In our study, the activation of hM4Di DREADDs blocks cyclic adenosine monophosphate (cAMP) production (by Gai protein blockade of adenylate cyclase), which results in neurons being unable to detect and respond to extracellular signals. Thus, DREADDs expression and activation on excitatory neurons likely prevents neurons from reliably responding to excitatory post-synaptic potentials, thereby causing disruption in activity, and the potential development of inhibitory synapses. It is well documented that excitatory synaptic activity regulates the development and maintenance of inhibitory synapses on excitatory neurons (Lin et al., 2008), and that deprivation of excitatory synaptic activity reduces the density of synaptic GABA receptors, and the number of functional inhibitory synapses in cortical cultures (Kilman et al., 2002) and hippocampal slices (Ramakers et al., 1994; Muramoto et al., 1996; Chub and O'Donovan, 1998). Furthermore, in early development, GABAR are predominantly depolarizing to promote cell proliferation, neurite growth and synapse formation (Ben-Ari, 2002). While it is still unclear when the shift from depolarization to hyperpolarization occurs (as there are significant

differences associated with sex, brain region and neuronal type) (Peerboom and Wierenga, 2021), disruption in this process due to prolonged inhibition may plausibly prevent the direction reversal of GABA currents through ionotropic GABAR leading to sustained or increased activity. In our study, the consequence of excitatory synaptic inhibition at 14 DIV was a subsequent increase in burstiness and synchrony in DCZ networks at baseline, indicating impaired inhibitory synaptic development and overall, less inhibition in the network.

Although the emerging picture is that E/I synaptic activity is the single most important factor regulating neural network bursting behavior, our results also indicate that there are intrinsic homeostatic mechanisms at work. This is especially relevant considering the recordings during response and recovery at the different perturbation days for the DCZ networks (**Figures 6–8**). According to the theory of homeostatic plasticity, network activity is stabilized by a negative feedback process where a forceful change in activity is resisted, and the system returns to a tolerated dynamic range (Turrigiano, 1999). This process typically operates on relatively slow time scales, from several hours to days, however, rapid presynaptic homeostatic plasticity following acute AMPAR blockade (Delvendahl et al., 2019), and rapid homeostatic plasticity *via* disinhibition after vision restriction (Kuhlman et al., 2013) have also been reported. The data presented in our study show that inhibited networks were able to recover network bursts during DCZ exposure, supporting several previous studies where networks bursts were maintained in the presence of activity suppressing chemogens (Chub and O'Donovan, 1998; Li et al., 2007; Zeldenrust et al., 2018). The exact mechanism for recovery during chemogenetic manipulation is unknown, however, we posit that several factors including alterations in neuromodulator levels and neurotransmitter release (Ramakers et al., 1994; Muramoto et al., 1996; Chub and O'Donovan, 1998) or sensitivity (Turrigiano et al., 1998; Desai et al., 1999) contributed to the network rescuing spontaneous activity.

Furthermore, an increase in burstiness and synchrony during DCZ silencing may indicate that silencing excitatory synaptic transmission may have lowered the spike threshold of excitatory neurons causing neurons to respond more robustly to activation, in a manner that reverberates in the network without much inhibitory control. We know from this study and others that *in vitro*, neurons tend to connect with each other in a modular organization of several clusters connected by both long- and short-range connections (Antonello et al., 2022). Within a network with reduced inhibition, as one module becomes activated whether spontaneously or due to external influence, the activity will quickly spread throughout the network in a positive feedback manner, increasing network synchronization (Huang et al., 2017). Our results also suggest that homeostatic mechanisms might play a role in the recovery of the DCZ networks at 28 DIV as seen with the decrease in burst duration and IBIs (**Figure 7**) as well as burstiness and synchrony (**Figure 8**) between 3rd phase response and 12 h recovery. We cannot entirely exclude, however, that such changes may be related to the media changes done in order to wash out DCZ from the networks. Also, though activity recovered in the sense that there was a decrease in burstiness and synchrony, the inhibited networks did not recover to baseline, but rather had drastically lower activity at both 12- and 24-h recovery as shown in **Figures 6–8**. This may indicate that recovery to baseline is a very slow process and takes longer than 24 h, especially before the networks reach 28 DIV. Since there was an increase in both baseline burstiness and coherence between 28 and 32 DIV for all networks as shown in **Figure 5**, it would be interesting to see whether this would stabilize as the networks get older and remain unperturbed and unstimulated.

Finally, an unexpected observation was a response to PBS vehicle between the baseline and 1st phase responses in PBS networks. PBS is often used as a vehicle in many *in vitro* and *in vivo* experiments. Addition of 10% PBS as a vehicle might have affected the concentration of media nutrients and caused a response in the firing activity. On the other hand, the observed effects may be merely due to intrinsic differences in each network in the PBS group. As it relates to the DCZ networks and the variability in the response between baseline and treatment 1st phase especially at 14 and 21 DIV, we cannot rule out that this may be due to where the DREADDs hM4Di are located in the network, and how they get activated. Although several protocols were tested to optimize the concentration of AAV DREADDs and DCZ ligand, we cannot be certain that the same DREADDs on the same neurons, or even on the same part of the network were being activated every time. To our knowledge, this combination using AAV DREADDs, and the novel synthetic ligand DCZ has not been used *in vitro* with dissociated primary neurons, so there are still great possibilities to explore in this area of research.

5. Conclusion and future directions

In this study, we investigated the responses of *in vitro* neural networks to transient selective inhibition of excitatory synaptic transmission, and network recovery from perturbation. We examined characteristics of network bursting dynamics over time, as well as network burstiness and synchrony. We found that while uninhibited networks developed with most of their spikes located in network bursts, inhibited networks overall exhibited more burstiness and synchrony at maturity. The burstiness and synchrony was also maintained during network response recordings, indicating homeostatic mechanisms restoring network activity in the presence of the ligand. The overall increase in burstiness and synchrony after the first perturbation, may be due to a decrease in endogenous inhibitory mechanisms caused by long term inhibitory synaptic modifications. In future studies it will be interesting to monitor the networks in the long term to see how the recovery profile changes with network maturity. As well as investigate the long-term implications of excitatory synaptic silencing on functional connectivity. There might have been some remodeling of synaptic attributes and/or reorganization of the structural network, which would make the network less efficient at information transmission due to the increased synchrony. This hypothesis can be tested further using high density MEAs that offer higher spatial resolution for network connectivity investigation.

Data availability statement

The raw data supporting the conclusions of this article will be made available by the authors, without undue reservation.

Author contributions

JW: conceptualization, investigation (cell experiments, protocol development and optimization, AAV investigations, immunocytochemistry, and electrophysiology recordings), data visualization, writing—original draft, and review and editing. NC: methodology, data analysis (preprocessing, scripts, and visualization), statistical analyses, and writing—review and editing. AS and IS: conceptualization, funding acquisition, writing—review and editing, and supervision. All authors contributed to the article and approved the submitted version.

Funding

This project is part of the SOCRATES (Self-Organizing Computational SubstRATES) project and is funded by the Research Council of Norway (NFR and IKT Pluss), grant number: 270961, and ALS Norge.

Acknowledgments

We would like to thank Prof. Morten Høydal, Department of Circulation and Medical Imaging, NTNU, for facilitating access to the Axion Electrophysiology System, and Dr. Rajeevkumar Nair Raveendran, Viral Vector Core Facility, Kavli Institute for Systems Neuroscience, NTNU, for the design and preparation of the AAV DREADDs constructs.

Conflict of interest

The authors declare that the research was conducted in the absence of any commercial or financial relationships that could be construed as a potential conflict of interest.

Publisher's note

All claims expressed in this article are solely those of the authors and do not necessarily represent those of their affiliated organizations, or those of the publisher, the editors and the reviewers. Any product that may be evaluated in this article, or claim that may be made by its manufacturer, is not guaranteed or endorsed by the publisher.

References

Alexander, G. M., Rogan, S. C., Abbas, A. I., Armbruster, B. N., Pei, Y., Allen, J. A., et al. (2009). Remote control of neuronal activity in transgenic mice expressing evolved G protein-coupled receptors. *Neuron* 63, 27–39. doi: 10.1016/j.neuron.2009.06.014

Antonello, P. C., Varley, T. F., Beggs, J., Porcionatto, M., Sporns, O., and Faber, J. (2022). Self-organization of in vitro neuronal assemblies drives to complex network topology. *Elife* 11:e74921. doi: 10.7554/eLife.74921

Arango-Restrepo, A., Barragán, D., and Rubi, J. M. (2021). A criterion for the formation of nonequilibrium self-assembled structures. *J. Phys. Chem. B* 125, 1838–1845. doi: 10.1021/acs.jpcb.0c07824

Armbruster, B. N., Li, X., Pausch, M. H., Herlitze, S., and Roth, B. L. (2007). Evolving the lock to fit the key to create a family of G protein-coupled receptors potently activated by an inert ligand. *Proc. Natl. Acad. Sci. U.S.A.* 104, 5163–5168. doi: 10.1073/pnas.0700293104

Bakkum, D. J., Radivojevic, M., Frey, U., Franke, F., Hierlemann, A., and Takahashi, H. (2013). Parameters for burst detection. *Front. Comput. Neurosci.* 7:193. doi: 10.3389/fncom.2013.00193

Baltz, T., De Lima, A., and Voigt, T. (2010). Contribution of GABAergic interneurons to the development of spontaneous activity patterns in cultured neocortical networks. *Front. Cell Neurosci.* 4:15. doi: 10.3389/fncel.2010.00015

Ben-Ari, Y. (2001). Developing networks play a similar melody. *Trends Neurosci.* 24, 353–360. doi: 10.1016/s0166-2236(00)01813-0

Ben-Ari, Y. (2002). Excitatory actions of gaba during development: The nature of the nurture. *Nat. Rev. Neurosci.* 3, 728–739. doi: 10.1038/nrn920

Bisio, M., Bosca, A., Pasquale, V., Berdondini, L., and Chiappalone, M. (2014). Emergence of bursting activity in connected neuronal sub-populations. *PLoS One* 9:e107400. doi: 10.1371/journal.pone.0107400

Bjorkli, C., Ebbesen, N. C., Julian, J. B., Witter, M. P., Sandvig, A., and Sandvig, I. (2022). Manipulation of neuronal activity in the entorhinal-hippocampal circuit affects intraneuronal amyloid-β levels. *bioRxiv [Preprint]* 2022.07.05.498797. doi: 10.1101/2022.07.05.498797

Blankenship, A. G., and Feller, M. B. (2010). Mechanisms underlying spontaneous patterned activity in developing neural circuits. *Nat. Rev. Neurosci.* 11, 18–29.

Burgard, E. C., and Hablitz, J. J. (1994). Developmental-changes in the voltage-dependence of neocortical NMDA responses. *Dev. Brain Res.* 80, 275–278. doi: 10.1016/0165-3806(94)90113-9

Calcagnotto, M. E., Paredes, M. F., Tihan, T., Barbaro, N. M., and Baraban, S. C. (2005). Dysfunction of synaptic inhibition in epilepsy associated with focal cortical dysplasia. *J. Neurosci.* 25, 9649–9657.

Chialvo, D. R. (2010). Emergent complex neural dynamics. *Nat. Phy.* 6, 744–750.

Chiappalone, M., Bove, M., Vato, A., Tedesco, M., and Martinoia, S. (2006). Dissociated cortical networks show spontaneously correlated activity patterns during in vitro development. *Brain Res.* 1093, 41–53.

Chiappalone, M., Novellino, A., Vajda, I., Vato, A., Martinoia, S., and Van Pelt, J. (2005). Burst detection algorithms for the analysis of spatio-temporal patterns in cortical networks of neurons. *Neurocomputing* 65–66, 653–662.

Chiappalone, M., Vato, A., Berdondini, L., Koudelka-Hep, M., and Martinoia, S. (2007). Network dynamics and synchronous activity in cultured cortical neurons. *Int. J. Neural. Syst.* 17, 87–103.

Chiu, C., and Weliky, M. (2001). Spontaneous activity in developing ferret visual cortex in vivo. *J. Neurosci.* 21, 8906–8914.

Chiu, C. Q., Barberis, A., and Higley, M. J. (2019). Preserving the balance: Diverse forms of long-term Gabaergic synaptic plasticity. *Nat. Rev. Neurosci.* 20, 272–281. doi: 10.1038/s41583-019-0141-5

Chub, N., and O'Donovan, M. J. (1998). Blockade and recovery of spontaneous rhythmic activity after application of neurotransmitter antagonists to spinal networks of the chick embryo. *J. Neurosci.* 18, 294–306. doi: 10.1523/JNEUROSCI.18-01-00294.1998

Cotterill, E., Charlesworth, P., Thomas, C. W., Paulsen, O., and Eglen, S. J. (2016). A comparison of computational methods for detecting bursts in neuronal spike trains and their application to human stem cell-derived neuronal networks. *J. Neurophysiol.* 116, 306–321. doi: 10.1152/jn.00093.2016

Darbon, P., Yvon, C., Legrand, J. C., and Streit, J. (2004). INaP underlies intrinsic spiking and rhythm generation in networks of cultured rat spinal cord neurons. *Eur. J. Neurosci.* 20, 976–988.

Delattre, V., Keller, D., Perich, M., Markram, H., and Muller, E. B. (2015). Network-timing-dependent plasticity. *Front. Cell Neurosci.* 9:220. doi: 10.3389/fncel.2015.00220

Delvendahl, I., Kita, K., and Müller, M. (2019). Rapid and sustained homeostatic control of presynaptic exocytosis at a central synapse. *Proc. Natl. Acad. Sci. U.S.A.* 116, 23783–23789. doi: 10.1073/pnas.1909675116

Desai, N. S., Rutherford, L. C., and Turrigiano, G. G. (1999). Plasticity in the intrinsic excitability of cortical pyramidal neurons. *Nat. Neurosci.* 2, 515–520.

Dizon, M. J., and Khodakhah, K. (2011). The role of interneurons in shaping Purkinje cell responses in the cerebellar cortex. *J. Neurosci.* 31, 10463–10473.

Dobrescu, R., and Purcarea, V. I. (2011). Emergence, self-organization and morphogenesis in biological structures. *J. Med. Life* 4, 82–90.

Eytan, D., Brenner, N., and Marom, S. (2003). Selective adaptation in networks of cortical neurons. *J. Neurosci.* 23, 9349–9356.

Fardet, T., Ballandras, M., Bottani, S., Metens, S., and Monceau, P. (2018). Understanding the generation of network bursts by adaptive oscillatory neurons. *Front. Neurosci.* 12:41. doi: 10.3389/fnins.2018.00041

Gal, A., Eytan, D., Wallach, A., Sandler, M., Schiller, J., and Marom, S. (2010). Dynamics of excitability over extended timescales in cultured cortical neurons. *J. Neurosci.* 30, 16332–16342.

Gandolfo, M., Maccione, A., Tedesco, M., Martinoia, S., and Berdondini, L. (2010). Tracking burst patterns in hippocampal cultures with high-density CMOS-MEAs. *J. Neural. Eng.* 7:056001. doi: 10.1088/1741-2560/7/5/056001

Geiger, J. R., Melcher, T., Koh, D. S., Sakmann, B., Seeburg, P. H., Jonas, P., et al. (1995). Relative abundance of subunit mRNAs determines gating and Ca2+ permeability of Ampa receptors in principal neurons and interneurons in rat CNS. *Neuron* 15, 193–204. doi: 10.1016/0896-6273(95)90076-4

Haaranen, M., Schafer, A., Jarvi, V., and Hyytia, P. (2020a). Chemogenetic stimulation and silencing of the insula, amygdala, nucleus accumbens, and their connections differentially modulate alcohol drinking in rats. *Front. Behav. Neurosci.* 14:580849. doi: 10.3389/fnbeh.2020.580849

Haaranen, M., Scuppa, G., Tambalo, S., Jarvi, V., Bertozzi, S. M., Armirotti, A., et al. (2020b). Anterior insula stimulation suppresses appetitive behavior while inducing forebrain activation in alcohol-preferring rats. *Transl. Psychiatry* 10:150. doi: 10.1038/s41398-020-0833-7

Harrington, D. L., Shen, Q., Theilmann, R. J., Castillo, G. N., Litvan, I., Filoteo, J. V., et al. (2018). Altered functional interactions of inhibition regions in cognitively normal Parkinson's disease. *Front. Aging Neurosci.* 10:331. doi: 10.3389/fnagi.2018.00331

Hestrin, S. (1993). Different glutamate receptor channels mediate fast excitatory synaptic currents in inhibitory and excitatory cortical neurons. *Neuron* 11, 1083–1091.

Hoehne, A., Mcfadden, M. H., and Digregorio, D. A. (2020). Feed-forward recruitment of electrical synapses enhances synchronous spiking in the mouse cerebellar cortex. *Elife* 9:e57344. doi: 10.7554/eLife.57344

Huang, Y. T., Chang, Y. L., Chen, C. C., Lai, P. Y., and Chan, C. K. (2017). Positive feedback and synchronized bursts in neuronal cultures. *PLoS One* 12:e0187276. doi: 10.1371/journal.pone.0187276

Jimbo, Y., Tateno, T., and Robinson, H. P. (1999). Simultaneous induction of pathway-specific potentiation and depression in networks of cortical neurons. *Biophys. J.* 76, 670–678. doi: 10.1016/S0006-3495(99)77234-6

Kaiser, M., and Hilgetag, C. C. (2010). Optimal hierarchical modular topologies for producing limited sustained activation of neural networks. *Front. Neuroinform.* 4:8. doi: 10.3389/fninf.2010.00008

Kamioka, H., Maeda, E., Jimbo, Y., Robinson, H. P., and Kawana, A. (1996). Spontaneous periodic synchronized bursting during formation of mature patterns of connections in cortical cultures. *Neurosci. Lett.* 206, 109–112. doi: 10.1016/s0304-3940(96)12448-4

Karsenti, E. (2008). Self-organization in cell biology: A brief history. *Nat. Rev. Mol. Cell. Biol.* 9, 255–262.

Khambhati, A. N., and Bassett, D. S. (2016). A powerful DREADD: Revealing structural drivers of functional dynamics. *Neuron* 91, 213–215. doi: 10.1016/j.neuron.2016.07.011

Kilman, V., Van Rossum, M. C. W., and Turrigiano, G. G. (2002). Activity deprivation reduces miniature IPSC amplitude by decreasing the number of postsynaptic GABA(A) receptors clustered at neocortical synapses. *J. Neurosci.* 22, 1328–1337. doi: 10.1523/JNEUROSCI.22-04-01328.2002

Kim, B., and Lee, K. J. (2022). Self-organized neuronal subpopulations and network morphology underlying superbursts. *New J. Phys.* 24:043047. doi: 10.1088/1367-2630/ac52c2

Klinshov, V. V., Teramae, J. N., Nekorkin, V. I., and Fukai, T. (2014). Dense neuron clustering explains connectivity statistics in cortical microcircuits. *PLoS One.* 9:e94292. doi: 10.1371/journal.pone.0094292

Kondo, S., and Asal, R. (1995). A reaction-diffusion wave on the skin of the marine angelfish Pomacanthus. *Nature* 376, 765–768. doi: 10.1038/376765a0

Kudela, P., Franaszczuk, P. J., and Bergey, G. K. (2003). Changing excitation and inhibition in simulated neural networks: Effects on induced bursting behavior. *Biol. Cybern.* 88, 276–285. doi: 10.1007/s00422-002-0381-7

Kuhlman, S. J., Olivas, N. D., Tring, E., Ikrar, T., Xu, X., and Trachtenberg, J. T. (2013). A disinhibitory microcircuit initiates critical-period plasticity in the visual cortex. *Nature* 501, 543–546.

Latham, P. E., Richmond, B. J., Nelson, P. G., and Nirenberg, S. (2000). Intrinsic dynamics in neuronal networks. I. Theory. *J. Neurophysiol.* 83, 808–827.

Lebonville, C. L., Paniccia, J. E., Parekh, S. V., Wangler, L. M., Jones, M. E., Fuchs, R. A., et al. (2020). Expression of a heroin contextually conditioned immune effect in male rats requires CaMKIIα-expressing neurons in dorsal, but not ventral, subiculum and hippocampal CA1. *Brain Behav. Immun.* 89, 414–422. doi: 10.1016/j.bbi.2020.07.028

Li, X., Zhou, W., Zeng, S., Liu, M., and Luo, Q. (2007). Long-term recording on multi-electrode array reveals degraded inhibitory connection in neuronal network development. *Biosens. Bioelectron.* 22, 1538–1543. doi: 10.1016/j.bios.2006.05.030

Lin, Y., Bloodgood, B. L., Hauser, J. L., Lapan, A. D., Koon, A. C., Kim, T. K., et al. (2008). Activity-dependent regulation of inhibitory synapse development by Npas4. *Nature* 455, 1198–1204.

Lisman, J. E. (1997). Bursts as a unit of neural information: Making unreliable synapses reliable. *Trends Neurosci.* 20, 38–43. doi: 10.1016/S0166-2236(96)10070-9

Magalhaes, K. S., Da Silva, M. P., Mecawi, A. S., Paton, J. F. R., Machado, B. H., and Moraes, D. J. A. (2021). Intrinsic and synaptic mechanisms controlling the expiratory activity of excitatory lateral parafacial neurones of rats. *J. Physiol.* 599, 4925–4948. doi: 10.1113/JP281545

Marom, S., and Shahaf, G. (2002). Development, learning and memory in large random networks of cortical neurons: Lessons beyond anatomy. *Q. Rev. Biophys.* 35, 63–87. doi: 10.1017/s0033583501003742

Muramoto, T., Mendelson, B., Phelan, K. D., Garcia-Rill, E., Skinner, R. D., and Puskarich-May, C. (1996). Developmental changes in the effects of serotonin and N-methyl-D-aspartate on intrinsic membrane properties of embryonic chick motoneurons. *Neuroscience* 75, 607–618. doi: 10.1016/0306-4522(96)00185-6

Nagai, Y., Miyakawa, N., Takuwa, H., Hori, Y., Oyama, K., Ji, B., et al. (2020). Deschloroclozapine, a potent and selective chemogenetic actuator enables rapid neuronal and behavioral modulations in mice and monkeys. *Nat. Neurosci.* 23, 1157–1167. doi: 10.1038/s41593-020-0661-3

Obien, M. E. J., Deligkaris, K., Bullmann, T., Bakkum, D. J., and Frey, U. (2015). Revealing neuronal function through microelectrode array recordings. *Front. Neurosci.* 8:423. doi: 10.3389/fnins.2014.00423

Okujeni, S., Kandler, S., and Egert, U. (2017). Mesoscale architecture shapes initiation and richness of spontaneous network activity. *J. Neurosci.* 37:3972. doi: 10.1523/JNEUROSCI.2552-16.2017

Opitz, T., De Lima, A. D., and Voigt, T. (2002). Spontaneous development of synchronous oscillatory activity during maturation of cortical networks in vitro. *J. Neurophysiol.* 88, 2196–2206.

Ozawa, A., and Arakawa, H. (2021). Chemogenetics drives paradigm change in the investigation of behavioral circuits and neural mechanisms underlying drug action. *Behav. Brain Res.* 406:113234. doi: 10.1016/j.bbr.2021.113234

Pachitariu, M., Lyamzin, D. R., Sahani, M., and Lesica, N. A. (2015). State-dependent population coding in primary auditory cortex. *J. Neurosci.* 35, 2058–2073.

Panthi, S., and Leitch, B. (2019). The impact of silencing feed-forward parvalbumin-expressing inhibitory interneurons in the cortico-thalamocortical network on seizure generation and behaviour. *Neurobiol. Dis.* 132:104610. doi: 10.1016/j.nbd.2019.104610

Pasquale, V., Martinoia, S., and Chiappalone, M. (2010). A self-adapting approach for the detection of bursts and network bursts in neuronal cultures. *J. Comput. Neurosci.* 29, 213–229. doi: 10.1007/s10827-009-0175-1

Passaro, A. P., Aydin, O., Saif, M. T. A., and Stice, S. L. (2021). Development of an objective index, neural activity score (NAS), reveals neural network ontogeny and treatment effects on microelectrode arrays. *Sci. Rep.* 11:9110. doi: 10.1038/s41598-021-88675-w

Peerboom, C., and Wierenga, C. J. (2021). The postnatal GABA shift: A developmental perspective. *Neurosci. Biobehav. Rev.* 124, 179–192.

Pena, F., and Ramirez, J. M. (2004). Substance P-mediated modulation of pacemaker properties in the mammalian respiratory network. *J. Neurosci.* 24, 7549–7556. doi: 10.1523/JNEUROSCI.1871-04.2004

Perez-Rando, M., Castillo-Gomez, E., Guirado, R., Blasco-Ibanez, J. M., Crespo, C., Varea, E., et al. (2017). NMDA receptors regulate the structural plasticity of spines and axonal boutons in hippocampal interneurons. *Front. Cell. Neurosci.* 11:166. doi: 10.3389/fncel.2017.00166

Ramakers, G. J., Corner, M. A., and Habets, A. M. (1990). Development in the absence of spontaneous bioelectric activity results in increased stereotyped burst firing in cultures of dissociated cerebral cortex. *Exp. Brain Res.* 79, 157–166. doi: 10.1007/BF00228885

Ramakers, G. J., Van Galen, H., Feenstra, M. G., Corner, M. A., and Boer, G. J. (1994). Activity-dependent plasticity of inhibitory and excitatory amino acid transmitter systems in cultured rat cerebral cortex. *Int. J. Dev. Neurosci.* 12, 611–621. doi: 10.1016/0736-5748(94)90013-2

Raus Balind, S., Magó, A., Ahmadi, M., Kis, N., Varga-Németh, Z., Lőrincz, A., et al. (2019). Diverse synaptic and dendritic mechanisms of complex spike burst generation in hippocampal CA3 pyramidal cells. *Nat. Commun.* 10:1859. doi: 10.1038/s41467-019-09767-w

Robinson, H. P., Kawahara, M., Jimbo, Y., Torimitsu, K., Kuroda, Y., and Kawana, A. (1993). Periodic synchronized bursting and intracellular calcium transients elicited

by low magnesium in cultured cortical neurons. *J. Neurophysiol.* 70, 1606–1616. doi: 10.1152/jn.1993.70.4.1606

Rozov, A. V., Valiullina, F. F., and Bolshakov, A. P. (2017). Mechanisms of long-term plasticity of hippocampal GABAergic synapses. *Biochemistry (Mosc)* 82, 257–263.

Sasai, Y. (2013). Cytosystems dynamics in self-organization of tissue architecture. *Nature* 493, 318–326. doi: 10.1038/nature11859

Schroeter, M. S., Charlesworth, P., Kitzbichler, M. G., Paulsen, O., and Bullmore, E. T. (2015). Emergence of rich-club topology and coordinated dynamics in development of hippocampal functional networks in vitro. *J. Neurosci.* 35, 5459–5470. doi: 10.1523/JNEUROSCI.4259-14.2015

Stephens, C. L., Toda, H., Palmer, T. D., Demarse, T. B., and Ormerod, B. K. (2012). Adult neural progenitor cells reactivate superbursting in mature neural networks. *Exp. Neurol.* 234, 20–30. doi: 10.1016/j.expneurol.2011.12.009

Sun, J. J., Kilb, W., and Luhmann, H. J. (2010). Self-organization of repetitive spike patterns in developing neuronal networks in vitro. *Eur. J. Neurosci.* 32, 1289–1299.

Suresh, J., Radojicic, M., Pesce, L. L., Bhansali, A., Wang, J., Tryba, A. K., et al. (2016). Network burst activity in hippocampal neuronal cultures: The role of synaptic and intrinsic currents. *J. Neurophysiol.* 115, 3073–3089.

Teppola, H., Acimovic, J., and Linne, M. L. (2019). Unique features of network bursts emerge from the complex interplay of excitatory and inhibitory receptors in rat neocortical networks. *Front. Cell. Neurosci.* 13:377. doi: 10.3389/fncel.2019.00377

Tetzlaff, C., Okujeni, S., Egert, U., Wörgötter, F., and Butz, M. (2010). Self-organized criticality in developing neuronal networks. *PLoS Comput. Biol.* 6:e1001013. doi: 10.1371/journal.pcbi.1001013

Turing, A. M. (1990). The chemical basis of morphogenesis. 1953. *Bull. Math. Biol.* 52, 153–197; discussion 119–152.

Turrigiano, G. G. (1999). Homeostatic plasticity in neuronal networks: The more things change, the more they stay the same. *Trends Neurosci.* 22, 221–227. doi: 10.1016/s0166-2236(98)01341-1

Turrigiano, G. G., Leslie, K. R., Desai, N. S., Rutherford, L. C., and Nelson, S. B. (1998). Activity-dependent scaling of quantal amplitude in neocortical neurons. *Nature* 391, 892–896.

Urban, D. J., and Roth, B. L. (2015). Dreadds (designer receptors exclusively activated by designer drugs): Chemogenetic tools with therapeutic utility. *Annu. Rev. Pharmacol. Toxicol.* 55, 399–417.

van Drongelen, W., Koch, H., Elsen, F. P., Lee, H. C., Mrejeru, A., Doren, E., et al. (2006). Role of persistent sodium current in bursting activity of mouse neocortical networks in vitro. *J. Neurophysiol.* 96, 2564–2577. doi: 10.1152/jn.00446.2006

van Pelt, J., Wolters, P. S., Corner, M. A., Rutten, W. L., and Ramakers, G. J. (2004). Long-term characterization of firing dynamics of spontaneous bursts in cultured neural networks. *IEEE Trans. Biomed. Eng.* 51, 2051–2062.

Verkhratsky, A., and Kirchhoff, F. (2007). NMDA receptors in glia. *Neuroscientist* 13, 28–37.

Wagenaar, D. A., Madhavan, R., Pine, J., and Potter, S. M. (2005). Controlling bursting in cortical cultures with closed-loop multi-electrode stimulation. *J. Neurosci.* 25, 680–688. doi: 10.1523/JNEUROSCI.4209-04.2005

Wagenaar, D. A., Pine, J., and Potter, S. M. (2006). An extremely rich repertoire of bursting patterns during the development of cortical cultures. *BMC Neurosci.* 7:11. doi: 10.1186/1471-2202-7-11

Waschke, L., Tune, S., and Obleser, J. (2019). Local cortical desynchronization and pupil-linked arousal differentially shape brain states for optimal sensory performance. *eLife* 8:e51501. doi: 10.7554/eLife.51501

Weir, K., Blanquie, O., Kilb, W., Luhmann, H. J., and Sinning, A. (2015). Comparison of spike parameters from optically identified GABAergic and glutamatergic neurons in sparse cortical cultures. *Front. Cell. Neurosci.* 8:460. doi: 10.3389/fncel.2014.00460

Whissell, P. D., Tohyama, S., and Martin, L. J. (2016). The use of DREADDs to deconstruct behavior. *Front. Genet.* 7:70. doi: 10.3389/fgene.2016.00070

Zeldenrust, F., Wadman, W. J., and Englitz, B. (2018). Neural coding with bursts-current state and future perspectives. *Front. Computat. Neurosci.* 12:48. doi: 10.3389/fncom.2018.00048

PAPER II

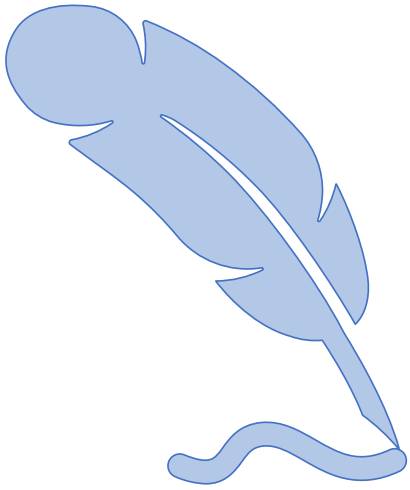

Inhibition of excitatory synaptic transmission alters functional organization and efficiency in cortical neural networks

Janelle S. Weir[1]*, Ola Huse Ramstad[1,2], Axel Sandvig[1,3,4,5], Ioanna Sandvig[1]*

[1]Department of Neuromedicine and Movement Science, Faculty of Medicine, Norwegian University of Science and Technology, Trondheim, Norway
[2]Department of Information Technology, Oslo Metropolitan University, Oslo, Norway
[3]Department of Neurology and Clinical Neurophysiology, St. Olav's University Hospital, Trondheim, Norway
[4]Department of Pharmacology and Clinical Neurosciences, Division of Neuro, Head and Neck, Umeå University Hospital, Umeå, Sweden,
[5]Department of Community Medicine and Rehabilitation, Division of Neuro, Head and Neck, Umeå University Hospital, Umeå, Sweden

*** Correspondence:** janelle.s.weir@ntnu.no ioanna.sandvig@ntnu.no

Word count: Abstract: 281 Body excluding figure captions and references: 4300
Number of tables: 1
Number of figures: 6
Keywords: Cortical neural networks, Modularity, Cluster coefficient, Path Length, Neuroplasticity, Network reorganization

Abstract

Fundamental neural mechanisms such as activity dependent Hebbian and homeostatic neuroplasticity are driven by balanced excitatory – inhibitory synaptic transmission, and work in tandem to coordinate and regulate complex neural network dynamics in both healthy and perturbed conditions. These neuroplasticity processes shape neural network activity, as well as structural and functional aspects of network organization, information transmission and processing. While crucial for all aspects of network function, understanding how the brain utilizes plasticity mechanisms to retain or regain function during and after perturbation is often challenging. This is because these processes occur at varying spatiotemporal scales simultaneously across diverse circuits and brain regions and are thus highly complicated to distinguish from other underlying mechanisms. However, neuroplasticity and self-organizing properties of the brain are largely conserved in *in vitro* biological neural networks, and as such, these networks enable us to investigate both structural and functional plasticity responses to perturbation networks at the micro and mesoscale level. In this study, we selectively silenced excitatory synaptic transmission in *in vitro* neural networks to investigate the impact of the perturbation on structural and functional network organization and resilience. Our results demonstrate that selective inhibition of excitatory transmission leads to transient de-clustering of modular structure, increased path length and degree in perturbed networks. These changes indicate a transient loss of network efficiency; with the network subsequently reorganizing to a state of increased clustering and short path lengths following recovery. These findings highlight the remarkable capacity of neural networks to reconfigure their functional organization following perturbation. The ability to detect and decode such processes as they evolve highlights the robustness of our models to investigate certain dynamic network properties that are often not accessible by *in vivo* methods.

1 Introduction

Complex self-organizing systems like *in vitro* neural networks spontaneously acquire structural and functional organization through dynamic activity independent (Goodman and Shatz 1993) and activity dependent (Kater, Davenport et al. 1994, Kirwan, Turner-Bridger et al. 2015) interactions between constituent elements of the network. During network development, structural connectivity is initially characterized by a dense meshwork of neurite connections and synapse overproduction which is subsequently sculpted by experience-driven synaptic pruning and connection refinement (Ivenshitz and Segal 2010, Fauth and Tetzlaff 2016, Millan, Torres et al. 2018). These processes occur concurrently with the maturation of excitatory and inhibitory synapses (Huang 2009), which have pivotal roles in initiating, regulating, and balancing the neural activity within these networks. While excitatory synapses enhance signal transmission, inhibitory synapses act as regulators, effectively controlling and modulating overall network activity levels. The precise coordination between these two types of synapses is crucial for establishing a well-functioning and adaptable neural network (Zhang and Sun 2011). As structural connectivity becomes more refined, these synapses mature and optimize their function, ultimately contributing to the establishment of efficient and effective neural circuitry (Najafi, Elsayed et al. 2020, Sukenik, Vinogradov et al. 2021) manifesting through the emergence of complex network activity such as network bursts and synchrony (Ben-Ari 2001, Opitz, De Lima et al. 2002, Wagenaar, Pine et al. 2006, Chiappalone, Vato et al. 2007).

A key characteristic of self-organizing neural networks is the progressive advancement from a less organized state to the formation of complex topologies and functional hierarchies over time (Karsenti 2008, Prokopenko 2009). The neuroplasticity processes involved in self-organization also dictate network wiring and, by large, information transmission and processing across ordered neural networks (Rubinov, Sporns et al. 2009). Neurons involved in the execution of a specific function tend to cluster together in specialized modules, for example, cells with the same eye preference grouped into ocular dominance columns in the visual system (Hubel and Wiesel 1969), are typically highly interconnected with each other. This organization is ubiquitous across neural networks, where high local clustering of neurons combined with rapid information transmission within and between clusters have been shown to have important implications for functional processing and efficiency (Bassett and Bullmore 2006, Bullmore and Sporns 2009, Meunier, Lambiotte et al. 2010). These modules perform segregated processing facilitated by dense short-range intra-module connections (edges) (Kaiser and Hilgetag 2010, Klinshov, Teramae et al. 2014, Okujeni, Kandler et al. 2017), with global integration with the rest of the network

by few long-range inter-module edges (Bullmore and Sporns 2012, Perinelli, Tabarelli et al. 2019). Thus, communication efficiency in the network is inversely proportional to the distance or number of edges (path length) separating processing modules (Kaiser and Hilgetag 2006, Sporns 2013, Sporns 2018).

In complex systems, network resilience to perturbation also plays a critical role in information processing, since failure in one part can trigger cascades of failures throughout the network (Albert, Jeong et al. 2000, Ivanov and Bartsch 2014). In disorders such as post-traumatic stress disorder (PTSD) (Suo, Lei et al. 2015), schizophrenia (Liu, Liang et al. 2008), epilepsy (Li, Chen et al. 2020) and during the prodromal stages of Alzheimer's disease (AD) (Pereira, Mijalkov et al. 2016), aberrant alterations in path length, clustering and modularity are highly correlated with pathophysiology progression, duration and / or severity. Nevertheless, neural networks can often compensate to maintain function despite any external perturbations or internal fluctuations. Much of this resilience stems from activity-dependent neuroplasticity, which is essential for the brain to function effectively, adapt to changing environments and protect itself against damage (Nakamura, Hillary et al. 2009, Overman and Carmichael 2013). However, since network topology, synaptic transmission and neuroplasticity responses are inextricably linked, quantifying their interdependence in healthy and perturbed conditions in the brain still presents major challenges. Consequently, there are unanswered questions regarding the implications of disrupting synaptic activity on global aspects of network organization and resilience. Specifically, it remains unclear whether the network can maintain its structural and functional organization during perturbation or if it undergoes reorganization, potentially leading to more efficient or less efficient functioning.

For this investigation, we expanded on our previous work using hM4Di designer receptors exclusively activated by designer drugs (DREADDs) (Urban and Roth 2015, Ozawa and Arakawa 2021) to selectively target and inhibit excitatory synaptic transmission in *in vitro* rat cortical networks interfaced with microelectrode arrays (MEAs) (Weir, Christiansen et al. 2023). In our previous work (Weir, Christiansen et al. 2023), we found that selective inhibition significantly influenced the functional electrophysiological dynamics in perturbed networks, which manifested as increased network burst rate, higher fractions of spikes in bursts, and increased synchrony. In the present study, perturbation resulted in transient but significant de-clustering of modules within the networks, with a decrease in clustering coefficient and small-worldness concomitantly with increased path length. These structural changes implied a shift to a random network organization, effectively creating a less optimized and less efficient network.

2 Materials and methods

2.1 Culture of cortical networks on microelectrode arrays and AAV transduction

Neuronal cultures of primary rat (Sprague Dawley) cortex neurons (Cat. No: A36511) were thawed and co-cultured with 15% primary rat cortical astrocytes (Cat. No: N7745100) both obtained from ThermoFisher Scientific (US). A small drop (80 µl) of the cell suspension containing about 60 x 10^4 cells were plated on the active area of PDL + Geltrex precoated complementary metal-oxide semiconductor (CMOS)-based high density multielectrode array (HD-MEA) (3Brain GmbH, Switzerland). Cells were incubated in a humidified incubator (5% CO_2, 37°C) for 6 hours to allow attachment, then the wells were filled with 1 mL Neurobasal™ Plus Medium supplemented with 2% B-27 Plus supplement and 0.5% GlutaMAX™ all from ThermoFisher Scientific. The day of plating was designated as day 0 and 50% media changes were carried out every 2-3 days. At 7 days in vitro (DIV), the cells were transduced with a vector encoding hM4Di-CaMKlla-DREADDs according to the protocol established in our previous paper (Weir, Christiansen et al. 2023). In short, 80% of the cell media was removed from the cultures and a drop containing 6 x 10^7 AAV viral particles encoding experimental hM4Di- CamKlla-DREADDs was added to the cells. The cultures were gently agitated for 30 seconds to distribute the viral particles in the media and then incubated for 8 hours. Afterwards, each culture was topped up with fresh Neurobasal Plus cell media and incubated for an additional 40 hours. After the incubation period, 50% media changes were carried out every second day as scheduled. The vector encodes mCherry which is a bright red fluorescent protein tag that makes it possible to visualize results soon after transduction.

2.2 Immunocytochemistry

At 14 DIV, samples on Nunc™ Lab -Tek™ chamber slides (Cat. No. 154534PK) were fixed with 4% Paraformaldehyde (PFA) for 20 minutes, then permeabilized with a buffer of 0.03% Triton X-100 and 5% goat serum diluted in DPBS for 2 hours at room temperature. Following blocking, antibodies at the indicated concentrations **(Table 1)** were added in a buffer of 0.01% Triton X-100 and 1% goat serum in DPBS. Nuclei were stained with Hoechst (bisbenzimide H 33342 trihydrochloride, 14533, Sigma-Aldrich, 1: 5000 dilution). Samples were washed, mounted on glass cover slides with anti-fade fluorescence mounting medium (ab104135, Abcam) and imaged. All sample images were acquired using an EVOS M5000 imaging system (Invitrogen, ThermoFisher Scientific). Images were processed using Fiji/ImageJ and Adobe Illustrator 2020 version: 24.0.0.

Table 1. Overview of primary and secondary antibodies, species, and concentration

Primaries			Secondaries		
Markers	**Catalogue #**	**Concentration**	**Fluorescent**	**Catalogue #**	**Concentration**
Ck mCherry	Ab205402 (Abcam)	1:1000	Goat-anti-Chicken AlexaFluor 568	Ab175477 (Abcam)	1:1000
Ms Calmodulin (CaMKll)	MA3-918 (Invitrogen)	1:250	Goat-anti-Mouse AlexaFluor 568	A11019 (Invitrogen)	1:1000
Ms NMDAR1	32-0500 (Invitrogen)	1:100	Goat-anti-Mouse AlexaFluor 647	A21236 (Invitrogen)	1:1000
Ms GABA	Ab86186 (Abcam)	1:250	Goat-anti-Mouse AlexaFluor 488	A11001 (Invitrogen)	1:1000
Ms TUJ	Ab78078 (Abcam)	1:500	Goat-anti-Rabbit AlexaFluor 568	A11011 (Invitrogen)	1:1000
Rb Glutamate decarboxylase (GAD65/67)	Ab183999 (Abcam)	1:100	Goat-anti-Rabbit AlexaFluor 647	A21244 (Invitrogen)	1:1000
Rb Map2	Ab32454 (Abcam)	1:250	Goat-anti-Rabbit AlexaFluor 488	A11008 (Invitrogen)	1:1000
Rb Glial fibrillary acidic protein (GFAP)	Ab278054 (Abcam)	1:500			

2.3 Deschloroclozapine (DCZ) activation of hM4Di DREADDs in neural networks

Networks for DCZ treatment were transiently inhibited once per day at 25, 26 and 27 DIV for 2 hours each time. The novel synthetic ligand deschloroclozapine (DCZ; 10 µM) was used to activate the DREADDs receptors to induce synaptic silencing in excitatory neurons (Bjorkli, Ebbesen et al. 2022, Weir, Christiansen et al. 2023). On the days of treatment, DCZ diluted in cell media was added to 20% media volume in the wells for a final DCZ concentration of 10 µM. Networks were incubated for 2 hours. Thereafter, DCZ was washed out by doing 3 x 80% media changes using fresh media. For each recording, samples were placed in the recording head stage for 10 minutes before starting data acquisition to reduce noise variations due to disturbances caused by moving the cells from the incubator (see **Figure 1** for a workflow). Electrophysiological data was recorded for 15 minutes.

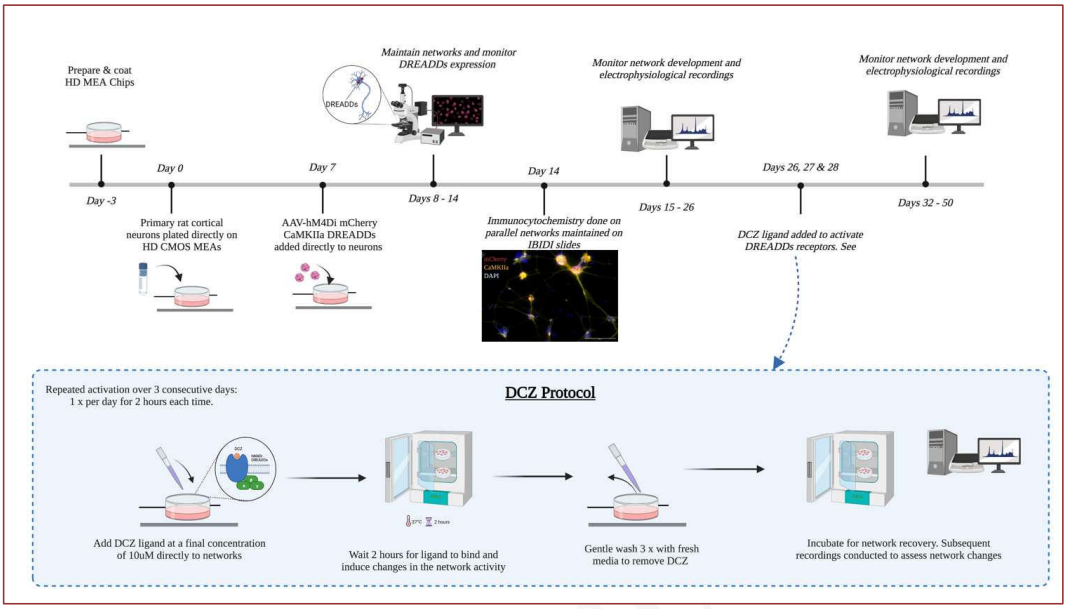

Figure 1. Workflow of experimental procedures. Timeline of experiment from preparation of HD MEAs and throughout the lifetime of the network. The DCZ protocol used for selectively perturbing DREADDs networks is illustrated in the bottom panel. *Figure created in Biorender.com.*

2.4 MEA setup and electrophysiological recording

Electrophysiological recordings were performed using the BioCam Duplex 3.0 platform with complementary metal-oxide semiconductor (CMOS) chips. Two models of CMOS chips (Arena and Accura) were used in this study due to availability (3Brain GmbH, Switzerland). The chips are integrated with 4096 square microelectrodes (21 µm x 21 µm) that are arranged in a 64 x 64 square grid on a seeding area of 2.67mm x 2.67mm (Arena) or 3.8mm x 3.8mm (Accura). The electrodes are aligned with 42 µm pitch (Arena) or 60 µm pitch (Accura) between electrodes. Recordings were done at a sampling rate of 20kHz, with a low pass cut off frequency at 100Hz and a high pass cut off frequency of 200 Hz. The raw data was visualized and preprocessed using the BrainWave software v5.1. Preprocessed data was analyzed offline in MATLAB.

2.5 Preprocessing: Spike detection and spike sorting using BrainWave 5 (3Brain GmbH, Switzerland)

Spike detection was performed using the Precise Timing Spike Detection (PTSD) algorithm which facilitates reliable and precise identification of spike events. Active channels were defined with a mean firing rate (MFR) of >0.10 spikes/s at a threshold of 7 x standard deviations (std) of the signal's biological and thermal noise. The peak lifetime period of spikes was set at 2.0 ms with the refractory period set at 1.0 ms. Spike sorting was performed using a K-Means & Silhouette clustering algorithm. Principle component analysis was used for feature extraction with the minimum number of spikes per cluster set at 2, and the maximum at 3. Outlier thresholds were set at 2 and all outliers and duplicate units were discarded. The duplication detection window was set at 0.1 ms with a threshold of 40%.

2.6 Network functional connectivity analyses

Connectivity data was analyzed offline using MATLAB (2021b). Functional connectivity was detected using Pearson cross-correlation. Prior to analyzing cross correlation, all potential connections were tested using Spearman's rank correlation and a bin size of 100 ms. Highly significant ($p < 0.001$) and strongly correlated ($r > 0.01$) connections were then further assessed using normalized Pearson cross correlation. For cross correlation, a bin size of 1 ms and a maximum lag of ±100ms was used and significant ($p< 0.1$) correlations were retained. Correlations of lag 0 were discarded. The weight of a connection in the adjacency matrix was set as the maximum normalized correlation coefficient within the specified lag. A final filtering step was performed to remove connections between distal electrodes with a biologically implausible lag, specifically exceeding 1 mm/ms.

Modularity was determined using functions from the Brain Connectivity toolbox (Rubinov and Sporns 2010) and the Community detection toolbox (https://github.com/mmitalidis/ComDetTB). For each adjacency matrix, the Louvain method of modularity detection (Blondel, Guillaume et al. 2008) was applied 100 times with a gamma of 1 and absolute weights. Each partitioning was then assessed for cluster validity using the node membership criterion as defined in the Community detection toolbox. The partition with the highest cluster validity, that is the strongest internal edge consistency for each module, was then selected. The Modularity Q values indicate the confidence of accurate network subdivision into modules. Modularity can either be positive or negative, with positive values indicating the possible presence of a community structure and negative values or zero indicating an undivided network (Newman 2006). Partitions with modularity Q greater than 0 indicate a community structure and > 0.1 indicate a

strong community structure (Newman 2006). In our results, partitions with modularity $Q < 0.01$ were discarded as too weakly clustered to qualify as a module.

For each module and giant component, the characteristic path length, clustering coefficient and participation coefficient (Guimerà and Nunes Amaral 2005) was detected using the Brain connectivity toolbox. The participation coefficient measures whether a node only interacts with nodes in its own module or if it shares edges with nodes from multiple modules. Path lengths were set as 1 minus the weight to account for stronger correlations being indicative of shorter paths. The intermodular path length describes the average distance between all nodes from one module to all nodes in another module. The clustering coefficient was calculated using binarized edges and describes the property of a node in the network and how well connected the neighborhood is. Mean degree describes the average number of connections that a node has to other nodes in the network. Small-world propensity (SWP) quantifies the extent to which a network displays small-world characteristics while accounting for variations in network density, and was calculated using the methods described in (Muldoon, Bridgeford et al. 2016) for weighted networks. The weighted clustering coefficient was calculated using the measure by (Onnela, Saramäki et al. 2005) and a threshold of $\phi_T = 0.6$ was set for the small-world propensity to classify networks as small-world, according to previous described (Muldoon, Bridgeford et al. 2016). The SWP was normalized so that values closer to 1 indicates that the network is more small-world.

3 Results

3.1 AAV2/1 Gi-DREADD expression found exclusively in CaMKIIa positive neurons with maturing excitatory and inhibitory synapses

Immunolabeling with antibodies specific for CaMKIIa expressed on excitatory neurons, and for mCherry expressed by DREADDs confirmed that both proteins colocalize in the network as shown in **(Figure 2A)**. In addition, there was no colocalization with mCherry and GAD65/67, a marker for inhibitory neurons **(Figure 2B)**. Furthermore, at 14 DIV the networks expressed NMDA receptors **(Figure 3A)** and GABA **(Figure 3B)** indicating the capacity for excitatory and inhibitory signaling at this stage.

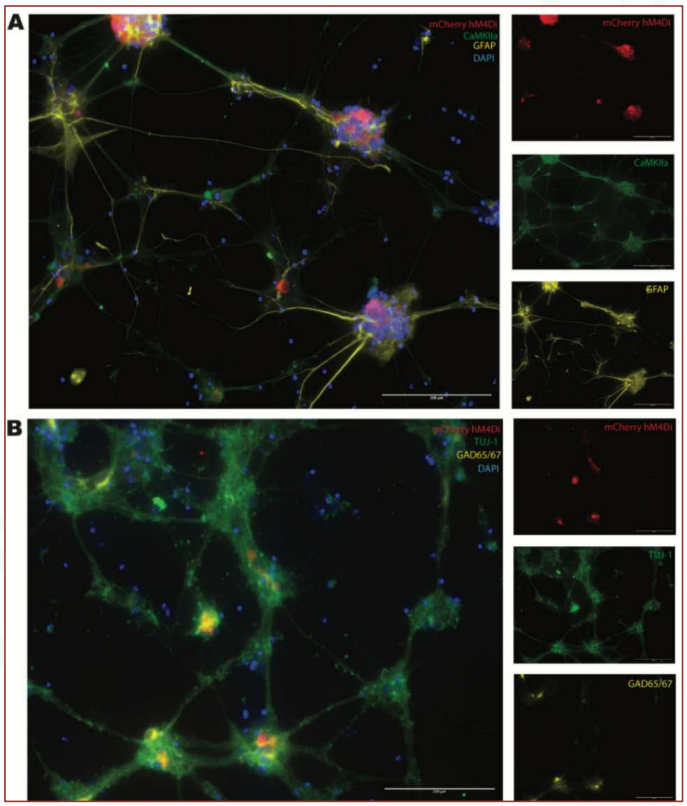

Figure 2. AAV2/1 hM4Di designer receptor exclusively activated by designer drugs (DREADDs) expressed in CaMKIIa positive neurons in vitro. (A) mCherry DREADDs expression was confirmed in CaMKIIa positive neurons **(B)** GAD65/67 expressing neurons (inhibitory neurons) did not express mCherry DREADDs. Scale bar = 250μm.

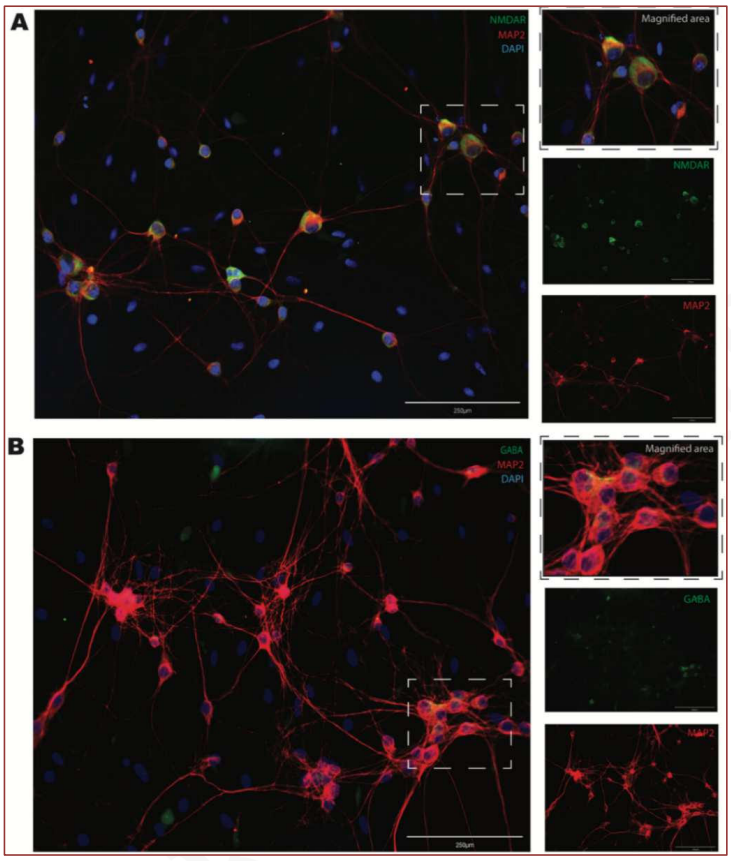

Figure 3. Neural networks positively stained for both NMDA receptors **(A)** and GABA **(B)** together with MAP2 neuronal cytoskeletal marker at 14 DIV. Scale bar = 250μm.

3.2 Network modularity develops over time and can be altered with inhibition of excitatory transmission

Spontaneous network activity was recorded between 14 DIV and up until 40 DIV. Graphs were created from the processed data to identify the different modules in the network and the nodes belonging to each module. These graphs are presented in **Figure 4** and show the modules for one network at 6 recording timepoints. At 14 DIV, the neural networks were still relatively immature and developing both structurally and functionally. Our results showed no distinct modules, and only a few active nodes were detected **(Figure 4A)**. At 21 and 26 DIV, almost all active nodes belonged to one of three modules detected **(Figure 4B, C; red, blue and yellow).** The graph shown at 28 DIV **(Figure 4D)** depicts the modular organization in the network 24 hours after selective inhibition of excitatory transmission. The

original 3 main modules from 26 DIV appeared to be fragmented into smaller clusters, with large areas where no activity was detected. Interestingly though, we found that by 32 DIV the network had begun reconfiguring itself, with more nodes organized into modules. By 40 DIV, the network had reconfigured itself back into 3 main modules, although with a different spatial positioning **(Figure 4E, F)**. Network organization at 40 DIV also showed that detected nodes within modules had more spatial distance compared to being positioned closer together at 21 DIV and 26 DIV.

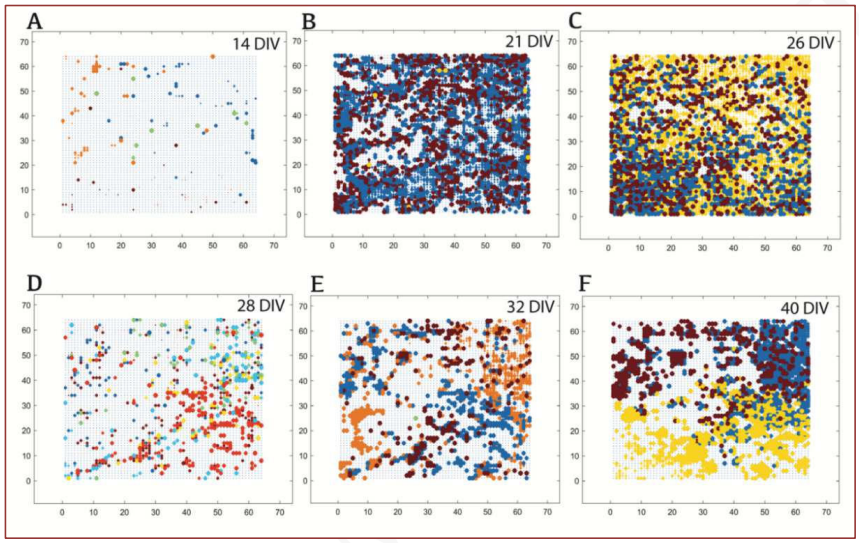

Figure 4. Inhibition results in functional de-clustering in modules with subsequent reorganization following recovery. Depicted here is a sample neural network across development. Modularity in the network at 14 DIV **(A)**, at 21 DIV **(B)** and at 26 DIV **(C)**. Network modular organization after perturbations at 28 DIV **(D)**, at 32 DIV **(E)** and at 40 DIV **(F)**. Each dot is one node and represents one active electrode at the time of recording. The colors indicate the module that the detected nodes belong to, and node sizes are scaled according to their participation coefficient.

3.3 Neural networks exhibited alterations in functional organization during and following selective perturbation

Further analyses were conducted to determine the extent to which both structural and functional organization had changed within the inhibited networks. **Figure *5*** depicts the results of these analyses for 3 experimental networks, from here onwards identified as Net1, Net2 and Net3 (see figure legend). We observed inconsistencies in the number of modules before and after selective inhibition of the networks, making it difficult to conclude exactly the structural changes taking place. For instance, in **Figure 5A**, networks had self-organized into 3 modules at 21 DIV before inhibition. During the period of inhibition between 25 and 27 DIV, there was no change in the number of modules in Net2, an increase in module number from 3 to 6 modules at 27 DIV for Net1, and a decrease from 3 to 1 module at 27 DIV for

Net3. During the network recovery period after inhibition, no modules were detected for Net2. The number of modules increased in Net1 and Net3, then returned to baseline number of 3 modules by 40 DIV.

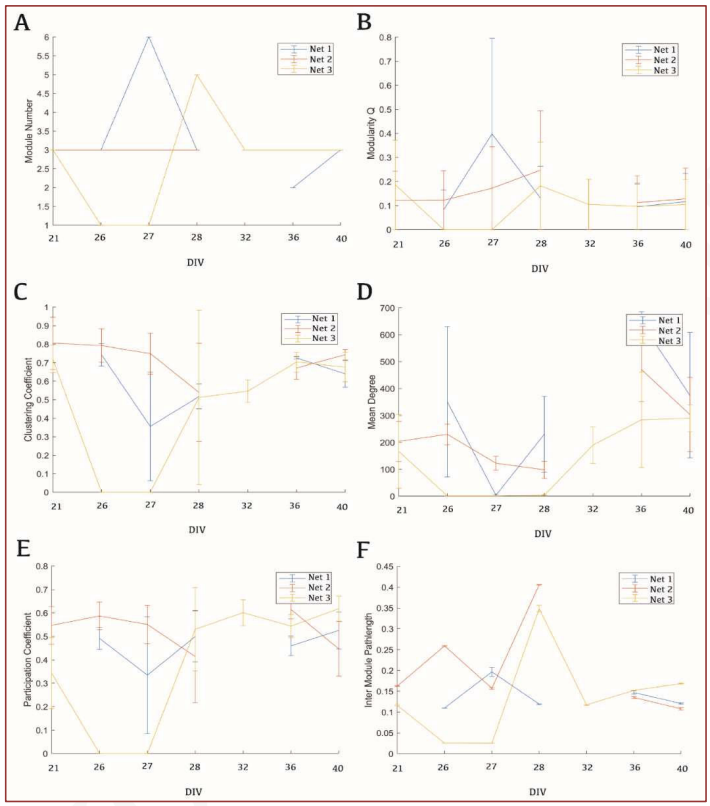

Figure 5. Neural networks exhibited transiently increased path lengths and decreased clustering due perturbation, with subsequent reconfiguration. Functional organization is described in terms of Module number **(A)**, Modularity Q **(B)**, Clustering coefficient **(C)**, Mean degree **(D)**, Participation coefficient **(E)**, and Inter module path length **(F)** with standard error bars.

For further analyses of network subdivision, analyses of the modularity Q were conducted, and the results highlighted that network organization reflected a community structure. Prior to perturbation, modularity Q = / > 0 but less than <0.2 **(Figure 5B)** indicating a community structure. Modularity Q appeared to increase (Q > 0.2) during perturbation for two networks (Net1 and Net3). One network decreased to Q = 0, indicating that there was low division during perturbation. Following perturbation and between 28 and 40 DIV, all networks appeared to stabilize with modularity Q values Q = 0.17 **(Figure 5B)**, which indicate varying modularity prior, during and after perturbation. Additional findings demonstrated that during the period of inhibition between 25 and 27 DIV, there was a decrease across all networks in

clustering coefficient **(Figure 5C)**, however, all networks restored high clustering with (values > 0.6) after perturbation suggesting some recovery of network functional organization. Similar results were observed for the participation coefficient **(Figure 5E)**. Furthermore, the average number of connections that each node had with other nodes in the network had decreased from above >150 connections to <110 connections for Net2 during perturbation, while the other 2 networks had no detected connections by 27 DIV. However, during the recovery period after inhibition, the networks gradually restored the connections such that all networks had mean degrees of approximately > 300 connections by 40 DIV **(Figure 5D)**. Our examination of intermodular path length showed that the number of edges connecting modules fluctuated greatly between recordings during the period of inhibition between 25 and 27 DIV, as well as immediately after inhibition at 28 DIV **(Figure 5F)**. Nevertheless, we observed that networks restored to pre-perturbation values between 32 and 40 DIV at < 0.2 intermodular path length.

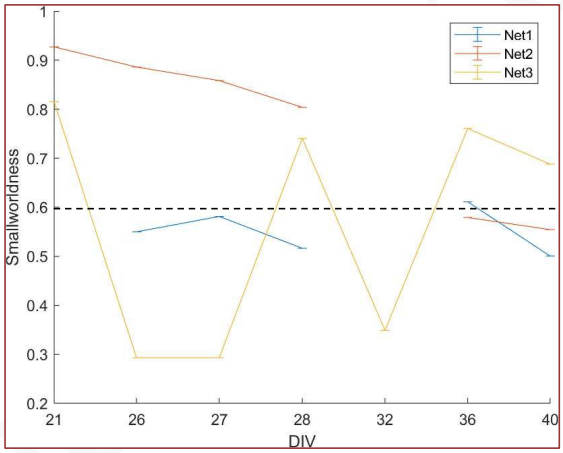

Figure 6. Neural networks exhibited transient decreases in SWP during perturbation, with subsequent recovery. The neural networks were analyzed as a weighted matrix with the dashed ling denoting the $\phi_T = 0.6$ threshold.

Finally, we found that the neural networks exhibited relatively large SWP values at 21 DIV ($\phi_T > 0.5$) indicating that the neural networks displayed small-world properties before perturbation **(Figure 6)**. During perturbation, two networks maintained high SWP values, while one network decreased to $\phi_T = 0.3$. There were fluctuations in values during recovery, but by 40 DIV, all networks restored to SWP values $\phi_T > 0.5$ although none restored to pre-inhibition values.

4 Discussion

Complex biological systems like the brain or *in vitro* neural networks can adjust their structural and functional organization in response to changes in sensory inputs or experiences. In healthy conditions, network topological architecture evolves in accordance with the principles of high efficiency of information transfer and processing. Networks achieve this by having segregated modules for specialized processing, and short pathways to connect the different areas of the network (van den Heuvel and Sporns 2013). It is also imperative that the relevant topologies are resilient i.e., they need to be adaptable to perturbations. The findings presented in this study demonstrate that perturbation of network activity via selective inhibition of excitatory synaptic transmission resulted into transient de-clustering of modular structures that corresponded to reduced clustering and decreased small-worldness. Other structural changes included a transient increase in path lengths during perturbation, with the network subsequently reorganizing to a state of increased clustering and short path lengths following recovery.

By structurally and functionally reorganizing information processing areas in response to impaired synaptic transmission, complex biological networks can adapt to altered inputs (Rezaul Karim, Proulx et al. 2021) and retain function. De-clustering refers to the process by which specialized brain regions or modules lose their distinct functional boundaries. It involves a reduction in the functional segregation or modular organization of the brain, leading to increased interactions and information flow between previously distinct brain regions (Park and Friston 2013, Joanna Su Xian, Kwun Kei et al. 2019). Several studies have shown that decreased clustering can occur in various contexts including during brain development and aging (Micheloyannis, Vourkas et al. 2009, Joanna Su Xian, Kwun Kei et al. 2019). De-clustering also represents a dynamic process of functional reorganization that allows for more flexible and efficient information processing during perturbation, learning and sensory input by enabling new information to be integrated into existing ensembles (Katori, Sakamoto et al. 2011, Pinotsis, Brincat et al. 2017). Our previous investigation showed that selective inhibition results in an increase in network wide bursts and synchrony (Weir, Christiansen et al. 2023), which is highly relevant here because it suggests that global activation increases as inhibited networks lose their structural boundaries. This also suggests that the transient loss of functional boundaries between processing areas in the network may be a compensatory response to restore synaptic drive with and across the perturbed areas of the network. As synaptic inputs to different parts of the network decrease due to inhibition, the remaining areas may have increased their synaptic capabilities, for example by either scaling up neurotransmitter release, increasing receptors on neurites or lowering the threshold for excitatory post-synaptic current (Bridi, de

Pasquale et al. 2018). As these synaptic modifications tend to occur on a slow time scale (Bridi, de Pasquale et al. 2018, Hobbiss, Ramiro-Cortés et al. 2018), it is entirely possible that they happen concomitantly with the increase in network synchrony since synchrony increases also occur gradually over several days (Weir, Christiansen et al. 2023).

Furthermore, the decrease in clustering coefficient and participation coefficient – two basic measurements of network communication and information flow – correspond with the reduction in the small-worldness in the network during and after inhibition. There are various factors that can influence small-worldness in neural networks, one of which is the lesioning of specific hubs. Although our perturbation did not target any particular area of the network, the observed effects closely align with other studies that have demonstrated the distinct impact of hub lesioning on the small-world structure of the remaining network (Sporns, Honey et al. 2007). Specifically, lesioning provincial hubs disturbs functional integration of the module to which they belong, which results in less segregation in the remaining network (Sporns, Honey et al. 2007). Evidently, by silencing excitatory synaptic transmission across the network, we also impaired hub function, which resulted in overall less discriminate processing. Provincial hubs play a pivotal role in functional processing in their module, while other hubs i.e., connector hubs, act as central communication transmission ports that receive and transfer a substantial bulk of information to the rest of the network (Bettencourt, Stephens et al. 2007). Since these hubs also make transmission faster by connecting several areas of the network, loss of hub processing will inevitably lead to some functional re-organization of paths in the network.

The findings presented in **Figure 5D, and F** indicate that the applied perturbation resulted in a decrease in mean degree, which implies a reduction in the average number of connections between nodes in the network. Additionally, the inter-module path length increased, indicating that transmission of signals between different areas of the network required more steps or intermediaries. These changes in network connectivity and information transmission have implications for the network's efficiency. According to the theory of brain efficiency and economic cost of signal propagation (Achard and Bullmore 2007, Bullmore and Sporns 2012), a more efficient network is characterized by high degree of connectivity with direct information flow between nodes. A shorter path length between communicating areas of the network is also associated with improved efficiency as it minimizes the number of transmission steps required.

As with all complex self-organizing systems, there is an innate desire to self-organize towards increased effectiveness. This drive was evident in our study, where we observed the remarkable ability of neural networks to reconfigure themselves following perturbations at 25 DIV, 26 DIV and 27 DIV. By 32 DIV, the networks had already begun re-configuring to restore their segregated processing and distinct modularity **(Figure 4)**. Furthermore, the networks also exhibited the restoration of high mean degree and low path lengths, which would contribute to overall more efficient information processing, transmission, and communication. Together, these findings highlight the dynamic flexibility and self-reglatory capabilities of neural networks.

5 Conclusions and future directions

In conclusion, the findings from this study shed light on the remarkable adaptability of neural networks in response to perturbation, both structurally and functionally. We showed that targeted inhibition of excitatory synaptic transmission resulted in a temporary disruption in modular organization, network clustering and short path lengths. The neural networks also demonstrated an innate capacity to adapt and reconfigure themselves in response to perturbation, with the ultimate goal of restoring their functional organization and optimized information processing. Understanding the self-regulatory capabilities of neural networks provides valuable insights into the mechanisms underlying neural plasticity, and recovery from disruptions. Therefore, our study highlights the significance of utilizing *in vitro* models as tools to explore these intricate structure-function relationships at a micro and mesoscale level in changing conditions in complex neural networks. Future analyses to validate and characterize other features of structural and functional organization such as, hub organization, degree distribution and specific measure of efficiency may help to strengthen the findings reported here. These further studies would also benefit greatly from expanding the sample size and data set to investigate network resilience at different timepoints in development i.e., early development and late maturity. Together, the results can enhance our understanding of adaptability in neural networks and may lead to the development of therapeutic strategies targeting neuroplasticity for function restoration in various neurological conditions.

Data availability statement

The raw data that support the findings of this study will be made available by the authors upon request.

Author Contributions

This study was conceived and designed by JSW, AS and IS. All data collection was done by JSW who also drafted the manuscript. OHR performed all data analysis. AS and IS helped with the manuscript revision process, and all authors have read and approved the final version of the manuscript.

Funding

This project was funded by The Research Council of Norway (NFR IKT Pluss; Self-Organizing Computational Substrates (SOCRATES)) Grant number: 270961,

Acknowledgement

The authors would like to thank Dr. Rajeevkumar Nair Raveendran at the Viral Vector Core Facility, Kavli Institute for Systems Neuroscience for designing and manufacturing the AAV vectors.

Conflict of Interest

The authors declare that the research was conducted in the absence of any commercial or financial relationships that could be construed as potential conflict of interest.

References

1. Achard, S. and E. Bullmore (2007). "Efficiency and Cost of Economical Brain Functional Networks." PLOS Computational Biology **3**(2): e17.
2. Albert, R., H. Jeong and A.-L. Barabási (2000). "Error and attack tolerance of complex networks." Nature **406**(6794): 378-382.
3. Bassett, D. S. and E. Bullmore (2006). "Small-world brain networks." Neuroscientist **12**(6): 512-523.
4. Ben-Ari, Y. (2001). "Developing networks play a similar melody." Trends Neurosci **24**(6): 353-360.
5. Bettencourt, L. M., G. J. Stephens, M. I. Ham and G. W. Gross (2007). "Functional structure of cortical neuronal networks grown in vitro." Phys Rev E Stat Nonlin Soft Matter Phys **75**(2 Pt 1): 021915.
6. Bjorkli, C., N. C. Ebbesen, J. B. Julian, M. P. Witter, A. Sandvig and I. Sandvig (2022). "Manipulation of neuronal activity in the entorhinal-hippocampal circuit affects intraneuronal amyloid-β levels." bioRxiv: 2022.2007.2005.498797.
7. Blondel, V. D., J.-L. Guillaume, R. Lambiotte and E. Lefebvre (2008). "Fast unfolding of communities in large networks." Journal of Statistical Mechanics: Theory and Experiment **2008**(10): P10008.
8. Bridi, M. C. D., R. de Pasquale, C. L. Lantz, Y. Gu, A. Borrell, S. Y. Choi, K. He, T. Tran, S. Z. Hong, A. Dykman, H. K. Lee, E. M. Quinlan and A. Kirkwood (2018). "Two distinct mechanisms for experience-dependent homeostasis." Nat Neurosci **21**(6): 843-850.
9. Bullmore, E. and O. Sporns (2009). "Complex brain networks: graph theoretical analysis of structural and functional systems." Nat Rev Neurosci **10**(3): 186-198.
10. Bullmore, E. and O. Sporns (2012). "The economy of brain network organization." Nat Rev Neurosci **13**(5): 336-349.
11. Chiappalone, M., A. Vato, L. Berdondini, M. Koudelka-Hep and S. Martinoia (2007). "Network dynamics and synchronous activity in cultured cortical neurons." Int J Neural Syst **17**(2): 87-103.
12. Fauth, M. and C. Tetzlaff (2016). "Opposing Effects of Neuronal Activity on Structural Plasticity." Front Neuroanat **10**: 75.
13. Goodman, C. S. and C. J. Shatz (1993). "Developmental Mechanisms That Generate Precise Patterns of Neuronal Connectivity." Cell **72**: 77-98.
14. Guimerà, R. and L. A. Nunes Amaral (2005). "Functional cartography of complex metabolic networks." Nature **433**(7028): 895-900.
15. Hobbiss, A. F., Y. Ramiro-Cortés and I. Israely (2018). Homeostatic Plasticity Scales Dendritic Spine Volumes and Changes the Threshold and Specificity of Hebbian Plasticity. iScience. **8:** 161-174.
16. Huang, Z. J. (2009). "Activity-dependent development of inhibitory synapses and innervation pattern: role of GABA signalling and beyond." The Journal of physiology **587**(Pt 9): 1881-1888.
17. Hubel, D. H. and T. N. Wiesel (1969). "Anatomical Demonstration of Columns in the Monkey Striate Cortex." Nature **221**(5182): 747-750.
18. Ivanov, P. C. and R. P. Bartsch (2014). Network physiology: Mapping interactions between networks of physiologic networks. Understanding Complex Systems**:** 203-222.
19. Ivenshitz, M. and M. Segal (2010). "Neuronal density determines network connectivity and spontaneous activity in cultured hippocampus." J Neurophysiol **104**(2): 1052-1060.
20. Joanna Su Xian, C., N. Kwun Kei, T. Jesisca, W. Chenhao, P. Jia-Hou, C. L. June, W. L. C. Michael and Z. Juan Helen (2019). "Longitudinal Changes in the Cerebral Cortex Functional Organization of Healthy Elderly." The Journal of Neuroscience **39**(28): 5534.
21. Kaiser, M. and C. C. Hilgetag (2006). "Nonoptimal component placement, but short processing paths, due to long-distance projections in neural systems." PLoS Comput Biol **2**(7): e95.
22. Kaiser, M. and C. C. Hilgetag (2010). "Optimal hierarchical modular topologies for producing limited sustained activation of neural networks." Front Neuroinform **4**: 8.
23. Karsenti, E. (2008). "Self-organization in cell biology: a brief history." Nat Rev Mol Cell Biol **9**(3): 255-262.
24. Kater, S. B., R. W. Davenport and P. B. Guthrie (1994). Filopodia as detectors of environmental cues: signal integration through changes in growth cone calcium levels. Progress in Brain Research. J. Van Pelt, M. A. Corner, H. B. M. Uylings and F. H. Lopes Da Silva, Elsevier. **102:** 49-60.

25. Katori, Y., K. Sakamoto, N. Saito, J. Tanji, H. Mushiake and K. Aihara (2011). "Representational Switching by Dynamical Reorganization of Attractor Structure in a Network Model of the Prefrontal Cortex." PLoS computational biology **7**: e1002266.
26. Kirwan, P., B. Turner-Bridger, M. Peter, A. Momoh, D. Arambepola, H. P. Robinson and F. J. Livesey (2015). "Development and function of human cerebral cortex neural networks from pluripotent stem cells in vitro." Development **142**(18): 3178-3187.
27. Klinshov, V. V., J.-n. Teramae, V. I. Nekorkin and T. Fukai (2014). "Dense Neuron Clustering Explains Connectivity Statistics in Cortical Microcircuits." PLOS ONE **9**(4): e94292.
28. Li, Y., Q. Chen and W. Huang (2020). "Disrupted topological properties of functional networks in epileptic children with generalized tonic-clonic seizures." Brain Behav **10**(12): e01890.
29. Liu, Y., M. Liang, Y. Zhou, Y. He, Y. Hao, M. Song, C. Yu, H. Liu, Z. Liu and T. Jiang (2008). "Disrupted small-world networks in schizophrenia." Brain **131**(Pt 4): 945-961.
30. Meunier, D., R. Lambiotte and E. T. Bullmore (2010). "Modular and hierarchically modular organization of brain networks." Front Neurosci **4**: 200.
31. Micheloyannis, S., M. Vourkas, V. Tsirka, E. Karakonstantaki, K. Kanatsouli and C. J. Stam (2009). "The influence of ageing on complex brain networks: a graph theoretical analysis." Hum Brain Mapp **30**(1): 200-208.
32. Millan, A. P., J. J. Torres, S. Johnson and J. Marro (2018). "Concurrence of form and function in developing networks and its role in synaptic pruning." Nat Commun **9**(1): 2236.
33. Muldoon, S. F., E. W. Bridgeford and D. S. Bassett (2016). "Small-World Propensity and Weighted Brain Networks." Scientific Reports **6**(1): 22057.
34. Najafi, F., G. F. Elsayed, R. Cao, E. Pnevmatikakis, P. E. Latham, J. P. Cunningham and A. K. Churchland (2020). "Excitatory and Inhibitory Subnetworks Are Equally Selective during Decision-Making and Emerge Simultaneously during Learning." Neuron **105**(1): 165-179.e168.
35. Nakamura, T., F. G. Hillary and B. B. Biswal (2009). "Resting Network Plasticity Following Brain Injury." PLOS ONE **4**(12): e8220.
36. Newman, M. E. J. (2006). "Modularity and community structure in networks." Proceedings of the National Academy of Sciences **103**(23): 8577-8582.
37. Okujeni, S., S. Kandler and U. Egert (2017). "Mesoscale Architecture Shapes Initiation and Richness of Spontaneous Network Activity." The Journal of Neuroscience **37**(14): 3972.
38. Onnela, J.-P., J. Saramäki, J. Kertész and K. Kaski (2005). "Intensity and coherence of motifs in weighted complex networks." Physical Review E **71**(6): 065103.
39. Opitz, T., A. D. De Lima and T. Voigt (2002). "Spontaneous development of synchronous oscillatory activity during maturation of cortical networks in vitro." Journal of neurophysiology **88**(5): 2196-2206.
40. Overman, J. J. and S. T. Carmichael (2013). "Plasticity in the Injured Brain: More than Molecules Matter." The Neuroscientist **20**(1): 15-28.
41. Ozawa, A. and H. Arakawa (2021). "Chemogenetics drives paradigm change in the investigation of behavioral circuits and neural mechanisms underlying drug action." Behav Brain Res **406**: 113234.
42. Park, H.-J. and K. Friston (2013). "Structural and Functional Brain Networks: From Connections to Cognition." Science **342**(6158): 1238411.
43. Pereira, J. B., M. Mijalkov, E. Kakaei, P. Mecocci, B. Vellas, M. Tsolaki, I. Kłoszewska, H. Soininen, C. Spenger, S. Lovestone, A. Simmons, L.-O. Wahlund, G. Volpe, E. Westman and f. t. A. s. D. N. I. AddNeuroMed consortium (2016). "Disrupted Network Topology in Patients with Stable and Progressive Mild Cognitive Impairment and Alzheimer's Disease." Cerebral Cortex **26**(8): 3476-3493.
44. Perinelli, A., D. Tabarelli, C. Miniussi and L. Ricci (2019). "Dependence of connectivity on geometric distance in brain networks." Scientific Reports **9**(1): 13412.
45. Pinotsis, D. A., S. L. Brincat and E. K. Miller (2017). "On memories, neural ensembles and mental flexibility." Neuroimage **157**: 297-313.
46. Prokopenko, M. (2009). "Guided self-organization." HFSP journal **3**(5): 287-289.
47. Rezaul Karim, A. K. M., M. J. Proulx, A. A. de Sousa and L. T. Likova (2021). "Neuroplasticity and Crossmodal Connectivity in the Normal, Healthy Brain." Psychol Neurosci **14**(3): 298-334.
48. Rubinov, M. and O. Sporns (2010). "Complex network measures of brain connectivity: uses and interpretations." Neuroimage ***52***(3): 1059-1069.

49. Rubinov, M., O. Sporns, C. van Leeuwen and M. Breakspear (2009). "Symbiotic relationship between brain structure and dynamics." BMC Neurosci **10**: 55.
50. Sporns, O. (2013). "Structure and function of complex brain networks." Dialogues Clin Neurosci **15**(3): 247-262.
51. Sporns, O. (2018). "Graph theory methods: applications in brain networks." Dialogues Clin Neurosci **20**(2): 111-121.
52. Sporns, O., C. J. Honey and R. Kotter (2007). "Identification and classification of hubs in brain networks." PLoS One **2**(10): e1049.
53. Sukenik, N., O. Vinogradov, E. Weinreb, M. Segal, A. Levina and E. Moses (2021). "Neuronal circuits overcome imbalance in excitation and inhibition by adjusting connection numbers." Proceedings of the National Academy of Sciences of the United States of America **118**(12).
54. Suo, X., D. Lei, K. Li, F. Chen, F. Li, L. Li, X. Huang, S. Lui, L. Li, G. J. Kemp and Q. Gong (2015). "Disrupted brain network topology in pediatric posttraumatic stress disorder: A resting-state fMRI study." Hum Brain Mapp **36**(9): 3677-3686.
55. Urban, D. J. and B. L. Roth (2015). "DREADDs (designer receptors exclusively activated by designer drugs): chemogenetic tools with therapeutic utility." Annu Rev Pharmacol Toxicol ***55***: 399-417.
56. van den Heuvel, M. P. and O. Sporns (2013). "An anatomical substrate for integration among functional networks in human cortex." J Neurosci **33**(36): 14489-14500.
57. Wagenaar, D. A., J. Pine and S. M. Potter (2006). "An extremely rich repertoire of bursting patterns during the development of cortical cultures." BMC Neurosci **7**: 11.
58. Weir, J. S., N. Christiansen, A. Sandvig and I. Sandvig (2023). "Selective inhibition of excitatory synaptic transmission alters the emergent bursting dynamics of in vitro neural networks." Frontiers in Neural Circuits **17**.
59. Zhang, Z. and Q. Q. Sun (2011). "The balance between excitation and inhibition and functional sensory processing in the somatosensory cortex." Int Rev Neurobiol **97**: 305-333.

PAPER III

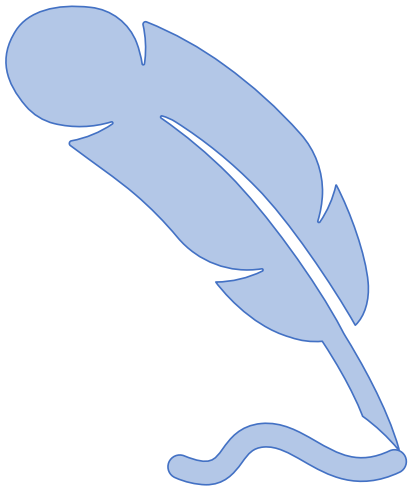

Altered structural organization and functional connectivity in feedforward neural networks after induced perturbation

Janelle S. Weir[1]*, Katrine Sjaastad Hanssen[1,2]*, Nicolai Winter-Hjelm[1], Axel Sandvig[1,3], Ioanna Sandvig[1]

[1]Department of Neuromedicine and Movement Science, Faculty of Medicine and Health Sciences, Norwegian University of Science and Technology (NTNU), Trondheim, Norway
[2] Kavli Institute for Systems Neuroscience, NTNU, Trondheim, Norway
[3] Department of Neurology and Clinical Neurophysiology, St Olav´s University Hospital, Trondheim, Norway

***These authors share first co-authorship**
Correspondence: janelle.s.weir@ntnu.no, katrine.s.hanssen@ntnu.no , ioanna.sandvig@ntnu.no

Keywords: Cortical network; neural engineering; electrophysiology; mutated tau; self-organization; neuroplasticity

Abstract

Reciprocal structure–function relationships underly both healthy and pathological behaviors in complex neural networks. Neuropathology can have widespread implications on the structural properties of neural networks, and drive changes in the functional interactions among network components at the micro- and mesoscale level. Thus, understanding network dysfunction requires a thorough investigation of the complex interactions between structural and functional network reconfigurations in response to perturbation. However, such network reconfigurations at the micro- and mesoscale level are often difficult to study *in vivo*. For example, subtle, evolving changes in synaptic connectivity, transmission, and electrophysiological shift from healthy to pathological states are difficult to study in the brain. Engineered *in vitro* neural networks are powerful models that enable selective targeting, manipulation, and monitoring of dynamic neural network behavior at the micro- and mesoscale in physiological and pathological conditions. In this study, we first established feedforward cortical neural networks using in-house developed two-nodal microfluidic chips with controllable connectivity interfaced with microelectrode arrays (mMEAs). We subsequently induced perturbations to these networks by adeno-associated virus (AAV) mediated expression of human mutated tau in the presynaptic node and monitored network structure and activity over three weeks. We found that induced perturbation in the presynaptic node resulted in altered structural organization and extensive axonal retraction starting in the perturbed node. Perturbed networks also exhibited functional changes in intranodal activity, which manifested as an overall decline in both firing rate and bursting activity, with a progressive increase in synchrony over time. We also observed impaired spontaneous and evoked internodal signal propagation between pre-and postsynaptic nodes in the perturbed networks. These results provide novel insights into dynamic structural and functional reconfigurations in engineered feedforward neural networks as a result of evolving pathology.

1. Introduction

One of the main structural pathological hallmarks of AD is the accumulation of neurofibrillary tangles in the brain as a result of the hyperphosphorylation of the microtubule associated protein tau (Braak et al., 1991). Tau proteins are mainly found in the axons of neurons (Götz et al., 2019) where they enrich microtubules to promote their assembly in axons (Baas et al., 2019; Qiang et al., 2018). However, under pathological conditions, tau becomes hyperphosphorylated, causing widespread morphological disruption in axons (Jackson et al., 2017; Kopeikina et al., 2013), ultimately affecting synaptic transmission and network function. The high interconnectivity of the brain also implies that neuronal axons and synapses may act as conduits for the spread of such pathology from affected areas, causing progressive, widespread disruption to the structural and functional integrity of the network (Adams et al., 2019; Kuhl, 2019). It has also been shown that hyperphosphorylated tau triggers hypoactivity in neurons (Ittner et al., 2011; Menkes-Caspi et al., 2015; Polanco et al., 2018; Wang et al., 2017), thus disturbing excitatory-inhibitory balance, and disrupting synaptic transmission and global integration across the network.

To elucidate how relevant pathological mechanisms gradually affect the structure and function of neural networks, it is imperative to study the underlying processes at the micro- and mesoscale. Such investigations are highly challenging, or de facto not feasible *in vivo* due to the size and complexity of the brain. This challenge can be overcome with the application of advanced cellular models based on engineered neural networks. Such networks develop with progressively increasing structural and functional complexity over time, essentially recapitulating fundamental aspects of neural network behavior as seen in the brain (Collingridge et al., 2010; Valderhaug et al., 2021; van de Wijdeven et al., 2019; Winter-Hjelm N, 2023). Engineered *in vitro* models thus enable longitudinal studies of dynamic network behavior and allow for selective perturbation and monitoring of network responses at the micro- and mesoscale level (Bauer et al., 2022; Bruno et al., 2020; Fiskum et al., 2021; Gribaudo et al., 2019; Nonaka et al., 2011; Valderhaug et al., 2021; Weir et al., 2023).

In the present study, we longitudinally investigated structural and functional changes in engineered two-nodal feedforward cortical neural networks, following induced expression of human mutated tau in the presynaptic nodes. Our primary aim was to longitudinally monitor and identify dynamic changes in neurite organization and electrophysiological activity of networks with evolving perturbation and compare this with control unperturbed networks. The two-nodal feedforward configuration of the engineered network enabled us to observe structural and functional reconfigurations in response to the perturbation in the affected node, while simultaneously monitoring dynamic changes in the postsynaptic node. Our results demonstrate that prior to perturbation, all neural networks developed

increasingly robust firing and bursting activity within the nodes. They had also developed prominent structural connections, and functional internodal connections with spontaneous and evoked feedforward burst propagation from the presynaptic to postsynaptic nodes. However, within four days of inducing perturbation by expression of human mutated tau in the presynaptic node, internodal connectivity was disrupted, manifested as progressive retraction of neurites from the entry zone near microtunnels in the presynaptic node, followed by retraction of neurites from the exit zones near the microtunnels towards the postsynaptic nodes. Neurite retraction persisted over a span of 3 weeks, during which period we observed a significant concomitant reduction in the overall intranodal mean firing rate, mean burst rate, and total number of bursts. Such structural or functional changes were not observed in control unperturbed networks. Furthermore, the neurite retraction and overall decrease in activity in the perturbed networks occurred simultaneously with a significant increase in network synchrony. Increased synchrony over time was not observed in control unperturbed networks. These results provide new insights into dynamic micro- and mesoscale network reconfigurations in response to induced perturbations and illustrate the utility of engineered feedforward neural networks as models of network function and dysfunction.

2. Methods

2.1. *In vitro* neural networks

An experimental timeline can be found in **Figure 1**. For this study, we used in-house developed microfluidic chips interfaced with microelectrode arrays (mMEAs; n=7) and 8-well chambered slides (Ibidi, 80841; n=2). Design and fabrication of the mMEAs was conducted as reported previously by our group (Winter-Hjelm N, 2023). Briefly, two compartments (from here on referred to as nodes) (5 mm wide/60 µm high) were connected by 20 microtunnels (700 µm long/10 µm wide/5 µm high) designed to promote unidirectional axonal outgrowth from the presynaptic to the postsynaptic node. Tesla valve microtopographies were included in the microchannels to redirect axons from the postsynaptic node back to their chamber of origin. Furthermore, axon traps were included on the postsynaptic side to misguide outgrowing axons and prevent them from entering the microtunnels. To prevent neuronal somata from entering the microtunnels, 4 µm pillars with 4 µm interspacing were positioned within the presynaptic node. This design promotes formation of feedforward networks by aiding axon outgrowth from the presynaptic node, but not vice versa. Impedance measurements and sterilization of the mMEAs were conducted as reported previously (Winter-Hjelm N, 2023). Prior to seeding of the cells, nodes were coated with 0.1 mg/mL Poly-l-Ornithine (PLO; Sigma-Aldrich, #P4957) for 30 min, subsequently replenished with fresh PLO for another 2h at 37°C/5% CO_2. Following this, all PLO was discarded, and the surfaces rinsed three times with distilled Milli-Q-water. Subsequently, the platforms were coated with laminin solution consisting of 16 µg/mL Mouse Natural Laminin (Gibco, #23017015) diluted in PBS (Sigma-Aldrich, D8537) for first 30 min, before being replenished with fresh laminin solution for another 2 h at 37°C/5% CO_2. To ensure proper flow of coating solution through the microtunnels, a hydrostatic pressure gradient was applied during all coating steps. Laminin solution was discarded and replaced by astrocyte media consisting of DMEM (Gibco™, 11885084) supplemented with 15% Fetal Bovine Serum (Sigma-Aldrich, F9665) and 2% Penicillin-Streptomycin (Sigma-Aldrich, #P4333) for 10 min at 37°C/5% CO_2 before rat primary cortical astrocytes (Gibco, #N7745100) were plated at a density of 100 cells/mm^2 48 hours prior to plating of neurons Subsequently, rat primary cortical neurons (Gibco, #A1084001) were plated at a density of 1,000 cells/mm^2 in neuronal media consisting of Neurobasal Plus Medium (Gibco™, A3582801) supplemented with 2% B27 Plus Medium (Gibco™, A358201), 2.5 mL/L Gluta-Max (Gibco™, 35050038) and 1% Penicillin-Streptomycin (Sigma-Aldrich, P4333). 4 and 24 hours after plating the neurons, 90% of the media was replenished. Thereafter, 50% of the media was replenished every 2 days.

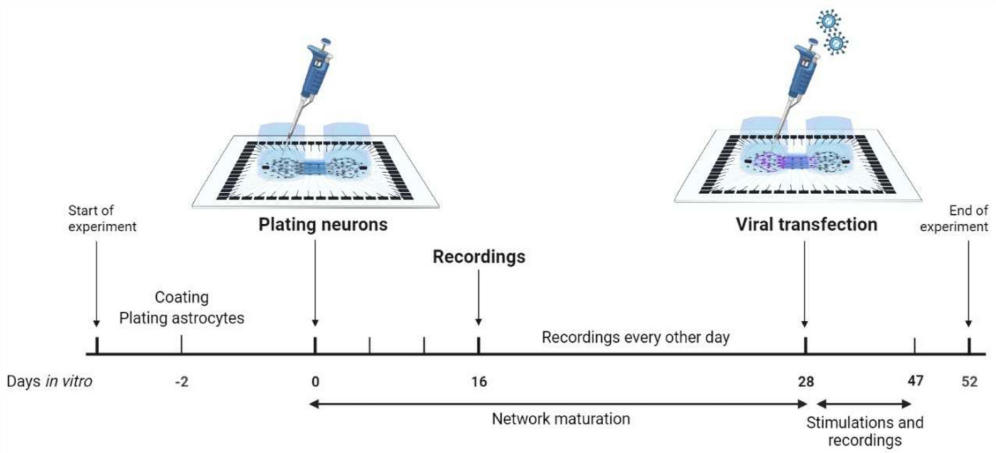

Figure 1. Schematic of the *in vitro* experimental timeline for establishing networks, transduction, and electrophysiological recordings. *Created with BioRender.com.*

2.1.1. AAV8 – GFP – 2A P301L Tau production and *in vitro* transduction

The viral vector encoding experimental AAV8 P301L mutated tau was kindly gifted by Dr. Christiana Bjørkli (Department of Neuromedicine and Movement Science, NTNU). Adeno associated virus (AAV) vector production and purification was performed in-house at the Viral Vector Core Facility (Kavli Institute for Systems Neuroscience, NTNU). Tittering of the viral stock was determined as approximately 10^{11} vg/mL. The viral stock was divided into 20 µl aliquots and stored at -80°C . Aliquots designated for use were thawed on ice, while any remaining virus was also aliquoted and stored at -80°C for future use. Each aliquot was thawed a maximum of 3 times. Viral units were introduced to healthy networks at 28 DIV to induce perturbation. Neurons were transduced by removing 70% of the cell media from the presynaptic nodes and directly adding 3 x 10^2 viral units per neuron diluted in cell media. After addition of the virus, the cultures were gently agitated for 30 s to ensure proper distribution and then incubated for 4 h. During our extensive testing of the protocol, we evaluated varying viral concentrations including low levels (between 1 x 10^2 and 8 x 10^2 viral units per neuron) and high levels (between 1 x 10^3 and 5 x 10^3 viral units per neuron). The final titer of viral units per neuron was decided by selecting the lowest concentration that achieved a balance between high transduction efficiency and prolonged cell culture longevity (results of the protocol testing not included). Afterwards, each well was topped up with fresh media without antibiotics and incubated for an additional 20 h at 37°C/5% CO_2. After the incubation period, 50% changes of the media were carried out as scheduled. To ensure comparable conditions with the control networks, an 80% media change was also conducted in the control unperturbed networks at the same time as the addition of

AAV P301L to the perturbed networks. The viral vector encoded a GFP fluorescent tag for easy visualization of transduction efficiency.

2.2. Immunocytochemistry

To assess network maturity including the expression of structural neuronal markers such as microtubule associated protein, immunocytochemistry (ICC) was performed as follows. Prior to immunostaining, cell media were aspirated and discarded from the culture plates, and the cultures were rinsed once with Dulbecco's Phosphate Buffered Saline (DPBS; Thermo Fischer Scientific, Cat #14040-117). Following this, networks were fixed with 4% Paraformaldehyde (Sigma-Aldrich, #P6148) for 10 min at room temperature followed by 3x10 min washes with DPBS. Further, all DPBS were discarded and replaced by blocking solution consisting of 5% Goat serum (Sigma-Aldrich, Cat# G9023) and 0.3% Triton-X (Thermo Fischer Scientific, Cat# 85111) in DPBS. Next, primary antibodies at the indicated concentration (**Table 1**) were added in a buffer of 0.01% Triton-X and 1% Goat Serum in DPBS overnight at 4°C. The following day, primary antibody solution was discarded, and cultures were rinsed 3x5 min with DBPS before secondary antibodies at the indicated concentration (**Table 1**) were added in a buffer of 0.01% Triton-X and 1% Goat Serum in DPBS for 2 h at room temperature. For staining cellular nuclei, Hoechst dye (bisbenzimide H 33342 trihydrochloride; Sigma-Aldrich, Cat# 14533) was added at 1:10.000 dilution for the last 10 min of the secondary antibody incubation. Samples from the 8-well Ibidi chips were washed with PBS, mounted on glass cover slides with anti-fade fluorescence mounting medium (Abcam, Cat#Ab104135) whereas microfluidic chips were filled with distilled Milli-Q-water before imaging. Immunolabelling was conducted at 22 DIV on control unperturbed neural network samples, as well as on perturbed neural networks that were transduced with AAV8 P301L at 20 DIV.

Table 1. List of primary and secondary antibodies with concentrations

Primary antibodies	**Concentration**	**Supplier**
Ck Map2	1:1000	Abcam, #Ab5392
Rb Phospho-Tau (Thr217) (pTau)	1:1000	Invitrogen, #44-744
Ms AT8 (Ser202/205)	1:1000	Invitrogen, #MN1020
Rb GAD65/67	1:100	Abcam, #Ab183999
Ms Calmodulin (CaMKIIa)	1:200	Invitrogen, #MA3-918
Rb GFAP	1:500	Abcam, #Ab278054
Secondary antibodies	**Concentration**	**Supplier**
Goat-Anti-Mouse Alexa Fluor 674	1:1000	Invitrogen, #A21236
Goat-Anti-Rabbit Alexa Fluor 488	1:1000	Invitrogen, #A21244
Goat-Anti-Chicken Alexa Fluor 568	1:1000	Abcam, #Ab175477

Ms: Mouse, Rb: rabbit, Ck: chicken.

2.2.1 Imaging

All samples from ICC were imaged using an EVOS M5000 microscope (Thermo Fischer Scientific, #AMF5000) connected to a LED light source and using an Olympus 20x/0.75 NA objective (N1480500), with the following filter sets/channels: DAPI (AMEP4650), CY5 (AMEP4656), GFP (AMEP4651) and TxRed (AMEP4655). Phase contrast images were taken using a Zeiss Axio Vert V.1 brightfield 20x/53 WD/0.4 NA objective with an Axiocam 202 mono. Images were processed using Adobe Photoshop 2020. To quantify for fluorescent intensity profile of AT8 and pTau in cell body clusters and axonal bundles in both perturbed and control unperturbed networks, fluorescent signal was measured in Fiji/ImageJ2. A total of six clusters of cell bodies and five axonal bundles were selected as regions of interest and assessment was done for total fluorescent signal (mean intensity/pixel) measured by mean grayscale. The data was further processed in Matlab R2021b. Additional statistical analysis of the mean grayscale values between perturbed and unperturbed networks using Statistical Package for the Social Sciences (SPSS) version 29.0.0.0.

2.3. Electrophysiological recordings

Electrophysiological activity of neural networks on mMEAs (n=7) was recorded using a MEA2100 recording system (Multichannel Systems, MCS, Reutlingen, Germany) at a sampling rate of 25,000 Hz. A 3D-printed in-house made plastic cap covered by a gas-permeable membrane was used to keep the cultures sterile during recordings. The stage temperature was set to 37°C (TC01, Multichannel Systems) and the cultures were allowed to equalize on the stage for 5 min before spontaneous electrophysiological activity was recorded for 15 min. All networks were recorded 24 h after media changes on the following days *in vitro* (DIV): 16, 20, 24, 26, 28, 31, 33, 35, 37, 39, 41, 43, 45 and 47. From 28 DIV onwards, networks were electrically stimulated and simultaneously recorded for 1 minute (directly following the 15 min recordings of spontaneous electrophysiological activity). Electrical stimulations were applied to one presynaptic electrode with the highest detected mean firing rate (Pasquale et al., 2010) during the 15 min recording. Stimulation consisted of a train of 60 spikes at ± 800 mV (positive phase first) of 200 µs duration with an interspike interval of 5s. This was according to previous studies demonstrating that persistent electrical stimulation in *in vitro* networks can increase network activity over time, resulting in enhanced evoked action potentials and an increased frequency of spikes in bursts (Brewer et al., 2009; Ide et al., 2010). Raw data was converted to an .h5 Hierarchical Data Format using Multichannel DataManager (V.1.14.4.22018) system and imported to Matlab R2021b for further analyses using adapted and custom-made scripts.

2.4. Data analysis

Electrophysiology data analysis was done as previously described (Winter-Hjelm N, 2023). Briefly, raw data was filtered using a 4th order Butterworth bandpass filter removing low frequency fluctuations below 300 Hz and high frequency noise above 3000 Hz. A notch filter was used to remove 50 Hz noise caused by the power supply mains. Stimulation data was filtered using the SALPA filter (Wagenaar et al., 2002), and each stimulation time point was followed by 15 ms blanking. Spike detection was conducted using the Precise Timing Spike Detection (PTSD) algorithm (Maccione et al., 2009) with a threshold of 11 times the standard deviation, a maximum peak duration set to 1 ms and a refractory period of 1.6 ms. Burst detection was conducted using the logISI approach (Pasquale et al., 2010), with a minimum of four consecutive spikes set as a minimum for a burst to be detected, and a hard threshold of 100 ms. Network bursts were detected using the logIBEI approach (Pasquale et al., 2010), with at least 20% of active electrodes required to participate during the span of a network burst. Network synchrony was measured using the coherence index (Timme et al., 2018).

2.5 Statistical analysis

Statistical Package for the Social Sciences (SPSS) version 29.0.0.0 was utilized for all statistical analyses. For comparison of the repeated measures, we used Generalized Linear Mixed-Effect Models (GLMMs) with network type (i.e., controls versus perturbed networks) as a fixed effect, and the network characteristics as targets. The network age (DIV) was used as a random effect. Only data from 31 DIV onwards were included in the analysis to specifically compare changes in network characteristics following perturbation to the control unperturbed networks. A gamma probability distribution with a log link function was chosen as the linear model. This selection was based on the Akaike information criterion and initial assessment of distribution fit to the predicted values. For multiple comparisons, we used sequential Bonferroni adjustment.

3. Results

3.1. Engineered feedforward cortical networks show intra- and internodal connectivity

Prior to perturbation, we validated that neurons were structurally connected with each other within the nodes and expressed markers for excitatory and inhibitory synaptic transmission. Our results showed that the neural networks organized into densely interconnected intranodal architectures, with outgrowing neurites in the microtunnels **(Figure 2A-B).** Additionally, ICC performed at 22 DIV revealed expression of the microtubule-associated protein 2 marker, MAP2 **(Figure 2C-D)**, the inhibitory neuronal marker glutamic acid decarboxylase 65/67, (GAD65/67) (Fukuda et al., 1997) **(Figure 2C)**, and the excitatory neuronal marker calcium-calmodulin (CaM) – dependent protein kinase II, (CaMKII) (Takao et al., 2005) **(Figure 2D)**. The presence of these markers indicated that the networks consisted of mature neurons with the capacity for excitatory and inhibitory synaptic transmission, a crucial aspect for achieving structural and functional network maturity.

To investigate whether the engineered networks were functionally connected, we monitored and recorded electrophysiological activity commencing at 16 DIV. By 26 DIV, the neural networks displayed a mature electrophysiological profile in line with previous studies (Chiappalone et al., 2006; Winter-Hjelm N, 2023). Specifically, raster plots of spontaneous activity within the network revealed both isolated spikes and synchronized bursts **(Figure 3A)**, while correlation matrices of network connectivity showed strong connectivity within pre- and postsynaptic nodes, as well as functional connectivity between the nodes **(Figure 3B)**. To further validate internodal connectivity, we applied electrical stimulations to the electrode with the highest firing rate within the presynaptic node at 26 DIV. We recorded and assessed the evoked activity in the postsynaptic node, which revealed that electrical stimulations caused a spiking response in the presynaptic node, followed by an on average 40 ms time delay before a subsequent spiking response was observed in the postsynaptic node **(Figure 3C)**. This effectively demonstrated that functional connectivity was established between the- pre and postsynaptic nodes.

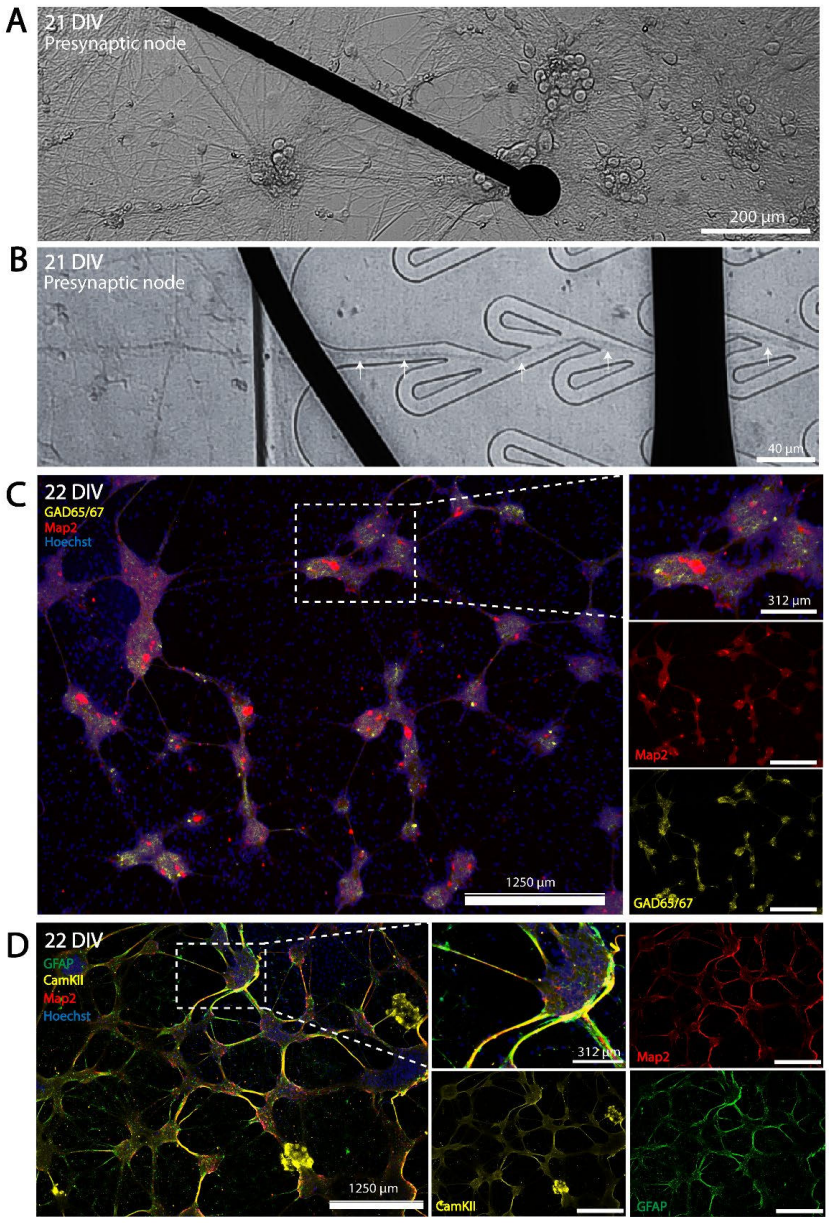

Figure 2. Developing structural organization and functional maturity of feedforward engineered neural networks (A-B) Phase contrast images of a neural network in the presynaptic node **(A)** with neurite projections going through the microtunnels **(B**) on a mMEA at 21 DIV. **(C-D)** Networks positively immunolabeled for the neuronal marker MAP2 in addition to the inhibitory marker GAD65/67 **(C)** and the excitatory neuron marker CaMKII **(D).** Glial fibrillary acidic protein (GFAP) antibody labelling of astrocytes in the network. DIV; days in vitro. Scale bar 1250 µm; (magnified area 312 µm).

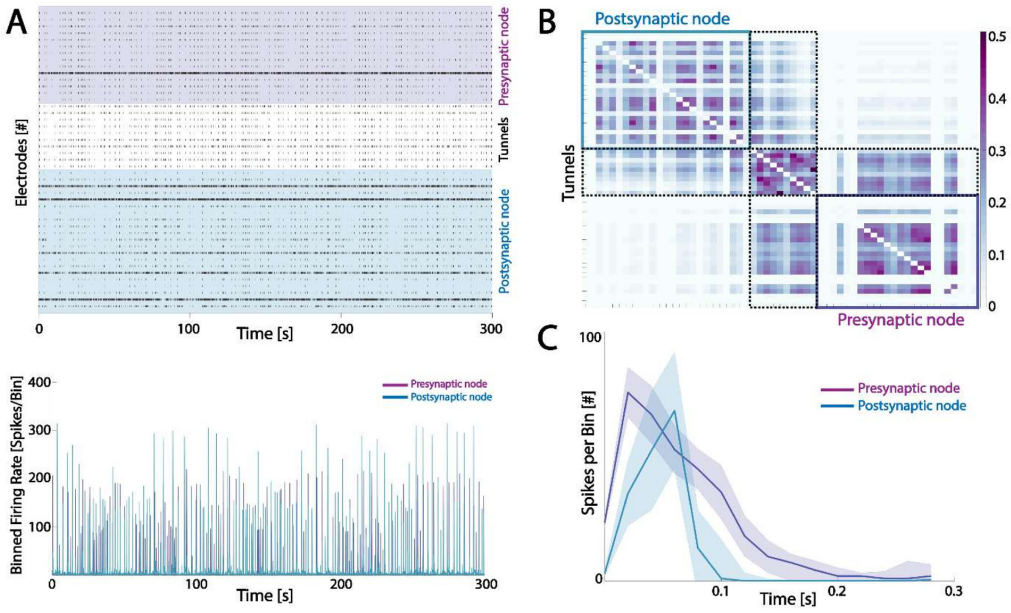

Figure 3. Neural networks displayed intra- and internodal functional connectivity at 26 DIV (A) Raster plots (300 seconds) of the recorded activity (top panel) and binned network activity (bottom panel) of corresponding total firing rate of one representative network. **(B)** Mutual information connectivity matrix showing the correlation in the network activity in nodes and tunnels. **(C)** Peristimulus time histogram of the pre- and postsynaptic response to an electrical stimulation in the presynaptic node. The graphs here show an initial response in the presynaptic node, followed by a delayed response in the postsynaptic node.

3.2. Perturbed networks express human mutated tau

At 28 DIV, we induced expression of human mutated tau protein in the presynaptic nodes of the engineered networks. The AAV construct encodes GFP, which allowed for easy visualization of transduction efficacy. Positive GFP expression was seen in the perturbed networks **(Figure 4B and Figure 5B)** which indicated effective AAV transduction. For additional verification of phosphorylated tau expression, we also labeled the networks for AT8 (Serine 202 and Threonine 205/ $tau^{202/205}$) and Phospho-Tau (Threonine 217/tau^{217}) proteins, hereon referred to as $tau^{202/205}$ and tau^{217}, respectively. Both $tau^{202/205}$ **(Figure 4B)** and tau^{217} **(Figure 5B)** were overexpressed in neuronal cytosols and axons along with GFP in perturbed networks. Perturbed networks had significantly higher expression of both $tau^{202/205}$ and tau^{217} (Rajbanshi et al., 2023) in the cytosolic compartments compared to controls, while a non-significant higher expression of $tau^{202/205}$ was found in axon bundles compared to controls. Additionally, we conducted primary exclusion immunolabeling for both $tau^{202/205}$ and tau^{217} to assess the specificity of the binding antigen, and no expression was found **(Figure 4C and 5C, respectively)**.

We also performed secondary antibody exclusion to assess the labeling specificity of the primary antibody and found no immunoexpression for either tau$^{202/205}$ or tau^{217} in the networks.

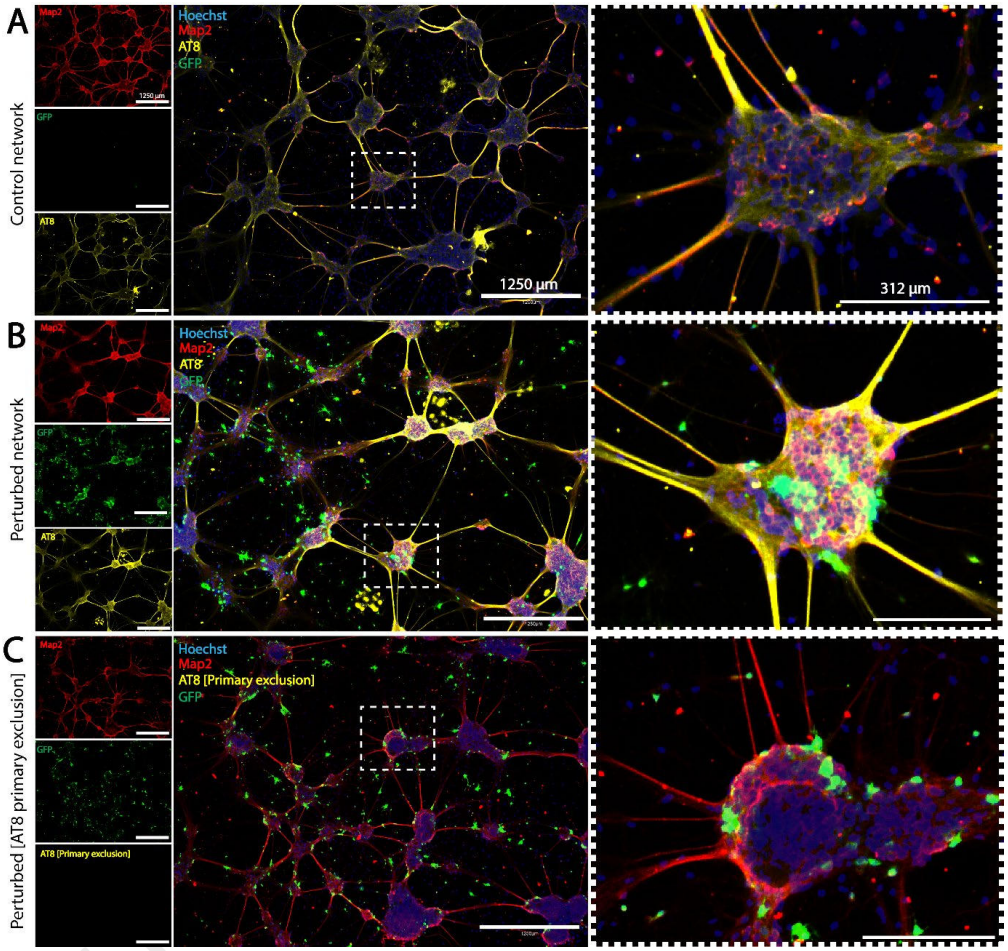

Figure 4. GFP expression exclusively in perturbed networks confirmed efficacy of viral transduction, further validated by AT8 expression. (A) Control unperturbed networks were not transduced with the AAV8-GFP-2A-P301L construct and thus did not express GFP. AT8 labeling was found primarily in axons. **(B)** Perturbed networks were positive for the GFP marker after transduction, with strong axonal and somato-dendritic AT8 expression. **(C)** Exclusion of the primary antibody AT8 to assess the specificity of antigen binding. Scale bar 1250 µm; (magnified area 312 µm).

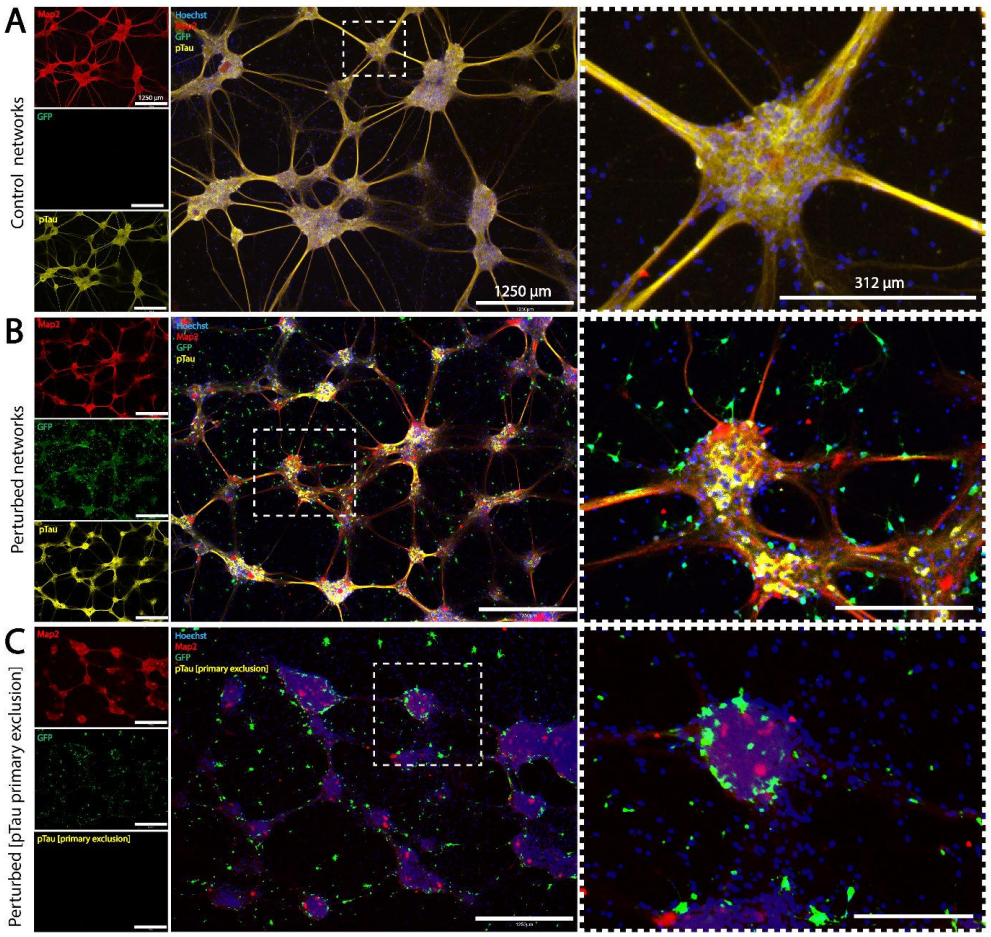

Figure 5. GFP expression exclusively in perturbed networks confirmed efficacy of viral transduction, further validated by pTau expression (A) Control unperturbed networks were not transduced with the AAV8-GFP-2A-P301L construct and thus did not express GFP. pTau labeling found in axons and cytosols. **(B)** Perturbed networks were positive for the GFP marker after transduction, with strong axonal and somato-dendritic pTau expression. **(C)** Primary exclusion of pTau to assess the specificity of antigen binding. Scale bar 1250 µm; (magnified area 312 µm).

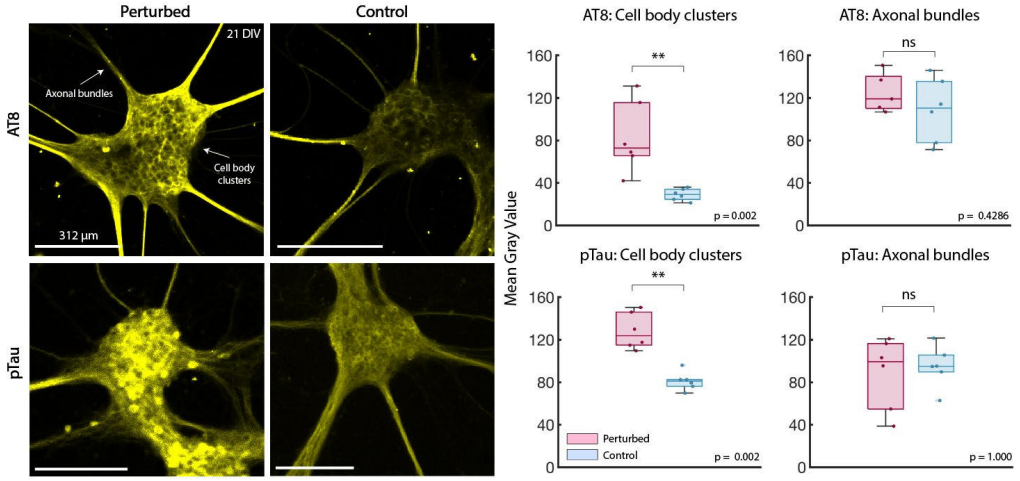

Figure 6. Quantification of fluorescent intensity of AT8 (tau$^{202/205}$) and pTau (tau^{217}) in perturbed and control unperturbed networks. Representative images from networks with AT8 and pTau labelling showing cell body clusters and axonal bundles. Bar graphs showing the mean gray value of cell body clusters.

3.3. Progressive internodal axonal retraction observed after perturbation

Prior to induced perturbation, phase contrast imaging of neural networks at 21 DIV confirmed structural connections between the pre- and postsynaptic neural nodes **(Figure 7A).** Interestingly, by four days post perturbation, i.e., at 32 DIV, the neurites within the presynaptic node of the perturbed networks started retracting from the entry zone near the unidirectional microtunnels, and by 52 DIV all structural connections between the presynaptic and postsynaptic nodes had been lost entirely **(Figure 7A).** Extensive neurite retraction was also observed in the postsynaptic node of the perturbed network by 52 DIV. In contrast, control unperturbed networks maintained robust neurite connections both at the entry zone of the presynaptic node microtunnels and the exit zone in the postsynaptic node **(Figure 7B).**

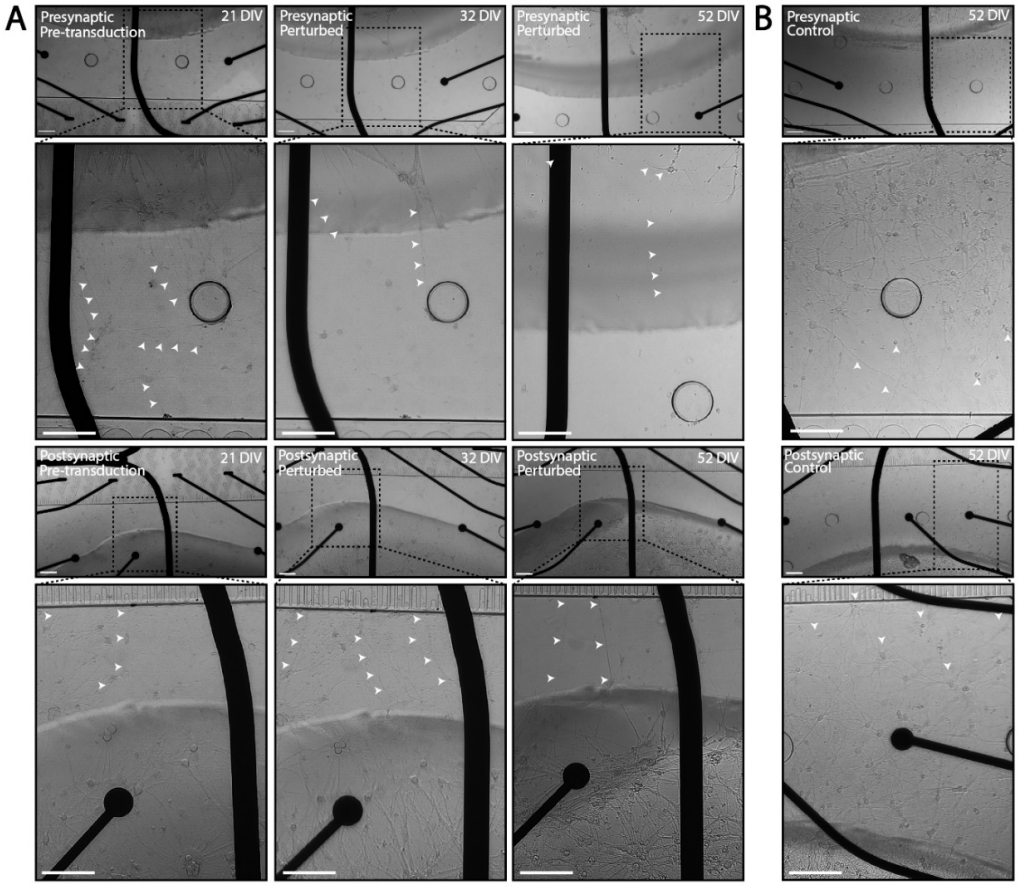

Figure 7. Progressive neurite retraction and active reorganization observed within networks following induced perturbation. (A) The leftmost column shows neurite extensions in the presynaptic node at the entry zone of the unidirectional microtunnels (top) and dense neurites in the postsynaptic node at the exit zone of the unidirectional microtunnels (bottom) at 21 DIV. The middle column is a snapshot of the same region in the network at 32 DIV showing retraction in the presynaptic node (top), but not in the postsynaptic node (bottom). The rightmost column shows extensive retraction in the presynaptic node (top) as well as in the postsynaptic node at 52 DIV (bottom). **(B)** Presynaptic (top) and postsynaptic (bottom) nodes of control unperturbed network depicting dense neurite connections at 52 DIV. Scale bar 100 µm.

3.4. Perturbed networks exhibit a decrease in overall network activity and an increase in network synchrony

Spontaneous network activity was recorded between 16 DIV and 47 DIV for both control unperturbed and perturbed networks. We captured network development from low activity to more mature profiles exhibited as increased mean firing rate **(Figure 8A)** and increased mean burst rate **(Figure 8B)**. Activity recorded from both pre- and postsynaptic nodes revealed the differences between control unperturbed and perturbed networks and their functional evolution. Specifically, the presynaptic nodes of control unperturbed networks exhibited a steady increase in electrical activity between 16 DIV and 31 DIV, consistent with previous studies by us and others capturing developing functional activity in cortical networks (Wagenaar et al., 2006; Weir et al., 2023). Both firing rate and burst rate increased between 33 DIV and 45 DIV in the presynaptic node but not in the postsynaptic node **(Figure 8A and B, respectively)**.

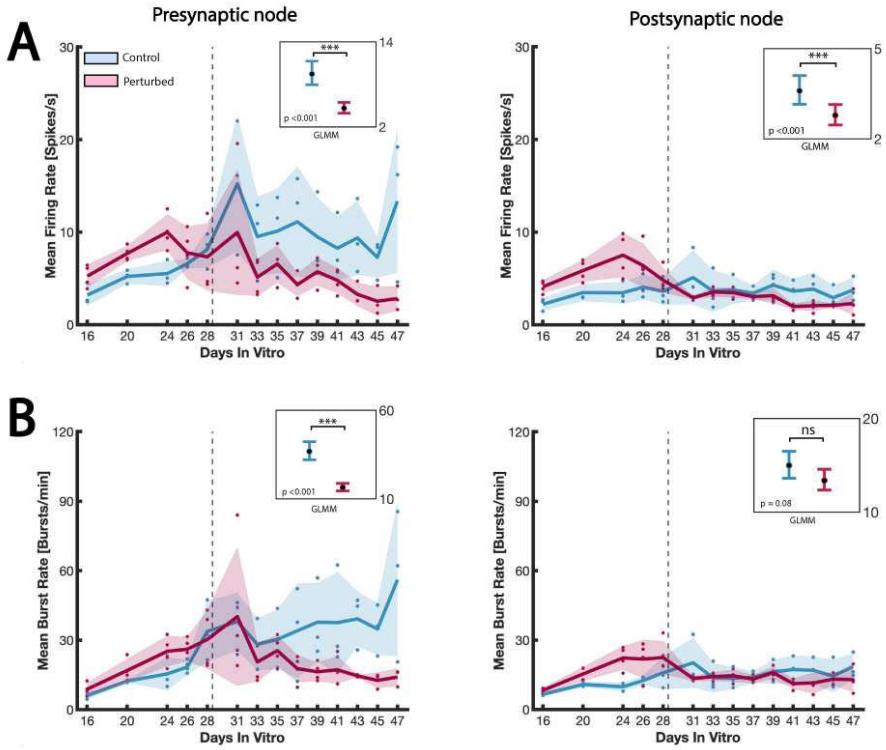

Figure 8. Electrophysiological recordings revealed progressive decrease in firing and burst rate in perturbed networks. (A) Mean firing rate (spikes/second) and **(B)** Mean burst rate (bursts/minute) in the presynaptic and post synaptic nodes for control unperturbed and perturbed networks. The solid lines denote the mean activity for the networks with the solid circles indicating individual data points. The shaded area denotes the standard error of the mean. The stippled line indicates the day of viral transduction in the perturbed networks (28 DIV). Plots showing the GLMM estimated group averages with 95% confidence intervals are depicted in the top right corner of the graphs.

Similarly, prior to induced expression of human mutated tau, the perturbed networks also exhibited a steady increase in both firing rate and burst rate in the presynaptic node between 16 DIV and 28 DIV. However, between 31 DIV and 47 DIV, they exhibited significantly lower firing ($p< 0.001$) and burst ($p< 0.001$) rates compared to healthy controls **(Figure 8A)**. The firing rate in the postsynaptic node of perturbed networks remained significantly lower ($p< 0.001$) than controls for the duration of the study **(Figure 8A)**. There were no significant differences in mean burst rate in the postsynaptic node between healthy controls and perturbed networks **(Figure 8B).**

The postsynaptic node of healthy controls had significantly longer bursts ($p= 0.001$) compared to perturbed networks **(Figure 9B)**, however, there were no significant differences in the mean burst duration in the presynaptic nodes between perturbed and healthy controls between 31 DIV and 47 DIV **(Figure 9A).** Furthermore, the total network activity (pre- and postsynaptic node activity combined) revealed that between 28 DIV and 47 DIV, healthy controls had significantly higher mean network burst duration ($p< 0.001$) compared to perturbed networks **(Figure 9C)**. Specifically, between 28 DIV and 33 DIV, control unperturbed networks exhibited a transient increase in mean network burst duration from 0.23 seconds to 0.26 seconds, however, there was a subsequent decrease between 33 DIV and 47 DIV **(Figure 9C)**. For the perturbed networks, the total network activity for pre- and postsynaptic nodes combined showed that between 33 DIV and 39 DIV there was a transient increase in network burst duration from 0.17 seconds to 0.22 seconds, with a subsequent decrease between 39 DIV and 47 DIV, similar to the healthy controls.

We also found that all networks had a general decrease in mean network burst size (analyzed as the percentage of active electrodes participating in network bursts), between 16 DIV and 28 DIV **(Figure 9D)**. The total bursting activity for pre-and postsynaptic nodes combined showed that control unperturbed networks decreased in burst size from 85% to 45% network participation **(Figure 9D)** between 16 DIV and 28 DIV**.** Similarly, networks before perturbation had a decrease in burst size from 82% to 43% network participation **(Figure 9D)**. Both groups had relatively stable burst size between 28 DIV and 47 DIV, however, perturbed networks had significantly larger network bursts ($p< 0.001$) by 47 DIV (61% of network participation) compared to control unperturbed networks (45% network participation) **(Figure 9D)**. Furthermore, when we examined network synchrony, measured by the coherence index, we observed a general decrease in both pre-and postsynaptic nodes of healthy controls between 16 DIV and 47 DIV **(Figure 9F)**. Both nodes of perturbed networks had progressively increased synchrony that was significantly higher ($p< 0.001$) than in control unperturbed networks between 31 DIV and 47 DIV **(Figure 9F)**.

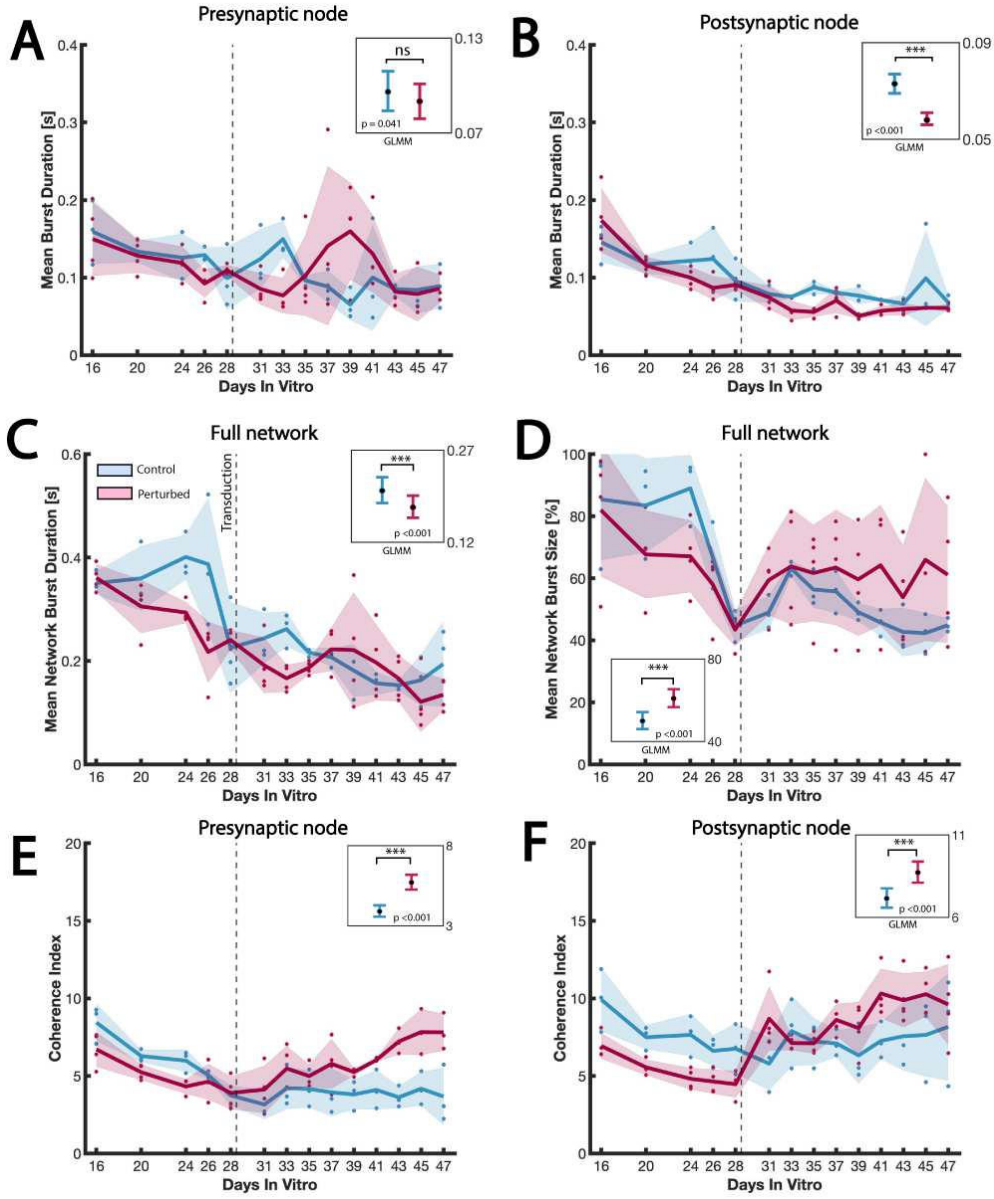

Figure 9. Electrophysiological recordings revealed a progressive increase in network burst size and synchrony in perturbed networks. ***(A)*** *Mean burst duration (seconds) in the pre-and* ***(B)*** *postsynaptic nodes of control and perturbed networks.* ***(C)*** *Mean network burst duration in the pre-and postsynaptic nodes combined for control and perturbed networks.* ***(D)*** *Mean network burst size (percentage) in the pre-and postsynaptic nodes combined for control and perturbed networks.* ***(E)*** *Coherence Index (measure of network synchrony) in the pre- and* ***(F)*** *postsynaptic nodes of control and perturbed networks. The solid line denotes the mean activity for the networks with solid circles indicating individual data points. The shaded area denotes the standard error of the mean. The stippled line indicates the day of transduction for the perturbed networks (28 DIV). Plots showing the GLMM estimated group averages with 95% confidence intervals are depicted in the top right corner of the graphs.*

3.5. Induced perturbation results in reduced propagation of spontaneous and evoked activity between nodes

Further analyses were conducted to determine the proportion of bursts propagating between the pre- and postsynaptic nodes in both control unperturbed and perturbed networks. We first evaluated the total number of network bursts exhibited by each network at each recording and identified the percentage of propagating bursts between the pre- and postsynaptic nodes in either direction **(Figure 10).** Our results showed that between 16 DIV and 28 DIV, both control unperturbed and perturbed networks had a steady increase in the total number of network bursts, with most or all bursts propagating in a feedforward manner from the presynaptic to the postsynaptic node **(Figure 10)**. Additionally, we found that for all subsequent recordings from 28 DIV onwards, burst propagation diminished in the control unperturbed networks to <2% by 47 DIV even though the total number of bursts within the network exceeded 2000 bursts/recording **(Figure 10)**. This implied that bursts were contained primarily within nodes of healthy controls. In contrast, perturbed networks exhibited a steady decline in the total number of network bursts between 33 DIV and 47 DIV (to less than10 bursts/recording by 43 DIV) **(Figure 10).**

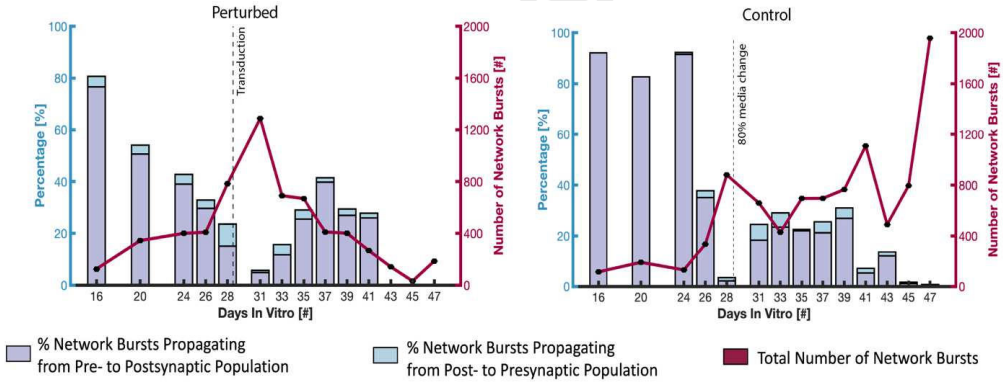

Figure 10. Feedforward burst propagation between pre- and postsynaptic nodes for perturbed (left) and control unperturbed (right) networks. The left y-axis on the graph denotes the percentage of network bursts propagating between the nodes, represented as the bars. The right y-axis denotes the total number of network bursts detected each day represented as the solid line. The x-axis denotes the day in vitro. The stippled line at 28 DIV indicates the day of transduction for the perturbed networks.

We also applied periodical electrical stimulations to the electrode with the highest firing rate in the presynaptic node to assess whether a presynaptic stimulus could evoke a postsynaptic response. The same electrode in each of the mMEAs was stimulated for 1 minute at each recording session between 28 DIV and 47 DIV. We found that electrical stimulation within the presynaptic node of control unperturbed networks produced a spike response followed by a postsynaptic spike response with an average delay time of 20 ms (31 DIV) and 40 ms (35 DIV) **(Figure 11A)**. Control unperturbed networks

also produced spike responses in the presynaptic node at 45 DIV and 47 DIV, although the tuning curves were of lower amplitudes than after previous stimulations. In addition, the spike responses in the postsynaptic node of control unperturbed networks at 45 DIV and 47 DIV were too low to allow for an evaluation of the delay time between the nodes. In contrast, stimulation in the presynaptic node of perturbed networks at 31 and 35 DIV resulted in a presynaptic spike response, with no spike response in the postsynaptic node **(Figure 11B)**. There was no response in presynaptic nor postsynaptic nodes at 45 DIV and 47 DIV in the perturbed networks.

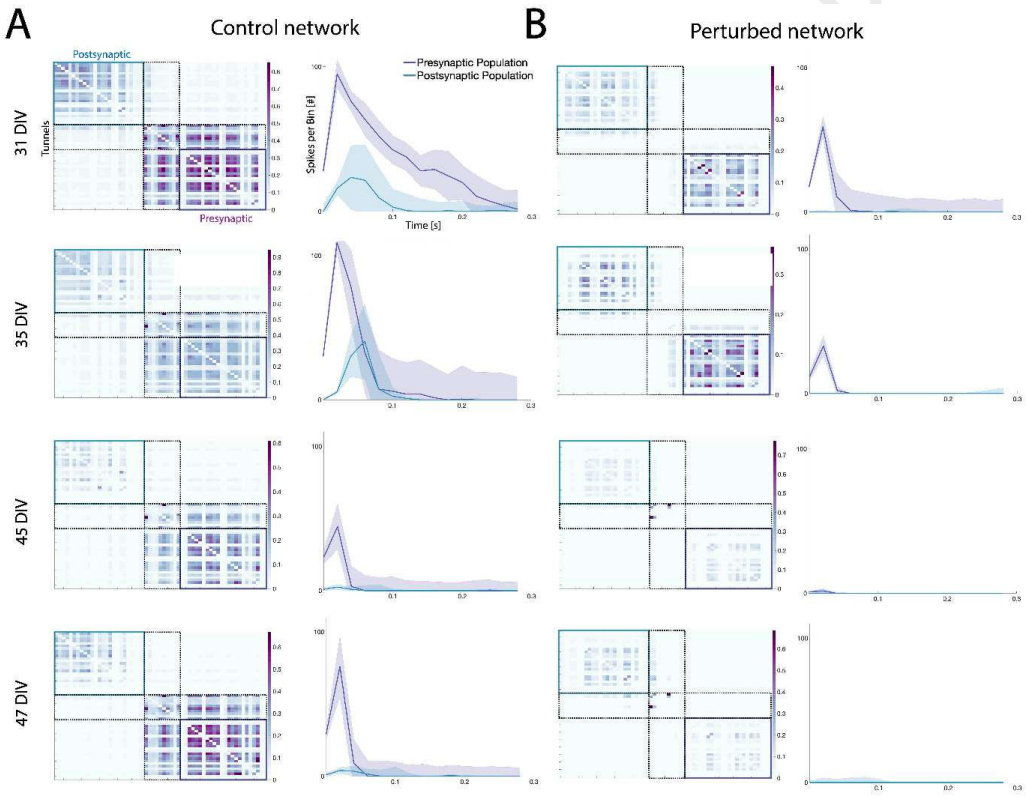

Figure 11. Induced perturbation resulted in progressive decline in presynaptic response to electrical stimulation between the pre-and postsynaptic nodes over time. (A) Mutual information connectivity matrices showing the network activity in chambers and tunnels (left column) and peristimulus time histograms of pre- and postsynaptic responses to electrical stimulations (right column) for control networks at 31, 35, 45 and 47 DIV. (B) Connectivity matrices showing the network activity in chambers and tunnels (left column) and peristimulus time histograms of pre- and postsynaptic responses to electrical stimulations (right column) for perturbed networks at 31, 35, 45 and 47 DIV. The curves show an initial response in the presynaptic network, followed by a delayed response in the postsynaptic network (for control networks) and no postsynaptic response (for perturbed networks). The shaded area denotes the standard error of the mean.

4. Discussion

Engineered neural networks *in vitro* self-organize into complex topologies and produce a complex profile of activity patterns ranging from individual spikes produced by single neurons to high frequency network bursts generated by neural assemblies (Chiappalone et al., 2006; van de Wijdeven et al., 2018; Weir et al., 2023). The development of complex network activity can be attributed to the structural properties of the network, as function tends to co-evolve with structure (Kapucu et al., 2017). Activity typically evolves with the maturity of neurons, and of excitatory and inhibitory synapses. As shown in **Figure 2**, our engineered neural networks expressed both the excitatory neuronal marker CaMKIIa, and the inhibitory neuronal marker GAD65/67 in conjunction with the neuronal marker MAP2 by 21 DIV, strongly indicating the capacity for excitatory – inhibitory synaptic transmission within the maturing networks. This was further verified through recordings of electrophysiological activity, which showed that in healthy conditions, networks developed highly dynamic and complex age-dependent firing activity and network bursts over time, in line with previous studies by us and others (Chiappalone et al., 2006; Chiappalone et al., 2007; Fiskum et al., 2021; van de Wijdeven et al., 2018; Weir et al., 2023).

The structural organization of neural networks is a crucial determining factor for the emergence of complex network dynamics and information processing. In our engineered feedforward networks, we showed that neurites extended from the presynaptic nodes into the microtunnels towards the postsynaptic nodes, thus establishing structural connections. Furthermore, electrical stimulation at 26 DIV confirmed that these networks were functionally interconnected, as evoked activity in the presynaptic node could propagate and elicit a response in the postsynaptic node (illustrated in **Figure 3**), in line with previous findings (Fair et al., 2009; Ma et al., 2018; Winter-Hjelm N, 2023). These results confirm recapitulation of a feedforward network *in vitro*, where information flows in a unidirectional manner, propagating sequentially from input nodes to output nodes (Barzegaran et al., 2022; Markov et al., 2014). Such feedforward hierarchical organizations are found in many parts of the brain (Markov et al., 2014; Siegle et al., 2021), and facilitate fast, efficient information processing between pre- and postsynaptic neuronal assemblies. We also observed spontaneous feedforward burst propagation in control unperturbed networks occurring from 16 DIV to 43 DIV, and perturbed networks from 16 DIV to 41 DIV **(Figure 10).** The ability of the network to spontaneously transmit information between the nodes is an essential factor in determining its functional capacity since this enables the integration of signals that support coordinated, complex information processing (Fauth et al., 2019; Fukushima et al., 2018; Senden et al., 2018). As such, our results confirmed the intended structural and functional organization of engineered feedforward cortical networks, with the presynaptic node providing input to the postsynaptic node **(Figure 3 and Figure 10)**.

These engineered feedforward networks also enabled us to selectively induce a perturbation, via AAV mediated expression of human mutated tau in the presynaptic node, and to monitor resulting effects within and between nodes. By utilizing this approach, we can effectively recapitulate and monitor a pathological process at the micro- and mesoscale. Such a process not only induces structural and functional changes in the immediately affected node, but also disrupts both structure and function in the postsynaptic node (Kuhl, 2019; Valderhaug et al., 2021). These findings are highly relevant for advanced modelling of evolving pathological processes in neurodegenerative diseases, such as AD, where an association between the progression of tau pathology and altered transsynaptic activity has been demonstrated (Liu et al., 2012). Such transsynaptic spread of tau pathology is attributed to the robust connection loops that exist between the putative origin points of tau pathology in the lateral entorhinal cortex layer II (Braak et al., 1991) and feedforward anatomical sites to hippocampal subregions (Liu et al., 2012; Stepan et al., 2015; Witter, 2007; Witter et al., 2017). This feedforward transsynaptic spread of hyperphosphorylated tau may contribute to structural impairments that disrupt the normal functioning of neural networks. In our study, by quantification of fluorescent signaling of $tau^{202/205}$ and tau^{217} expression, we find prominent differences, i.e., increased tau^{217} and $tau^{202/205}$ in the cytosol of neurons in the perturbed networks compared to the control unperturbed ones, signifying detrimental effects of tau phosphorylation. Normal phosphorylation at $tau^{202/205}$ sites is found in maturing brain and is associated with neural development (Goedert et al., 1995), while tau^{217} phosphorylation is found to be associated with the normal development of postsynaptic sites (Rajbanshi et al., 2023). This means that some phosphorylation of tau at these sites is to be expected in control unperturbed networks as shown in **Figure 6**. Furthermore, studies have shown that the phosphorylation of tau at a single site does not preferentially induce neurotoxic effects (Steinhilb et al., 2007). It appears then that the neurotoxic effects of tau depend on a combined high phosphorylation pattern at multiple sites in axons and/or cytosol, which we have demonstrated in our perturbed networks **(Figure 6)**. In addition, recent findings also reported a correlation between high tau^{217} expression and AD pathology progression (Rajbanshi et al., 2023) associated with synaptic decline. Therefore, our finding of increased expression of both $tau^{202/205}$ and tau^{217} in the cytosol of neurons within the perturbed networks suggests that the introduction of human mutated tau, capable of inducing detrimental synaptic effects, has impacted both the structural and functional dynamics of these networks.

This result is further supported by the differences found in the electrophysiological activity of perturbed networks compared to unperturbed controls. Initially, both unperturbed control and perturbed networks had diminished burst propagation between pre- and postsynaptic nodes over time, with very little propagation from 41 DIV in healthy controls, and no propagation after 43 DIV in

the perturbed networks, as illustrated in **Figure 10**. The decreased level of spontaneous activity propagation in healthy networks with age, i.e., DIV, is suggestive of local information processing within nodes, rather than internodal processing. This is further supported by the drastic increase in the total number of bursts detected within nodes of controls (>1800 bursts/recording by 47 DIV), at the same time as the perturbed networks experienced a drastic decline in the total number of bursts within nodes (<10 bursts/recording by 47 DIV) as shown in **Figure 10.** The perturbed networks exhibited differences that can be attributed to increased tau hyperphosphorylation, which, when combined with feedforward propagation between the immediately affected node and the healthy node, precipitated the spread of perturbation effects, leading to disruption in normal synaptic activity across the entire network.

Other studies have found that severity of neuronal loss and atrophy of cortical structures as a result of tau pathology tend to positively correlate with the severity of functional network decline (Adamec et al., 2002; Rascovsky et al., 2005), thus highlighting the complex interrelationship between network structure and function in pathology. The present study revealed such dynamic structural and functional changes in perturbed networks, attributable to the induced expression of human mutated tau at 28 DIV. Between 32 DIV and 52 DIV, we observed progressive neurite retraction from the entry zone near the microtunnels in the presynaptic nodes in the perturbed networks. We also noticed that retraction from the exit zone near the postsynaptic nodes also occurred within weeks of presynaptic retraction as shown in **Figure 7A**. This was not observed in the unperturbed control networks, which maintained a dense neurite network in the zones near the microtunnels in both nodes as seen in **Figure 7B**. The significance of these changes in perturbed networks lies in their potential to adversely affect the network's ability to transmit and integrate information. Prolonged expression of mutant P301L tau exacerbates axonal destabilization (Biswas et al., 2018; Qiang et al., 2018) and impairment of presynaptic terminals (Hunsberger et al., 2021). Furthermore, both maintenance of presynaptic integrity and synaptic plasticity depend on active anterograde and retrograde axonal transport systems (Cai et al., 2011), thus impairment of tau in axons can affect such processes (Lacovich et al., 2017) and severely disrupt synaptic functions between pre- and postsynaptic nodes in perturbed networks. Furthermore, the observed subsequent neurite retraction in the postsynaptic node of the perturbed networks (shown in **Figure 7A)**, suggested that the loss of presynaptic input triggered reorganization within postsynaptic nodes. These observations thus indicated a dynamic process of structural and functional reconfiguration across the entire feedforward network in response to presynaptic node perturbation.

The prominent structural changes observed following induced perturbation occurred concomitantly with changes in the electrophysiological profile of the perturbed networks between 28 DIV and 47

DIV. Prior to perturbation and between 16 DIV and 28 DIV, all networks in our study exhibited similar trends in activity patterns such as firing and burst rate **(Figure 8)**, burst duration and synchrony **(Figure 9)** and burst propagation **(Figure 10)**. In healthy conditions, gradually increasing firing and burst patterns are crucial for the establishment and maintenance of functional synapses, and the elaboration of the network topology into hierarchical processing. Bursts also contribute to the formation and refinement of neural circuits especially during early network formation (between 9 and 21 DIV) [49], where they facilitate the integration of immature neurons into the maturing network. It is therefore expected that all healthy networks would inherently follow this developmental trend of increasing firing and burst rates prior to perturbation. Following the induced expression of human mutated tau, perturbed networks exhibited a steady decline in both firing rate and burst rate in comparison to control unperturbed networks, which continued to display a steady increase over time **(Figure 8)**. Furthermore, these differences in firing rate following perturbation were found to be significant between control unperturbed and perturbed networks in both pre- and postsynaptic nodes. This suggested that perturbed networks became less electrophysiologically active as they underwent structural reorganization, including neurite retraction. The observed decrease in firing and bursting activity also aligned with *in vivo* findings showing that neurons in a mouse model with the Tau-P301 mutation gradually became more hypoactive (Busche et al., 2019). However, Busche et al., (Busche, 2019) also suggested that the disruption in network activity occurred before any prominent structural tau abnormalities were observed in vivo. We have shown however, that the decline in general network activity correlated strongly with the progressive loss of synaptic connectivity and pre- and postsynaptic neurite reorganization. These changes are highly challenging to detect and correlate *in vivo*.

Another interesting result in our study was the significant increase in network burst size and synchrony, as measured by the coherence index, observed in the perturbed networks between 28 DIV and 47 DIV **(Figure 9 E and F)**. Network bursts, which are coordinated patterns of neuronal activity exhibited by multiple interconnected neurons within the network, are ubiquitous for normal network function (Weir et al., 2023). Coordinated neuronal activity also leads to network synchrony (Salinas et al., 2001), and is thus important for information processing, coding, and synaptic integration of distributed signals (Gansel, 2022). Synchrony may also promote activity-dependent establishment of synaptic connections via spike-timing dependent plasticity (STDP) (Anisimova et al., 2022) to support network function. In a recent study by our group, we found that networks that were perturbed by selective silencing of excitatory synaptic transmission also demonstrated increased synchrony during network recovery (Weir et al., 2023). Such behavior may thus be crucial for the network's ability to restore its functional and structural organization within specific time windows after a perturbation.

On the other hand, increased synchrony may also have adverse effects, such as facilitating the spread of perturbations through axons and synapses to affect the entire interconnected network (Uhlhaas et al., 2006), as has been found in AD pathology (Liu et al., 2012; Wang et al., 2017). Furthermore, excessive network bursts and synchrony have been implicated in various neurological disorders, including epilepsy, where they signify a disruption in normal network physiology i.e., impaired excitatory-inhibitory dynamics (Kudela et al., 2003; Wu et al., 2015). Therefore, while a degree of network synchrony is necessary for normal functioning, too much can be problematic. This raises a crucial question regarding whether the observed synchrony in the perturbed networks in our study may represent an adaptive or maladaptive network response to induced perturbation.

Interestingly, synchrony increased concurrently with neurite retraction at 32 DIV, and while firing and burst rate declined. We found that, following perturbation, networks began exhibiting fewer, yet larger synchronized bursts, which can be interpreted as a homeostatic compensatory response to maintain network activity as the overall firing and burst rates declined. In response to low network activity levels, homeostatic scaling, which occurs gradually and over several hours to days, can increase overall input to counteract hypoactivity (Chowdhury et al., 2018; Turrigiano, 2008). This may explain the observation of increasing synchrony between 31 DIV and 47 DIV **(Figure 9 E and F).** However, increased synchrony could also signify pathophysiological changes in the underlying network since it occurred concomitant with the evolution of induced pathology. *In vivo,* induced perturbation caused by hyperphosphorylated tau can disrupt the structural and functional integrity of the affected network, and subsequently result in increased inflammation leading to apoptotic or necrotic cell death (Dong et al., 2022; Thal et al., 2022). Furthermore, it has been suggested that the presence of diverse connections and pathways within a neural network can provide alternative routes for information flow to reduce the reliance on a single synchronized pathway (Kirst et al., 2016), thus acting as a gatekeeping mechanism to prevent excessive synchrony and enhancing overall network robustness. In our study, as induced perturbation led to progressive structural and functional disruption in the network, it is likely that information flow within the network might have been hindered, as there were insufficient alternative routes to effectively distribute activity, ultimately leading to excessive synchrony. This is further supported by observations in control unperturbed during the same time frame between 31 DIV and 47 DIV. During this time, control networks exhibited significantly higher mean firing and burst rates **(Figure 8)** and comparatively more bursts within nodes **(Figure 10)**, without showing excessive synchrony. These networks also maintained the dense neurite architectures between the nodes. This effectively suggests that the unperturbed control networks possessed the ability to maintain their activity within a dynamic range to prevent excessive network wide activation, an ability which the perturbed networks appeared to gradually lose. Based on these

findings, increased network synchrony after induced perturbation might be associated with the deterioration of overall network function in response to the perturbation, rather than serving as an adaptive purpose.

Lastly, to further investigate whether perturbation affected structural and functional connectivity between the nodes, we applied periodic electrical stimulation to one electrode within the presynaptic node and assessed the postsynaptic response. We found that although control unperturbed exhibited a consistent presynaptic spike response to electrical stimulation, there was a gradual decline in the postsynaptic response over time as illustrated in **Figure 11A**. This could be due to activity dependent long-term synaptic changes in the vicinity of the stimulating electrode, such as a reduction in synapse number or downscaling of synaptic receptors on neurons, as previously reported (Collingridge et al., 2010). Such activity dependent structural changes would likely reduce the amplitude of the presynaptic response, thus reducing the strength of the propagating signal (as shown in **Figure 11A)**. For perturbed networks, we found that there was no response to presynaptic stimulation in the postsynaptic node by 31 DIV (**Figure 11B)**. This outcome was anticipated as we had already observed extensive neurite retraction in the presynaptic node by the specific time point, indicating the severance of connectivity between nodes. No response to stimulation was observed in the presynaptic node at 45 DIV and 47 DIV, which may be due to possible progressive neuron loss in the network, or structural reorganization of any remaining neurons to areas outside the vicinity of the stimulating electrode. Nevertheless, the differences in response to electrical stimulation between perturbed and control unperturbed networks may reflect the functional capacity of each network, although determination of whether these differences were indeed related to the networks´ functional capacity was beyond the scope of this study. In this paper, our objective was to monitor ongoing changes in both structure and function, a goal we successfully demonstrated through our results. This underscores the efficacy of our platform in investigating dynamic changes to perturbation at the network level. Additionally, it could potentially allow for the examination of how mutated tau affects neurons at the molecular level, including phenomena like mitochondrial changes. This, in turn, may facilitate the assessment of critical molecular shifts throughout the timeline of network alterations, although this specific aspect falls beyond the scope of our present study. These findings have significant implications for future research endeavors and their ability to tract and analyze such intricate processes.

5. Conclusions and future directions

Using engineered two-nodal feedforward neural networks with controllable afferent-efferent connections, we longitudinally monitored and assessed dynamic structural and functional behaviors in healthy conditions and in response to induced perturbation via expression of human mutated tau. We found that prior to perturbation, both control unperturbed and perturbed networks followed a similar developmental trajectory consistent with relevant literature. The effects of the induced perturbation were evident within one week, with perturbed networks exhibiting significant decreases in firing rate, burst rate and total number of bursts in comparison to the relevant increases observed in control unperturbed networks. These changes align with reported adverse effects of tau hyperphosphorylation. Furthermore, over time, while healthy controls showed a steady decline in burst size and synchrony, perturbed networks showed significant increases in both, suggesting that all the activity was contained within a few, large, synchronized network bursts. Increasing synchrony, coupled to neurite retraction and the overall decline in firing and burst rates also suggested that the observed synchrony may be a maladaptive, rather than an adaptive, response. Importantly, the relevant changes seen in the perturbed networks were not observed in healthy controls, suggesting that the changes were attributable to the induced perturbation, rather than physiological endogenous tau expression. However, a valuable enhancement for future studies will involve designing a control virus featuring a wild-type tau with the same structure as the experimental virus to enable a more thorough comparison of the effects induced by mutated tau. Although the control unperturbed networks served as a sufficient baseline for evaluating structural and functional changes, introducing a control virus would heighten the study's validity by establishing a baseline to differentiate any alterations attributed to the virus itself as a foreign entity within the culture. Nevertheless, our current findings do provide significant new insights into dynamic structural and functional reconfigurations at the micro- and mesoscale in engineered feedforward neural networks as a result of evolving tau-associated pathology.

Conflict of Interest

The authors declare that the research was conducted in the absence of any commercial or financial relationships that could be construed as potential conflict of interest.

Author Contributions

The author contribution follows the CRediT system. JSW, KSH: Conceptualization, Investigation (Cell experiments; Protocol development and optimization; AAV investigations, Immunocytochemistry and Electrophysiological recordings), Writing – Original Draft, Review and Editing, Illustration. NWH: Methodology, Software, Investigation (chip design & manufacturing, electrophysiology, formal analysis), Writing – Review and Editing. AS, IS: Conceptualization, Methodology, Writing – Review & Editing, Funding acquisition, Supervision.

Funding

This project was funded by The Research Council of Norway (NFR, IKT Pluss; Self-Organizing Computational Substrates (SOCRATES)) Grant number: 27096; NTNU Enabling Technologies and The Liaison Committee for education, research, and innovation in Central Norway.

Acknowledgements

The authors would like to thank Dr. Christiana Bjørkli for the technical support in developing the transduction protocol and gifting us the AAV8-GFP-2a-P301Ltau-virus, originally designed, and produced by Dr. Rajeevkumar Nair Raveendran at the Viral Vector Core Facility, Kavli Institute for Systems Neuroscience. Prof. Michela Chiappalone and Prof. Sergio Martinoia, University of Genova for generously providing the scripts for the Precise Timing Spike Detection algorithm and the logISI burst detection. Prof. Menno P. Witter and Dr. Asgeir Kobro-Flatmoen, Kavli Institute for Systems Neuroscience for kindly reading and proving feedback. The Research Council of Norway is acknowledged for the support to the Norwegian Micro- and Nano-Fabrication Facility, NorFab, project number 295864.

Data availability statement

The raw data that support the findings of this study will be made available by the authors upon request.

References

Adamec, E., Murrell, J. R., Takao, M., Hobbs, W., Nixon, R. A., Ghetti, B., & Vonsattel, J. P. (2002). P301L tauopathy: confocal immunofluorescence study of perinuclear aggregation of the mutated protein. *J Neurol Sci, 200*(1-2), 85-93. doi:10.1016/s0022-510x(02)00150-8

Adams, J. N., Maass, A., Harrison, T. M., Baker, S. L., & Jagust, W. J. (2019). Cortical tau deposition follows patterns of entorhinal functional connectivity in aging. *Elife, 8*. doi:10.7554/eLife.49132

Anisimova, M., van Bommel, B., Wang, R., Mikhaylova, M., Wiegert, J. S., Oertner, T. G., & Gee, C. E. (2022). Spike-timing-dependent plasticity rewards synchrony rather than causality. *Cereb Cortex, 33*(1), 23-34. doi:10.1093/cercor/bhac050

Barzegaran, E., & Plomp, G. (2022). Four concurrent feedforward and feedback networks with different roles in the visual cortical hierarchy. *PLoS Biol, 20*(2), e3001534. doi:10.1371/journal.pbio.3001534

Bauer, U. S., Fiskum, V., Nair, R. R., van de Wijdeven, R., Kentros, C., Sandvig, I., & Sandvig, A. (2022). Validation of Functional Connectivity of Engineered Neuromuscular Junction With Recombinant Monosynaptic Pseudotyped ΔG-Rabies Virus Tracing. *Front Integr Neurosci, 16*, 855071. doi:10.3389/fnint.2022.855071

Biswas, S., & Kalil, K. (2018). The Microtubule-Associated Protein Tau Mediates the Organization of Microtubules and Their Dynamic Exploration of Actin-Rich Lamellipodia and Filopodia of Cortical Growth Cones. *J Neurosci, 38*(2), 291-307. doi:10.1523/jneurosci.2281-17.2017

Brewer, G. J., Boehler, M. D., Ide, A. N., & Wheeler, B. C. (2009). Chronic electrical stimulation of cultured hippocampal networks increases spontaneous spike rates. *J Neurosci Methods, 184*(1), 104-109. doi:10.1016/j.jneumeth.2009.07.031

Bruno, G., Colistra, N., Melle, G., Cerea, A., Hubarevich, A., Deleye, L., . . . Dipalo, M. (2020). Microfluidic Multielectrode Arrays for Spatially Localized Drug Delivery and Electrical Recordings of Primary Neuronal Cultures. *Front Bioeng Biotechnol, 8*, 626. doi:10.3389/fbioe.2020.00626

Braak, H., & Braak, E. (1991). Neuropathological stageing of Alzheimer-related changes. *Acta Neuropathol, 82*(4), 239-259. doi:10.1007/bf00308809

Busche, M. A. (2019). Tau suppresses neuronal activity in vivo, even before tangles form. *Brain, 142*(4), 843-846. doi:10.1093/brain/awz060

Busche, M. A., Wegmann, S., Dujardin, S., Commins, C., Schiantarelli, J., Klickstein, N., . . . Hyman, B. T. (2019). Tau impairs neural circuits, dominating amyloid-β effects, in Alzheimer models in vivo. *Nat Neurosci, 22*(1), 57-64. doi:10.1038/s41593-018-0289-8

Baas, P. W., & Qiang, L. (2019). Tau: It's Not What You Think. *Trends Cell Biol, 29*(6), 452-461. doi:10.1016/j.tcb.2019.02.007

Cai, Q., Davis, M. L., & Sheng, Z. H. (2011). Regulation of axonal mitochondrial transport and its impact on synaptic transmission. *Neurosci Res, 70*(1), 9-15. doi:10.1016/j.neures.2011.02.005

Chiappalone, M., Bove, M., Vato, A., Tedesco, M., & Martinoia, S. (2006). Dissociated cortical networks show spontaneously correlated activity patterns during in vitro development. *Brain Res, 1093*(1), 41-53. doi:10.1016/j.brainres.2006.03.049

Chiappalone, M., Vato, A., Berdondini, L., Koudelka-Hep, M., & Martinoia, S. (2007). Network dynamics and synchronous activity in cultured cortical neurons. *Int J Neural Syst, 17*(2), 87-103. doi:10.1142/s0129065707000968

Chowdhury, D., & Hell, J. W. (2018). Homeostatic synaptic scaling: molecular regulators of synaptic AMPA-type glutamate receptors. *F1000Res, 7*, 234. doi:10.12688/f1000research.13561.1

Collingridge, G. L., Peineau, S., Howland, J. G., & Wang, Y. T. (2010). Long-term depression in the CNS. *Nat Rev Neurosci, 11*(7), 459-473. doi:10.1038/nrn2867

Dong, Y., Yu, H., Li, X., Bian, K., Zheng, Y., Dai, M., . . . Kong, W. (2022). Hyperphosphorylated tau mediates neuronal death by inducing necroptosis and inflammation in Alzheimer's disease. *J Neuroinflammation, 19*(1), 205. doi:10.1186/s12974-022-02567-y

Fair, D. A., Cohen, A. L., Power, J. D., Dosenbach, N. U., Church, J. A., Miezin, F. M., . . . Petersen, S. E. (2009). Functional brain networks develop from a "local to distributed" organization. *PLoS Comput Biol, 5*(5), e1000381. doi:10.1371/journal.pcbi.1000381

Fauth, M. J., & van Rossum, M. C. (2019). Self-organized reactivation maintains and reinforces memories despite synaptic turnover. *Elife, 8*. doi:10.7554/eLife.43717

Fiskum, V., Sandvig, A., & Sandvig, I. (2021). Silencing of Activity During Hypoxia Improves Functional Outcomes in Motor Neuron Networks in vitro. *Front Integr Neurosci, 15*, 792863. doi:10.3389/fnint.2021.792863

Fornito, A., Zalesky, A., & Breakspear, M. (2015). The connectomics of brain disorders. *Nat Rev Neurosci, 16*(3), 159-172. doi:10.1038/nrn3901

Fukuda, T., Heizmann, C. W., & Kosaka, T. (1997). Quantitative analysis of GAD65 and GAD67 immunoreactivities in somata of GABAergic neurons in the mouse hippocampus proper (CA1 and CA3 regions), with special reference to parvalbumin-containing neurons. *Brain Res, 764*(1-2), 237-243. doi:10.1016/s0006-8993(97)00683-5

Fukushima, M., Betzel, R. F., He, Y., van den Heuvel, M. P., Zuo, X. N., & Sporns, O. (2018). Structure-function relationships during segregated and integrated network states of human brain functional connectivity. *Brain Struct Funct, 223*(3), 1091-1106. doi:10.1007/s00429-017-1539-3

Gansel, K. S. (2022). Neural synchrony in cortical networks: mechanisms and implications for neural information processing and coding. *Front Integr Neurosci, 16*, 900715. doi:10.3389/fnint.2022.900715

Goedert, M., Jakes, R., & Vanmechelen, E. (1995). Monoclonal antibody AT8 recognises tau protein phosphorylated at both serine 202 and threonine 205. *Neurosci Lett, 189*(3), 167-169. doi:10.1016/0304-3940(95)11484-e

Gribaudo, S., Tixador, P., Bousset, L., Fenyi, A., Lino, P., Melki, R., . . . Perrier, A. L. (2019). Propagation of α-Synuclein Strains within Human Reconstructed Neuronal Network. *Stem Cell Reports, 12*(2), 230-244. doi:10.1016/j.stemcr.2018.12.007

Götz, J., Halliday, G., & Nisbet, R. M. (2019). Molecular Pathogenesis of the Tauopathies. *Annu Rev Pathol, 14*, 239-261. doi:10.1146/annurev-pathmechdis-012418-012936

Henderson, J. A., & Gong, P. (2018). Functional mechanisms underlie the emergence of a diverse range of plasticity phenomena. *PLoS Comput Biol, 14*(11), e1006590. doi:10.1371/journal.pcbi.1006590

Hunsberger, H. C., Setti, S. E., Rudy, C. C., Weitzner, D. S., Pfitzer, J. C., McDonald, K. L., . . . Reed, M. N. (2021). Differential Effects of Human P301L Tau Expression in Young versus Aged Mice. *Int J Mol Sci, 22*(21). doi:10.3390/ijms222111637

Ide, A. N., Andruska, A., Boehler, M., Wheeler, B. C., & Brewer, G. J. (2010). Chronic network stimulation enhances evoked action potentials. *J Neural Eng, 7*(1), 16008. doi:10.1088/1741-2560/7/1/016008

Ittner, L. M., & Götz, J. (2011). Amyloid-β and tau--a toxic pas de deux in Alzheimer's disease. *Nat Rev Neurosci, 12*(2), 65-72. doi:10.1038/nrn2967

Jackson, J. S., Witton, J., Johnson, J. D., Ahmed, Z., Ward, M., Randall, A. D., . . . Ashby, M. C. (2017). Altered Synapse Stability in the Early Stages of Tauopathy. *Cell Rep, 18*(13), 3063-3068. doi:10.1016/j.celrep.2017.03.013

Kapucu, F. E., Valkki, I., Christophe, F., Tanskanen, J. M. A., Johansson, J., Mikkonen, T., & Hyttinen, J. A. K. (2017). On electrophysiological signal complexity during biological neuronal network development and maturation. *Annu Int Conf IEEE Eng Med Biol Soc, 2017*, 3333-3338. doi:10.1109/embc.2017.8037570

Katsuno, M., Sahashi, K., Iguchi, Y., & Hashizume, A. (2018). Preclinical progression of neurodegenerative diseases. *Nagoya J Med Sci, 80*(3), 289-298. doi:10.18999/nagjms.80.3.289

Kirst, C., Timme, M., & Battaglia, D. (2016). Dynamic information routing in complex networks. *Nat Commun, 7*, 11061. doi:10.1038/ncomms11061

Kopeikina, K. J., Polydoro, M., Tai, H. C., Yaeger, E., Carlson, G. A., Pitstick, R., . . . Spires-Jones, T. L. (2013). Synaptic alterations in the rTg4510 mouse model of tauopathy. *J Comp Neurol, 521*(6), 1334-1353. doi:10.1002/cne.23234

Kudela, P., Franaszczuk, P. J., & Bergey, G. K. (2003). Changing excitation and inhibition in simulated neural networks: effects on induced bursting behavior. *Biol Cybern, 88*(4), 276-285. doi:10.1007/s00422-002-0381-7

Kuhl, E. (2019). Connectomics of neurodegeneration. *Nat Neurosci, 22*(8), 1200-1202. doi:10.1038/s41593-019-0459-3

Lacovich, V., Espindola, S. L., Alloatti, M., Pozo Devoto, V., Cromberg, L. E., Čarná, M. E., . . . Falzone, T. L. (2017). Tau Isoforms Imbalance Impairs the Axonal Transport of the Amyloid Precursor Protein in Human Neurons. *J Neurosci, 37*(1), 58-69. doi:10.1523/jneurosci.2305-16.2016

Liu, L., Drouet, V., Wu, J. W., Witter, M. P., Small, S. A., Clelland, C., & Duff, K. (2012). Trans-synaptic spread of tau pathology in vivo. *PLoS One, 7*(2), e31302. doi:10.1371/journal.pone.0031302

Ma, Z., Ma, Y., & Zhang, N. (2018). Development of brain-wide connectivity architecture in awake rats. *Neuroimage, 176*, 380-389. doi:10.1016/j.neuroimage.2018.05.009

Maccione, A., Gandolfo, M., Massobrio, P., Novellino, A., Martinoia, S., & Chiappalone, M. (2009). A novel algorithm for precise identification of spikes in extracellularly recorded neuronal signals. *J Neurosci Methods, 177*(1), 241-249. doi:10.1016/j.jneumeth.2008.09.026

Markov, N. T., Vezoli, J., Chameau, P., Falchier, A., Quilodran, R., Huissoud, C., . . . Kennedy, H. (2014). Anatomy of hierarchy: feedforward and feedback pathways in macaque visual cortex. *J Comp Neurol, 522*(1), 225-259. doi:10.1002/cne.23458

Menkes-Caspi, N., Yamin, H. G., Kellner, V., Spires-Jones, T. L., Cohen, D., & Stern, E. A. (2015). Pathological tau disrupts ongoing network activity. *Neuron, 85*(5), 959-966. doi:10.1016/j.neuron.2015.01.025

Moore, A. K., Weible, A. P., Balmer, T. S., Trussell, L. O., & Wehr, M. (2018). Rapid Rebalancing of Excitation and Inhibition by Cortical Circuitry. *Neuron, 97*(6), 1341-1355.e1346. doi:10.1016/j.neuron.2018.01.045

Nonaka, T., & Hasegawa, M. (2011). In vitro recapitulation of aberrant protein inclusions in neurodegenerative diseases: New cellular models of neurodegenerative diseases. *Commun Integr Biol, 4*(4), 501-502. doi:10.4161/cib.4.4.15779

Pasquale, V., Martinoia, S., & Chiappalone, M. (2010). A self-adapting approach for the detection of bursts and network bursts in neuronal cultures. *J Comput Neurosci, 29*(1-2), 213-229. doi:10.1007/s10827-009-0175-1

Polanco, J. C., Li, C., Durisic, N., Sullivan, R., & Götz, J. (2018). Exosomes taken up by neurons hijack the endosomal pathway to spread to interconnected neurons. *Acta Neuropathol Commun, 6*(1), 10. doi:10.1186/s40478-018-0514-4

Qiang, L., Sun, X., Austin, T. O., Muralidharan, H., Jean, D. C., Liu, M., . . . Baas, P. W. (2018). Tau Does Not Stabilize Axonal Microtubules but Rather Enables Them to Have Long Labile Domains. *Curr Biol, 28*(13), 2181-2189.e2184. doi:10.1016/j.cub.2018.05.045

Rajbanshi, B., Guruacharya, A., Mandell, J. W., & Bloom, G. S. (2023). Localization, induction, and cellular effects of tau phosphorylated at threonine 217. *Alzheimers Dement*. doi:10.1002/alz.12892

Rascovsky, K., Salmon, D. P., Lipton, A. M., Leverenz, J. B., DeCarli, C., Jagust, W. J., . . . Galasko, D. (2005). Rate of progression differs in frontotemporal dementia and Alzheimer disease. *Neurology, 65*(3), 397-403. doi:10.1212/01.wnl.0000171343.43314.6e

Rubinov, M., Sporns, O., van Leeuwen, C., & Breakspear, M. (2009). Symbiotic relationship between brain structure and dynamics. *BMC Neurosci, 10*, 55. doi:10.1186/1471-2202-10-55

Salinas, E., & Sejnowski, T. J. (2001). Correlated neuronal activity and the flow of neural information. *Nat Rev Neurosci, 2*(8), 539-550. doi:10.1038/35086012

Senden, M., Reuter, N., van den Heuvel, M. P., Goebel, R., Deco, G., & Gilson, M. (2018). Task-related effective connectivity reveals that the cortical rich club gates cortex-wide communication. *Hum Brain Mapp, 39*(3), 1246-1262. doi:10.1002/hbm.23913

Siegle, J. H., Jia, X., Durand, S., Gale, S., Bennett, C., Graddis, N., . . . Koch, C. (2021). Survey of spiking in the mouse visual system reveals functional hierarchy. *Nature, 592*(7852), 86-92. doi:10.1038/s41586-020-03171-x

Steinhilb, M. L., Dias-Santagata, D., Fulga, T. A., Felch, D. L., & Feany, M. B. (2007). Tau phosphorylation sites work in concert to promote neurotoxicity in vivo. *Mol Biol Cell, 18*(12), 5060-5068. doi:10.1091/mbc.e07-04-0327

Stepan, J., Dine, J., & Eder, M. (2015). Functional optical probing of the hippocampal trisynaptic circuit in vitro: network dynamics, filter properties, and polysynaptic induction of CA1 LTP. *Front Neurosci, 9*, 160. doi:10.3389/fnins.2015.00160

Takao, K., Okamoto, K., Nakagawa, T., Neve, R. L., Nagai, T., Miyawaki, A., . . . Hayashi, Y. (2005). Visualization of synaptic Ca2+ /calmodulin-dependent protein kinase II activity in living neurons. *J Neurosci, 25*(12), 3107-3112. doi:10.1523/jneurosci.0085-05.2005

Tarawneh, R., & Holtzman, D. M. (2012). The clinical problem of symptomatic Alzheimer disease and mild cognitive impairment. *Cold Spring Harb Perspect Med, 2*(5), a006148. doi:10.1101/cshperspect.a006148

Thal, D. R., & Tomé, S. O. (2022). The central role of tau in Alzheimer's disease: From neurofibrillary tangle maturation to the induction of cell death. *Brain Res Bull, 190*, 204-217. doi:10.1016/j.brainresbull.2022.10.006

Timme, N. M., & Lapish, C. (2018). A Tutorial for Information Theory in Neuroscience. *eNeuro, 5*(3). doi:10.1523/eneuro.0052-18.2018

Turrigiano, G. G. (2008). The self-tuning neuron: synaptic scaling of excitatory synapses. *Cell, 135*(3), 422-435. doi:10.1016/j.cell.2008.10.008

Uhlhaas, P. J., & Singer, W. (2006). Neural synchrony in brain disorders: relevance for cognitive dysfunctions and pathophysiology. *Neuron, 52*(1), 155-168. doi:10.1016/j.neuron.2006.09.020

Valderhaug, V. D., Heiney, K., Ramstad, O. H., Bråthen, G., Kuan, W. L., Nichele, S., . . . Sandvig, I. (2021). Early functional changes associated with alpha-synuclein proteinopathy in engineered human neural networks. *Am J Physiol Cell Physiol, 320*(6), C1141-c1152. doi:10.1152/ajpcell.00413.2020

Vale, C., Alonso, E., Rubiolo, J. A., Vieytes, M. R., LaFerla, F. M., Giménez-Llort, L., & Botana, L. M. (2010). Profile for amyloid-beta and tau expression in primary cortical cultures from 3xTg-AD mice. *Cell Mol Neurobiol, 30*(4), 577-590. doi:10.1007/s10571-009-9482-3

van de Wijdeven, R., Ramstad, O. H., Bauer, U. S., Halaas, Ø., Sandvig, A., & Sandvig, I. (2018). Structuring a multi-nodal neural network in vitro within a novel design microfluidic chip. *Biomed Microdevices, 20*(1), 9. doi:10.1007/s10544-017-0254-4

van de Wijdeven, R., Ramstad, O. H., Valderhaug, V. D., Köllensperger, P., Sandvig, A., Sandvig, I., & Halaas, Ø. (2019). A novel lab-on-chip platform enabling axotomy and neuromodulation in a multi-nodal network. *Biosens Bioelectron, 140*, 111329. doi:10.1016/j.bios.2019.111329

Wagenaar, D. A., Pine, J., & Potter, S. M. (2006). An extremely rich repertoire of bursting patterns during the development of cortical cultures. *BMC Neurosci, 7*, 11. doi:10.1186/1471-2202-7-11

Wagenaar, D. A., & Potter, S. M. (2002). Real-time multi-channel stimulus artifact suppression by local curve fitting. *J Neurosci Methods, 120*(2), 113-120. doi:10.1016/s0165-0270(02)00149-8

Wang, Y., Balaji, V., Kaniyappan, S., Krüger, L., Irsen, S., Tepper, K., . . . Mandelkow, E. M. (2017). The release and trans-synaptic transmission of Tau via exosomes. *Mol Neurodegener, 12*(1), 5. doi:10.1186/s13024-016-0143-y

Weir, J. S., Christiansen, N., Sandvig, A., & Sandvig, I. (2023). Selective inhibition of excitatory synaptic transmission alters the emergent bursting dynamics of in vitro neural networks. *Front Neural Circuits, 17*, 1020487. doi:10.3389/fncir.2023.1020487

Winter-Hjelm N, T. Å. B., Sikoriski P, Sandvig A, Sandvig I. (2023). Structure-Function Dynamics of Engineered, Modular Neuronal Networks with Controllable Afferent-Efferent Connectivity. *Journal of Neural Engineering* doi:DOI 10.1088/1741-2552/ace37f

Witter, M. P. (2007). The perforant path: projections from the entorhinal cortex to the dentate gyrus. *Prog Brain Res, 163*, 43-61. doi:10.1016/s0079-6123(07)63003-9

Witter, M. P., Doan, T. P., Jacobsen, B., Nilssen, E. S., & Ohara, S. (2017). Architecture of the Entorhinal Cortex A Review of Entorhinal Anatomy in Rodents with Some Comparative Notes. *Front Syst Neurosci, 11*, 46. doi:10.3389/fnsys.2017.00046

Wu, Y., Liu, D., & Song, Z. (2015). Neuronal networks and energy bursts in epilepsy. *Neuroscience, 287*, 175-186. doi:10.1016/j.neuroscience.2014.06.046

Yamamoto, H., Moriya, S., Ide, K., Hayakawa, T., Akima, H., Sato, S., . . . Hirano-Iwata, A. (2018). Impact of modular organization on dynamical richness in cortical networks. *Sci Adv, 4*(11), eaau4914. doi:10.1126/sciadv.aau4914

ISBN 978-82-326-7676-7 (printed ver.)
ISBN 978-82-326-7675-0 (electronic ver.)
ISSN 1503-8181 (printed ver.)
ISSN 2703-8084 (online ver.)

NTNU

Norwegian University of
Science and Technology